Understanding the enzyme-inhibitor interaction within the substrate pocket of protein tyrosine kinases

by

Shana Marie Santos

A dissertation submitted in partial fulfillment
of the requirements for the degree of
Doctor of Philosophy
(Chemistry)
in the University of Michigan
2013

Doctoral Committee:
Assistant Professor Matthew Bryan Soellner, Chair
Professor Anna K. Mapp
Professor E. Neil G. Marsh
Professor Henry I. Mosberg

Dedication

To Mindy, my mother, who through her hard work, strength and endless love pushed me to become the person I am today.

To Seth, my best friend and hero, who battled the graduate school monster alongside me and never let me give up.

Acknowledgements

I owe a lot of my stubbornness and determination to my amazing support system, my family. Without them, I am not sure I would have made it this far. Because of this, I would like to thank my parents, Mindy and Manny, for their support, love and endless encouragement. I feel incredibly fortunate that they always worked hard to provide me with any and every opportunity I could ever imagine. Between soccer games and practices, band concerts, and the endless school science projects I am positive that I was a handful. But, in between chauffeuring me around the state for my activities, consoling me when I was discouraged, and celebrating with me those happy moments, I never heard one complaint (other than my own). For this I am beyond thankful and I feel truly blessed. Also, I cannot forget my little brother, Derek, who without him I would have never learned patience and the ability to think of witty come-backs for his endless amount of snark. To the rest of my family, aunts, uncles, cousins, grandparents, you have all been there to encourage me through every choice I have ever made and I could not have done any of this without all of those loud and fun family dinners and talks. Furthermore, I would like to mention and thank the Hogg family for their endless encouragement and support throughout my graduate education.

I would like to extend a great thanks to my teachers and professors who have offered me encouragement and guidance through the years, especially Mrs. Joan Cavallo, my high

school chemistry teacher, who first sparked my interest in chemistry with her passion for science and that stressful end of the term “determine the unknown” lab experiment. I would not have entered an undergraduate program in chemistry if not for her encouragement and advice while in her general chemistry and advanced placement chemistry courses and because of this, I am forever grateful to her. A big thanks to Dr. Eddie Luzik, for mentoring me throughout undergraduate research and encouraging me to set great goals for myself all while making research seem like so much fun. I also could not forget the opportunities that Dr. Michael Saliby afforded me by being able to serve as a laboratory assistant for him, even if it meant that the AA or the GC-MS broke too often and we had to call him at night while he was at home, making him return to campus in his Converse sneakers (Sorry Dr. Saliby).

Over the course of five years at the University of Michigan, I have had the pleasure of working with some talented and wonderful colleagues. I would like to acknowledge my labmates for their support and help with my projects. First, I want to thank Dr. Peter Barker for his unending support, encouragement and teasing. Without him, I would never have remembered to take mass spec of my reactions. Thank you to Kristin Ko for being my cubby-mate for the past year and a half and for our countless coffee runs. I probably would not have made it through the last stretch without being able to bother you constantly. Christel Fox, thank you for always being there to listen to me and send me cute cat photos when I really needed them. Also, I want to thank Dr. Sonali Kurup for being my previous cubby-mate as well as for her friendship, encouragement and help in synthesizing the biphenyl library. I would like to extend a big thanks to Michael Steffey for his help on all of my projects as well as having patience to explain the cell proliferation studies to me many times. Thank you to the rest of the

Soellner lab: Dr. Steven Bremmer, Meg Breen, Kris Branvold, Sameer Phadke, Frank Kwarcinski and Taylor Johnson for making the Soellner lab a great place to have spent the past five years. You all have helped me in so many different ways and I am very grateful for your friendships and knowledge.

I would like to sincerely thank the members of my committee, Dr. Anna Mapp, Dr. Neil Marsh, Dr. Henry Mosberg and Dr. Matthew Soellner. Thank you all for agreeing to serve on my committee as well as for your support and advice. I would like to especially thank Dr. Matthew Soellner for allowing me to be his first chemistry student to join his lab and for taking a chance on me. I appreciate being able to learn so much from you over these past years.

Lastly and most importantly, I want to thank Seth Hogg. Without you, I would not have been able to make it through all of the obstacles that I have faced. You are the strongest, most caring, and intelligent person that I have ever known. Not to mention, one of the best cooks. You support and encourage me so much, that you make me feel like I can conquer anything. Thank you for being my best friend and thank you for helping me get through the tough spots, celebrating the happy times with me and for teaching me to laugh even though I might want to cry. Thank you for making me a better, stronger and more caring person than I ever was. I am so lucky to have met you and to have you in my life. I am excited to see where this new chapter of our lives leads us.

Table of Contents

List of Tables

List of Figures

List of Appendices

List of Abbreviations

ADP:	Adenosine diphosphate
Ala (A):	Alanine
aPK:	Atypical protein kinase
Asp (D):	Aspartic acid
ATP:	Adenosine triphosphate
BiPH:	Biphenyl
BOC:	Di-tert-butyl dicarbonate protecting group
CBZ:	Carboxybenzyl protecting group
Cl:	Chloro-/Chlorine
DMSO:	Dimethyl sulfoxide
ePK:	Eukaryotic protein kinase
F:	Fluoro-/Fluorine
FDA:	US Food and Drug Administration
Fmoc:	Fluorenylmethyloxycarbonyl protecting group
Gly (G):	Glycine
GTP:	Guanosine triphosphate
Glu (E):	Glutamic acid
H:	Hydrogen
HER/EGFR:	Human epidermal growth factor receptor family
HT-29:	Human colon carcinoma cell line
IR:	Insulin receptor kinase

IC_{50}:	Half maximal inhibitory concentration
K_M:	The concentration of substrate required to observe the reaction rate at one half V_{max}
LE:	Ligand efficiency
Me:	Methyl
Met (M):	Methionine
NDPK:	Nucleoside-diphosphate kinase
NPTK:	Nonreceptor (cytosolic) protein tyrosine kinase
OMe:	Methoxy
Phe (F):	Phenylalanine
PK:	Protein kinase
PTK:	Protein tyrosine kinase
Pro (P):	Proline
pY:	Phosphorylated tyrosine
Ro3:	Rule of three
RPTK:	Receptor tyrosine kinase
SAR:	Structure-activity relationship
SH1/SH2/SH3:	Src homology domain
SK-BR-3:	Breast cancer cell line
Src WT:	Wild type Src
Src KD:	Kinase domain Src
Src 3D:	Three domain Src
Src T338M:	Gatekeeper mutation of Src
Thr (T):	Threonine
TK:	Tyrosine kinase
TR-FRET:	Time resolved fluorescence resonance energy transfer
Tyr (Y):	Tyrosine

V_{max}: Maximal velocity

Abstract

Protein phosphorylation occurs through enzymatic transfer of the γ-phosphate of adenosine triphosphate (ATP) to the hydroxyl moieties of the amino acid residues serine, threonine, and tyrosine. This post-translational modification is catalyzed by a group of enzymes classified as protein kinases. The phosphotransfer event initiates signal transduction cascades that are instrumental in the regulation of diverse cell functions. Aberrant protein kinase activity has been associated with various disease states. Because of this, academic as well as pharmaceutical efforts have been aimed at the understanding of kinase activity and understanding the related disease states. The work described herein focuses specifically on the development and evaluation of protein tyrosine kinase inhibitors in hopes to glean further knowledge regarding the substrate-binding region of the protein tyrosine kinase, c-Src.

Chapter 2 will discuss the use of a privileged scaffold, the biphenyl moiety, to screen for potential substrate-competitive inhibitors of the protein tyrosine kinase, c-Src. A 300 member library of biphenyl-containing compounds was synthesized and evaluated. From this study one compound, **BiPH 65**, emerged as a low micromolar affinity, substrate-competitive inhibitor of c-Src (IC_{50}: 60.4 micromolar). Thorough evaluation of the compound revealed inhibitory activity not only against the kinase domain of the protein, but also against the physiologically relevant three domain c-Src (IC_{50}: 17.2 micromolar), as well as the clinically relevant T338M c-Src (IC_{50}: 26.4 micromolar). Chapter 3 examines the use of an inhibitor peptide to arrive at truncated,

tetrafluorinated peptidomimetic small molecule inhibitors of c-Src. Although initially promising, these compounds were eventually found to bind competitively with ATP. Lastly, Chapter 4 details the study performed using a purchased fragment library. This fragment library was screened with hopes to elucidate a new scaffold on which to further optimize and design substrate-competitive inhibitors. However, we were happily surprised to find a compound that data suggest binds allosterically to the protein tyrosine kinase, c-Src. Although the lead compound, **[1]**, does not inhibit cell growth of a human colon carcinoma cell line, compound **[1c]**, the methyl ester analog of **[1]**, inhibits cell growth of a human breast cancer cell line (GI_{50}: 23.5 micromolar).

Chapter 1:

Introduction

1.1: Kinase Background

The regulation of cellular processes is critical for sustaining life. This occurs on a biochemical level through the processing of intracellular signals. These signals are interpreted by various proteins that can be switched from an on or active state to an off or inactive state depending on cellular environmental stimuli including changes in substrate concentration. Through fluctuations in enzymatic conformations, cellular processes such as cell growth, differentiation and proliferation are modulated. The processing of cellular signals occurs at a cost of a supply of energy. This energy supply is conserved through events such as the hydrolysis of nucleoside triphosphates like ATP and GTP. Since cellular activities can be likened to a system of checks and balances, every signaling event is paired with an energy providing biochemical reaction and is observed through post-translational modifications of the signaling protein.[1]

Post-translational modifications are reversible reactions that are catalyzed by enzymes. The most prevalent post-translational modification is reversible phosphorylation as it affects one-third of cellular proteins.[1] A majority of signal transduction pathways are involved with a phosphotransfer cascade.[2] Protein phosphorylation is catalyzed by a class of enzymes known as

protein kinases. These enzymes facilitate the transfer of the γ-phosphate of adenosine triphosphate (ATP) to the hydroxyl moieties of amino acid residues, serine, threonine and tyrosine of the natural peptide substrate.[1,3,4] (**Figure 1.1**) The protein kinase reaction occurs as the two substrates, ATP and a protein, bind to the catalytic domain of the kinase. Following the transfer of the γ-phosphate from ATP to the protein substrate, the phosphorylated product and ADP are released.[5] This phosphotransfer thus initiates signaling cascades that regulate cell functions such as cell growth, differentiation, proliferation, angiogenesis, metabolism, and apoptosis.[3-7] The kinase domain not only binds the protein substrate, but also binds magnesium, a cofactor.[5]

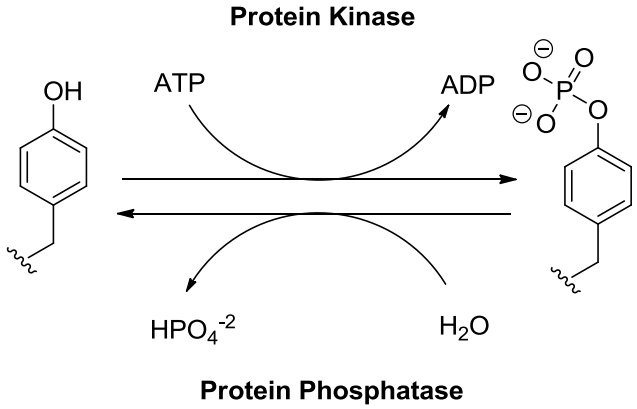

Figure 1.1: The reversible phosphorylation reaction facilitated by a protein kinase and a protein phosphatase. Adapted from Marks, et. al. 2009.

1.1.1: Kinase Families

The human kinome encompasses both lipid kinases as well as protein kinases.[5] The protein kinase superfamily consists of 518 individual kinases and comprises 1.7% of genes in the human genome.[1,2,5,7] Most protein kinases (478) contain an eukaryotic protein kinase (ePK) catalytic domain, whereas the other 40 kinases lack this conserved catalytic domain and are

regarded as atypical protein kinases (aPK).[5,7] Eight principle sub-families define the protein kinase superfamily. They include the tyrosine kinases (TK), tyrosine kinase-like (TKL), STE20 STE11 STE7 related (STE), casein kinase 1 (CK1), protein kinase A, protein kinase G and protein kinase C related (AGC), Ca^{2+}/calmodulin-dependent kinases (CAMK), Cdk MAPK GSK and Cdk-like related (CMGC), and finally receptor guanylyl cyclase (RGC).[3,5,7] Regarding cellular protein bound phosphoamino acids, approximately 95% exist as phosphoserine, 5% exist as phosphothreonine, while only 0.01-0.1% is found as phosphotyrosine.[3,8] More generally, protein kinases can phosphorylate either serine/threonine residues or tyrosine residues. Only 90 out of the 518 known kinases are capable of phosphorylating tyrosine residues.[9] Although small in number, this sub-family of protein tyrosine kinases (PTKs) is instrumental in many diverse cellular regulatory functions.[3,4,10] In addition to the regulation of cell growth, differentiation and development, cell survival and apoptosis, transcriptional regulation and glucose uptake, PTKs control T-cell and B-cell activation, as well as extracellular stimuli response, mitogenesis, angiogenesis, oncogenesis, platelet activation, cell shape and attachment, and lastly, neurotransmitter signaling.[3,4,10]

1.1.2: The Protein Tyrosine Kinase Family

The PTK family can be further divided into two smaller sub-classes: receptor protein tyrosine kinases (RPTK) and non-receptor (cytosolic) protein tyrosine kinases (NPTK). RPTKs are transmembrane proteins with inherent PTK catalytic activity. The N-terminus of a RPTK resides outside the confines of the cell and serves as the ligand binding domain, while the cytoplasmic domain contains a protein kinase catalytic domain.[5,11-13] RPTKs main function is to transduce a

signal from the extracellular binding of a ligand into the cytoplasm of the cell.[12] Examples of RPTKs include the insulin receptor (IR) and the human epidermal growth factor receptor family (HER/EGFR).[5] However, the NPTK sub-class of PTKs are more diverse as they not only are cytoplasmic proteins, but also membrane-associated as well as nuclear proteins.[12] There are 10 NPTK families[14], ABL[15,16], ACK[17], CSK[18,19], FAK[20-23], FES[24,25], FRK[26-29], JAK[30-33], SRC[34-38], TEC[39-42], and SYK[43,44]. The scope of this work focuses solely on the NPTK family of kinases and most specifically on the SRC family of protein tyrosine kinases as their implication in disease states is not only interesting, but not entirely understood. Our work aims to elucidate a better understanding of the NPTK, c-Src.

1.1.3: The Src Family of NPTKs

The Src family is further segregated into two subfamilies, A and B. The Src-A family consists of FGR, FYN, SRC, and YES1 while the Src-B family consists of BLK, HCK, LCK, and LYN.[8,12,14] **Figure 1.2** illustrates the general structure of Src and the Src family kinases.[45-47]

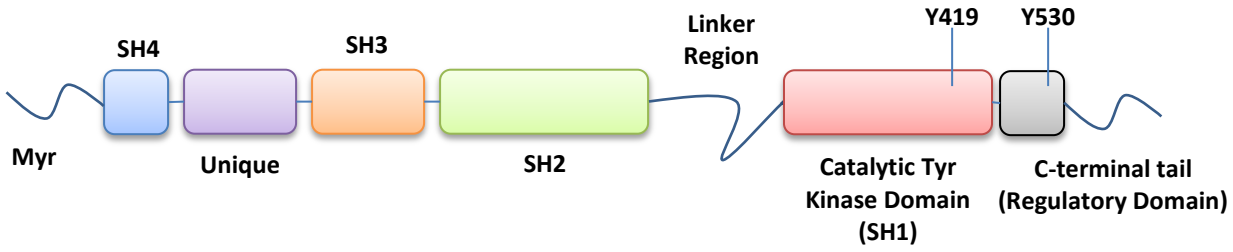

Figure 1.2: A schematic of the structural components of the SRC family kinases. Adapted from Finn, 2008, Sen, 2011 and Roskoski, 2004.

A myristoylation sequence is situated at the N-terminal of the kinase that is attached to a SH4 domain. A unique domain is connected to the SH3 domain followed by a SH2 domain. By means of a linker region, the SH2 domain is appended to the SH1 domain. The SH1 domain is the

catalytic tyrosine kinase domain. Lastly, a C-terminal regulatory segment is found following the SH1 domain.[46]

Membrane association of the kinase is facilitated by the myristoylation of the N-terminus of the kinase. This modification of the kinase aids in attachment and localization to the plasma membrane.[8,46-50] The first amino acid of the N-terminal tail, methionine 1, is removed and glycine 2 is myristoylated increasing the hydrophobicity of the N-terminal tail and aiding in the attachment to the membrane.[8] Furthermore, the SH4 domain serves to regulate cellular management of other different Src family kinases in the cell.[46] The unique domain of the kinase structure is not conserved throughout the family members and imparts distinctive properties to each kinase.[8,46]

Both the SH3 and SH2 domains are involved with regulation of protein-protein interactions.[51] The SH3 domain consists of approximately 60 amino acid residues that characteristically bind to proline-rich sequences allowing for interactions between substrate and enzyme as well as other intramolecular reactions.[8,46,48,52] The slightly larger SH2 domain (approximately 100 amino acids) binds to phosphorylated tyrosine residues either on the regulatory C-terminal tail or those of other protein sequences that the particular kinase has preference.[46] The preferred ligand binding motif of Src family PTKs is pY-E-E-I.[4,8,47] Tyr 530 resides on the C-terminal tail; when this residue is phosphorylated, it is bound to the SH2 domain of the kinase rendering the kinase in the inactive form. When this residue becomes unphosphorylated and Tyr 419 of the SH1 domain is phosphorylated, the kinase is said to be in

the active conformation.[46] **Figure 1.3** illustrates the interactions of the various domains of the kinase in both the inactive and active forms of the src family kinases.[47]

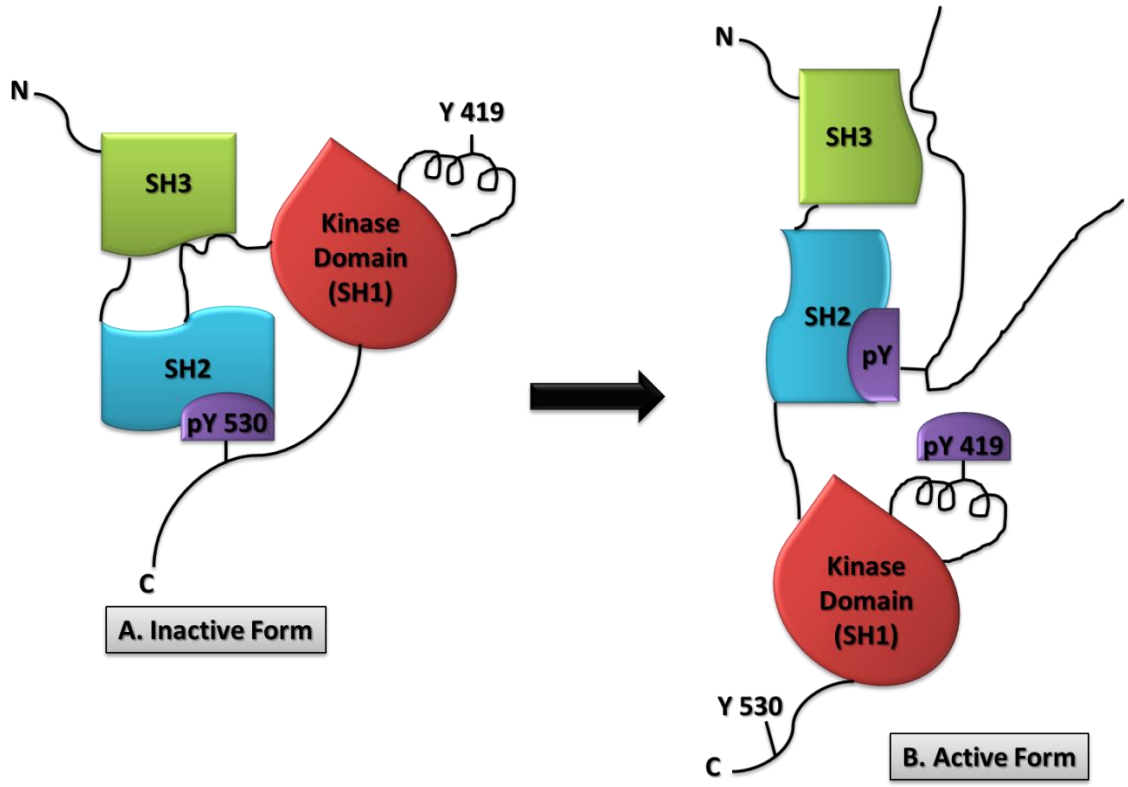

Figure 1.3: An illustration of the structural domains of the SRC family kinases in the inactive and active conformations. Adapted from Roskoski, 2004.

The catalytic tyrosine kinase domain or SH1 domain is bi-lobed in structure and contains approximately 250 amino acid residues. The smaller N-terminal lobe (approximately 70 amino acids) principally aids in the binding of ATP by the use of a glycine-rich loop to coordinate the phosphate groups of ATP.[47,53] Structurally, the N-terminal lobe consists of a five stranded β-sheet and an α-helix.[53] ATP binds in a pocket formed between the two lobes and makes critical hydrogen bonds with the so called hinge region.[53] Primarily α-helical, the larger C-terminal lobe consists of approximately 180 amino acid residues.[47,53] The C-terminal lobe is responsible for

the binding of the protein substrate.[47] This is due to the activation loop with two conserved sequences, Asp-Phe-Gly (or DFG) as well as Ala-Pro-Glu (or APE). Through the coordination of magnesium ions, the aspartate residue allows the substrate to interact with the phosphate groups of ATP.[53] The movement of both lobes allows for the binding of ATP and the release of ADP. Furthermore, the movement of the activation loop is instrumental in generating the inactive and active conformations of the kinase. When the DFG sequence is in a closed conformation, facing into the kinase, the kinase is said to be in the active form. Conversely, when the DFG sequence is in an open conformation, or out, the kinase is in an inactive conformation.[53,54]

1.2: Kinases and Disease

Initially discovered by Peyton Rous in 1911 due to his studies of viruses, src is regarded as the oldest known oncogene.[45,55] In 1976, the SRC gene was defined as the first proto-oncogene and later in 1980, c-Src protein was identified as the first protein tyrosine kinase.[48,55] c-Src assumes an integral role in the regulation of important cellular processes such as survival, differentiation, angiogenesis, motility, migration and invasion, and cell proliferation.[45,55] (**Figure 1.4**)

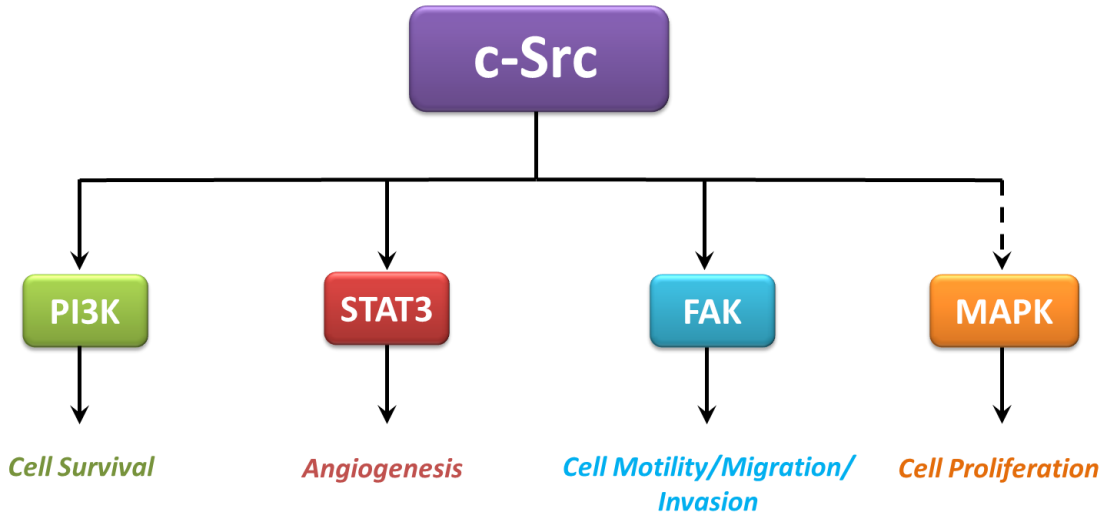

Figure 1.4: The physiological roles of c-Src. Adapted from Finn, 2008.

Activated by cytosolic proteins such as focal adhesion kinase (FAK) or Crk-associated substrate (CAS), as well as the dephosphorylation of Tyr 530 and phosphorylation of Tyr 419, Src interacts with substrates and downstream signaling molecules.[45] As shown in **Figure 1.4**, Src directly affects PI3K, STAT3 and FAK resulting in the onset of diverse cellular processes. Although not directly activated by Src, the Ras/Raf pathway, MAPK and cell proliferation are regulated by c-Src.[45]

The overexpression, the enhancement of kinase catalytic efficiency as well as the dysregulation of protein kinases have been found to be instrumental in the onset of disease states. This is due to abnormal levels of protein kinase reaction products in the cell.[56] Aberrant protein kinase activity has been correlated with a multitude of diseases including: cancer, rheumatoid arthritis, cardiovascular disease and neurodegenerative disease.[10] c-Src has been found over-expressed in specific cancers that include: breast, colon, pancreatic, and ovarian.[45,55,57] In spite of these facts, c-Src has yet to be shown as a central oncogene in human

cancers, though it is thought that the interruption of the Src signaling cascade could disrupt oncogenic pathways.[45] Furthermore, increased c-Src concentration alone has not been directly reported, however, the increase of c-Src concentration aids greatly in the increased signaling between pathways.[45]

Because of this, inhibiting c-Src activation may lead to the delay of disease progression or prevent the reoccurrence of the disease state.[45] One such example rests with HER2-positive breast cancer. The HER2 oncogene has not only been correlated to being overexpressed in 20% of human breast cancers but also has been associated with reduced patient survival. Trastuzumab (Herceptin) treatment is often used to treat HER2-positive breast cancer patients. However, these patients eventually tend to develop resistance to the Trastuzumab (Herceptin) treatment. Through thorough study, Zhang and coworkers have suggested that the subsequent downstream activation of c-Src is the reason for the drug resistance.[58,59] With hopes to combat such resistance, the inhibition of c-Src has been explored and may have clinical success to the benefit of HER2-positive breast cancer patients.[58,59] Additionally, c-Src has been associated with tamoxifen resistance.[59]

1.3: Inhibition of Kinases

Because of their role in cellular regulation, protein kinases have been intensely studied not only by academia, but thirty percent of pharmaceutical efforts have been extended for the study and development of protein kinase inhibitors. This only falls second to G-protein-coupled receptor research targets.[13,60-65] Hiroyoshi Hidaka developed the first protein kinase inhibitors in the 1980s. These inhibitors were naphthalene sulphonamides that had been previously

developed for a different target, calmodulin.[66] When the naphthalene moiety was replaced with an isoquinoline, they no longer affected calmodulin, but instead were inhibitors of protein kinases. One of these inhibitors, **H8**, is shown in **Figure 1.5**.[66] Difficulty with these inhibitors was noted as the compounds were of low potency and nonselective.

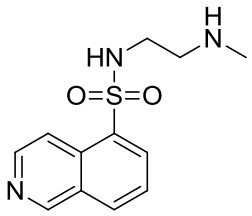

H8

Figure 1.5: One of the first protein kinase inhibitors developed by Hiroyoshi Hidaka in the 1980s.

1.3.1: Current Approved Inhibitors of Protein Kinases

To date, there are over 130 inhibitors of protein kinases at various stages of clinical development and trials.[62,63] Despite the amount of effort and time dedicated to protein kinases, the U.S. Food and Drug Administration (FDA) has only approved a total of eleven kinase inhibitors for use as therapeutics.[63] (**Table 1.1**) All approved therapeutics bind the kinase in an ATP-competitive fashion.[63,67]

Inhibitor	Kinase Target
Imatinib	ABL1-2, PDGFR, KIT
Gefitinib	EGFR
Erlotinib	EGFR
Lapatinib	EGFR, ERBB2
Dasatinib	ABL1-2, PDGFR, KIT, SRC
Nilotinib	ABL1-2, PDGFR, KIT
Sunitinib	VEGFR1-3, KIT, PDGFR, RET, CSF1R, FLT3
Sorafenib	VEGFR2, KIT, PDGFR, FLT3, BRAF
Pazopanib	VEGFR1-3, KIT, PDGFR
Everolimus	mTOR
Temsirolimus	mTOR
Bosutinib	ABL, SRC
Ruxolitinib	JAK1-2

Table 1.1: FDA approved kinase inhibitors and their target kinases. Adapted from Fabbro, 2012.

1.4: Types of Kinase Inhibition

The characterization of protein kinase inhibitors is broadly defined by the mode of binding between the inhibitor and the kinase target.[67,68] Current inhibitor research and development can be organized into various sub-types of protein kinase inhibitors. Each inhibitor type affects the kinase in a unique manner and has its own benefits and disadvantages. Often, selectivity, potency and lack of structural knowledge are challenging obstacles to overcome in inhibitor design.

1.4.1: Type I and II Inhibitors

Protein kinase inhibitors that bind to the ATP binding pocket and compete directly with ATP concentrations are classified as Type I or Type II protein kinase inhibitors. Type I kinase inhibitors bind to the active conformation of the kinase, when the DFG motif is in the “in”

position. Type I inhibitors interact with the hinge region of the protein kinase and are capable of making the same interactions as ATP with the kinase.[62] In contrast, Type II inhibitors are said to trap the inactive conformation of the protein kinase, when the activation loop DFG motif is in an "out" position.[68] Type II inhibitors bind not only to the ATP pocket, but also extend into the hydrophobic pocket that is created by the "out" position of the DFG motif.[62]

ATP competitive inhibitors often are extremely potent and successful in clinical studies as all FDA approved kinase inhibitors are either classified as Type I or Type II inhibitors. However, the ATP binding pocket of protein kinases is highly conserved.[69] Because this pocket singularly serves to bind a molecule of ATP, these inhibitors often suffer from a lack of selectivity. Additionally, in a cancer cell, the cellular concentrations of ATP can be as high as 10 mM; a concentration much higher than the K_M of ATP for the protein kinase. This high ATP concentration ultimately dictates that the ATP-competitive inhibitor must be very potent in order to compete against such high levels of ATP.[60,65,68]

Although their Type I counterparts are known to lack selectivity, Type II inhibitors gain some selectivity from their role in binding to the hydrophobic pocket created by the DFG "out" conformation, as they prevent the kinase from adapting the active conformation.[62,68] Both imatinib and sorafenib are regarded as Type II inhibitors.[68]

Both Type I and Type II inhibitors are affected by mutations within the ATP binding pocket. One clinically relevant mutation is that of the gatekeeper residue. This residue resides in a hydrophobic pocket in the back of the ATP pocket. When this residue is mutated, from a

threonine to a larger hydrophobic residue, access to the pocket is restricted often resulting in resistance to the inhibitor.[68]

1.4.2: Type III Inhibitors

With push to develop equally as potent yet more selective inhibitors than the Type I and Type II counterparts, Type III protein kinase inhibitors emerged with the discovery of the highly potent and selective MEK inhibitor, PD318088.[62,68] Furthermore, Rauh and co-workers have discovered other Type III inhibitors fortuitously through *in vitro* library screens.[68,70] Like Type II inhibitors, Type III inhibitors stabilize an inactive conformation of the protein kinase by binding to the hydrophobic pocket formed by the DFG "out" conformation but not extending into the hinge region as Type II inhibitors characteristically do.[68] Uniquely, Type III inhibitors stabilize an inactive form of the kinase in which the hinge region is in a closed, active conformation but an essential glutamate residue is skewed in such a way that catalysis cannot occur.[68]

1.4.3: Substrate-Competitive Inhibitors

Substrate-competitive inhibitors characteristically probe the substrate binding region of protein kinases. The substrate-binding pockets of kinases, are, in general, less conserved than the ATP-binding pockets of protein kinases. A small number of natural substrate peptides or proteins with unique sequences bind selectively to various kinases. Because of this, it is hypothesized that probing the substrate pocket for the design and development of substrate-competitive inhibitor compounds would yield compounds that have a high specificity for the desired kinase target, resulting in a more selective probe or therapeutic. Since natural peptide or protein substrates often exist in the cell at concentrations at or below their K_M, these types

of inhibitors need not have the extreme potency that ATP-competitive inhibitors (Type I and II) must possess.[3,66,71,72]

The development of substrate-competitive inhibitors presents a variety of challenges as there is a significant lack of structural data for many protein kinases. Therefore, the rational design of such inhibitors is difficult. Furthermore, in addition to only being able to achieve low micromolar affinities for the kinase target, the substrate pocket is often shallow and solvent exposed further hindering any rational design.[68] See chapters 2, 3 and 4 for a discussion of work in this area.

1.4.4: Type IV Inhibitors – Allosteric Inhibitors

Type IV inhibitors are regarded as purely allosteric in nature. Such compounds target regions of the kinase apart from the ATP binding pocket and active site.[62,68] Truly allosteric inhibitors have been elucidated for protein kinases such as Akt as well as Plk1.[62] Additionally, the compound GNF-2, developed by Nathanael Gray and coworkers, has been described as an allosteric inhibitor of c-Abl and c-Arg.[73-75] (**Figure 1.6**) See chapter 4 for work performed in this area.

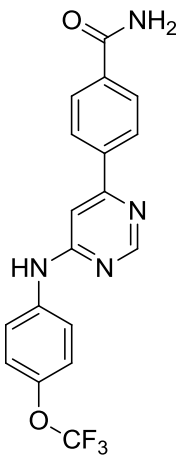

GNF-2

Figure 1.6: The structure of the allosteric c-Abl, c-Arg inhibitor, **GNF-2**.

1.4.5: Type V Inhibitors

Divided into two subgroups, Type V inhibitors aim to combine the high affinity properties of some inhibitors with the high selectivity properties of others by combining the two different compounds to produce one compound with desirable qualities. These compounds target two distinct regions of the protein kinase and are known as bisubstrate (Type Va) or bivalent (Type Vb).[62]

Type Va bisubstrate inhibitors target both the ATP binding region as well as the substrate binding region concurrently.[62,76,77] More generally, Type Vb bivalent inhibitors target any arrangement of regions of the protein kinase.[62,68] Type V inhibitors as a whole aim to garner optimal selectivity and potency using the knowledge gleaned from various Type I-IV inhibitors and their kinase targets.[62,68]

1.5: Scope of the work to be presented

The work presented in this dissertation aims to explore the development and evaluation of substrate-competitive inhibitors of the protein tyrosine kinase c-Src. In order to accomplish this study, various approaches were considered and utilized. To begin with, chapter 2 discusses how a privileged scaffold was exploited to design a library of 300 compounds containing a biphenyl moiety. This library screen resulted in the discovery of a substrate-competitive c-Src inhibitor. Additionally, chapter 2 outlines the use of a specialized TR-FRET screen developed in our laboratory to efficiently characterize substrate-competitive inhibitors. Secondly, chapter 3 describes how we delved into the design of an inhibitor from an inhibitor peptide. Through truncation of the parent peptide, we arrived at a peptidomimetic compound that unfortunately did not bind in the desired substrate-competitive mode. Lastly, chapter 4 explores the results from our study on the use of a fragment library supplied by the Maybridge Chemical Company, and how we were able to elucidate a fragment that binds to c-Src in an allosteric manner.

1.6: References

(1) Marks, F.; Klingmüller, U.; Müller-Decker, K. *Cellular Signal Processing: An Introduction to the Molecular Mechanisms of Signal Transduction*; Garland Science: New York, 2009.
(2) Zhang, J.; Yang, P. L.; Gray, N. S. *Nature Reviews: Cancer* **2009**, *9*, 28.
(3) Al-Obeidi, F. A.; Wu, J. J.; Lam, K. S. *Biopolymers* **1998**, *47*, 197.
(4) Al-Obeidi, F. A.; Lam, K. S. *Oncogene* **2000**, *19*, 5690.
(5) Duong-Ly, K. C.; Peterson, J. R. *Curr. Protoc. Pharmacol.* **2013**, *2.9.1 - 2.9.14*.
(6) Matthews, D. J.; Gerritsen, M. E. *Targeting Protein Kinases for Cancer Therapy*; John Wiley & Sons: Hoboken, NJ, 2010.
(7) Manning, G. *Science* **2002**, *298*, 1912.
(8) Mustelin, T. *Src Family Tyrosine Kinases in Leukocytes*; R.G. Landes Company: Austin, 1994.

(9) Pearson, M.; Garcia-Echeverria, C.; Fabbro, D. In *Protein Tyrosine Kinases: From Inhibitors to Useful Drugs*; Fabbro, D., McCormick, F., Eds.; Humana Press, Inc.: Totowa, New Jersey, 2006, p 1.
(10) Giamas, G.; Man, Y. L.; Hirner, H.; Bischof, J.; Kramer, K.; Khan, K.; Lavina-Ahmed, S. S.; Stebbing, J.; Knippschild, U. *Cell. Signal.* **2010**, *22*, 984.
(11) Hunter, T.; Lindberg, R. A. In *Protein Kinases*; Woodgett, J. R., Ed.; IRL Press - Oxford University Press: New York, 1994, p 177.
(12) Courtneidge, S. A. In *Protein Kinases*; Woodgett, J. R., Ed.; IRL Press - Oxford University Press: New York, 1994, p 212.
(13) Eglen, R.; Reisine, T. *Pharmacol. Ther.* **2011**, *130*, 144.
(14) Robinson, D. R.; Wu, Y.-M.; Lin, S.-F. *Oncogene* **2000**, *19*, 5548.
(15) Lanier, L. M.; Gertler, F. B. *Curr. Opin. Neurobiol.* **2000**, *10*, 80.
(16) Laneuville, P. *Semin. Immunol.* **1995**, *7*, 255.
(17) Mott, H. R.; Owen, D.; Nietlispach, D.; Lowe, P. N.; Manser, E.; Lim, L.; Laue, E. D. *Nature* **1999**, *399*, 384.
(18) Sondhi, D.; Cole, P. A. *Biochemistry* **1999**, *38*, 11147.
(19) Klages, S.; Adam, D.; Class, K.; Fargnoli, J.; Bolen, J. B.; Penhallow, R. C. *Proc Natl Acad Sci U S A* **1994**, *91*, 2597.
(20) Avraham, H.; Park, S. Y.; Schinkmann, K.; Avraham, S. *Cell. Signal.* **2000**, *12*, 123.
(21) Girault, J. A.; Costa, A.; Derkineren, P.; Studler, J. M.; Toutant, M. *Trends Neurosci.* **1999**, *22*, 257.
(22) Schlaepfer, D. D.; Hunter, T. *Trends Cell Biol.* **1999**, *8*, 151.
(23) Weisberg, E.; Sattler, M.; Ewaniuk, D. S.; Salgia, R. *Crit. Rev. Oncog.* **1997**, *8*, 343.
(24) Smithgall, T. E.; Rogers, J. A.; Peters, K. L.; Li, J.; Briggs, S. D.; Lionberger, J. M.; Cheng, H.; Shibata, A.; Scholtz, B.; Schreiner, S.; Dunham, N. *Crit. Rev. Oncog.* **1998**, *9*, 43.
(25) Pendergast, A. M. *Curr. Opin. Cell Biol.* **1996**, *8*, 174.
(26) Lee, H.; Kim, M.; Lee, K. H.; Kang, K. N.; Lee, S. T. *Mol. Cell* **1998**, *8*, 401.
(27) Vasioukhin, V.; Tyner, A. L. *Proc Natl Acad Sci U S A* **1997**, *94*, 14477.
(28) Kohmura, N.; Yagi, T.; Tomooka, Y.; Oyanagi, M.; Kominami, R.; Takeda, N.; Chiba, J.; Ikawa, Y.; Aizawa, S. *Mol. Cell. Biol.* **1994**, *14*, 6915.
(29) Lee, J.; Wang, Z.; Luoh, S. M.; Wood, W. I.; Scadden, D. T. *Gene* **1994**, *138*, 247.
(30) Danial, N. N.; Rothman, P. *Oncogene* **2000**, *19*, 2523.
(31) Imada, K.; Leonard, W. J. *Mol. Immunol.* **2000**, *37*, 1.
(32) Aringer, M.; Cheng, A.; Nelson, J. W.; Chen, M.; Sudarshan, C.; Zhou, Y. J.; O'Shea, J. J. *Life Sci* **1999**, *64*, 2173.
(33) Leonard, W. J.; O'Shea, J. J. *Annu. Rev. Immunol.* **1998**, *16*, 293.
(34) Abram, C. L.; Courtneidge, S. A. *Exp. Cell Res.* **2000**, *254*, 1.
(35) Schlessinger, J. *Cell* **2000**, *100*, 293.
(36) Schwartzberg, P. L. *Oncogene* **1998**, *17*, 1463.
(37) Thomas, S. M.; Brugge, J. S. *Annu. Rev. Cell Dev. Biol.* **1997**, *13*, 513.
(38) Chow, L. M.; Veillette, A. *Semin. Immunol.* **1995**, *7*, 207.
(39) Schaeffer, E. M.; Schwartzberg, P. L. *Curr. Opin. Immunol.* **2000**, *12*, 282.
(40) Yang, W. C.; Collette, Y.; Nunes, J. A.; Olive, D. *Immunity* **2000**, *12*, 373.

(41) Mano, H. *Cytokine Growth Factor Rev.* **1999**, *10*, 267.
(42) Rawlings, D. J.; Witte, O. N. *Semin. Immunol.* **1995**, *7*, 237.
(43) Turner, M.; Schweighoffer, E.; Colucci, F.; Di Santo, J. P.; Tybulewicz, V. L. *Immunol. Today* **2000**, *21*, 148.
(44) Chu, D.; Morita, C. T.; Weiss, A. *Immunol. Rev.* **1998**, *165*, 167.
(45) Finn, R. S. *Ann. Oncol.* **2008**, *19*, 1379.
(46) Sen, B.; Johnson, F. M. *Journal of Signal Transduction* **2011**, *2011*, 1.
(47) Roskoski, R. *Biochem. Biophys. Res. Commun.* **2004**, *324*, 1155.
(48) Brown, M. T.; Cooper, J. A. *Biochemica et Biophysica Acta* **1996**, *1287*, 121.
(49) Courtneidge, S. A.; Levinson, A. D.; Bishop, J. M. *Proc Natl Acad Sci U S A* **1980**, *77*, 3783.
(50) Cross, F. R.; Garber, E. A.; Pellman, D.; Hanafusa, H. *Mol. Cell. Biol.* **1984**, 1834.
(51) McDowall, J. In *SRC, proto-oncogene tyrosine-protein kinase.* http://www.ebi.ac.uk/interpro/potm/2003_2/Page_2.htm.
(52) Cohen, G. B.; Ren, R.; Baltimore, D. *Cell* **1995**, *80*, 237.
(53) Cowan-Jacob, S. W.; Ramage, P.; Stark, W.; Fendrich, G.; Jahnke, W. In *Protein Tyrosine Kinases: From Inhibitors to Useful Drugs*; Fabbro, D., McCormick, F., Eds.; Humana Press: Totowa, New Jersey, 2006, p 187.
(54) Zuccotto, F.; Ardini, E.; Casale, E.; Angiolini, M. *J Med Chem* **2010**, *53*, 2681.
(55) Martin, S. G. *Nature Reviews: Molecular Cell Biology* **2001**, *2*, 467.
(56) Copeland, R. A. *Evaluation of Enzyme Inhibitors in Drug Discovery: A Guide for Medicinal Chemists and Pharmacologists*; John Wiley & Son: Hoboken, NJ., 2005.
(57) Frame, M. C. *Biochemica et Biophysica Acta* **2002**, *1602*, 114.
(58) Zhang, S.; Huang, W.-C.; Li, P.; Guo, H.; Poh, S.-B.; Brady, S. W.; Xiong, Y.; Tseng, L.-M.; Li, S.-H.; Ding, Z.; Sahin, A. A.; Esteva, F. J.; Hortobagyi, G. N.; Yu, D. *Nat. Med.* **2011**, *17*, 461.
(59) Muthuswamy, S. K. *Nat. Med.* **2011**, *17*, 416.
(60) Knight, Z. A.; Shokat, K. M. *Chem. Biol. (Cambridge, MA, U. S.)* **2005**, *12*, 621.
(61) Morphy, R. *J Med Chem* **2010**, *53*, 1413.
(62) Cox, K. J.; Shomin, C. D.; Ghosh, I. *Future Med. Chem.* **2011**, *3*, 29.
(63) Fabbro, D.; Cowan-Jacob, S. W.; Möbitz, H.; Martiny-Baron, G. In *Kinase Inhibitors: Methods and Protocols*; Kuster, B., Ed.; Humana Press: 2012; Vol. 795, p 1.
(64) Han, K.-C.; Kim, S. Y.; Yang, E. G. *Curr. Pharm. Des.* **2012**, *18*, 2875.
(65) Kirkland, L. O.; McInnes, C. *Biochem. Pharmacol.* **2009**, *77*, 1561.
(66) Cohen, P. *Nature Reviews: Drug Discovery* **2002**, *1*, 309.
(67) Grant, S. K. *Cell. Mol. Life Sci.* **2009**, *66*, 1163.
(68) Lamba, V.; Ghosh, I. *Curr. Pharm. Des.* **2012**, *18*, 2936.
(69) Bikker, J. A.; Brooijmans, N.; Wissner, A.; Mansour, T. S. *J Med Chem* **2009**, *52*, 1493.
(70) Simard, J. R.; Kluter, S.; Grutter, C.; Getlik, M.; Rabiller, M.; Rode, H. B.; Rauh, D. *Nat. Chem. Biol.* **2009**, *5*, 394.
(71) Ye, G.; Tiwari, R.; Parang, K. *Curr. Opin. Investig. Drugs* **2008**, *9*, 605.

(72) Songyang, Z.; Carraway, K. L.; Eck, M. J.; Harrison, S. C.; Feldman, R. A.; Mohammadi, M.; Schlessinger, J.; Hubbard, S. R.; Smith, D. P.; Eng, C.; Lorenzo, M. J.; Ponder, B. A. J.; Mayer, B. J.; Cantley, L. C. *Nature* **1995**, *373*, 536.
(73) Choi, Y.; Seeliger, M. A.; Panjarian, S. B.; Kim, H.; Deng, X.; Sim, T.; Couch, B.; Koleske, A. J.; Smithgall, T. E.; Gray, N. S. *J. Biol. Chem.* **2009**, *284*, 29005.
(74) Fabbro, D.; Manley, P. W.; Jahnke, W.; Liebetanz, J.; Szyttenholm, A.; Fendrich, G.; Strauss, A.; Zhang, J.; Gray, N. S.; Adrian, F.; Warmuth, M.; Pelle, X.; Grotzfeld, R.; Berst, F.; Marzinzik, A.; Cowan-Jacob, S. W.; Furet, P.; Mestan, J. *Biochimica et Biophysica Acta (BBA) - Proteins and Proteomics* **2010**, *1804*, 454.
(75) Zhang, J.; Adrián, F. J.; Jahnke, W.; Cowan-Jacob, S. W.; Li, A. G.; Iacob, R. E.; Sim, T.; Powers, J.; Dierks, C.; Sun, F.; Guo, G.-R.; Ding, Q.; Okram, B.; Choi, Y.; Wojciechowski, A.; Deng, X.; Liu, G.; Fendrich, G.; Strauss, A.; Vajpai, N.; Grzesiek, S.; Tuntland, T.; Liu, Y.; Bursulaya, B.; Azam, M.; Manley, P. W.; Engen, J. R.; Daley, G. Q.; Warmuth, M.; Gray, N. S. *Nature* **2010**, *463*, 501.
(76) Lavogina, D.; Enkvist, E.; Uri, A. *ChemMedChem* **2010**, *5*, 23.
(77) Parang, K.; Cole, P. A. *Pharmacol. Ther.* **2002**, *93*, 145.

Chapter 2:

The Biphenyl as a Privileged Scaffold

2.1: Abstract

Protein tyrosine kinases (PTKs) have been implicated in diseases including cancer, inflammation, and diabetes.[1] All FDA approved therapeutics targeting PTKs are ATP-competitive inhibitors.[2,3] Although these inhibitors are extremely potent, the ATP-binding pockets of protein kinases share a high sequence similarity and therefore, selectivity is difficult to achieve.[4] We hypothesize that substrate-competitive inhibition of PTKs can offer advantages over ATP-competitive inhibition, such as improved selectivity through the more highly conserved substrate-binding pocket as well as the ability to address the clinically relevant ATP-binding pocket mutations. Thus, we aim to develop small molecule, substrate-competitive PTK inhibitors.

The biphenyl framework was chosen for its ability to mimic protein-protein interactions as well as its characteristic binding promiscuity.[5-7] Thus, a library of approximately 300 biphenylethylacetimides, and other compounds similar in structure was screened against wild type c-Src (kinase domain and 3-domain) as well as the c-Src gatekeeper T338M mutant. The average molecular weight of the compounds within the library was 365.8. This study resulted in one compound of great interest, (4-morpholino)biphenylethylacetimide, as it inhibited kinase domain c-Src with an IC_{50} of 52 μM and 3-domain c-Src with an IC_{50} of 16 μM. Most notably, the lead compound inhibited the gatekeeper c-Src T338M mutant with an IC_{50} of 26 μM.

Additionally, Lineweaver-Burke plot analysis suggests that the lead compound binds in the desired ATP-noncompetitive, substrate-competitive mode.

2.2: Introduction

Over 500 different enzymes construct the general class known as protein kinases. Protein tyrosine kinases (PTKs) represent a small group of kinases within the kinome. Functionally, these 90 kinases facilitate the transfer of the γ-phosphate of an adenosine triphosphate molecule to its substrate's phenolic tyrosine residue resulting in the initiation of signaling cascades imperative for cell functions such as cell growth, cell division, and apoptosis.[8,9] Dysregulation of such cellular events results in various disease states including cancer, rheumatoid arthritis, cardiovascular disease, as well as neurodegenerative disease.[1] Second only to G-protein coupled receptors, PTKs are a superfamily of intensely investigated enzymes. Thirty percent of pharmaceutical research efforts are directed toward the discovery of inhibitors of protein kinases.[10-14] Of the 90 known PTKs, our interest lies with the non-receptor PTK c-Src as it regulates diverse cellular processes involving: survival, angiogenesis, motility, migration and invasion, as well as cell proliferation. As the first proto-oncogene discovered, it is known to be over-expressed in cancers such as breast, colon, pancreatic and ovarian.[15,16] Over-expressed in 20% of human breast cancers, HER2-positive patients have been found to have or eventually develop trastuzumab resistance during treatment. Zhang and coworkers suggest that the subsequent downstream activation of c-Src is a result of drug resistance. Therefore, to combat this resistance, inhibition of c-Src may have clinical success and benefit in HER2-positive breast cancer patients.[17,18]

Although the importance of therapeutic design is imperative to combat current cancer threats, the design of selective, small molecule inhibitors is paramount for the further understanding of enzymatic activity. Off-target binding of inhibitors often leads to negative effects and toxicity.[19] These selective, small molecules act as specific kinase probes that investigate the modes of binding and kinase activity that may not be completely understood at this time as well as to thwart the incidence of toxic effects due to off-target binding. In the end, these molecules may also aid in the rational design of later therapeutics. Selectivity allows for the more precise study of the kinase in question as well as its role in various signal transduction pathways.

Probing the activity of PTKs involves the prevention of the phosphate transfer from ATP to kinase substrate. Current approaches include ATP-competition as well as substrate-competition among others. To date, all FDA approved PTK inhibitors are ATP-competitive in nature. Thus, the inhibitor in question must out-compete high concentrations of cellular ATP to bind to the dysregulated kinase halting kinase activity.[12] This class of compounds, although highly potent and successful in clinical studies, suffers from a lack of selectivity amongst the more than 500 kinase family members. Low selectivity results from the highly conserved ATP-binding pocket of kinases.[4] This pocket, formed in each kinase, singularly serves to bind a molecule of ATP. High pocket conservation renders ATP-competitive inhibitors quite promiscuous, as they can bind to their target kinase as well as many other kinases downstream. Off-target binding plays a major role in the toxicity of the inhibitors.[13,19-21]

Another mode of inhibition currently under investigation rests upon out-competing the substrate peptide or protein that would in turn undergo phosphorylation by the abundance of

ATP in cancerous cells.[13,21] The substrate-binding pockets of kinases are, in general, less conserved than the ATP-binding pockets of fellow kinase family members as they bind a small number of substrate peptides with unique sequences.[8,13,21-23] This characteristic of the substrate-binding pocket is hypothesized to provide optimized specificity for desired kinase targets and therefore, better therapeutics. Additionally, the inhibitor does not compete with high concentrations of substrate peptide, as the substrate peptides exist in much lower concentrations than ATP in cancerous cells.[8,23]

Although substrate-competitive inhibitors have tremendous potential, their development presents many challenges. Currently, no structural data exists for many PTKs. Lack of structural understanding hinders the rational design of such inhibitors, as not much is known about the often shallow and solvent exposed substrate-binding pocket. Furthermore, substrate-competitive inhibitors historically achieve only micromolar affinities for the kinase.[8,13,21,23] Through rational design and the use of a privileged scaffold, we designed, synthesized and evaluated a series of inhibitors containing a biphenyl side chain showing great potential in the development of an optimized substrate-competitive c-Src inhibitor.

2.3: The Biphenyl Library

The biphenyl moiety was hypothesized to be a promising scaffold as it is found in 4.3% of all molecular frameworks of known drugs and high throughput screening libraries.[5-7] Its advantageous size and shape allows for high-affinity binding to various pockets on diverse protein surfaces.[5-7] Additionally, this privileged scaffold provides a means for versatility through facile optimization. A library of 300 compounds, organized into three subgroups, containing the biphenyl moiety was synthesized. The average molecular weight of the compounds within the

library was 365.8. The first group investigated was substituted biphenylethylacetamides. Further, acetyl replacements of these substituted biphenylethylacetamides were synthesized and evaluated. The third subgroup was comprised of compounds more peptidic in nature; as they resembled N-acetyl substituted biphenyl amino acids. (**Figure 2.1**) This work was completed with help from Dr. Sonali Kurup.

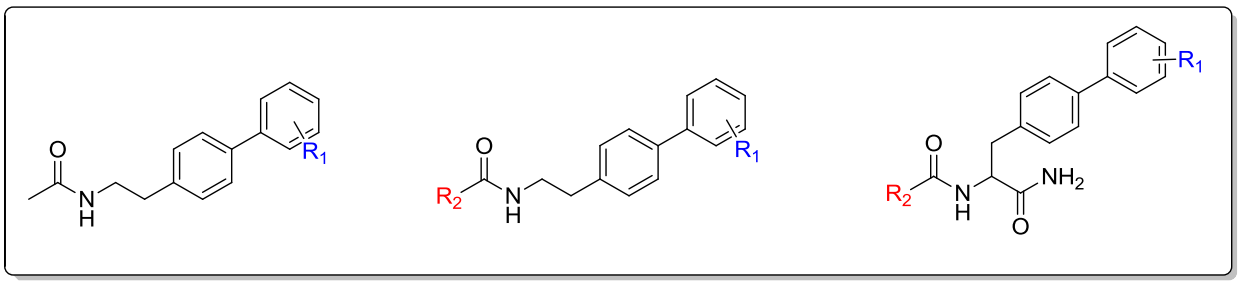

Figure 2.1: Common substructures of molecules within the biphenyl library

2.3.1: Top Ring Substitutions and Acetyl Replacements

In an effort to efficiently prepare compounds that would sufficiently probe the substrate pocket, the unsubstituted biphenylethylacetamide compounds could be easily optimized not only at the top ring, but also at the acetyl moiety. Therefore, the subsequent sub-library of compounds that was prepared not only contained top ring modifications, but also employed various replacements for the acetyl moiety.

The first group of compounds synthesized was the substituted biphenylethylacetamides prepared through Suzuki reactions involving various substituted phenyl boronic acids and acetylated 4-bromo(phenylethyl)amine. (**Figure 2.2**) Focusing primarily on the boronic acids available, a diverse set of electron-withdrawing groups as well as electron-donating groups were explored. These compounds would hopefully lend to the better understanding of the

tolerance and flexibility of the substrate binding pocket. Thus, this subgroup of the biphenyl library explored only modifications of the biphenyl top ring.

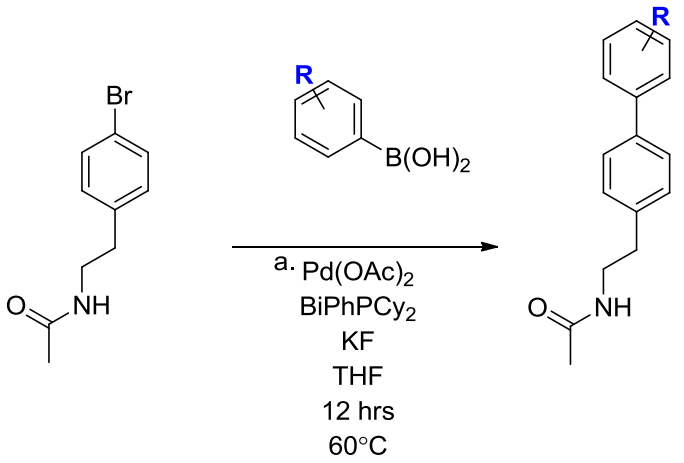

Figure 2.2: Synthesis scheme for the preparation of the substituted biphenylethylacetamides. [a.]This is the most common route to synthesize the compounds, however, synthetic optimizations were utilized when needed.

To further explore the size constraints of the substrate-binding pocket, acetyl replacements were employed on the substituted biphenylethylacetamides. These replacements varied from peptidic, such as amino acids, to substituted benzoyl chlorides and benzoic acids. The use of these diverse replacements allows for the better understanding of the substrate-binding pocket's flexibility.

2.3.2: N-acetyl Substituted Biphenyl Amino Acids

In order to instill diversity into the biphenyl library, we designed, synthesized and evaluated the third sub-group of the biphenyl library, the N-acetyl substituted biphenyl amino acids. These compounds investigated amino acid-like inhibitors of c-Src. Structurally, the sub-group of N-acetyl substituted biphenyl amino acids consists of the biphenyl appended to an amino acid that is 'capped' by an acetyl group, or an acetyl replacement at the N-terminus. Again, retaining a similar strategy to the biphenylethylacetamides, both top ring substitutions

and acetyl replacements were investigated to further probe the substrate-binding pocket's flexibility.

2.4: Evaluation

With such a large library, it was critical to devise an appropriate approach that carefully, yet efficiently concentrates the large number of compounds into a more manageable subset of compounds. Because of this, our lab developed a time-resolved fluorescence resonance energy transfer (TR-FRET) binding assay which allowed for the primary evaluation of the library in such a manner that those compounds that bind undesirably to the ATP-binding pocket could be easily identified and removed from any further screens. Simultaneously, the compounds were screened using the TR-FRET method for substrate-competitive binding. Secondarily, once a smaller subset of compounds of interest was generated, evaluating the affinity of the compounds using a pyrene substrate fluorescence assay proved more practicable.[24] The design and optimization of the TR-FRET assay was performed by Dr. Steven Bremmer.

2.4.1: TR-FRET Evaluation

In order to elucidate only those compounds with the propensity to bind in the substrate pocket of c-Src, the entire library was subjected to analysis by two separate antibody-based TR-FRET binding assays. (**Figure 2.3**) In order to better assess the mode of binding of the inhibitors, the library was incubated with one of two probes along with His-tag labeled c-Src protein and a Europium labeled His-tag antibody. The inhibitor's ability to out-compete the binding of an ATP-binding probe as well as a bivalent-binding probe was evaluated. The compounds of interest would then not affect the FRET signal measured by fluorescence of the ATP-binding probe, as they would not bind in the ATP pocket. However, the compound would not allow a FRET signal

to occur, as demonstrated by a decrease in fluorescence, when in the presence of the bisubstrate-binding probe. The inhibitor binds to the substrate pocket, thereby preventing the probe from binding to form a FRET pair. The inhibitors chosen from this initial screen did not compete with the ATP-binding probe, but out-compete the bisubstrate-binding probe greater than or equal to 50 percent. Consequently, fourteen compounds were carried through to a secondary screen using the pyrene substrate fluorescence assay. (**Figure 2.4**)

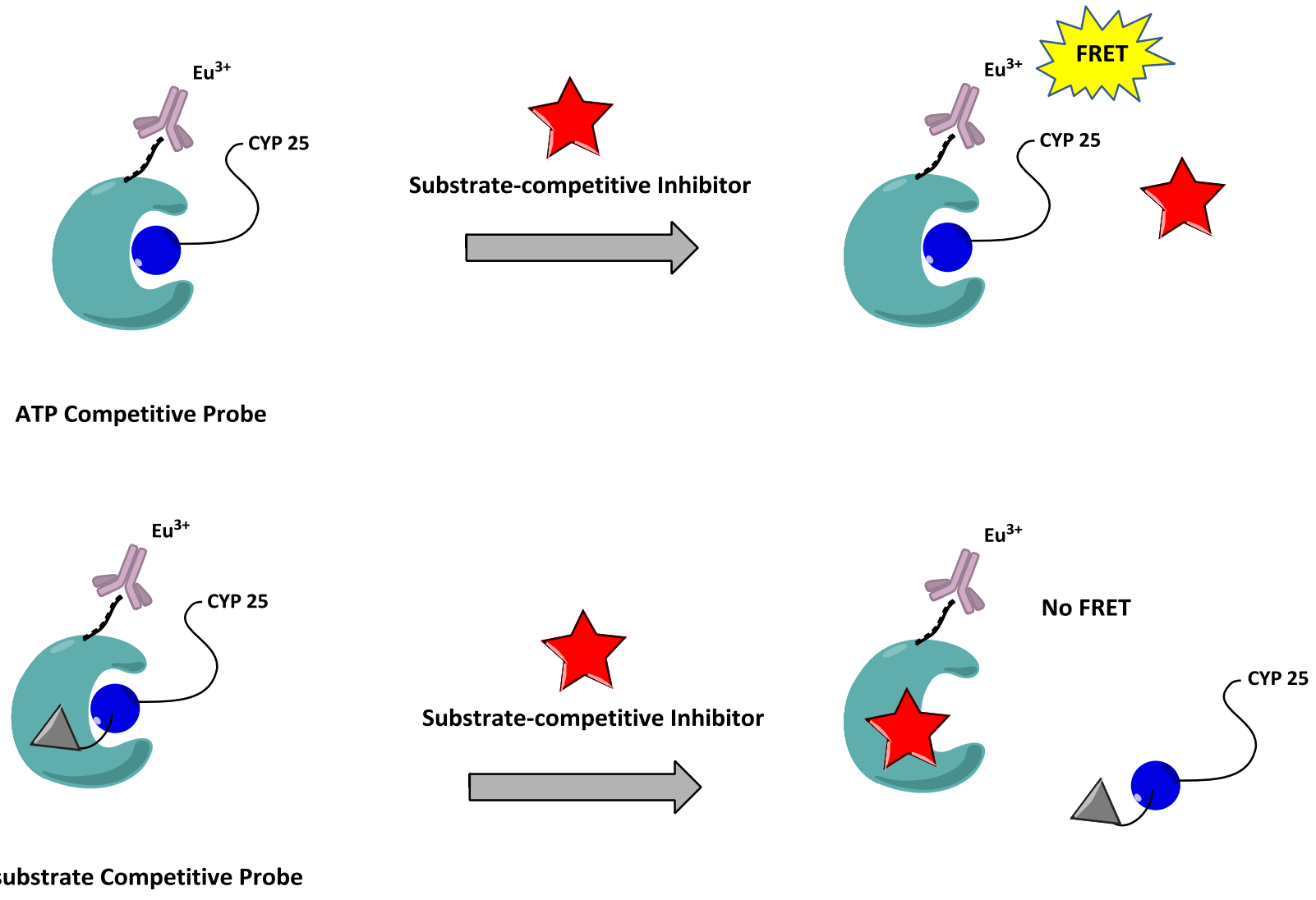

Figure 2.3: A schematic of the TR-FRET assay used as a primary screen to evaluate the biphenyl library

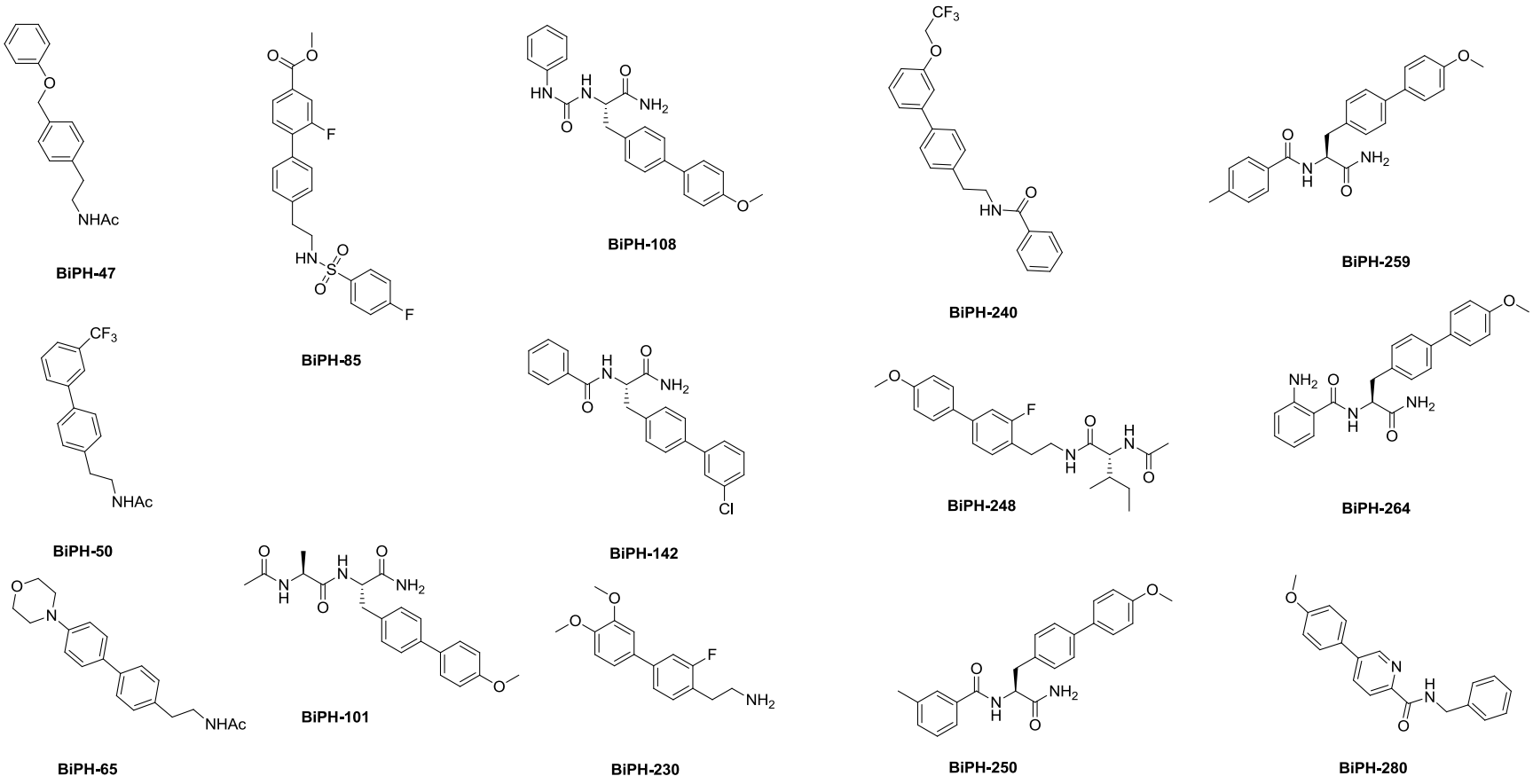

Figure 2.4: The 14 biphenyl compounds extracted from the TR-FRET primary screen

2.4.2: Pyrene Substrate Fluorescence Assay Evaluation

These fourteen compounds were then evaluated by a pyrene substrate fluorescence assay.[24] In this kinetic assay, a pyrene-containing c-Src substrate was incubated with the inhibitor and the kinase domain of c-Src while fluorescence was measured. The pyrene side chain and tyrosine side chain of the substrate are involved in a π-π stacking interaction which results in a quench of the ability of the pyrene to fluoresce. If the tyrosine is phosphorylated by the kinase, this interaction is disrupted and fluorescence is detected. A good inhibitor would then prevent the phosphorylation event and a decrease of fluorescence would occur. (**Figure 2.5**) The IC_{50} values of the fourteen compounds were obtained against c-Src including the kinase domain, three-domain wild type c-Src, and T338M c-Src (the gatekeeper mutation).

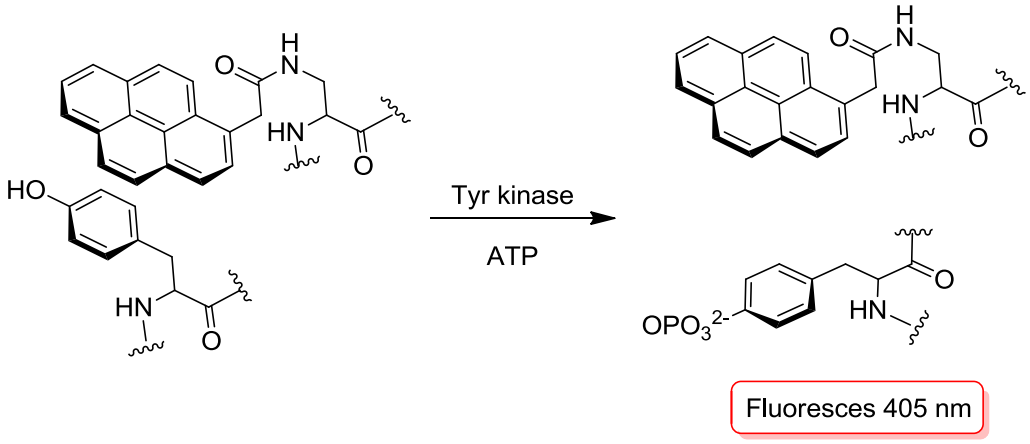

Figure 2.5: A schematic of the pyrene substrate fluorescence assay used as a secondary screen to evaluate the biphenyl library

2.4.2.1: Results

Utilizing the pyrene substrate fluorescence assay, the compounds were evaluated for efficacy against c-Src kinase domain (KD), the physiologically relevant c-Src three domain (3D), and the clinically observed mutation of the ATP-binding pocket, c-Src T338M. When evaluating a compound against the kinase domain alone, we hope to screen the compounds for the ability to bind to the substrate-binding pocket of the kinase. Whereas, evaluating the compounds against the entire protein aims to screen the compound in more physiological-like conditions with the hope that the compound can still inhibit the kinase. Furthermore, we also evaluated the compounds against the T338M c-Src mutation. This mutation is found in the hinge region between the N and C lobes of the PTK. This gatekeeper residue regulates the accessibility of a hydrophobic pocket in the back of the ATP-binding pocket of an active kinase. Resistance against known ATP-competitive inhibitors and therapeutics can originate with a mutation at this residue.[25-27] **Table 2.1** displays the IC_{50} values obtained for these screens.

BiPH	c-Src Kinase Domain Ave IC_{50}[a]	Std Dev	c-Src Three Domain Ave IC_{50}[a]	Std Dev	c-Src T338M Ave IC_{50}[a]	Std Dev
47	> 1000	-	298.3	52.3	> 1000	-
50	560.2	65.9	545.3	627.1	605.6	281.9
65	60.4	31.2	17.2	10.9	26.4	12.6
85	260.0	3.3	61.5	75.0	500.5	7.9
101	191.5	30.6	130.4	101.4	217.9	39.0
108	1147.3	440.9	NA[b]	NA[b]	> 1000	-
142	218.4	97.2	NA[b]	NA[b]	NA[b]	NA[b]
230	570.6	50.1	636.5	545.3	333.6	23.5
240	74.1	3.3	40.7	42.6	145.9	19.2
248	> 1000	-	> 1000	-	77.6	16.3
250	97.4	20.9	126.8	157.2	54.1	18.8
259	22.3	4.0	6.9	0.2	28.0	2.7
264	378.0	14.5	88.4	48.6	197.6	34.6
280	181.7	10.5	150.0	33.9	329.5	207.0

[a.] *All reported values in µM*
[b.] *Compound was not evaluated under these conditions*
Conditions: 1 mM ATP, 45 µM pyrene substrate, 30 nM enzyme

Table 2.1: Data from the screens against the fourteen compounds of interest

The structures of the highlighted compounds shown in **Table 2.1**, are shown below in **Figure 2.6**. **BiPH 65** is a substituted biphenylethylacetamide, while **BiPH 250** and **BiPH 259** are examples of the N-acetyl substituted biphenyl amino acid sub-group within the biphenyl library. Interestingly, both **BiPH 250** and **BiPH 259** are structural isomers, as **BiPH 250** is the 3-methylphenyl isomer and **BiPH 259** is the 4-methylphenyl isomer. Additionally, both compounds **BiPH 65** and **BiPH 259** have similar ligand efficiencies of about 0.100 kcal/mol/non H atoms. However, **BiPH 250** has a much lower ligand efficiency of 0.043 kcal/mol/non H atoms. Ligand efficiency has been previously used to serve as a means to evaluate and optimize

fragment or lead compound hits as it quantifies the ability of a compound to bind with relation to the non-hydrogen atoms.[28,29]

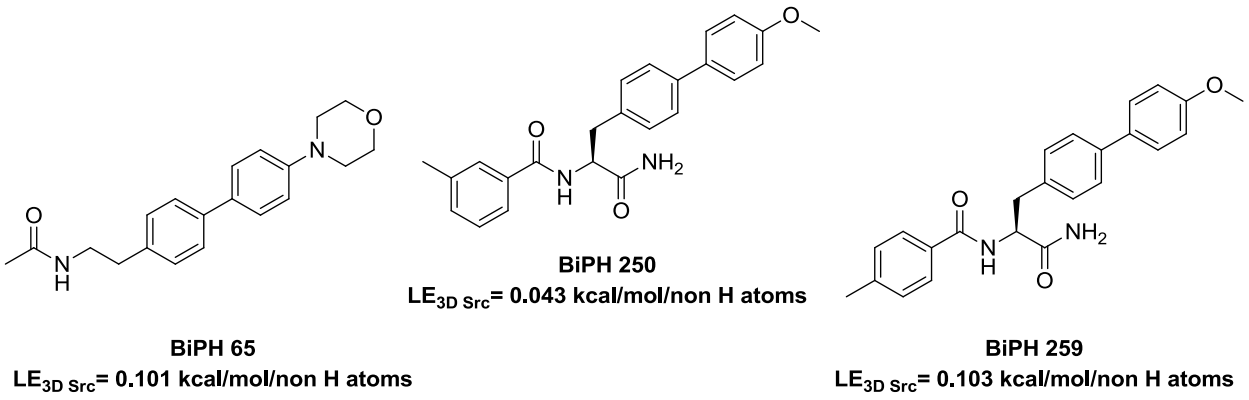

Figure 2.6: Compounds of interest from the secondary screen

Compounds **BiPH 65**, **BiPH 250**, and **BiPH 259** not only displayed IC_{50} values of interest for c-Src kinase domain, but they also inhibited the full three domain c-Src as well as the gatekeeper mutation. The three compounds of interest have affinities for the c-Src protein kinase domain (KD) and the full c-Src protein in the low, double digit micromolar range. Most notably, when evaluated against the T338M gatekeeper mutation of the c-Src protein, **BiPH 65** was 2-fold more potent (IC_{50} 26.4 μM). Both **BiPH 250** and **BiPH 259** also inhibit all three c-Src forms in the low double digit micromolar range. However, **BiPH 259** inhibits the three-domain c-Src with a single digit IC_{50} of 6.9 μM.

Controls using high and low ATP concentrations as well as high substrate concentrations were carried out with all three compounds against kinase domain c-Src. (**Table 2.2**) This evaluation provided us with a quick means to evaluate whether or not the compounds may be binding ATP competitive through the comparison of the changes in IC_{50} values.

BiPH	High [ATP][b] Ave IC_{50}[a]	Low [ATP][c] Ave IC_{50}[a]	High [substrate][d] Ave IC_{50}[a]	Normal Conditions Ave IC_{50}[a]
65	14.8	18.7	188.0	60.4
250	80.4	63.7	40.2	97.4
259	85.4	83.6	336.4	22.3

[a.] *All reported values in μM*
[b.] *5 mM ATP, 45 μM pyrene substrate*
[c.] *100 μM ATP, 45 μM pyrene substrate*
[d.] *500 μM pyrene peptide, 1 mM ATP*
[e.] *1 mM ATP, 45 μM pyrene substrate*

Table 2.2: Table of data obtained from control experiments using high and low [ATP] and high [substrate]

2.4.2.2: Lineweaver-Burk Analysis of compounds

As previously demonstrated, both compound **BiPH 65** and **BiPH 259** show some competition with substrate concentrations. This was illustrated by the increased IC_{50} values when the concentration of substrate was increased. **BiPH 250** seems to lack substrate-competitive binding to c-Src, and it is hypothesized that this compound may bind in an allosteric manner to c-Src. In order to further illustrate the modes of binding for the compounds, Lineweaver-Burk analysis of **BiPH 65** and **BiPH 259** was used. Such plots allow for further refinement of the binding mode as they suggest that compound **BiPH 259** binds in a mixed mode, being both ATP-competitive as well as substrate-competitive. (**Figures 2.7**, **2.8**) The data for these plots unfortunately do not follow a clear trend. This makes the characterization of the binding mode of compound **BiPH 259** difficult. However, the analysis of **BiPH 65**, shown below, strongly suggests the compound binds in the desired ATP-noncompetitive, substrate-competitive binding mode. (**Figures 2.9**, **2.10**) Additionally, as shown

in the K_M plots for this analysis provided in **Appendix A**, we notice that the K_M values remain constant, while the V_{max} values decrease slightly with respect to ATP. This trend is characteristic of non-competitive inhibition. With respect to the substrate plot, we notice that the K_M values increase, while the V_{max} remains constant. This trend is characteristic of competitive inhibition.

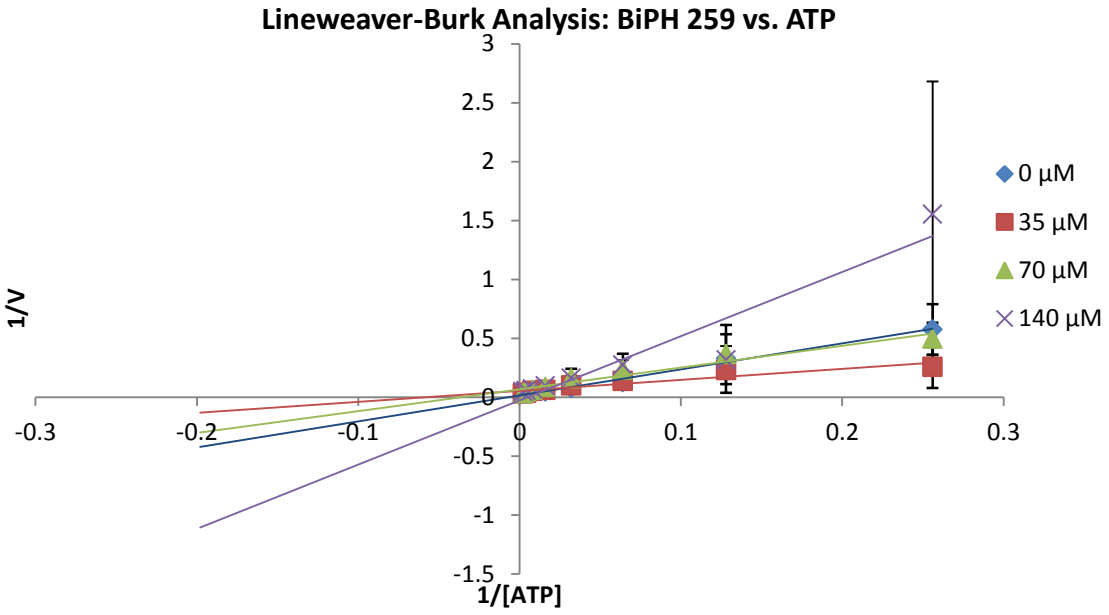

Figure 2.7: Lineweaver-Burk Plot of compound **BiPH 259** vs. ATP

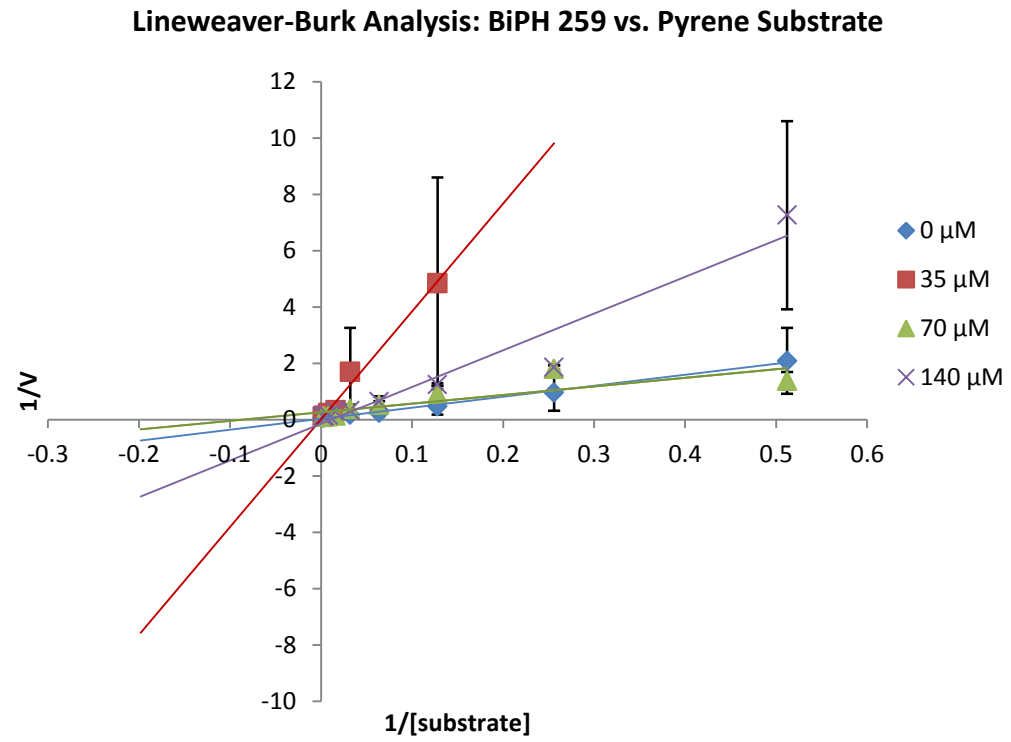

Figure 2.8: Lineweaver-Burk Plot of compound **BiPH 259** vs. pyrene substrate

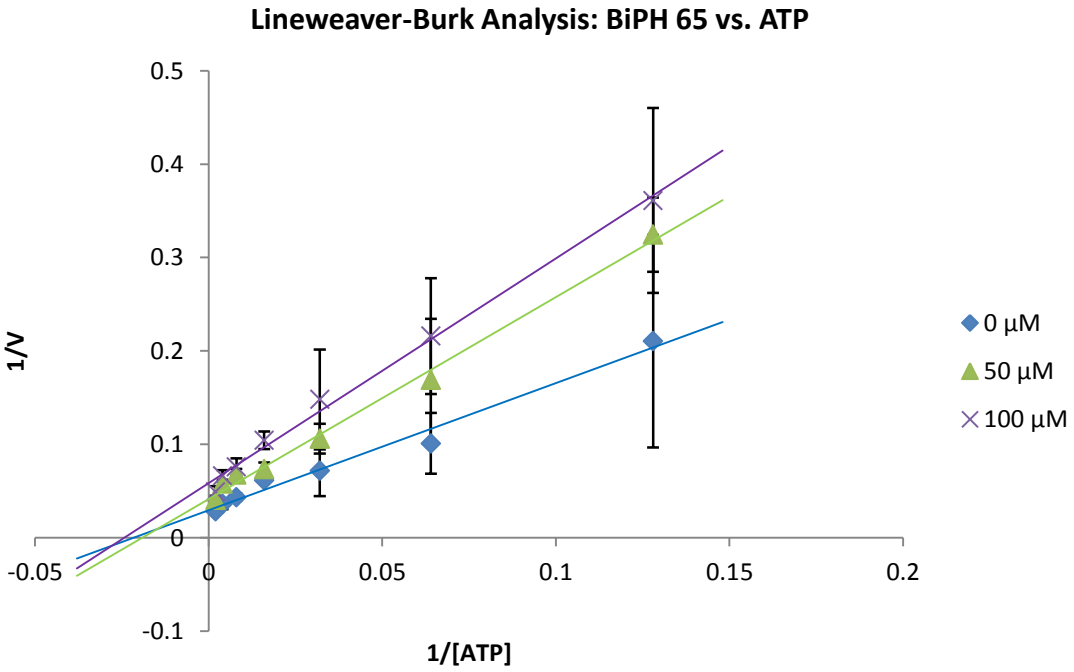

Figure 2.9: Lineweaver-Burk Plot of compound **BiPH 65** vs. ATP

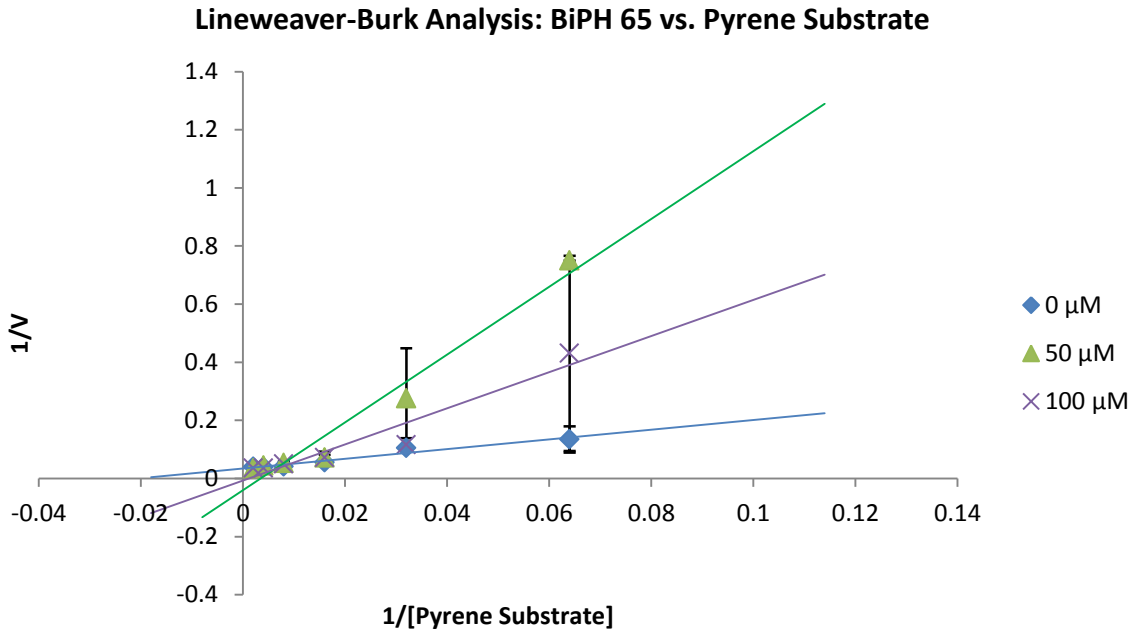

Figure 2.10: Lineweaver-Burk Plot of compound **BiPH 65** vs. pyrene substrate

Additional plots that explore the binding modes of compounds **BiPH 65** and **BiPH 259** are included in **Appendix D**. Please refer to this appendix for the Hanes analysis of these two compounds. We believe that the Hanes analysis for **BiPH 65** vs. ATP may further support the ATP-noncompetitive binding mode. However, the Hanes analysis for **BiPH 259** is less clear and consequently inconclusive.

The binding mode of **BiPH 65** was further characterized through the use of the TR-FRET assay. Full dose response curves were run with each probe, ATP-competitive and bisubstrate-competitive. Using the same principles as described with the primary screen, we predicted that **BiPH 65** would not out-compete the ATP-competitive probe and therefore, we would generate a FRET signal at any concentration of the inhibitor. Supporting this idea, the average EC_{50} of the compound when evaluated against the ATP-competitive probe is greater than 1000 µM. Conversely, we would then assume that **BiPH 65** would in fact out-compete the bisubstrate-

competitive probe and an EC_{50} curve would be generated. The average EC_{50} of the compound when evaluated against the bisubstrate-probe is 112.8 ± 41.9 µM.

2.4.2.3: Analogs of BiPH 65

In hopes to gain potency, analogs of **BiPH 65** were synthesized focusing on replacing the acetyl group. Benzyl, phenyl, phenyl urea, phenyl sulfonamide, and acetyl glycine replacements were employed. Regrettably, no analog displayed better potency for c-Src kinase domain than the parent compound. (**Figure 2.11**, **Table 2.3**)

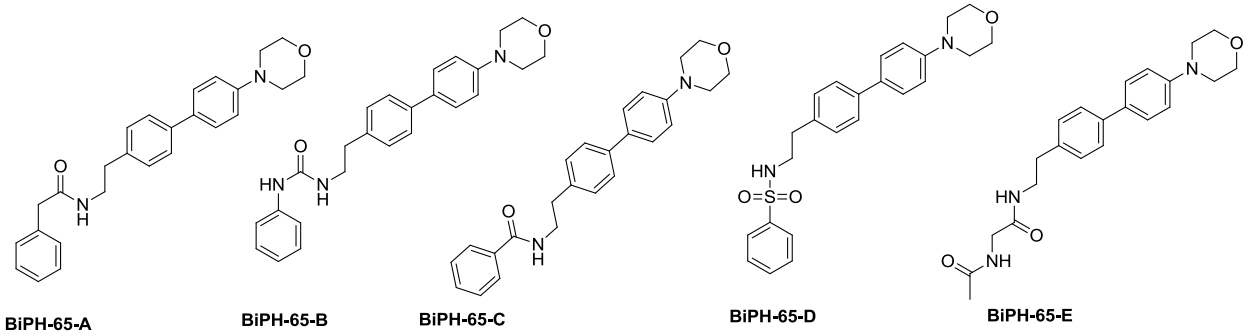

Figure 2.11: Analogs of **BiPH 65** prepared

Compound	c-Src KD Ave IC_{50}[a]
BiPH 65	60.4
BiPH 65-A	> 1000
BiPH 65-B	> 1000
BiPH 65-C	> 1000
BiPH 65-D	> 1000
BiPH 65-E	168.8

[a] All reported values in µM
Conditions: 1 mM ATP, 45 µM pyrene substrate, 30 nM enzyme

Table 2.3: IC_{50} values of **BiPH 65** analogs prepared

2.4.2.4: Molecular Dynamics Simulations

Molecular modeling simulations were performed on **BiPH 65** by Dr. Kelly L. Damm-Ganamet. These simulations further suggest an ATP-noncompetitive mode of binding as the compound appears to favor binding in a pocket formed by the activation loop of c-Src. Additionally, through binding at the activation loop, we hypothesized that the compound may stabilize the inactive conformation of the kinase. (**Figure 2.12**)

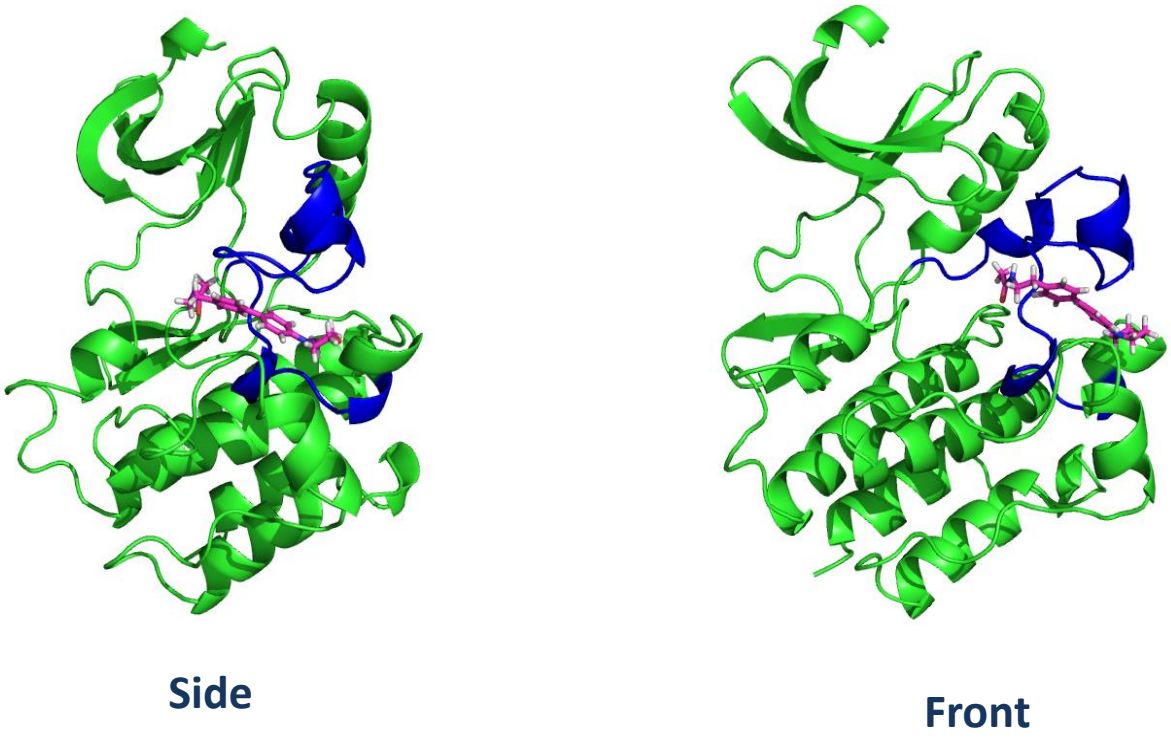

Figure 2.12: Molecular modeling of **BiPH 65** and c-Src. Shown in magenta, **BiPH 65** prefers binding in an ATP-noncompetitive mode as it appears to prefer binding to the inactive conformation of the kinase at the activation loop (blue).

To experimentally investigate this, **BiPH 65** was evaluated against the constitutively active, pY-416 c-Src. Assay data gleaned from this evaluation support the inability of the compound to bind the active conformation of c-Src (IC_{50} >1000 μM). The T338M c-Src data also support such a binding mode, as it is suggested that the gatekeeper mutation favors the inactive conformation of the protein and shown previously, **BiPH 65** is two-fold more potent for the gatekeeper than the kinase domain of c-Src.[26]

2.4.2.5: Selectivity of BiPH 65

In the rational design of kinase inhibitors, as mentioned above, an important property of the inhibitor is its ability to be selective for the kinase of interest as off-target kinase binding correlates with heightened toxicity effects. To investigate the selectivity of **BiPH 65** we evaluated its potency against two PTKs sharing significant sequence similarity with c-Src. The first, Hck, is a Src-family PTK that shares 72% sequence similarity, 59% sequence identity with c-Src.[30] The second, c-Abl, is not a member of the Src-family but shares 49% sequence identity and 68% sequence similarity with c-Src. The thought is that in utilizing such highly homologous proteins, if the compound was not selective for c-Src, it would bind with similar potency to these other PTKs. After evaluation with both of these PTKs it was discovered that **BiPH 65** did not inhibit either PTK (Hck IC_{50} > 500 μM, c-Abl IC_{50} > 500 μM) and therefore has selectivity for c-Src over c-Abl and c-Hck.

2.4.2.6: Cellular proliferation studies

Cellular proliferation studies were performed with **BiPH 65** using the HT-29, human colon carcinoma, cell line. Following a 72 hour exposure to the selective inhibitor, the 50%

growth inhibition value was 10.3 µM. (**Figure 2.13**) Therefore, **BiPH 65** is a compound capable of entering the cell and inhibiting cell growth.

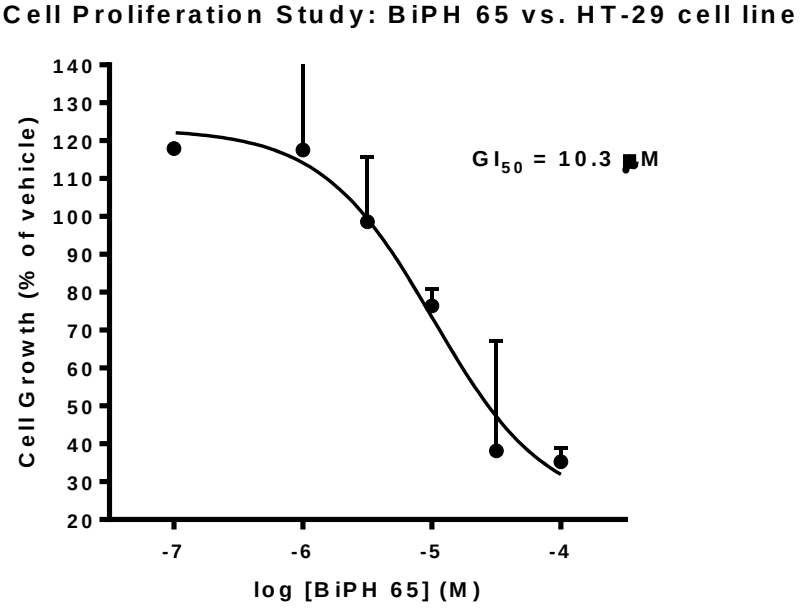

Figure 2.13: GI_{50} curve of **BiPH 65** and HT-29 cells

2.5: Conclusion

The design of substrate-competitive inhibitors of PTKs is a challenging task. Furthermore, the design of a selective substrate-competitive inhibitor is daunting as there is little to no structural data available for the substrate binding pocket of these kinases. Therefore, the rational design of such compounds can be executed by means of exploiting the use of privileged scaffolds often found in high throughput screening libraries, as they are known to be promiscuous binding fragments. We demonstrated that through the use of the privileged biphenyl scaffold we were able to design a compound that does not compete with ATP in binding to c-Src. Additionally, this compound is cell permeable and selective with regards to other highly homologous PTKs. **BiPH 65** is a c-Src selective, substrate-competitive inhibitor that

may prove to be a useful tool in probing the biological activity of the kinase as it favors binding to the inactive conformation of c-Src. We further outline the importance of the use of our newly developed, specialized TR-FRET screen. With this screen, we were able to easily and efficiently evaluate a large number of compounds for not only ATP-competitiveness, but also for substrate-competitiveness.

2.6: References

(1) Giamas, G.; Man, Y. L.; Hirner, H.; Bischof, J.; Kramer, K.; Khan, K.; Lavina-Ahmed, S. S.; Stebbing, J.; Knippschild, U. *Cell. Signal.* **2010**, *22*, 984.

(2) Fabbro, D.; Cowan-Jacob, S. W.; Möbitz, H.; Martiny-Baron, G. In *Kinase Inhibitors: Methods and Protocols*; Kuster, B., Ed.; Humana Press: 2012; Vol. 795, p 1.

(3) Grant, S. K. *Cell. Mol. Life Sci.* **2009**, *66*, 1163.

(4) Bikker, J. A.; Brooijmans, N.; Wissner, A.; Mansour, T. S. *J Med Chem* **2009**, *52*, 1493.

(5) Hajduk, P. J.; Bures, M.; Praestgaard, J.; Fesik, S. W. *J Med Chem* **2000**, *43*, 3443.

(6) Bemis, G. W.; Murcko, M. A. *J Med Chem* **1996**, *39*, 2887.

(7) Horton, D. A.; Bourne, G. T.; Smythe, M. L. *Chem. Rev.* **2003**, *103*, 893.

(8) Al-Obeidi, F. A.; Wu, J. J.; Lam, K. S. *Biopolymers* **1998**, *47*, 197.

(9) Al-Obeidi, F. A.; Lam, K. S. *Oncogene* **2000**, *19*, 5690.

(10) Knight, Z. A.; Shokat, K. M. *Chem. Biol. (Cambridge, MA, U. S.)* **2005**, *12*, 621.

(11) Morphy, R. *J Med Chem* **2010**, *53*, 1413.

(12) Melnikova, I.; Golden, J. *Nat. Rev. Drug Discovery* **2004**, *3*, 993.

(13) Cohen, P. *Nature Reviews: Drug Discovery* **2002**, *1*, 309.

(14) Manning, G. *Science* **2002**, *298*, 1912.

(15) Finn, R. S. *Ann. Oncol.* **2008**, *19*, 1379.

(16) Martin, S. G. *Nature Reviews: Molecular Cell Biology* **2001**, *2*, 467.

(17) Muthuswamy, S. K. *Nat. Med.* **2011**, *17*, 416.

(18) Zhang, S.; Huang, W.-C.; Li, P.; Guo, H.; Poh, S.-B.; Brady, S. W.; Xiong, Y.; Tseng, L.-M.; Li, S.-H.; Ding, Z.; Sahin, A. A.; Esteva, F. J.; Hortobagyi, G. N.; Yu, D. *Nat. Med.* **2011**, *17*, 461.

(19) Force, T.; Krause, D. S.; Van Etten, R. A. *Nat. Rev. Cancer* **2007**, *7*, 322.

(20) Zhang, J.; Yang, P. L.; Gray, N. S. *Nature Reviews: Cancer* **2009**, *9*, 28.

(21) Ye, G.; Tiwari, R.; Parang, K. *Curr. Opin. Investig. Drugs* **2008**, *9*, 605.

(22) Frame, M. C. *Biochemica et Biophysica Acta* **2002**, *1602*, 114.

(23) Songyang, Z.; Carraway, K. L.; Eck, M. J.; Harrison, S. C.; Feldman, R. A.; Mohammadi, M.; Schlessinger, J.; Hubbard, S. R.; Smith, D. P.; Eng, C.; Lorenzo, M. J.; Ponder, B. A. J.; Mayer, B. J.; Cantley, L. C. *Nature* **1995**, *373*, 536.

(24) Wang, Q.; Cahill, S. M.; Blumenstein, M.; Lawrence, D. S. *J. Am. Chem. Soc.* **2006**, *128*, 1808.
(25) Zuccotto, F.; Ardini, E.; Casale, E.; Angiolini, M. *J Med Chem* **2010**, *53*, 2681.
(26) Azam, M.; Seeliger, M. A.; Gray, N. S.; Kuriyan, J.; Daley, G. Q. *Nat. Struct. Mol. Biol.* **2008**, *15*, 1109.
(27) Krishnamurty, R.; Maly, D. J. *ACS Chem. Biol.* **2010**, *5*, 121.
(28) Kuntz, I. D.; Chen, K.; Sharp, K. A.; Kollman, P. A. *Proc Natl Acad Sci U S A* **1999**, *96*, 9997.
(29) Abad-Zapatero, C. *Expert Opinion on Drug Discovery* **2007**, *2*, 469.
(30) Courtneidge, S. A. In *Protein Kinases*; Woodgett, J. R., Ed.; IRL Press - Oxford University Press: New York, 1994, p 212.

Chapter 3:

The Investigation of 4-fluorotyrosine as a Suitable Scaffold to Prepare Substrate-Competitive c-Src Inhibitors

3.1: Abstract

The class of enzymes known as protein tyrosine kinases (PTKs) has been associated with disease states such as cancer, inflammation and diabetes when kinase activity is dysregulated. The non-receptor protein tyrosine kinase c-Src regulates diverse cellular processes that include cell survival, angiogenesis, motility, migration and invasion as well as cell proliferation. Discovered and classified in the 1970s, the c-Src proto-oncogene is characteristically overexpressed in various cancers such as breast, colon, pancreatic and ovarian.[1-3] Although regarded as the first PTK characterized, there is limited structural data that exists for c-Src pertaining to the substrate binding pocket.[2,4-8] This fact holds true for many PTKs. The end result is that the rational design of inhibitors is hindered, as not much is known about the often shallow and solvent exposed substrate-binding pocket. The main motivation behind our work rests in better understanding this PTK and, more specifically, garnering knowledge about the substrate-binding site of the kinase. We aim to develop peptidomimetic compounds that act not only as inhibitors of the kinase activity, but which also probe the substrate pocket to provide more structural information.

Previously published literature outlined the use of peptides containing fluorinated tyrosyl residues as substrate-competitive inhibitors of the insulin receptor kinase, a fellow PTK

family member.[9,10] Due to this documented success, an effort in our laboratory was made to further investigate this fluorinated tyrosyl residue with respect to the development of inhibitors of c-Src. Through stepwise modifications of the inhibitor peptide Ac-EEEI(4F)YGEFEA-NH_2, a library of (4F)tyrosine containing peptidomimetics were synthesized and evaluated as inhibitors for c-Src. A full range of SAR optimizations on the parent compound were synthesized and evaluated. Although initially very promising, these fluorinated peptidomimetics undesirably bound to c-Src in an ATP-competitive, substrate-noncompetitive mode.

3.2: Introduction

Protein tyrosine kinases (PTKs) are a family of 90 enzymes that catalyze the transfer of adenosine triphosphate's (ATP) γ-phosphate to the hydroxyl moiety of a tyrosine of the natural peptide substrate and thusly, initiate signaling cascades that are critical for cell functions including cell growth, cell division, and apoptosis.[11,12] Disease states arise when cellular events such as these are dysregulated by aberrant kinase activity. Examples of disease states correlated with this activity include cancer, rheumatoid arthritis, cardiovascular disease and neurodegenerative disease.[13] Because of this, PTKs provide an attractive therapeutic target and the 518 member protein kinase family consumes thirty percent of pharmaceutical research efforts toward the discovery of inhibitors to target and regulate such activity.[14-18]

In 1976, c-Src was determined to be the first proto-oncogene and only four years later the enzyme was classified as the first PTK.[2] Cell survival, angiogenesis, motility, migration and invasion, and cell proliferation are regulated by c-Src.[1,2] Furthermore, the over-expression of c-Src has been linked to cancers such as breast, colon, pancreatic, and ovarian.[1,2] Twenty percent

of HER2-positive breast cancers have been linked with c-Src over-expression, and thus, the excessive downstream activation of the PTK has been thought to be in part, the cause of HER2-positive breast cancer resistance to the drug, Herceptin.[19,20] The inhibition of c-Src would explore a new means by which to combat this clinically relevant resistance.

Current approved therapeutics aimed at regulating PTK activity are all ATP-competitive in nature. This class of inhibitors binds within the ATP pocket of the PTK and competes with cellular levels of ATP. Although extremely potent, these compounds often suffer from issues of selectivity being that the ATP pocket of each of the individual 518 protein kinases is highly conserved. As such, ATP-competitive inhibitors bind promiscuously, and this off-target binding can lead to issues with undesired toxicity.[17,21-23] Secondarily, these inhibitors must compete with concentrations of ATP as high as 10 mM within a cancer cell although kinases typically have an affinity for ATP only in the low micromolar range.[14,17,24] The excess of cellular ATP assures the saturation of the ATP pocket and thus, requires high affinity inhibitors in the low nanomolar to picomolar range in order to achieve *in vivo* activity. Lastly, common mutations of the ATP-binding pocket often lead to rapid drug resistance and loss of efficacy. Such clinically relevant mutations include the T338M mutation of c-Src.

Determined to design selective inhibitors of c-Src, we focused on the investigation of substrate-competitive inhibitors. Unlike the ATP-binding pocket, the substrate-binding pocket is less conserved among PTKs. Unfortunately, there is little known structural knowledge existing about the substrate-binding pocket.[2,4-8] The shallow pocket is thought to be solvent exposed and most likely becomes more defined upon the binding of a substrate. By targeting the

substrate pocket, we strive to improve the selectivity of our inhibitors. Additionally, most natural substrates are found present in cells at or below their K_M values allowing for compounds that do not necessarily need low nanomolar potencies, but which may have low micromolar affinity for the kinase.[22,24,25] Notably, the common mutations that are found with ATP-competitive inhibitors could potentially be avoided as the inhibitor targets another pocket within the catalytic domain.

In order to explore the substrate-binding pocket, we began with peptidic substrates that bind to c-Src favorably. Upon elucidating such peptides, we aimed to replace the phosphorylatable hydroxyl moiety of tyrosine of the substrate with a non-phosphorylatable pharmocaphore which would, by design, inhibit the kinase activity. From there, truncation through a stepwise fashion would allow for the evaluation of small peptidomimetic inhibitor compounds. With this in mind, previous reports on the development of peptidic inhibitors for the PTK, insulin receptor kinase, utilized a (4F)tyrosyl residue and provided a foundation for this project.[9,10] Compared to tyrosine, the (4F)tyrosine and its derivatives have altered ionic and nucleophilic character of the phenolic moiety.[9] Further, a fluorine atom is only slightly larger than a hydrogen atom and therefore, significant steric interference should not be observed. Due to this, the inhibitor would mimic the natural substrate, but would not allow for phosphorylation.[9] Using the insulin receptor kinase (4F)tyrosine inhibitor model, we set out to develop peptidomimetic inhibitors of c-Src that would desirably bind at the substrate pocket. Peptidomimetic compounds are thought to be able to bind similarly to the kinase target as the larger peptide in addition to providing a higher proteolytic stability and a higher bioavailability than the natural peptide.[26]

3.3: Initial studies

Determined to develop a substrate-competitive inhibitor, our foundation for compound design rested with a known c-Src substrate sequence. The binding affinity (K_M) for the c-Src optimal substrate peptide sequence, Ac-EEEIYGEFEA-NH_2, is 34 ± 8 μM. Replacing the tyrosine in this sequence with a (4F)tyrosine residue, the resulting peptide (Ac-EEEI(4F)YGEFEA-NH_2) was synthesized via standard Fmoc solid phase peptide synthesis (SPPS) methods on Rink amide resin using microwave-assisted peptide coupling. (**Figure 3.1**)

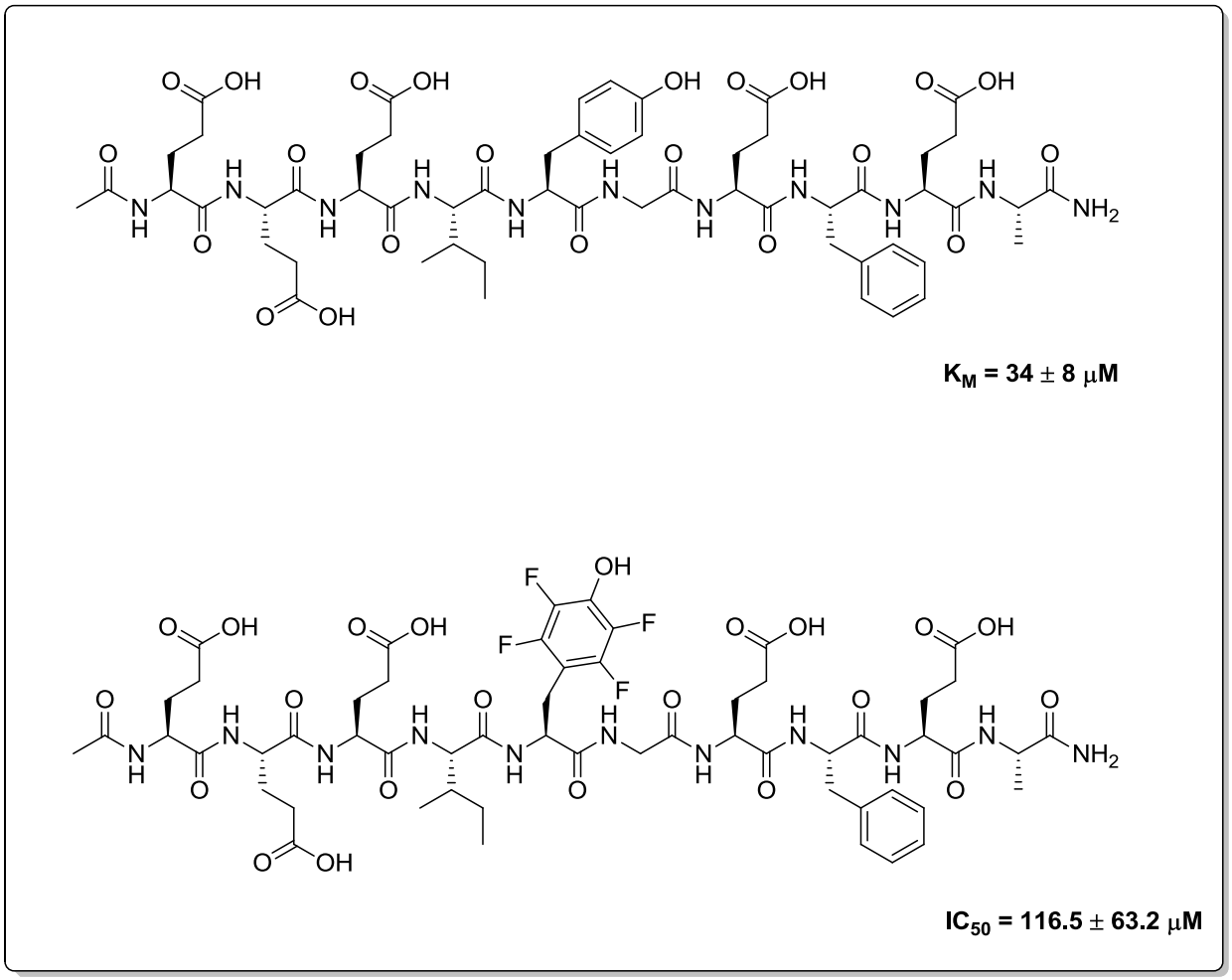

Figure 3.1: (Top) The structure of the c-Src optimal peptide, Ac-EEEIYGEFEA-NH_2. (Bottom) The structure of the Ac-EEEI(4F)YGEFEA-NH_2 inhibitor peptide.

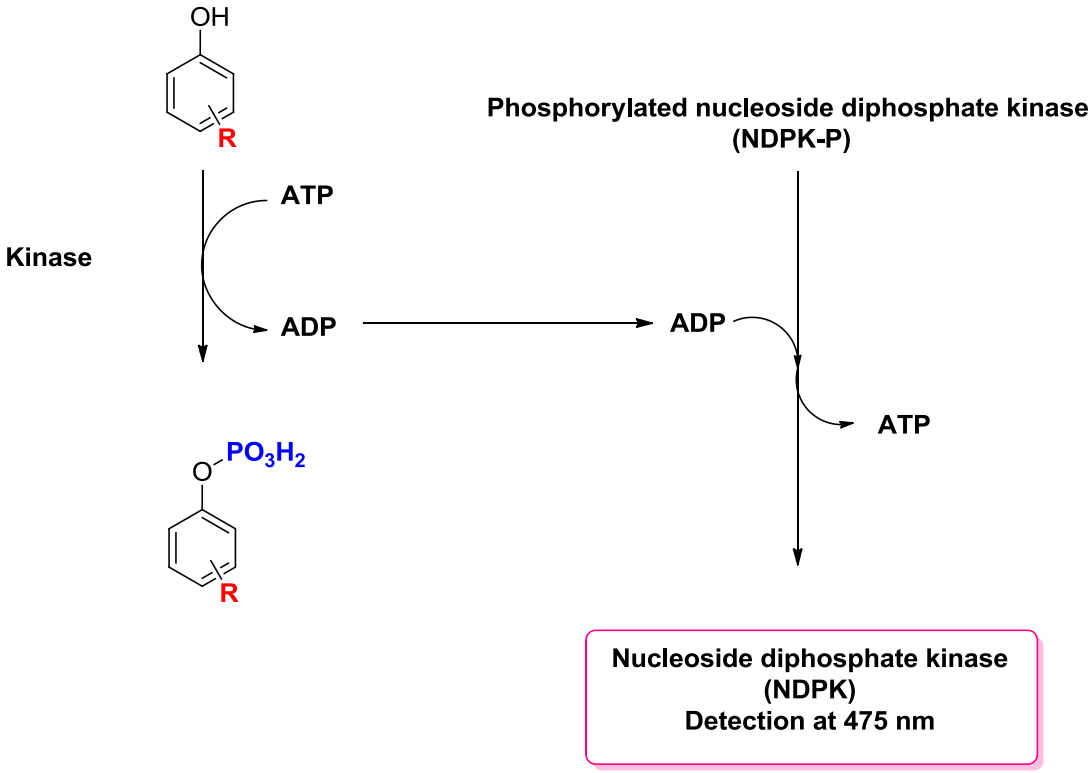

Figure 3.2: A schematic of the nucleoside diphosphate kinase assay (NDPK)

This potential inhibitor peptide sequence was first evaluated using a nucleoside diphosphate kinase assay (NDPK).[27] (**Figure 3.2**) This coupled fluorescence-based assay incorporates the use of a phosphorylated nucleoside diphosphate kinase bound to a fluorescent cumerin (NDPK~P). As the kinase uses ATP to phosphorylate the substrate, ADP is produced. This ADP binds to NDPK~P, the phosphate is transferred to ADP, producing ATP and a measureable decrease in fluorescence is observed and quantified as enzyme activity.[27] The data gleaned from this study suggest that the tetrafluorotyrosine containing peptide does not become phosphorylated by c-Src as no fluorescence is observed correlating to a lack of enzyme activity. (**Figure 3.3**)

Since the data suggest that the tetrafluorotyrosine containing peptide does not become phosphorylated, the peptide was evaluated as an inhibitor using the pyrene substrate fluorescence assay.[28] This assessment demonstrated that Ac-EEEI(4F)YGEFEA-NH_2 inhibits c-Src with an IC_{50} of 116.5 ± 63.2 µM. (**Figure 3.4**) With these encouraging results in our hands, we aimed to begin work in the design of small tetrafluorotyrosine containing peptidomimetic compounds. These initial studies were performed by Meghan E. Breen in our laboratory.

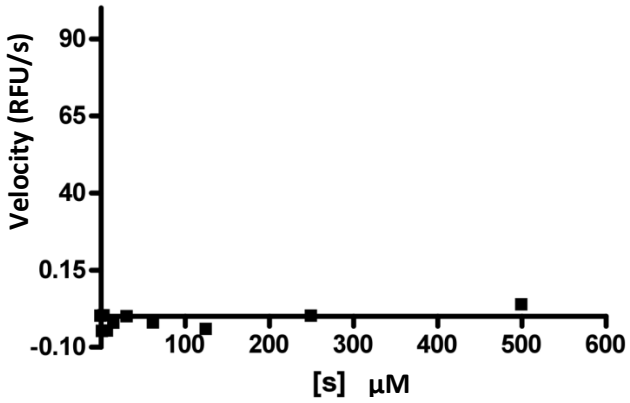

Figure 3.3: NDPK assay results evaluating Ac-EEEI(4F)YGEFEA-NH_2 against c-Src, illustrates a lack of phosphorylation by c-Src as no fluorescence is observed.

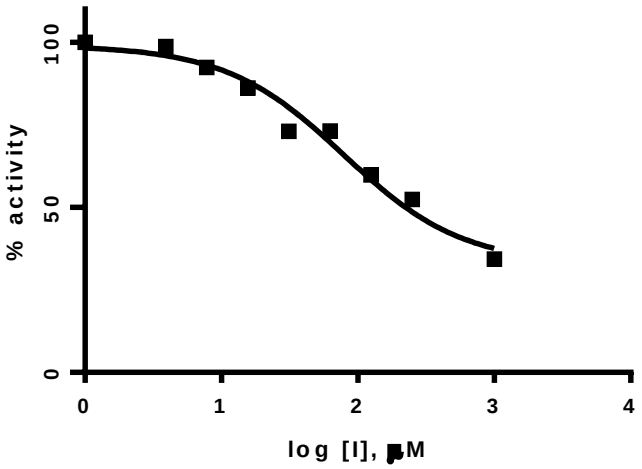

Figure 3.4: Pyrene substrate assay results evaluating Ac-EEEI(4F)YGEFEA-NH_2 against c-Src. IC_{50} 116.5 ± 63.2 µM

3.4: Library Generation

Focusing on our initial studies, we began with the truncation of the peptide to a single residue, Fmoc-4F-Tyrosine-OH. This amino acid was synthesized via reported synthetic methods shown in **Figure 3.5**.[29] The allyl group was removed as the last step of the synthesis of the compound. The preliminary library would focus on the optimizations of the C-terminus, while retaining the Fmoc N-terminus protecting group. The second library would explore Fmoc replacements of the tetrafluorotyrosine residue. Our evaluations show that these compounds would prove to be not very potent. Thus, in the final group of compounds prepared, we utilized solid phase peptide synthesis techniques to quickly investigate optimizations on the best Fmoc replacement, the phenyl urea, on a carboxylamide amino acid scaffold.

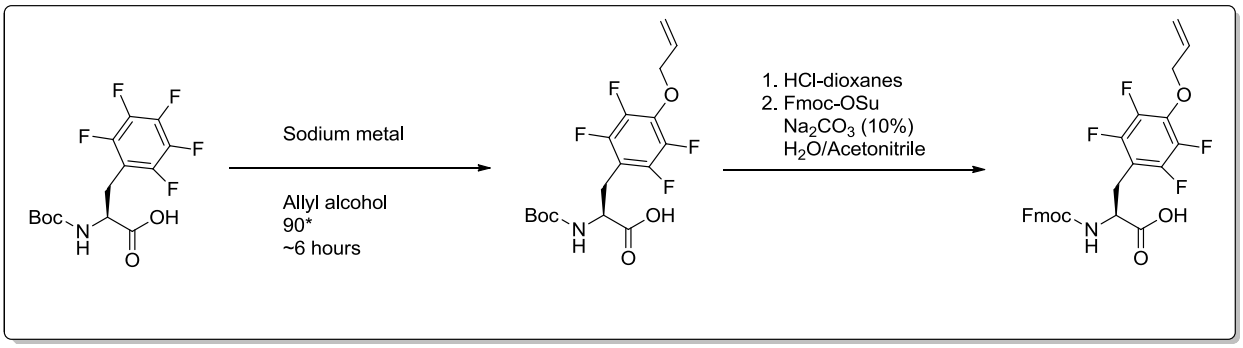

Figure 3.5: Preparation of the allyl protected Fmoc-(4F)Tyrosine-OH amino acid

3.4.1: C-terminus Optimization

The C-terminus optimization series numbered 3 compounds in total. We aimed to append an easily modified moiety to the parent carboxylamide compound. Thus, we evaluated the parent compound (**IV-sms-93**), a phenyl substitution (**IV-sms-80**), and lastly a benzyl substitution (**IV-sms-89**). (**Figure 3.6**)

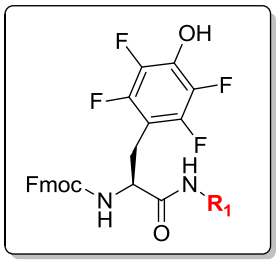

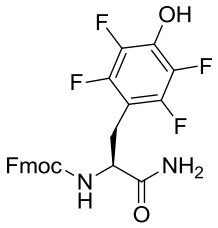

IV-sms-93
c-Src WT KD IC_{50}: 302.1 ± 141.8 μM

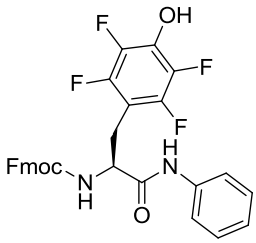

IV-sms-80
c-Src WT KD IC_{50} : 144.6 ± 21.2 μM

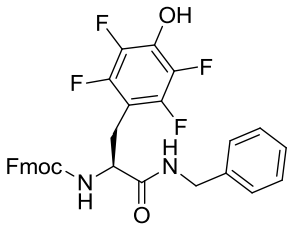

IV-sms-89
c-Src WT KD IC_{50} : 131.2 ± 22.3 μM

Figure 3.6: The C-terminus library of the (4F)Tyrosine compounds

The carboxylamide analog provided the least potent evaluation of this small library. As it stood, this compound (**IV-sms-93**) did not inhibit c-Src very well. However, both the phenyl and benzyl analogs proved to be of slightly more interest. Of these two analogs, the most potent analog was the benzyl C-terminal replacement, **IV-sms-89**. With an IC_{50} of 131 μM, it was hypothesized that further optimizations of both the benzyl group and the replacement of the Fmoc protecting group could provide a fully optimized and potent inhibitor of c-Src. Prior to performing a SAR study on the benzyl moiety, the next set of optimizations to be performed would be on the N-terminus of the compound, exploring replacements of the large Fmoc protecting group while preserving the newly discerned benzyl C-terminus optimization.

3.4.2: N-terminus Optimization

Retaining the C-terminus benzyl, a series of eight compounds was synthesized. These compounds would explore various replacements for the Fmoc protecting group. These analogs are illustrated in **Figure 3.7**.

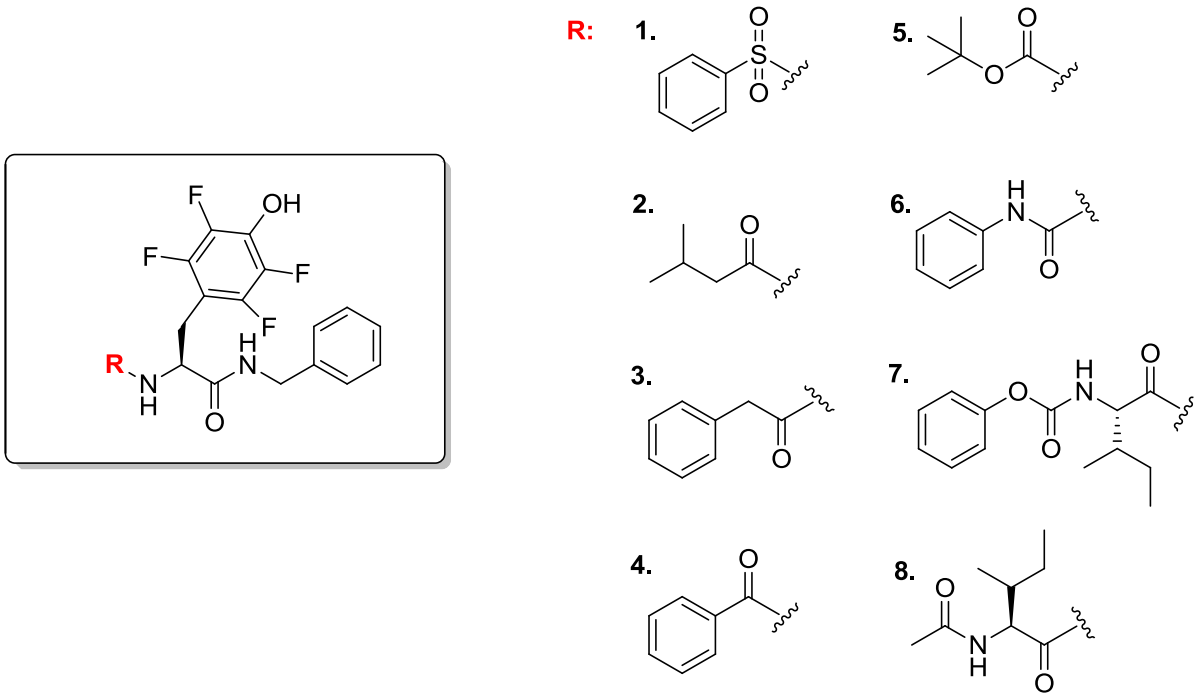

Figure 3.7: The N-terminus library of the (4F)Tyrosine compounds

In addition to a benzyl (**3**), phenyl (**4**), phenyl sulfonamide (**1**) and phenyl urea (**6**) replacements, we evaluated the potency of compounds that contained more peptidic substitutions by incorporating amino acid residues such as acetylated isoleucine (**8**) and CBZ protected isoleucine (**7**), as well as evaluating an isovaleryl replacement (**2**) and a BOC group replacement (**5**) of the Fmoc group.

Of these eight compounds, none displayed potency significantly greater than that of the Fmoc-containing parent compound (IC_{50}: 131 μM). These values are compiled in **Table 3.1**.

R	Ave IC_{50} (μM)
1	796 ± 184
2	318 ± 67
3	> 1000
4	346 ± 53
5	> 1000
6	**129 ± 25**
7	> 1000
8	> 1000

Table 3.1: Evaluation of N-terminus optimization library

Disappointingly, the analogs did not provide the increase in potency we had hypothesized. However, it should be noted that analog (**6**), the phenyl urea containing compound, did have similar potency to the parent compound as it inhibited c-Src with an IC_{50} of 129 ± 25 μM.

3.4.3: Carboxylamide Compounds

Although we could not find a suitable optimization within the N-terminus library, we wished to delve further into investigating the phenyl urea modification. In order to increase the ease of preparing this library, we focused only on modifying the N-terminal. We achieved this by appending the Fmoc-(4F)tyrosine-OH to Rink amide resin via standard Fmoc solid phase peptide synthesis methods. Once coupled and Fmoc deprotected, the resin was dried and split. Utilizing a diverse library of substituted phenyl isocyanates, we prepared a SAR library of sixteen carboxylamide compounds. (**Figure 3.8**) Each compound was cleaved from the resin, purified and evaluated using the pyrene substrate fluorescence assay.[28] The parent compound of this library is denoted by H in **Table 3.2**.

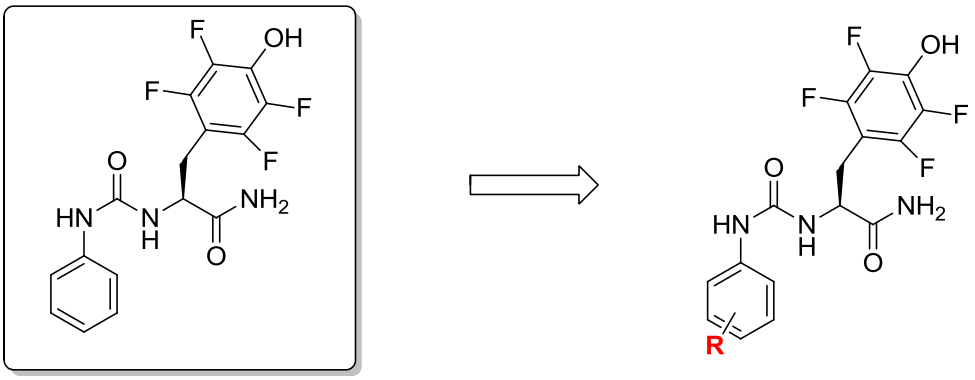

Figure 3.8: The carboxylamide library of the (4F)Tyrosine compounds

R	Ave IC_{50} (μM)
H	**119 ± 33**
2Cl	683 ± 96
3Cl	800 ± 133
4Cl	605 ± 123
2CF_3	1098 ± 138
3CF_3	687 ± 4
4CF_3	> 500
2F	414 ± 94
3F	**12 ± 4**
4F	681 ± 118
2OMe	> 500
3OMe	268 ± 69
4OMe	> 500
2Me	28 ± 4
3Me	159 ± 49
4Me	307 ± 59

Table 3.2: Carboxylamide analog library evaluation

Out of this library, we discovered one compound of particular interest. The (3F)phenyl urea analog was evaluated to have an IC_{50} of 12 ± 4 μM for c-Src. This was rather encouraging as

most analogs previously evaluated did not have potencies in the low double digit micromolar range. Additionally, because this compound is peptidic in nature, being an amino acid analog, we anticipated that it would bind in the substrate pocket in an ATP-noncompetitive, substrate-competitive desired binding mode with c-Src.

Further evaluation of the (3F)phenyl urea analog included a selectivity study. While our current assay protocol screens the compounds against the kinase domain of c-Src, we wanted to assess the ability of the compound to inhibit the physiological relevant c-Src protein. To do this, we tested the compound against the full three domain protein (c-Src WT 3D). Additionally, we wished to gather data pertaining to the compound's ability to inhibit a clinically relevant mutation of c-Src (c-Src T338M). Lastly, we would evaluate the (3F)phenyl urea analog against two PTKs that share high sequence similarity with c-Src, these PTKs are c-Abl and c-Hck. The data are expressed in **Table 3.3**.

Kinase	Ave IC_{50} (μM)
c-Src WT KD	12 ± 4 μM
c-Src T338M	> 500 μM
c-Src WT 3D	12 ± 0.4 μM
c-Abl	46 ± 18 μM
c-Hck	23 ± 2 μM

Conditions: 1 mM ATP, 45 μM pyrene substrate, 30 nM enzyme

Table 3.3: Lead compound evaluation

The (3F)phenyl urea analog inhibits the full three domain protein with a similar potency as it inhibits the kinase domain alone. However, the analog unfortunately does not inhibit the T338M gatekeeper mutant. Nevertheless, the (3F)phenyl urea analog does show some selectivity for c-Src over the other PTKs evaluated (4-fold over c-Abl, 2-fold over c-Hck).

In order to investigate the binding mode of the (3F)phenyl urea analog, we ran control experiments that would evaluate the compound at high and low concentrations of ATP and high concentrations of substrate. From these experiments, we were disappointed to find that the data suggest the analog may compete with ATP. As shown in **Table 3.4**, at high concentrations of ATP, the IC_{50} increases, while at low concentrations of ATP, the IC_{50} decreases. Interestingly, the IC_{50} of the compound decreased at high substrate concentrations. This data suggests that the compound is not substrate-competitive. In order to make a more informed judgment on the binding of the (3F)phenyl urea analog, Lineweaver-Burk analysis was performed.

Control Experiment	Ave IC_{50} (μM)
High ATP *(5 mM ATP, 45 μM pyrene substrate)*	16 ± 2 μM
Low ATP *(100 μM ATP, 45 μM pyrene substrate)*	5 ± 2 μM
High Pyrene Substrate *(1 mM ATP, 500 μM pyrene substrate)*	5 ± 3 μM
Standard Conditions *(1 mM ATP, 45 μM pyrene substrate)*	12 ± 4 μM

Table 3.4: Control experiment data

Much to our disappointment, Lineweaver-Burk analysis suggests that with respect to ATP, the compound shows a trend characteristic of mixed inhibition. These results appear to be inconclusive. The substrate analysis suggests a competitive binding mode. The plots are provided in **Figure 3.9** and **Figure 3.10.**

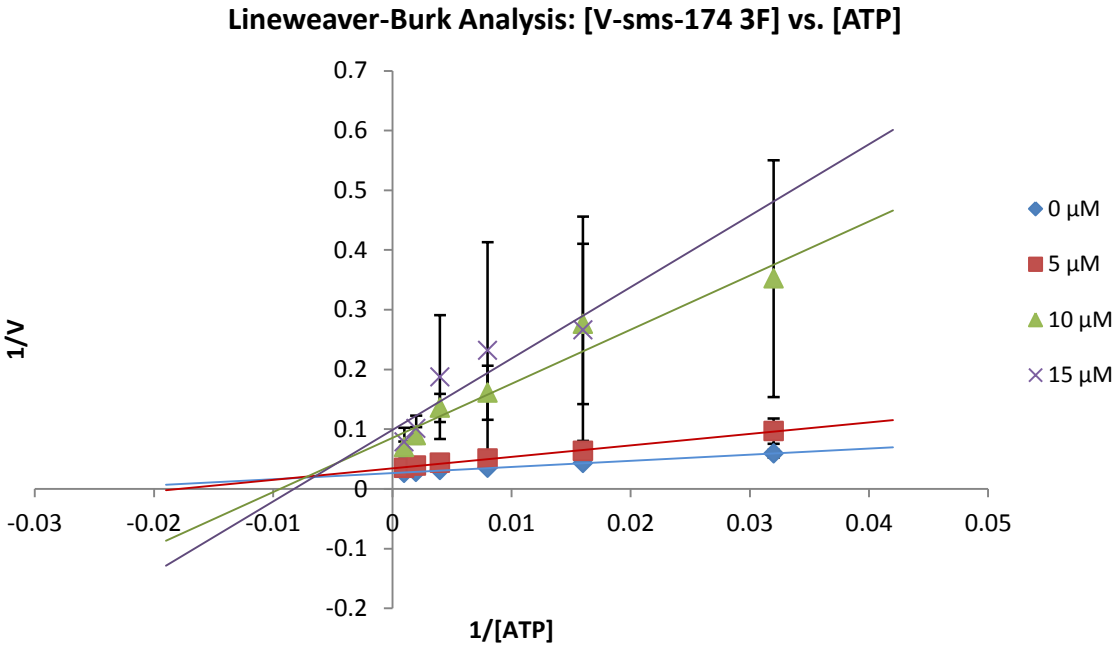

Figure 3.9: Lineweaver-Burk analysis of the (3F)phenyl urea analog against varying concentrations of ATP.

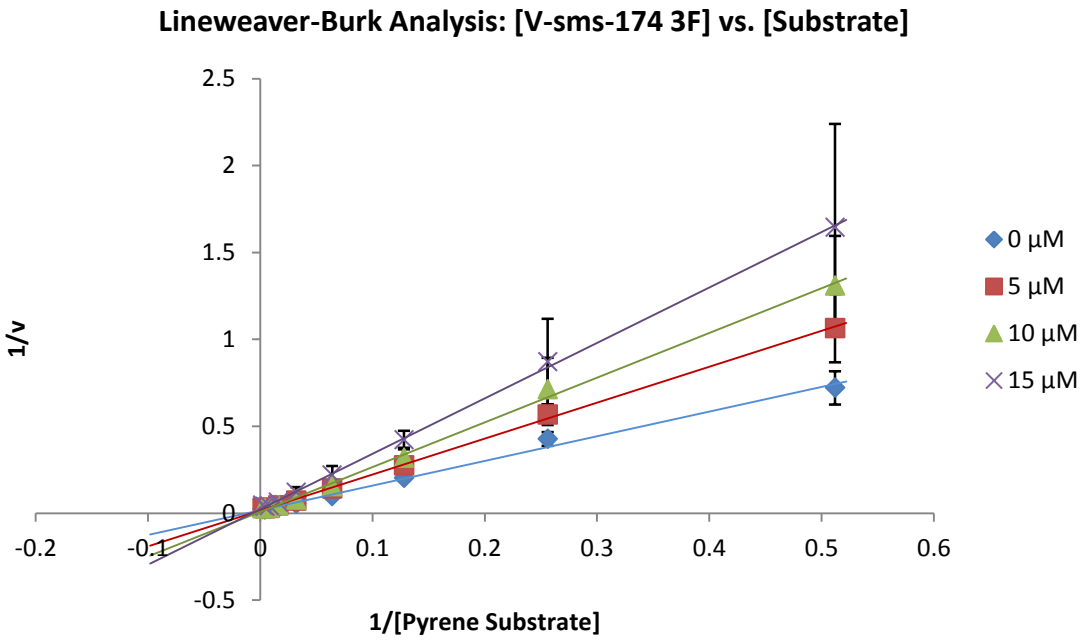

Figure 3.10: Lineweaver-Burk analysis of the (3F)phenyl urea analog against varying concentrations of pyrene substrate.

This mode of binding is further illustrated with K_M plots for these analyses, provided in **Appendix B**. As a means to better characterize the binding mode of the compound, we also analyzed the data using a Hanes plot. This data is provided in **Appendix D**. Much to our disappointment, this method of analysis provides us with more inconclusive results. With respect to compound **V-sms-174 3F**, we cannot yet conclusively characterize the binding mode.

3.5: Conclusions

Although initially promising, it can be deduced from this project that small peptidomimetic inhibitor compounds may not bind in the same manner as their larger peptide counterparts. Following the synthesis and evaluation of a diverse analog library utilizing a full

range of SAR optimizations of the parent compound, we arrived at a compound that had very promising IC_{50} values for a substrate-competitive inhibitor. Unfortunately, after control experiments and Lineweaver-Burk analysis, we were saddened to learn that we cannot easily interpret the binding mode of the compound.

Despite our unfortunate discoveries with regards to the design of a substrate-competitive tetrafluorinated tyrosine containing inhibitor, peptidomimetic inhibitors still serve as a general basis for the development of future substrate-competitive inhibitors. By taking a known substrate peptide and replacing the phosphorylatable residue with a non-phosphorylatable pharmacophore, an inhibitor peptide can be elucidated. Through the truncation of this then known inhibitor peptide, there is a great potential to arrive at small peptidomimetic compounds that have the likelihood of binding in the substrate pocket to potently inhibit the kinase target.

3.6: References

(1) Finn, R. S. *Ann. Oncol.* **2008**, *19*, 1379.
(2) Martin, S. G. *Nature Reviews: Molecular Cell Biology* **2001**, *2*, 467.
(3) Frame, M. C. *Biochemica et Biophysica Acta* **2002**, *1602*, 114.
(4) Kamath, J. R.; Liu, R.; Enstrom, A. M.; Lou, Q.; Lam, K. S. *J. Pept. Res.* **2003**, *62*, 260.
(5) Alfaro-Lopez, J.; Yuan, W.; Phan, B. C.; Kamath, J.; Lou, Q.; Lam, K. S.; Hruby, V. J. *J Med Chem* **1998**, *41*, 2252.
(6) Wu, J. J.; Phan, H.; Salmon, S. E.; Lam, K. S. *Letters in Peptide Science* **1996**, *3*, 309.
(7) Songyang, Z.; Carraway, K. L.; Eck, M. J.; Harrison, S. C.; Feldman, R. A.; Mohammadi, M.; Schlessinger, J.; Hubbard, S. R.; Smith, D. P.; Eng, C.; Lorenzo, M. J.; Ponder, B. A. J.; Mayer, B. J.; Cantley, L. C. *Nature* **1995**, *373*, 536.
(8) Brown, M. T.; Cooper, J. A. *Biochemica et Biophysica Acta* **1996**, *1287*, 121.
(9) Yuan, C.-J.; Jakes, S.; Elliott, S.; Graves, D. J. *J. Biol. Chem.* **1990**, *265*, 16205.
(10) Ablooglu, A. J.; Till, J. H.; Kim, K.; Parang, K.; Cole, P. A.; Hubbard, S. R.; Kohanski, R. A. *J. Biol. Chem.* **2000**, *275*, 30394.

(11) Al-Obeidi, F. A.; Wu, J. J.; Lam, K. S. *Biopolymers* **1998**, *47*, 197.
(12) Al-Obeidi, F. A.; Lam, K. S. *Oncogene* **2000**, *19*, 5690.
(13) Giamas, G.; Man, Y. L.; Hirner, H.; Bischof, J.; Kramer, K.; Khan, K.; Lavina-Ahmed, S. S.; Stebbing, J.; Knippschild, U. *Cell. Signal.* **2010**, *22*, 984.
(14) Knight, Z. A.; Shokat, K. M. *Chem. Biol. (Cambridge, MA, U. S.)* **2005**, *12*, 621.
(15) Morphy, R. *J Med Chem* **2010**, *53*, 1413.
(16) Melnikova, I.; Golden, J. *Nat. Rev. Drug Discovery* **2004**, *3*, 993.
(17) Cohen, P. *Nature Reviews: Drug Discovery* **2002**, *1*, 309.
(18) Manning, G. *Science* **2002**, *298*, 1912.
(19) Zhang, S.; Huang, W.-C.; Li, P.; Guo, H.; Poh, S.-B.; Brady, S. W.; Xiong, Y.; Tseng, L.-M.; Li, S.-H.; Ding, Z.; Sahin, A. A.; Esteva, F. J.; Hortobagyi, G. N.; Yu, D. *Nat. Med.* **2011**, *17*, 461.
(20) Muthuswamy, S. K. *Nat. Med.* **2011**, *17*, 416.
(21) Zhang, J.; Yang, P. L.; Gray, N. S. *Nature Reviews: Cancer* **2009**, *9*, 28.
(22) Ye, G.; Tiwari, R.; Parang, K. *Curr. Opin. Investig. Drugs* **2008**, *9*, 605.
(23) Force, T.; Krause, D. S.; Van Etten, R. A. *Nat. Rev. Cancer* **2007**, *7*, 322.
(24) Morin, M. J. *Oncogene* **2000**, *19*, 6574.
(25) Smyth, L. A.; Collins, I. *J. Chem. Biol.* **2009**, *2*, 131.
(26) Grauer, A.; König, B. *European Journal of Organic Chemisry* **2009**, *30*, 5099.
(27) Brune, M.; Corrie, J. E. T.; Webb, M. R. *Biochemistry* **2001**, *40*, 5087.
(28) Wang, Q.; Cahill, S. M.; Blumenstein, M.; Lawrence, D. S. *J. Am. Chem. Soc.* **2006**, *128*, 1808.
(29) Wang, F.; Luoheng, Q.; Wong, P.; Gao, J. *Org. Lett.* **2011**, *13*, 236.

Chapter 4:

The Identification of Small Molecule, Allosterically-binding c-Src Kinase Inhibitors through the use of a Screening Library.

4.1: Abstract

The non-receptor protein tyrosine kinase c-Src is known to regulate many diverse cellular processes including cell survival, angiogenesis, motility, migration and invasion, as well as cell proliferation. Discovered in the 1970s, the proto-oncogene is known to be over-expressed in breast, colon, pancreatic and ovarian cancers.[1-3] Our motivations behind this work were to elucidate new molecular scaffolds on which to develop substrate-competitive small molecule inhibitors of c-Src.

Using a 1000 compound-containing library obtained from Maybridge Chemical, we evaluated the compounds against the clinically relevant T338M c-Src 'gatekeeper' mutant kinase. This screen was performed using high ATP concentrations in hope of eliminating any fragments that may preferentially bind to the ATP binding pocket of the kinase, as we desire to elucidate structures that would favorably bind to the substrate binding pocket of the kinase. The data from this exploratory screen gleaned nine compounds that displayed favorable inhibitory activity in the biochemical assay for c-Src. The compounds of interest inhibited T338M c-Src at a value greater than or equal to 50 percent inhibition. This inhibition value was chosen as it was greater than three standard deviations from the mean percent inhibition value of the entire 1000 compound library evaluated. Of these nine compounds, three compounds

were further studied due to the predicted ease of modification and optimization of the fragment. Preliminary controls testing for an ATP-noncompetitive mode of binding found only one fragment: **[1]**. (**Figure 4.1**) This compound, 5-chlorobenzo[b]thiophene-3-carboxylic acid, inhibited the T338M c-Src 'gatekeeper' mutant with an IC_{50} of 7.9 μM and the wild type c-Src protein with an IC_{50} of 9.4 μM. Additionally, this compound exhibits selectivity for c-Src over other closely related PTKs (c-Abl, c-Hck). Lineweaver-Burk data supports an ATP-noncompetitive binding mode. However, substrate Lineweaver-Burk plots are more inconclusive, hinting at the possibility that **[1]** may bind in an allosteric pocket.

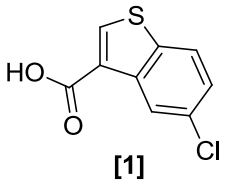

[1]

Figure 4.1: Maybridge fragment **[1]** pulled from the primary screen, 5-chlorobenzo[b]thiophene-3-carboxylic acid.

4.2: Introduction

Protein tyrosine kinases (PTKs) are a class of proteins totaling 90 different enzymes that functionally facilitate the transfer of the γ-phosphate of a molecule of adenosine triphosphate (ATP) to a substrate's phenolic tyrosine residue. This transfer initiates signaling cascades critical for important cell processes such as cell growth, cell division, and programmed cell death.[4,5] The interruption of these cellular events has been found to be influential in various disease states including cancer, rheumatoid arthritis, cardiovascular disease, as well as

neurodegenerative disease.[6] Due to their critical role in such processes, PTKs have been intensely studied and targeted. Pharmaceutical research devotes thirty percent of its efforts to the elucidation of therapeutics that target this superfamily of enzymes.[7-11]

Discovered in 1976, c-Src was deemed to be the first proto-oncogene and later in 1980, was further classified as a PTK.[1] c-Src is known to regulate various cellular processes such as survival, angiogenesis, motility, migration and invasion, as well as cell proliferation. c-Src has been found to be over-expressed in specific cancers including: breast, colon, pancreatic, and ovarian.[1,2] Attributable to its over-expression in twenty percent of HER2-positive breast cancers, c-Src's activity is thought to be a cause of Herceptin-resistant HER2-positive breast cancer.[12,13] As such, the inhibition of c-Src has been explored as a therapeutic means to combat this resistance.

The understanding of enzymatic activity is fundamental to the rational design of effective therapeutics in the current struggle to combat cancer. Therefore, the design of selective, small molecule inhibitors is imperative as these molecules can reveal information about the enzyme as they lend to the targeting of a specific protein without broadly affecting other closely related proteins. This selective probe can study the specific kinase in question, leading to a more precise investigation of the kinase activity. Selectivity of these small molecule probes is important, as off-target binding of inhibitors can lead to certain toxicity.[14]

To date, all FDA approved PTK inhibitors are ATP-competitive as they bind in the highly conserved ATP pocket of kinases. These inhibitors are highly potent and therefore are able to out compete the high concentrations of cellular ATP often found in cancer cells.[9] Although

these inhibitors bind with high affinity, they are often impaired by their lack of selectivity.[15] As a result, ATP-competitive inhibitors are promiscuous due to their ability to bind to many kinases downstream from the kinase of interest. These off-target effects are a significant reason for toxicity of such inhibitors.[10,14-17]

Our interest rests in the development of substrate-competitive inhibitors for c-Src. Such inhibition only involves the competition between a small molecule binding to the substrate-binding pocket of the kinase and the natural protein substrate.[10,17] As a general rule of thumb, the substrate-binding pocket is less conserved throughout the 518 member PK families than the ATP-binding pockets since kinases bind a number of protein substrates with unique sequences.[4,18] These protein-protein binding sites are often shallow and solvent exposed, producing difficult conditions with which to rationally design small, substrate-competitive molecules.[8] The lack of structural understanding of various PTKs and their substrate binding sites renders the rational design of substrate-competitive inhibitors much more difficult without the aid of a crystal structure to model possible inhibitory scaffolds. In order to begin work on developing a new set of substrate-competitive small molecule probes for c-Src, we chose to evaluate a fragment library sold by Maybridge Chemicals using a biased screen. Our motivations in performing this screen were to ultimately obtain a compound that has desirable inhibitory activity for c-Src which can be easily optimized to increase the potency of the inhibitor. The resulting compound, 5-chlorobenzo[b]thiophene-3-carboxylic acid, **[1]**, displayed interesting properties, as it was ATP-noncompetitive and data from Lineweaver-Burk analysis appeared to support the hypothesis that **[1]** binds allosterically to c-Src with an IC_{50} value of 9.4

± 2.8 μM (1 mM ATP, 45 μM substrate). Furthermore, from controls performed with highly similar PTKs, **[1]** displays promising selectivity for c-Src.

A true allosteric protein kinase inhibitor, or type IV inhibitor, binds to regions of the kinase not associated with the active site of the protein. These inhibitors regulate kinase activity through unique mechanisms particular to the specific kinase as they bind to regions distant from the ATP-binding pocket.[19,20] While the propensity for these compounds to have higher selectivity is unknown, these binding sites often tend to be more structurally distinct.[7,8,20] With regards to both substrate-competitive and allosteric inhibitors, there are promising advantages; however, their development is faced with many troubles. Lack of structural understanding as well as low micromolar affinities for the PTK are some of the obstacles that the design of such inhibitors faces. Here we desire to discuss our findings with **[1]**.

4.3: Initial studies - The Maybridge Library

The Maybridge Chemical Fragment Library is comprised of 1000 compounds with noted diversity of structure. This library satisfies the Rule of Three (Ro3) as all of the compounds have molecular weights less than or equal to 300, 3 or less hydrogen bond acceptors, 3 or less hydrogen bond donors, 3 or less rotatable bonds and a cLogP of 3 or less.[21] Through the use of high ATP concentrations, we anticipated hits obtained from this library would provide us with a molecular framework upon which to develop new substrate-competitive inhibitors as we hoped to eliminate ATP-competitive inhibitors from those fragments that are substrate-competitive in the library.

4.3.1: Preliminary Evaluation

The preliminary evaluation of the entire 1000 compound library was performed in our laboratory by Michael E. Steffey. Using the pyrene substrate fluorescence assay reported by Lawrence and coworkers,[22] the 1000 compounds were evaluated for inhibitory potency against the T338M c-Src kinase. This was performed by collecting single point percent inhibitory data for each compound at 50 μM. The motivations for using this particular c-Src gatekeeper mutation rest in clinically relevant mutations that lead to resistance of many tyrosine kinase inhibitors. Because of its position in the hinge region between the N and C lobes of the PTK, the gatekeeper mutation regulates the accessibility of a pocket in the hydrophobic back cavity of the ATP-binding pocket of an active kinase. Subsequently, a mutation of this residue from a threonine to a larger, more hydrophobic residue will change the size of this particular back pocket and therefore, can lead to resistance of known ATP-competitive inhibitors.[23-25] We wished to develop a substrate competitive inhibitor that not only inhibits the wild type c-Src kinase, but also those mutations that have been shown to be clinically relevant in the discovery of inhibitors and therapeutics. Additionally, the compounds were screened at high concentrations of ATP [5 mM] with hopes that this level of ATP would prevent the binding of those fragments with the susceptibility of binding in an ATP-competitive mode. **Figure 4.2** shows a histogram displaying the percent inhibition results from the initial screen of the Maybridge Library screen.

From these 1000 compounds, the nine compounds shown in **Figure 4.3** emerged with favorable percent inhibition values. These nine compounds represent 0.9% of the entire library.

The mean percent inhibition value was 1.25% and the standard deviation was 21.1% inhibition. We were interested in compounds that showed percent inhibition values that were three times the standard deviation (64.6%). However, in order to ensure that we evaluated every possible lead, we broadened our search and considered those compounds that had a percent inhibition of 50% or greater. Based off of their structures and high percent inhibition values, compounds **[1]**, **[2]** and **[3]** were chosen to be carried forward for additional screening. Although **[4]** was reported to have 75.9% inhibition, we concluded that there was minimal opportunity to further optimize the scaffold and therefore, we chose to forgo its further evaluation. Compounds **[1]**, **[2]** and **[3]** were hypothesized to provide interesting new scaffolds to begin design of new substrate-competitive inhibitors of c-Src. IC_{50} values of these compounds were obtained at both 5 mM and 1 mM ATP concentrations, 25 μM substrate concentration for the T338M c-Src kinase. This control would allow for in the further evaluation of the compounds to be binding in an ATP-competitive mode. Shown below in **Figures 4.4** and **4.5** are the IC_{50} curves of these compounds at both concentrations of ATP.

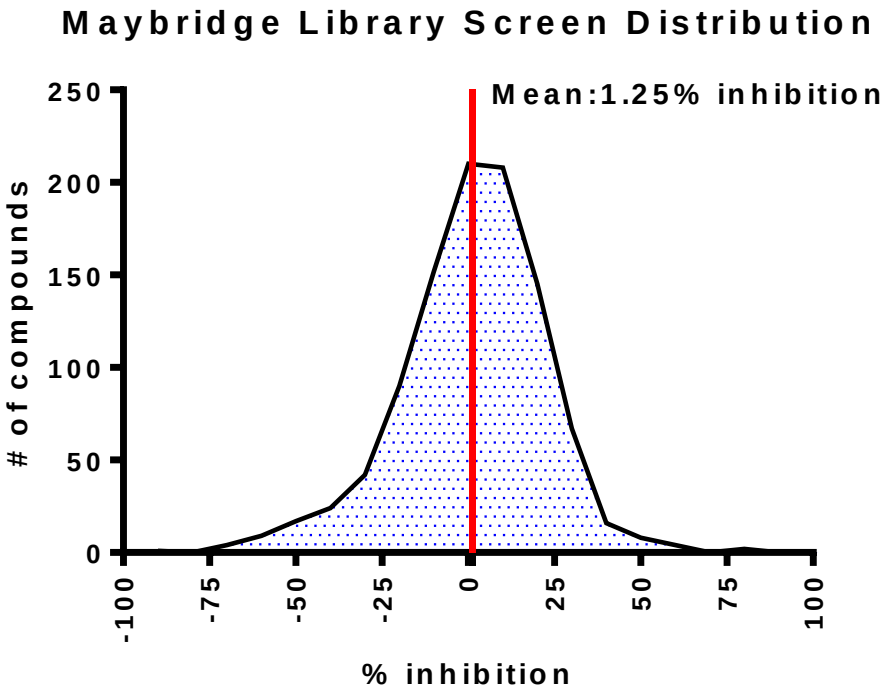

Figure 4.2: Histogram of the results from the Maybridge fragment library screen against T338M c-Src kinase. The compounds were assayed at 50 µM (n=1) against 30 nM kinase in the presence of 5 mM ATP and 25 µM pyrene substrate. Fluorescence was measured in kinetic mode and mean velocity of the reaction was calculated over the linear rate from 0.5 - 3 minutes of the reaction. Percent inhibition was calculated against the vehicle control (1% DMSO).

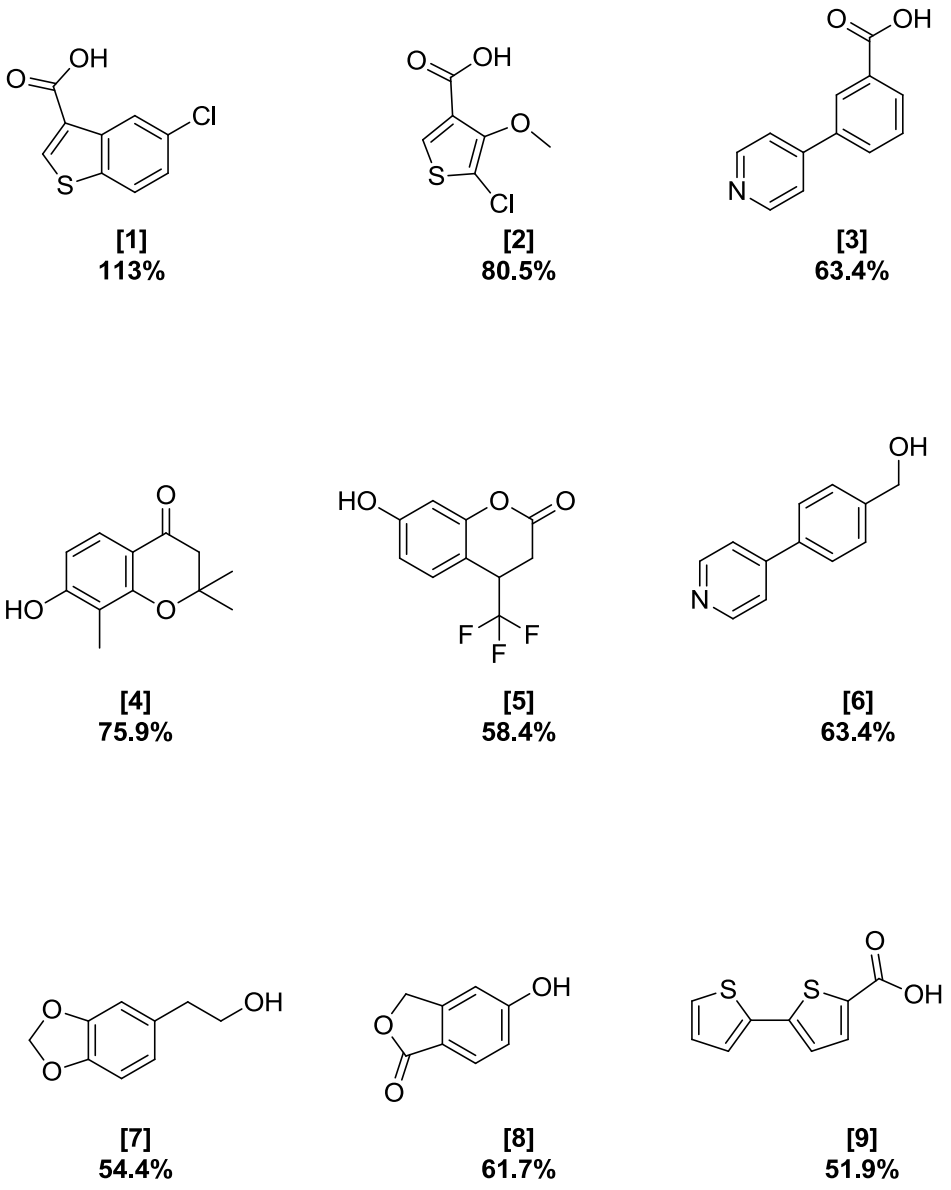

Figure 4.3: The nine compounds that were pulled from the initial screen of the Maybridge compounds and their percent inhibition values for T338M c-Src. Compounds **[1]**, **[2]**, and **[3]** were further evaluated in a secondary screen in which full IC_{50} curves were obtained for the compounds at varying concentrations of ATP.

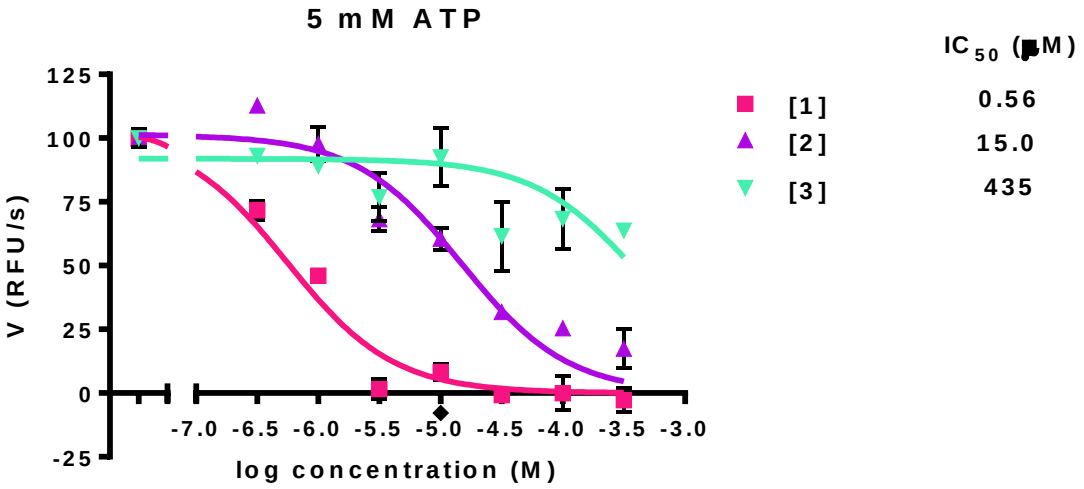

Figure 4.4: The IC_{50} curves of compounds **[1]**, **[2]** and **[3]** at high concentration of ATP [5 mM] and 25 µM substrate.

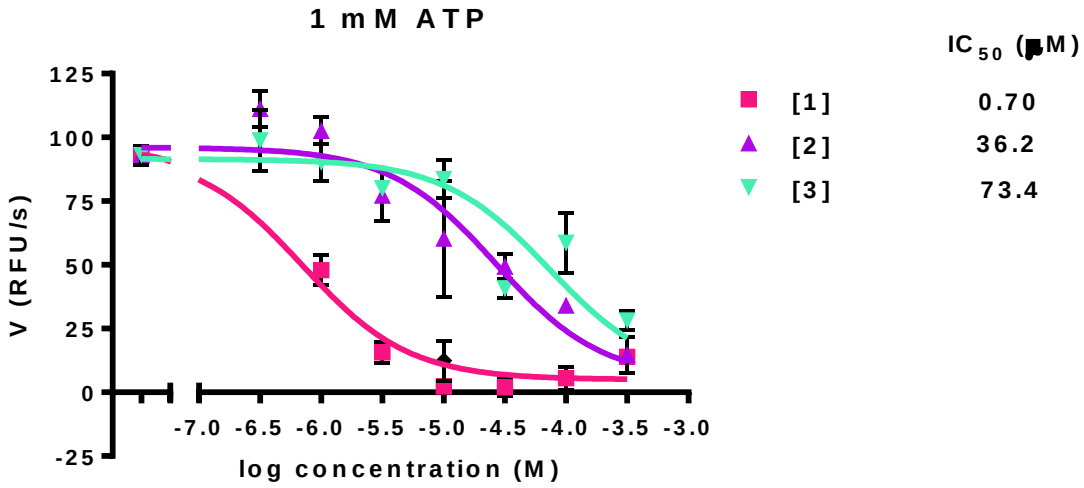

Figure 4.5: The IC_{50} curves of compounds **[1]**, **[2]** and **[3]** at a normal concentration of ATP [1 mM] and 25 µM substrate.

4.3.2: 5-Chlorobenzo[b]thiophene-3-carboxylic acid as a lead compound

The evaluation of compounds **[1]** and **[2]** implies that at varying ATP concentrations, the IC_{50} values of these compounds do not change significantly. This is a characteristic trend of non-competitive inhibition. However, the data for **[3]** appears to suggest that it is ATP-competitive, as the IC_{50} value increases significantly in the presence of high concentrations of ATP. Due to this, **[3]** was no longer of interest for further evaluation. With this, our focus shifted to the further evaluation of compound **[1]** as it is more potent than compound **[2]**. From this data, compound **[1]** was subjected to evaluation of IC_{50} values for the T338M c-Src kinase at varying substrate concentrations. (**Figure 4.6)**

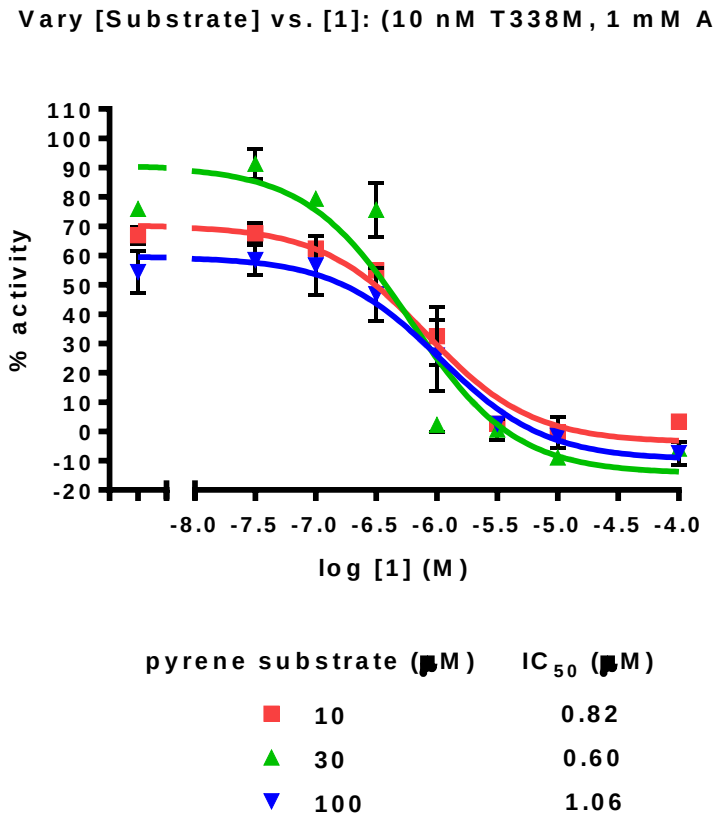

Figure 4.6: The IC_{50} curves of compound **[1]** against the T338M c-Src kinase with varying concentrations of substrate.

As seen above, when the concentration of the pyrene substrate is varied, the IC_{50} values of **[1]** do not change significantly. Unfortunately, this trend is characteristic of a non-competitive relationship between the inhibitor and substrate. Knowing this, further evaluation of the compound was performed with hopes to fully characterize the lead compound. Compound **[1]** was evaluated against c-Src wild type kinase domain (IC_{50} 9.4 μM, 1 mM ATP, 45 μM substrate) to confirm that the inhibitor not only could bind to the mutation but also the wild type protein. Since **[1]** inhibits both wild type c-Src as well as the gatekeeper mutant with low micromolar potency, the subsequent evaluation to perform would focus on the selectivity of the compound. In order to do this, we evaluated its potency against two PTKs that share significant sequence similarity with c-Src. As a Src-family PTK, c-Hck shares 72% sequence similarity and 59% sequence identity with c-Src.[26] c-Abl, while not a member of the Src-family, shares 49% sequence identity and 68% sequence similarity with c-Src. In utilizing such highly homologous proteins, we assume that if the compound was not selective for c-Src alone, it would also bind to these other PTKs with similar affinities. When evaluated against these PTKs, compound **[1]** failed to inhibit either kinase well as c-Src: c-Abl (IC_{50}: 195.0 μM) and c-Hck (IC_{50} > 125 μM).

4.3.2.1: Lineweaver-Burk Analysis

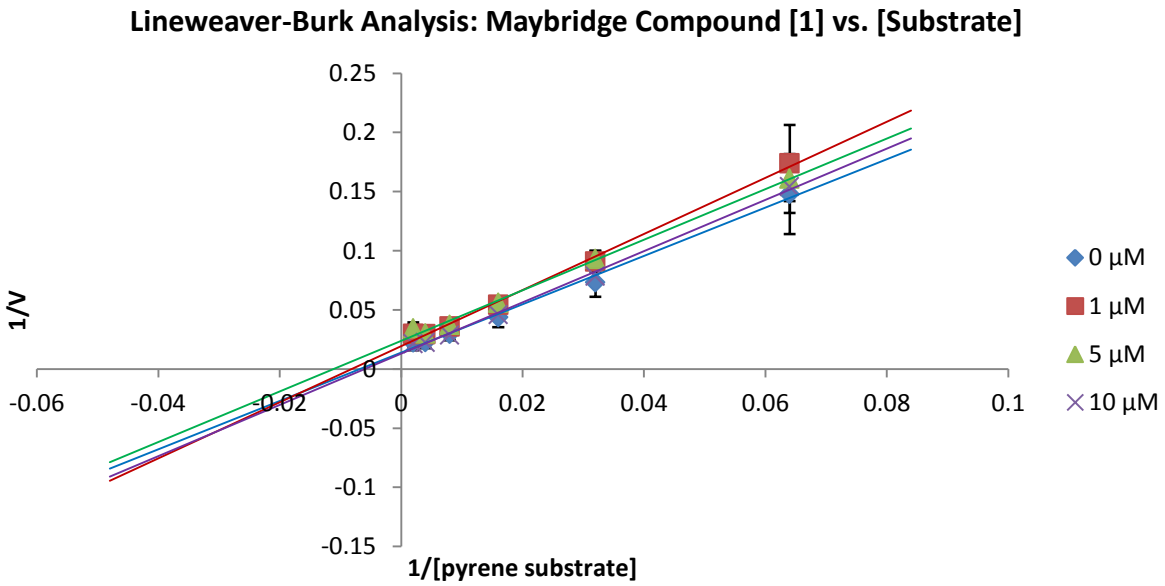

Figure 4.7: The Lineweaver-Burk analysis of **[1]** with respect to substrate.

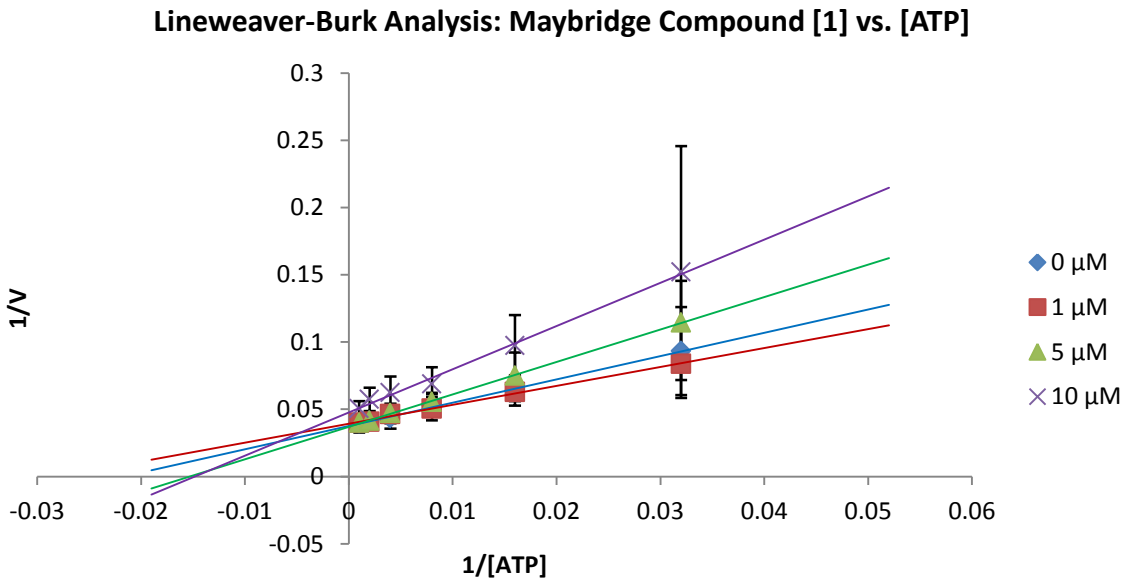

Figure 4.8: The Lineweaver-Burk analysis of **[1]** with respect to ATP.

A Lineweaver-Burk analysis was performed on the compound in order to better understand the binding mode of the compound. The data suggests that **[1]** may bind in an ATP-noncompetitive mode or possibly with mixed inhibition. Additionally, the substrate data is equally ambiguous with respect to compound **[1]**. (**Figure 4.7**, **Figure 4.8**) This is further illustrated with the K_M plots for these analyses, provided in section **Appendix C**. With hopes to better illustrate the binding mode of compound **[1]**, we evaluated the Lineweaver-Burk data using a Hanes analysis. This data is provided in **Appendix D**. Although the substrate data still is unclear, the ATP data may suggest an ATP-noncompetitive mode of binding. Overall, the ambiguity of this data leads us to believe that the compound is binding in an allosteric pocket on the protein.

4.3.2.2: Cellular proliferation studies and [1] analog library

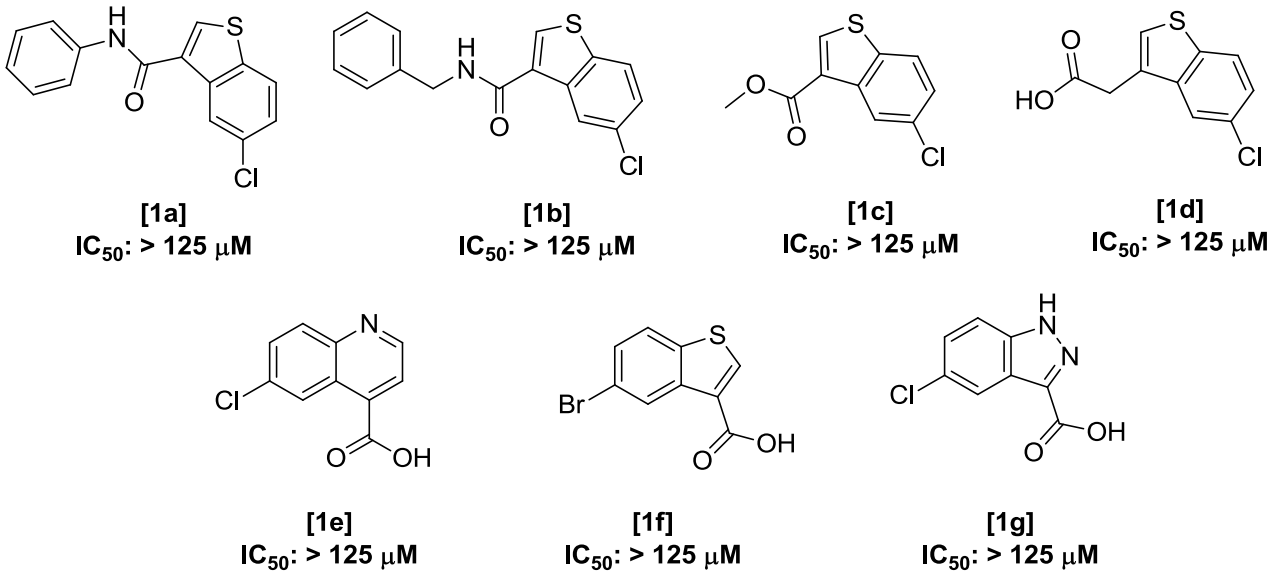

Figure 4.9: The **[1]** analog library with IC_{50} data

Cellular proliferation studies were performed on the compound in a human breast cancer cell line, SK-BR-3 cells. However, **[1]** did not show any cell growth inhibition. Despite the inability for this compound to enter the cell, a library of seven analogs were synthesized or purchased in order to refine the scaffold and arrive at a compound that would be able to permeate the cell membrane. The compounds (**Figure 4.9**) were initially evaluated against wild type c-Src; unfortunately, not one of the compounds displayed any inhibitory activity against the kinase.

Although not active in kinetic assays, the methyl ester analog of **[1]**, **[1c]**, was evaluated in a cellular proliferation study using SK-BR-3 cells. Following a 72-hour exposure to the cells, compound **[1c]** inhibited the growth of the SK-BR-3 cells with a GI_{50} of 22.5 μM. (**Figure 4.10**) It is assumed that **[1c]** acts as a prodrug of **[1]** as the methyl ester is cell permeable and become metabolized to the carboxylic acid containing **[1]** upon entering the cell.

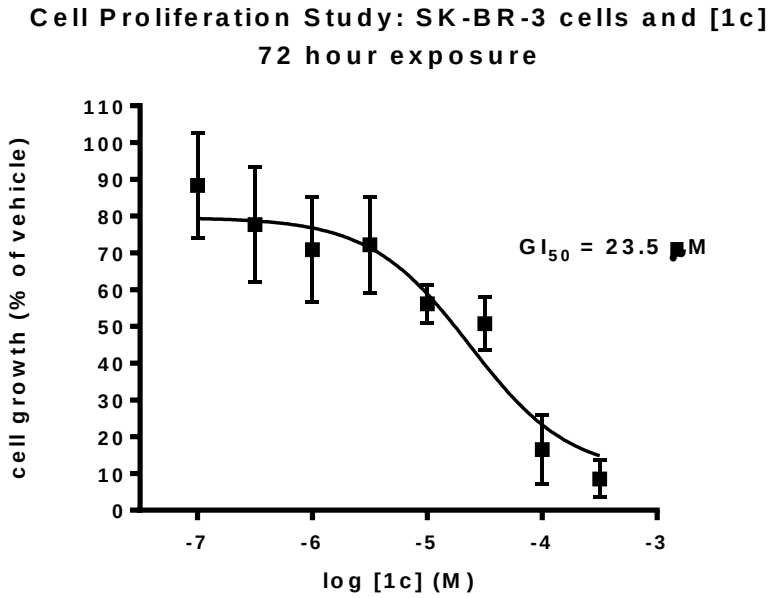

Figure 4.10: The GI_{50} curve of compound **[1c]** against SK-BR-3 cells.

4.4: Conclusions

Using a fragment library, we were able to discover a thiophene scaffold that is an inhibitor of the PTK, c-Src. The parent compound, **[1]** displays selectivity for c-Src over other similar PTKs, c-Abl and c-Hck. Additionally, compound **[1]** inhibits the clinically relevant T338M c-Src mutant (IC_{50} 7.9 μM). Furthermore, Lineweaver-Burk data supports that this compound does not bind the PTK as an ATP-competitive manner, but in an allosteric pocket as our evaluation suggests ambiguous substrate inhibition data. Although the carboxylic acid containing parent compound does not enter cells, the methyl ester analog, **[1c]**, of the compound inhibits the growth of a human breast cancer cell line with a GI_{50} of 23.5 μM.

4.5: References

(1) Martin, S. G. *Nature Reviews: Molecular Cell Biology* 2001, *2*, 467.
(2) Finn, R. S. *Ann. Oncol.* 2008, *19*, 1379.
(3) Frame, M. C. *Biochemica et Biophysica Acta* 2002, *1602*, 114.
(4) Al-Obeidi, F. A.; Wu, J. J.; Lam, K. S. *Biopolymers* 1998, *47*, 197.
(5) Al-Obeidi, F. A.; Lam, K. S. *Oncogene* 2000, *19*, 5690.
(6) Giamas, G.; Man, Y. L.; Hirner, H.; Bischof, J.; Kramer, K.; Khan, K.; Lavina-Ahmed, S. S.; Stebbing, J.; Knippschild, U. *Cell. Signal.* 2010, *22*, 984.
(7) Knight, Z. A.; Shokat, K. M. *Chem. Biol. (Cambridge, MA, U. S.)* 2005, *12*, 621.
(8) Morphy, R. *J Med Chem* 2010, *53*, 1413.
(9) Melnikova, I.; Golden, J. *Nat. Rev. Drug Discovery* 2004, *3*, 993.
(10) Cohen, P. *Nature Reviews: Drug Discovery* 2002, *1*, 309.
(11) Manning, G. *Science* 2002, *298*, 1912.
(12) Zhang, S.; Huang, W.-C.; Li, P.; Guo, H.; Poh, S.-B.; Brady, S. W.; Xiong, Y.; Tseng, L.-M.; Li, S.-H.; Ding, Z.; Sahin, A. A.; Esteva, F. J.; Hortobagyi, G. N.; Yu, D. *Nat. Med.* 2011, *17*, 461.
(13) Muthuswamy, S. K. *Nat. Med.* 2011, *17*, 416.
(14) Force, T.; Krause, D. S.; Van Etten, R. A. *Nat. Rev. Cancer* 2007, *7*, 322.
(15) Bikker, J. A.; Brooijmans, N.; Wissner, A.; Mansour, T. S. *J Med Chem* 2009, *52*, 1493.
(16) Zhang, J.; Yang, P. L.; Gray, N. S. *Nature Reviews: Cancer* 2009, *9*, 28.
(17) Ye, G.; Tiwari, R.; Parang, K. *Curr. Opin. Investig. Drugs* 2008, *9*, 605.

(18) Songyang, Z.; Carraway, K. L.; Eck, M. J.; Harrison, S. C.; Feldman, R. A.; Mohammadi, M.; Schlessinger, J.; Hubbard, S. R.; Smith, D. P.; Eng, C.; Lorenzo, M. J.; Ponder, B. A. J.; Mayer, B. J.; Cantley, L. C. *Nature* 1995, *373*, 536.
(19) Cox, K. J.; Shomin, C. D.; Ghosh, I. *Future Med. Chem.* 2011, *3*, 29.
(20) Lamba, V.; Ghosh, I. *Curr. Pharm. Des.* 2012, *18*, 2936.
(21) Maybridge; Vol. 2013, http://www.maybridge.com/images/pdfs/ro3frag.pdf.
(22) Wang, Q.; Cahill, S. M.; Blumenstein, M.; Lawrence, D. S. *J. Am. Chem. Soc.* 2006, *128*, 1808.
(23) Zuccotto, F.; Ardini, E.; Casale, E.; Angiolini, M. *J Med Chem* 2010, *53*, 2681.
(24) Azam, M.; Seeliger, M. A.; Gray, N. S.; Kuriyan, J.; Daley, G. Q. *Nat. Struct. Mol. Biol.* 2008, *15*, 1109.
(25) Krishnamurty, R.; Maly, D. J. *ACS Chem. Biol.* 2010, *5*, 121.
(26) Courtneidge, S. A. In *Protein Kinases*; Woodgett, J. R., Ed.; IRL Press - Oxford University Press: New York, 1994, p 212.

Chapter 5:

Conclusions

Although the protein tyrosine kinase, c-Src has been well-studied and investigated, there are still many characteristics that are unknown and undocumented. Herein lies the biggest challenge to the rational development of a selective substrate-competitive inhibitors. Despite being the first protein tyrosine kinase discovered, we do not have extensive knowledge of its substrate-binding region.

The principle motivations behind this collection of work were to elucidate a better understanding of the substrate-binding pocket of c-Src for future rational design of inhibitors to target the kinase. Using various approaches to develop series of compounds, we struggled to truly uncover any concrete binding trends. As witnessed with the biphenyl library of Chapter 2, we can note that despite having similar scaffolds, small molecule inhibitors targeting the substrate pocket can bind promiscuously and do not necessarily bind in a similar manner to one another. However, from our study on biphenyl containing compounds, we were encouraged to elucidate the (4-morpholino)biphenylethylacetamide (**BiPH 65**) as a low micromolar substrate-competitive, ATP-noncompetitive inhibitor of c-Src. It is noteworthy to mention that this compound not only inhibits the kinase domain and physiologically relevant three domain forms of c-Src, it also can inhibit the clinically relevant T338M c-Src protein. Furthermore, we have not only shown selectivity for c-Src over other closely related or highly similar protein tyrosine

kinases: c-Abl and c-Hck, but we have also demonstrated the ability of **BiPH 65** to inhibit cell growth of a human colon carcinoma cell line, HT-29, with a GI_{50} of 10.3 μM. From this intensive study of the biphenyl library, we were able to demonstrate the importance of our very specialized TR-FRET screen. Developed in our laboratory, these TR-FRET screens allowed us to not only characterize ATP-competitive binding compounds, but also, those compounds that bound the kinase in a substrate-competitive fashion simultaneously. The specialized TR-FRET assay provided a means to evaluate and characterize our compounds for a predicted binding mode quickly and efficiently. Without the work done previously in our lab by Dr. Bremmer on the development of this screen, we may not have arrived at our best compound, **BiPH 65** as quickly.

Chapter 3 highlighted the struggles with the design and development of substrate-competitive inhibitors. The motivations behind this project focused on the truncation of a peptidic inhibitor based on a natural substrate sequence to a small peptidomimetic compound to serve as a substrate-competitive inhibitor. However, from this study we observed that, although truncated from a larger peptidic inhibitor that binds to the substrate pocket of the kinase, the peptidomimetic compounds synthesized and evaluated were more promiscuous, and bound to other regions of the kinase as well. Despite the lack of success with this project, a good lesson was learned about this particular approach to the design of substrate-competitive inhibitors and the potential promiscuity of peptidomimetic compounds. We can conclude that compounds derived from peptide structures do not necessarily bind in the same manner as their larger counterparts. Furthermore, we also concluded that our general assay does not

provide a biased and specialized enough means by which to characterize substrate-competitive inhibitors.

Chapter 4 detailed our evaluation of a commercially available fragment library as we began a search for a new substrate-competitive scaffold on which to design new inhibitors. Although we were unable to elucidate a substrate-competitive inhibitor, our study revealed evidence of an allosteric inhibitor of c-Src, **[1]**. Although **[1]** is unable to inhibit the growth of a cancer cell line, we demonstrated that **[1c]**, the methyl ester analog of **[1]**, acts in a pro-drug fashion and inhibits the cell growth of the SK-BR-3 cells, a breast cancer cell line, with a GI_{50} of 23.5 μM. The use of a biased screen in this study allowed us to better characterize and remove more ATP-competitive inhibitors than our general screen. However, even a biased screen did not fully allow us to easily find substrate-competitive binding compounds.

In order to fully characterize the compounds of interest developed in the projects discussed in chapters 2 and 4, obtaining crystal structures of the compound bound to the protein would surely aid in the understanding of the inhibitor compound's interactions with c-Src. This would conclusively confirm the substrate-competitive mode of binding of **BiPH 65** as well as provide some insight as to where, exactly, the Maybridge fragment **[1]** is binding allosterically to the protein tyrosine kinase. Despite current laboratory efforts in these matters, a successful and usable crystal structure has yet to be resolved.

Appendices

Appendix A:
Supplemental Information for Chapter 2

A.1: General synthetic methods Unless otherwise noted, all reagents were obtained from commercially available sources and used without further purification. All ^{1}H and ^{13}C NMR spectra were measured with an Inova 500 spectrometer. Samples were taken in $CDCl_3$ or DMSO-*d6***,** spectra were referenced to chloroform peak. High resolution mass spectrometry (HRMS) was carried out by the University of Michigan Mass Spectrometry Facility (J. Windak, Director).

A.2: Synthesis of compounds

Synthesis of S1

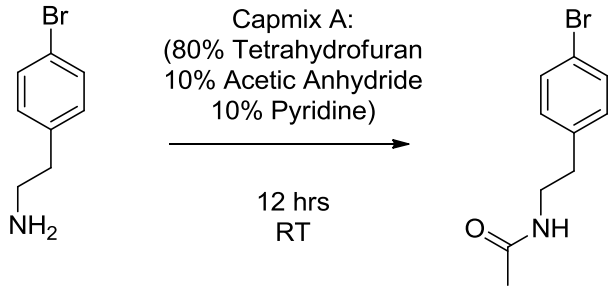

S1

90% yield

In a dried, round-bottom flask equipped with a stir bar, 4-bromophenethyl amine was added (0.500 mL, 3.22 mmol) and dissolved in 5.00 mL of Capmix A (80% Tetrahydrofuran, 10% Acetic Anhydride, 10% Pyridine). The solution was allowed to stir overnight at room temperature. The organics were removed under reduced pressure. The resulting oil was solubilized in ethyl acetate (20 mL), washed with 10% aqueous citrate (1 x 10 mL), followed by a wash with a brine solution (1 x 10 mL). The resulting organic layer was dried over anhydrous $MgSO_4$ and filtered. The solvent was removed under reduced pressure to provide the crude product, which was purified via automated silica gel chromatography (Linear gradient of 0 → 10% methanol in DCM) to yield compound **S1** as a white solid (696.5 mg, 90% yield) **Spectral data**. ^{1}H NMR (500 MHz, Chloroform-*d*) δ 7.45 – 7.37 (m, 2H), 7.08 – 7.01 (m, 2H), 5.77 (s, 1H), 3.44 (td, *J* = 7.0, 5.9 Hz, 2H), 2.75 (t, *J* = 7.0 Hz, 2H), 1.91 (s, 3H). ^{13}C NMR (500 MHz, Chloroform-*d*) δ 170.37, 137.95,

131.58, 130.51, 130.46, 120.23, 40.53, 35.02, 23.15, 19.55. HRMS-ESI (*m/z*): $[M+H]^+$ calcd for $C_{10}H_{12}BrNO$ 242.0175; found 242.0169.

Synthesis of BiPH 47

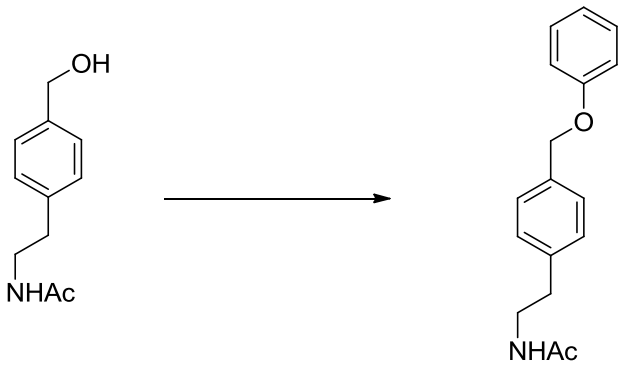

BiPH 47

27% yield

Synthesis of BiPH 47: N-acetyltyramine (179 mg, 1.0 mmol) was dissolved in 5 mL anhydrous DMF. K_2CO_3 (138 mg, 1.0 mmol) was added followed by benzylbromide (0.13 mL, 1.1 mmol), and the reaction was heated at 60 C under N_2 for 24 h. The reaction was cooled to RT, diluted with 20 mL H_2O, and extracted with EtOAc (3 x 20 mL). The combined organic extracts were washed with brine, dried over $MgSO_4$, and concentrated to give a colorless oil. Purification via automated silica gel chromatography (Linear gradient of 1 → 10% MeOH in DCM) gave **BiPH 47** as a white crystalline solid (73 mg, 27% yield). **Spectral data**. ^{1}H NMR (500 MHz, Chloroform-*d*) δ 7.47 – 7.29 (m, 5H), 7.15 – 7.07 (m, 2H), 6.96 – 6.89 (m, 2H), 5.48 – 5.44 (m, 1H), 5.05 (s, 2H), 3.48 (td, *J* = 6.9, 5.8 Hz, 2H), 2.75 (t, *J* = 6.9 Hz, 2H), 1.94 (s, 3H).^{13}C NMR (500 MHz, Chloroform-*d*) δ 170.02, 157.50, 137.01, 131.13, 129.71, 128.60, 127.98, 127.48, 115.01, 77.30, 77.04, 76.79, 70.04, 67.20, 40.80, 34.73, 23.38. HRMS-ESI (*m/z*): $[M+H]^+$ calcd for $C_{17}H_{19}NO_2$ 270.1489; found 270.1485.

Synthesis of BiPH 50

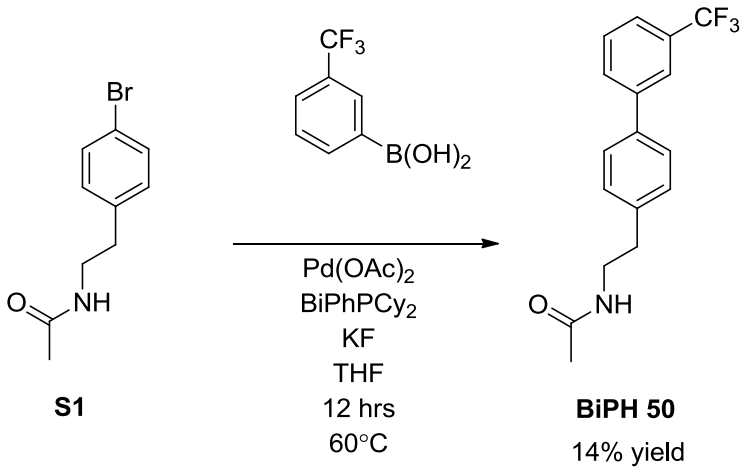

In a dried, round-bottom flask equipped with a stir bar, **S1** (242 mg, 1 mmol), palladium (II) acetate (12 mg, 0.5 mmol), 2-(Dicyclohexylphosphino)biphenyl (35 mg, 0.1 mmol), and potatssium fluoride (174 mg, 3 mmol), were dissolved in anhydrous THF 5 mL). 3-trifluoromethylphenyl boronic acid (228 mg, 1.2 mmol) was added and the contents of the flask were heated to 60°C in an oil bath and allowed to stir overnight. The reaction was quenched with water (20 mL) and was extracted with DCM (2 x 10 mL). The organic layer was washed with brine (1 x 10 mL) and dried over anhydrous $MgSO_4$ and filtered. The solvent was removed under reduced pressure to provide the crude product, which was purified via automated silica gel chromatography (Linear gradient of 0 → 100% ethyl acetate in hexanes) to yield compound **BiPH 50** as a white crystalline solid (41.8 mg, 14% yield) **Spectral data**. ^{1}H NMR (500 MHz, Chloroform-*d*) δ 7.82 (td, *J* = 1.6, 0.8 Hz, 1H), 7.75 (dt, *J* = 7.7, 1.5 Hz, 1H), 7.63 – 7.52 (m, 4H), 7.36 – 7.27 (m, 2H), 5.75 (s, 1H), 3.56 (td, *J* = 7.0, 5.8 Hz, 2H), 2.89 (t, *J* = 7.0 Hz, 2H), 1.97 (s, 3H). ^{13}C NMR (500 MHz, Chloroform-*d*) δ 170.25, 141.57, 138.91, 137.95, 131.24, 130.98, 130.24, 129.40, 129.27, 128.72, 128.63, 127.36, 125.27, 123.90, 40.67, 35.30, 23.29. HRMS-ESI (*m/z*): $[M+H]^+$ calcd for $C_{17}H_{16}F_3NO$ 308.1257; found 308.1254.

Synthesis of BiPH 65

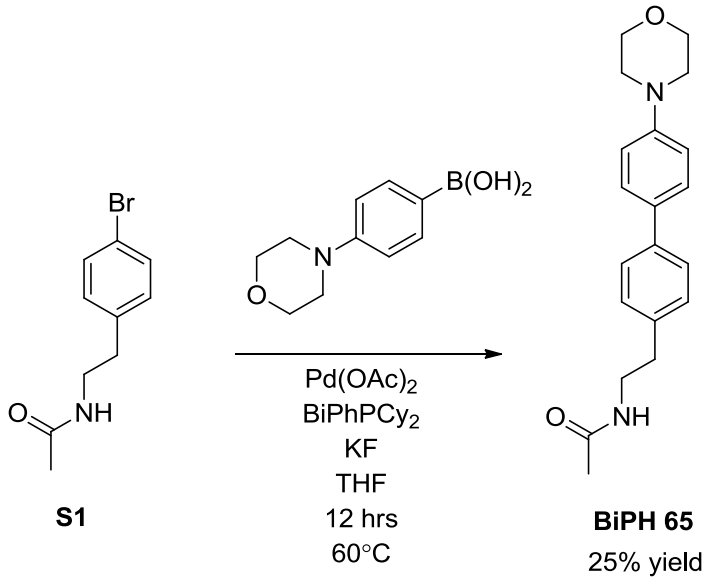

In a dried, round-bottom flask equipped with a stir bar, **S1** (242 mg, 1 mmol), palladium (II) acetate (12 mg, 0.05 mmol), 2-(Dicyclohexylphosphino)biphenyl (35 mg, 0.1 mmol), and potatssium fluoride (174 mg, 3 mmol), were dissolved in anhydrous THF (5 mL). 4-morpholinophenyl boronic acid (248.4 mg, 1.2 mmol) was added and the contents of the flask were heated to 60°C in an oil bath and allowed to stir overnight. The reaction was quenched with water (20 mL) and was extracted with DCM (2 x 10 mL). The organic layer was washed with brine (1 x 10 mL) and dried over anhydrous $MgSO_4$ and filtered. The solvent was removed under reduced pressure to provide the crude product, which was purified via automated silica gel chromatography (Linear gradient of 1 → 10% methanol in dichloromethane) to yield compound **BiPH 65** as a brown solid (82.3 mg, 25% yield) **Spectral data**. ^{1}H NMR (500 MHz, Chloroform-*d*) δ 7.54 – 7.39 (m, 3H), 7.34 – 7.16 (m, 1H), 7.10 – 7.03 (m, 1H), 7.02 – 6.84 (m, 3H), 5.48 (dd, *J* = 14.7, 8.5 Hz, 1H), 3.90 – 3.81 (m, 4H), 3.50 (dtd, *J* = 30.4, 7.0, 5.9 Hz, 2H), 3.23 – 3.12 (m, 4H), 2.80 (dt, *J* = 34.1, 6.9 Hz, 2H), 1.94 (d, *J* = 5.1 Hz, 3H). ^{13}C NMR (500 MHz, Chloroform-*d*) δ 170.08, 137.86, 137.10, 131.70, 130.48, 129.19, 129.13, 127.63, 127.20, 126.72, 120.36, 115.77, 115.70, 66.94, 66.89, 49.35, 49.15, 40.64, 35.09, 23.32. HRMS-ESI (*m/z*): $[M+H]^+$ calcd for $C_{20}H_{24}N_2O_2$ 325.1911; found 325.1904.

Synthesis of BiPH 85

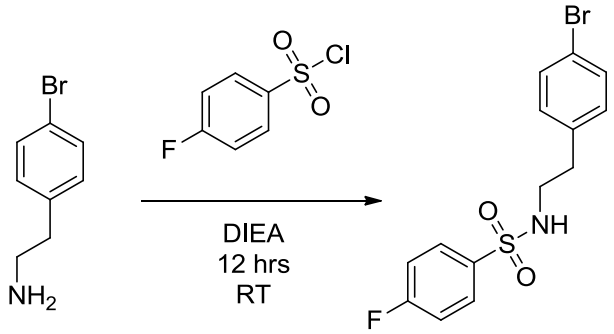

S9

84% yield

Synthesis of **S9**. In a dried, round-bottom flask equipped with a stir bar, 4-bromophenethyl amine (0.390 mL, 2.5 mmol) was added and dissolved in DCM (10 mL). 4-fluorophenylsulfonyl chloride (535.2 mg, 2.75 mmol) and diisopropyl ethyl amine (0.87 mL, 5 mmol) were added last and the solution was allowed to stir overnight at room temperature. The organics were removed under reduced pressure. The resulting oil was solubilized in ethyl acetate (20 mL), washed with 10% aqueous citrate (1 x 10 mL), followed by a wash with a brine solution (1 x 10 mL). The resulting organic layer was dried over anhydrous $MgSO_4$ and filtered. The solvent was removed under reduced pressure to provide the crude product, which was purified via automated silica gel chromatography (Linear gradient of 0 → 10% methanol in DCM) to yield compound **S9** as a yellow solid (758.8 mg, 84% yield) **Spectral data**. ^{1}H NMR (500 MHz, Chloroform-d) δ 7.93 – 7.85 (m, 2H), 7.50 – 7.43 (m, 2H), 7.30 – 7.22 (m, 2H), 7.10 – 7.02 (m, 2H), 4.81 (t, J = 6.3 Hz, 1H), 3.29 (q, J = 6.8 Hz, 2H), 2.83 (t, J = 7.0 Hz, 2H). ^{13}C NMR (500 MHz, Chloroform-*d*) δ 221.47, 166.06, 165.87, 164.03, 160.33, 158.35, 137.93, 135.89, 133.38, 130.55, 129.80, 129.72, 129.00, 125.60, 117.47, 117.27, 116.43, 116.25, 52.44, 44.10, 35.59. HRMS-ESI (*m/z*): $[M+Na]^+$ calcd for $C_{14}H_{13}BrFNO_2S$ 379.9727; found 379.9727.

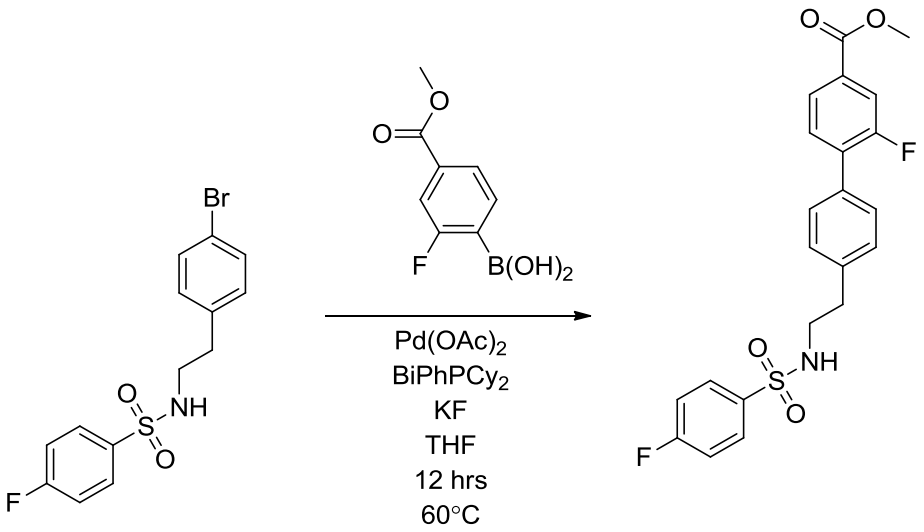

In a dried, round-bottom flask equipped with a stir bar, **S9** (213 mg, 0.56 mmol), palladium (II) acetate (6.73 mg, 0.03 mmol), 2-(Dicyclohexylphosphino)biphenyl (21.02 mg, 0.06 mmol), and potatssium fluoride (105 mg, 1.8 mmol), were dissolved in anhydrous THF (5 mL). 4-COOMe, 2-F phenyl boronic acid (200 mg, 1.1 mmol) was added and the contents of the flask were heated to 60°C in an oil bath and allowed to stir overnight. The reaction was quenched with water (20 mL) and was extracted with DCM (2 x 10 mL). The organic layer was washed with brine (1 x 10 mL) and dried over anhydrous $MgSO_4$ and filtered. The solvent was removed under reduced pressure to provide the crude product, which was purified via automated silica gel chromatography (Linear gradient of 0 → 100% ethyl acetate in hexanes) to yield compound **BiPH 85** as a tan crystalline solid (40 mg, 17% yield) **Spectral data**. ^{1}H NMR (500 MHz, Chloroform-*d*) δ 7.99 – 7.84 (m, 4H), 7.58 – 7.51 (m, 3H), 7.28 – 7.18 (m, 4H), 4.58 (t, *J* = 6.3 Hz, 1H), 4.01 (s, 3H), 3.34 (q, *J* = 6.7 Hz, 2H), 2.90 (t, *J* = 6.9 Hz, 2H).^{13}C NMR (500 MHz, $CDCl_3$): δ 221.47, 166.06, 165.87, 164.03, 160.33, 158.35, 137.93, 135.89, 133.38, 130.55, 129.80, 129.72, 129.00, 125.60, 117.47, 117.27, 116.43, 116.25, 52.44, 44.10, 35.59. HRMS-ESI (*m/z*): $[M+Na]^+$ calcd for $C_{22}H_{19}F_2NO_4S$ 454.0895; found 454.0892.

Synthesis of BiPH 108

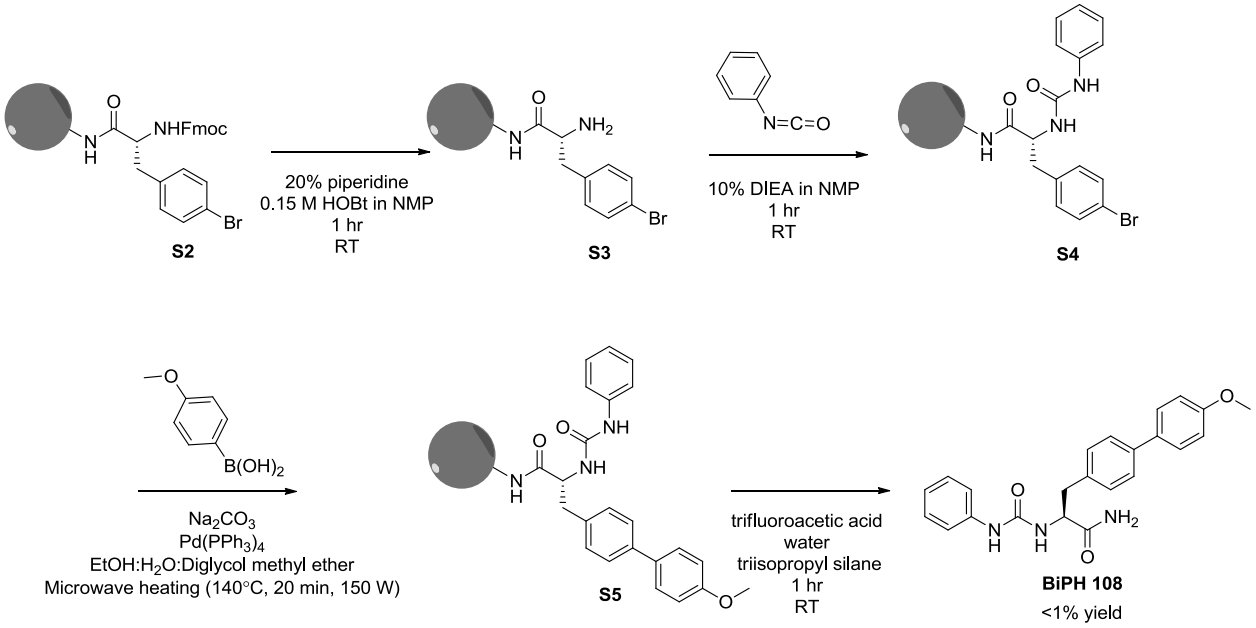

Synthesis of **S2** and **S3**. Into a plastic, microwave peptide vessel, Rink Amide resin (639 mg, 0.1 mmol) was added and swollen with n-methyl-2-pyrrolidone (7 mL). The vessel was placed on a shake plate for 1 hour at room temperature. Following this period, the solvent in the vessel was evacuated and to it, deprotection solution (7 mL, 20% piperidine, 0.15 M HOBt in NMP) was added. Again, the vessel was placed on a shake plate for 1 hour at room temperature and subsequently the solvent was evacuated and the beads were washed with NMP (3 x 10 mL). The resin beads were evaluated for complete Fmoc deprotection through the use of the Kaiser test.[1] The resin beads were washed with DCM (3 x 5 mL) and dried. A solution of Fmoc-(4-Br)phenylalanine-OH (560 mg, 1.2 mmol) and HBTU (500 mg, 1.3 mmol) and activator solution (10% Diisopropylethylamine in NMP, 4 mL) was prepared and added to another vessel containing deprotected rink amide resin beads (200 mg of deprotected beads). The vessel was allowed to shake at room temperature overnight. Upon solvent evacuation and the washing of the beads (NMP, 3 x 10 mL), the resin beads were evacuated with the Kaiser test to insure complete coupling of the amino acid to the resin beads, arriving at compound **S2**. Lastly, the beads were deprotected, Kaiser tested, and dried as previously described to arrive at **S3**.

Synthesis of **S4**. To the resin beads of compound **S3**, a solution of phenyl isocyanate (5% in 4 mL of activator solution) was added and allowed to shake at room temperature overnight. The vessel was then evacuated, washed with NMP (3 x 5 mL) and evaluated by Kaiser Test to ensure complete coupling of the phenyl isocyanate. The beads were subsequently rinsed with DCM (3 x 5 mL) and dried arriving at compound **S4**.

Synthesis of compound **S5**. The resin beads containing compound **S4** were transferred to a dried, glass microwave vessel equipped with a stir bar. To this vessel, 4-methoxyphenyl boronic acid (304 mg, 2.0 mmol), sodium carbonate (212 mg, 2.0 mmol), tetrakis(triphenylphosphine)palladium (0) (24 mg, 0.021 mmol) were added. A solvent mixture of ethanol:water:diglycol methyl ether (2:1:10) was subsequently added and the reaction vessel was placed into a CEM microwave synthesizer. The reaction was heated to 140 °C for 20 minutes at 150 W of power. After cooling, the reaction mixture was washed with deionized water (~50 mL), NMP (3 x 10 mL), Methanol (3 x 10 mL), Diglycol methyl ether (3 x 10 mL), and DCM (3 x 10 mL), resulting in the preparation of compound **S5** on resin.

Synthesis of **BiPH 108**. Compound **S5** was separated from resin using cleavage conditions (trifluoroacetic acid 3.8 mL, water 0.1 mL, triisopropyl silane 0.1 mL) for 1 hour with intermittent stirring. The resulting solution was filtered, collected and the solvent was removed under reduced pressure. The resulting oil was purified via reverse-phase chromatography (linear gradient of 5 → 95% CH_3CN (0.1% HOAc) in H_2O (0.1% HOAc)) to yield **BiPH 108** as a white crystalline solid (2 mg, < 1% yield). **Spectral data**. ^{1}H NMR (500 MHz, DMSO-d_6) δ 8.68 (s, 1H), 7.64 – 7.49 (m, 5H), 7.37 – 7.29 (m, 2H), 7.29 – 7.16 (m, 2H), 7.14 (d, *J* = 2.0 Hz, 1H), 7.03 – 6.96 (m, 2H), 6.91 – 6.84 (m, 1H), 6.30 (d, *J* = 8.1 Hz, 1H), 4.46 (td, *J* = 7.8, 5.1 Hz, 1H), 3.78 (s, 3H), 3.04 (dd, *J* = 13.8, 5.2 Hz, 1H), 2.86 (dd, *J* = 13.8, 7.6 Hz, 1H). ^{13}C NMR (500 MHz, DMSO-d_6) δ 173.81, 159.17, 157.07, 155.00, 140.78, 138.58, 132.80, 130.32, 129.12, 127.99, 126.28, 121.51, 117.86, 114.77, 55.59, 54.05, 14.45. HRMS-ESI (*m/z*): $[M+H]^+$ calcd for $C_{23}H_{23}N_3O_3$ 390.1812; found 390.1805.

Synthesis of BiPH 101

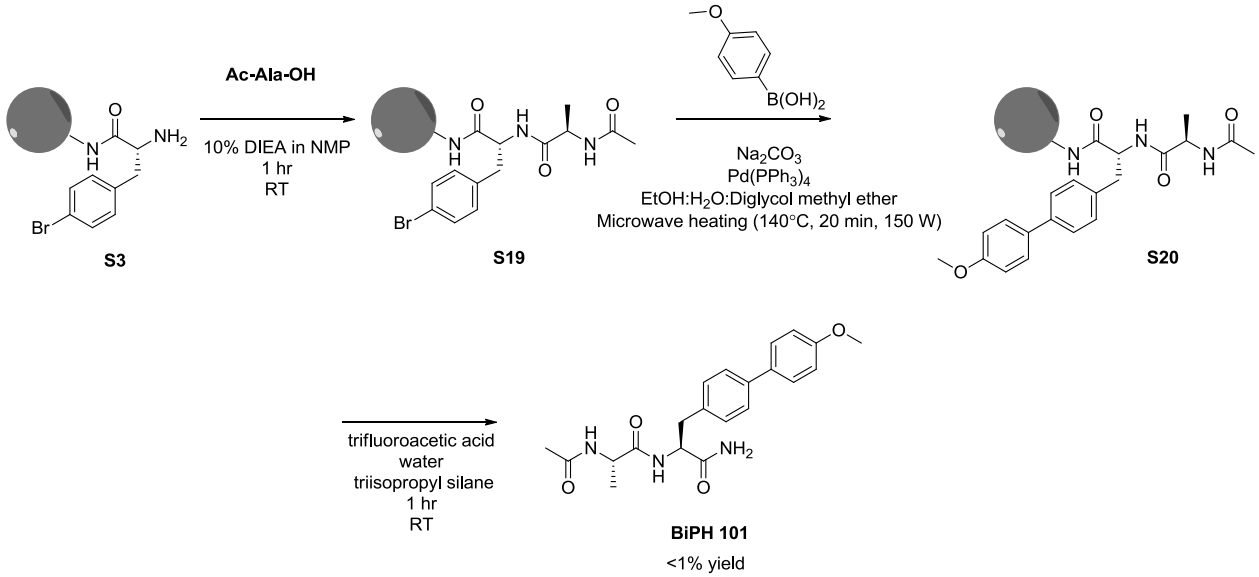

Synthesis of **S19**. To the resin beads of compound **S3** (200 mg), a solution of Ac-Ala-OH (131 mg, 1 mmol) and HBTU (380 mg, 1.0 mmol) in 4 mL activator solution was added and allowed to shake at room temperature overnight. The vessel was then evacuated, washed with NMP (3 x 5 mL) and evaluated by Kaiser Test to ensure complete coupling. The beads were subsequently rinsed with DCM (3 x 5 mL) and dried arriving at compound **S19** on resin.

Synthesis of compound **S20**. The resin beads containing compound **S19** were transferred to a dried, glass microwave vessel equipped with a stir bar. To this vessel, 4-methoxyphenyl boronic acid (304 mg, 2.0 mmol), sodium carbonate (212 mg, 2.0 mmol), tetrakis(triphenylphosphine)palladium (0) (24 mg, 0.021 mmol) were added. A solvent mixture of ethanol:water:diglycol methyl ether (2:1:10) was subsequently added and the reaction vessel was placed into a CEM microwave synthesizer. The reaction was heated to 140 °C for 20 minutes at 150 W of power. After cooling, the reaction mixture was washed with deionized water (~50 mL), NMP (3 x 10 mL), Methanol (3 x 10 mL), Diglycol methyl ether (3 x 10 mL), and DCM (3 x 10 mL), resulting in the preparation of compound **S20** on resin.

Synthesis of **BiPH 101**. Compound **S20** was separated from resin using cleavage conditions (trifluoroacetic acid 3.8 mL, water 0.1 mL, triisopropyl silane 0.1 mL) for 1 hour with intermittent stirring. The resulting solution was filtered, collected and the solvent was removed under reduced pressure. The resulting oil was purified via reverse-phase chromatography (linear gradient of 5 → 95% CH_3CN (0.1% HOAc) in H_2O (0.1% HOAc)) to yield **BiPH 101** as a white crystalline solid (2 mg, <1% yield). **Spectral data**. ^{1}H NMR (500 MHz, DMSO-d_6) δ 8.02 (dd,

J = 7.9, 4.5 Hz, 1H), 7.81 (d, *J* = 8.3 Hz, 1H), 7.52 (dt, *J* = 38.4, 8.3 Hz, 6H), 7.25 (dd, *J* = 18.0, 7.6 Hz, 2H), 7.07 – 6.96 (m, 2H), 4.40 (dtd, *J* = 18.7, 9.6, 9.1, 5.0 Hz, 1H), 4.15 (q, *J* = 7.9, 7.4 Hz, 1H), 3.77 (s, 4H), 3.30 (s, 3H), 3.00 (ddd, *J* = 25.0, 13.9, 4.8 Hz, 1H), 2.88 – 2.79 (m, 1H), 1.84 – 1.71 (m, 3H), 1.09 (d, *J* = 6.9 Hz, 3H).^{13}C NMR (500 MHz, DMSO-d_6) δ 170.39, 170.28, 159.16, 144.94, 136.68, 132.77, 130.18, 127.99, 126.21, 114.77, 62.47, 55.60, 54.26, 40.46, 25.42, 23.02, 18.20, 14.73.HRMS-ESI (*m/z*): $[M+Na]^+$ calcd for $C_{21}H_{25}N_3O_4$ 406.1737; found 406.1746.

Synthesis of BiPH 142

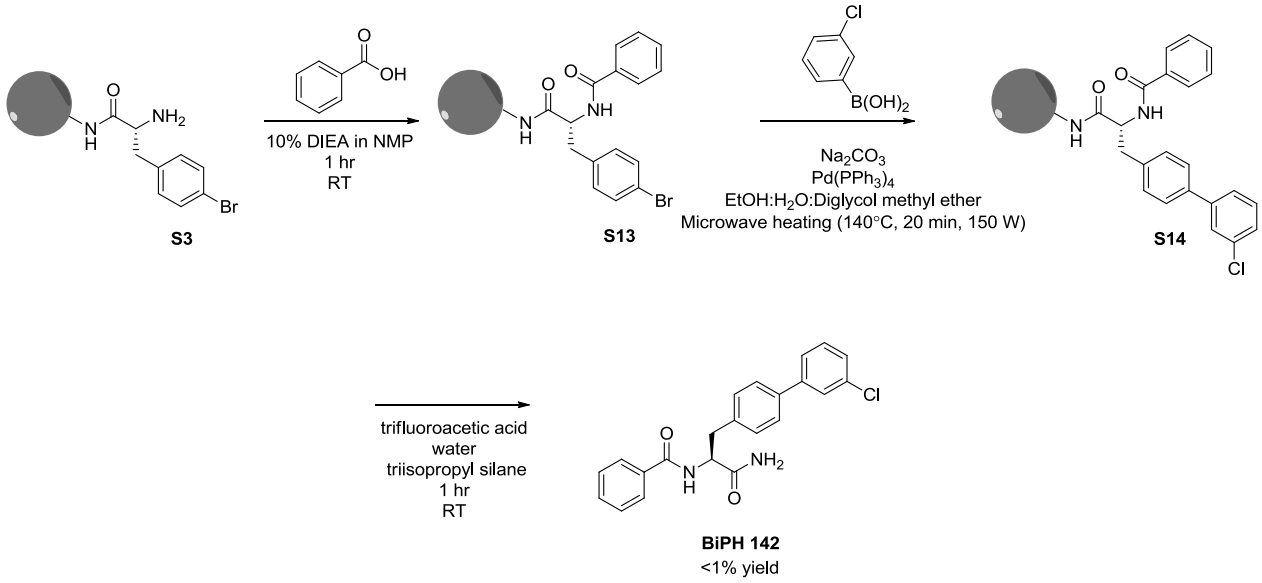

Synthesis of **S13**. To the resin beads of compound **S3** (200 mg), a solution of benzoic acid (200 mg, 1.64 mmol) and HBTU (380 mg, 1.0 mmol) in 4 mL activator solution was added and allowed to shake at room temperature overnight. The vessel was then evacuated, washed with NMP (3 x 5 mL) and evaluated by Kaiser Test to ensure complete coupling. The beads were subsequently rinsed with DCM (3 x 5 mL) and dried arriving at compound **S13** on resin.

Synthesis of compound **S14**. The resin beads containing compound **S13** were transferred to a dried, glass microwave vessel equipped with a stir bar. To this vessel, 3-chlorophenyl boronic acid (312 mg, 2.0 mmol), sodium carbonate (212 mg, 2.0 mmol), tetrakis(triphenylphosphine)palladium (0) (24 mg, 0.021 mmol) were added. A solvent mixture of ethanol:water:diglycol methyl ether (2:1:10) was subsequently added and the reaction vessel was placed into a CEM microwave synthesizer. The reaction was heated to 140 °C for 20 minutes at 150 W of power. After cooling, the reaction mixture was washed with deionized

water (~50 mL), NMP (3 x 10 mL), Methanol (3 x 10 mL), Diglycol methyl ether (3 x 10 mL), and DCM (3 x 10 mL), resulting in the preparation of compound **S14** on resin.

Synthesis of **BiPH 142**. Compound **S14** was separated from resin using cleavage conditions (trifluoroacetic acid 3.8 mL, water 0.1 mL, triisopropyl silane 0.1 mL) for 1 hour with intermittent stirring. The resulting solution was filtered, collected and the solvent was removed under reduced pressure. The resulting oil was purified via reverse-phase chromatography (linear gradient of 5 → 95% CH_3CN (0.1% HOAc) in H_2O (0.1% HOAc)) to yield **BiPH 142** as a white crystalline solid (2 mg, <1% yield). **Spectral data**. ^{1}H NMR (500 MHz, DMSO-d_6) δ 8.57 (d, *J* = 8.4 Hz, 1H), 7.85 – 7.78 (m, 2H), 7.63 – 7.56 (m, 1H), 7.56 – 7.30 (m, 8H), 7.14 (d, *J* = 2.2 Hz, 1H), 4.68 (m, 1H), 3.16 (dd, *J* = 13.8, 4.1 Hz, 1H), 3.06 (dd, *J* = 13.8, 10.7 Hz, 1H). ^{13}C NMR (500 MHz, DMSO-d_6) δ 173.79, 166.81, 140.07, 138.71, 138.63, 136.99, 136.87, 134.62, 131.94, 131.72, 131.69, 130.28, 129.44, 129.39, 128.60, 127.91, 127.88, 55.10, 40.30, 37.30, 14.38. HRMS-ESI (*m/z*): $[M+Na]^+$ calcd for$C_{22}H_{19}ClN_2O_2$ 401.1027; found 401.1020.

Synthesis of BiPH 230

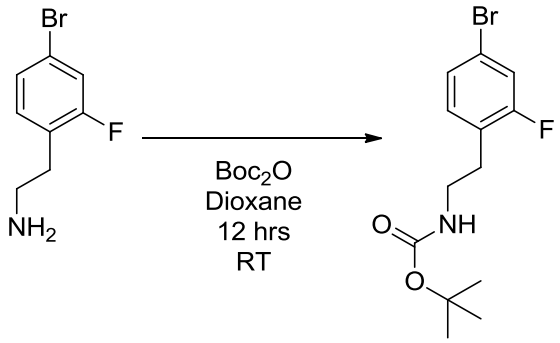

S15
67% yield

Synthesis of **S15**. In a dried, round-bottom flask equipped with a stir bar, 4-bromo-2-fluorophenyl ethyl amine (55 mg, 0.253 mmol) was solubilized in dioxane (10 mL). To this solution, boc anhydride (61 mg, 0.278 mmol) and NaOH (0.100 mL, 0.6 M) were added. The reaction was allowed to stir overnight at room temperature. Following this, the solvent was removed under reduced pressure. The crude product was dissolved in ethyl acetate (10 mL) and washed with water (2 x 10 mL). The organic layer was dried over anhydrous $MgSO_4$ and filtered. The solvent was removed under reduced pressure to provide the crude product, which was purified via automated silica gel chromatography (Linear gradient of 5 → 40% ethyl acetate in hexanes) to yield compound **S15** as a white solid (53.9 mg, 67% yield) **Spectral data**. ^{1}H NMR (500 MHz, Chloroform-*d*) δ 7.22 (ddd, *J* = 9.5, 4.7, 2.0 Hz, 2H), 7.07 (t, *J* = 8.1 Hz, 1H), 4.55 (s,

1H), 3.35 (q, *J* = 7.1 Hz, 2H), 2.80 (t, *J* = 6.7 Hz, 2H), 1.42 (s, 9H).[13]C NMR (500 MHz, Chloroform-*d*): δ 162.08, 160.09, 155.79, 132.26, 127.37, 125.08, 120.35, 119.09, 118.89, 79.39, 40.34, 29.35, 19.32. HRMS-ESI (*m/z*): $[M+Na]^+$ calcd for $C_{13}H_{17}BrFNO_2$ 340.0319; found 340.0313.

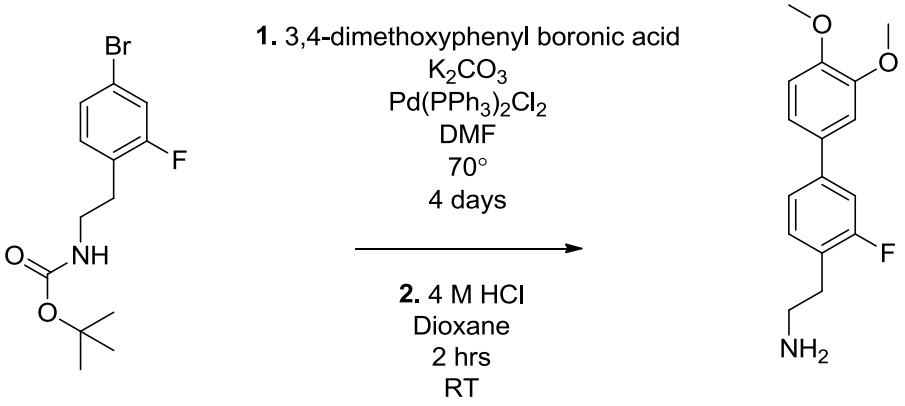

S15 **BiPH 230**

7.4% yield

Synthesis of **BiPH 230**. In a dried, round-bottom flask equipped with a stir bar, **S15** (25.8 mg, 0.081 mmol) was solubilized in DMF (1 mL). To this solution, Palladium(II)bis(triphenylphosphine) dichloride (11.4 mg, 0.016 mmol), potassium carbonate (33.8 mg, 0.244 mmol), 3,4-dimethoxyphenyl boronic acid (30 mg, 0.163 mmol) was added and the contents of the flask were heated to 70°C in an oil bath and allowed to stir for 4 days. The solvent was removed under reduced pressure to provide the crude product, (230 mg, brown oil) which was promptly used without further purification. The BOC-protected crude brown oil was solubilized in a solution of HCl in dioxane (10 mL, 4 M) and was allowed to stir for 2 hours. The solvent was removed under reduced pressure to provide the crude product, which was purified via reverse-phase chromatography (linear gradient of 5 → 95% CH_3CN (0.1% HOAc) in H_2O (0.1% HOAc)) to yield **BiPH 230** as a white solid, trifluroacetic acid salt (1.71 mg, 7.4% yield). **Spectral data**. [1]H NMR (500 MHz, Chloroform-*d*) δ 8.21 (s, 2H), 7.26 (s, 2H), 7.11 – 6.98 (m, 3H), 6.90 (d, *J* = 8.1 Hz, 1H), 3.98 (s, 3H), 3.94 – 3.88 (m, 3H), 3.25 (s, 2H), 3.09 (s, 2H). [13]C NMR (500 MHz, Chloroform-*d*) δ 160.61, 153.24, 135.99, 134.57, 131.29, 129.48, 122.76, 121.07, 119.30, 117.50, 111.44, 110.11, 107.17, 55.94, 39.70, 27.48. [19]F NMR (376 MHz, DMSO-d_6) δ -73.52 , -118.37 (t, *J* = 9.7 Hz). HRMS-ESI (*m/z*): $[M+H]^+$ calcd for $C_{16}H_{18}FNO_2$ 276.1394; found 276.1398.

Synthesis of BiPH 240

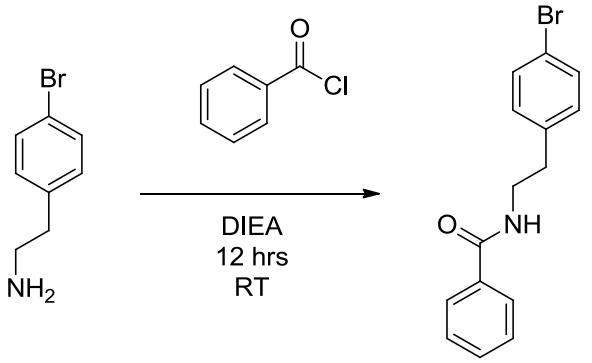

S6

82% yield

Synthesis of **S6**. In a dried, round-bottom flask equipped with a stir bar, 4-bromophenethyl amine (0.390 mL, 2.5 mmol) was added and dissolved in DCM (10 mL). Benzoyl chloride (0.32 mL, 2.75 mmol) and diisopropyl ethyl amine (0.87 mL, 5 mmol) were added last and the solution was allowed to stir overnight at room temperature. The organics were removed under reduced pressure. The resulting oil was solubilized in ethyl acetate (20 mL), washed with 10% aqueous citrate (1 x 10 mL), followed by a wash with a brine solution (1 x 10 mL). The resulting organic layer was dried over anhydrous $MgSO_4$ and filtered. The solvent was removed under reduced pressure to provide the crude product, which was purified via automated silica gel chromatography (Linear gradient of 0 → 10% methanol in DCM) to yield compound **S6** as a grey crystalline solid (620 mg, 82% yield) **Spectral data** ^{1}H NMR (500 MHz, Chloroform-*d*) δ 7.72 – 7.66 (m, 2H), 7.53 – 7.37 (m, 5H), 7.14 – 7.07 (m, 2H), 6.24 – 6.18 (m, 1H), 3.68 (td, *J* = 6.9, 5.9 Hz, 2H), 2.89 (t, *J* = 6.9 Hz, 2H). ^{13}C NMR (500 MHz, Chloroform-d) δ 221.67, 167.56, 137.93, 134.45, 131.73, 131.52, 130.55, 128.60, 126.83, 120.41, 81.61, 41.02, 35.15, 19.51, 19.49. HRMS-ESI (*m/z*): $[M+H]^+$ calcd for $C_{15}H_{14}BrNO$ 304.0332; found 304.0332.

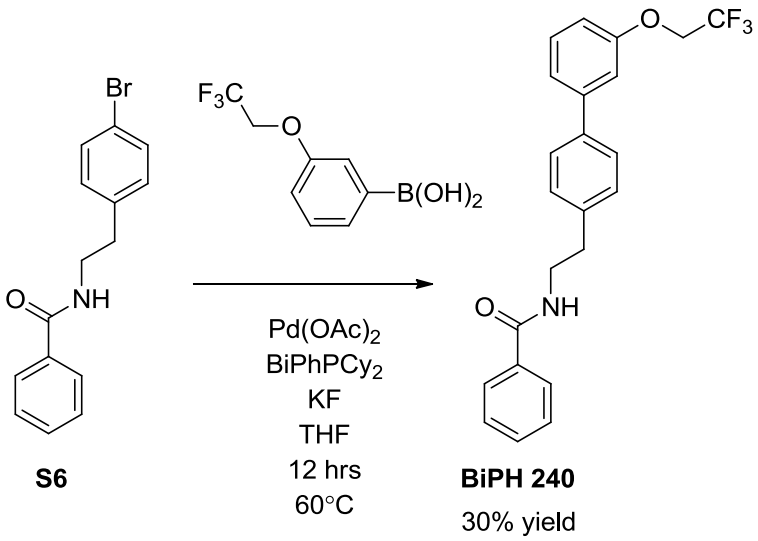

S6

BiPH 240

30% yield

Synthesis of **BiPH 240**. In a dried, round-bottom flask equipped with a stir bar, **S6** (100 mg, 0.330 mmol), palladium (II) acetate (4 mg, 0.017 mmol), 2-(Dicyclohexylphosphino)biphenyl (12 mg, 0.033 mmol), and potatssium fluoride (58 mg, 0.99 mmol), were dissolved in anhydrous THF (4 mL). 4-morpholinophenyl boronic acid (87 mg, 0.40 mmol) was added and the contents of the flask were heated to 60°C in an oil bath and allowed to stir overnight. The reaction was quenched with water (20 mL) and was extracted with DCM (2 x 10 mL). The organic layer was washed with brine (1 x 10 mL) and dried over anhydrous $MgSO_4$ and filtered. The solvent was removed under reduced pressure to provide the crude product, which was purified via automated silica gel chromatography (Linear gradient of 7 → 70% ethyl acetate in hexanes) to yield compound **BiPH 240** as a white solid (40 mg, 30% yield) **Spectral data.** ^{1}H NMR (500 MHz, Chloroform-d) δ 7.71 (d, J = 7.4 Hz, 2H), 7.60 – 7.29 (m, 8H), 7.29 – 7.12 (m, 2H), 6.92 (dd, J = 8.4, 2.6 Hz, 1H), 6.21 – 6.15 (m, 1H), 4.41 (q, J = 8.1 Hz, 2H), 3.76 (q, J = 6.6 Hz, 2H), 2.99 (t, J = 6.9 Hz, 2H). ^{13}C NMR (500 MHz, Chloroform-*d*) δ 167.52, 157.79, 142.73, 138.78, 138.52, 134.60, 131.48, 130.07, 129.33, 128.60, 127.43, 126.81, 121.28, 113.89, 113.37, 77.28, 77.03, 76.77, 67.14, 66.07, 65.78, 41.12, 35.37. HRMS-ESI (*m/z*): $[M+H]^+$ calcd for $C_{23}H_{20}F_3NO_2$ 400.1519; found 400.1516.

Synthesis of BiPH 248

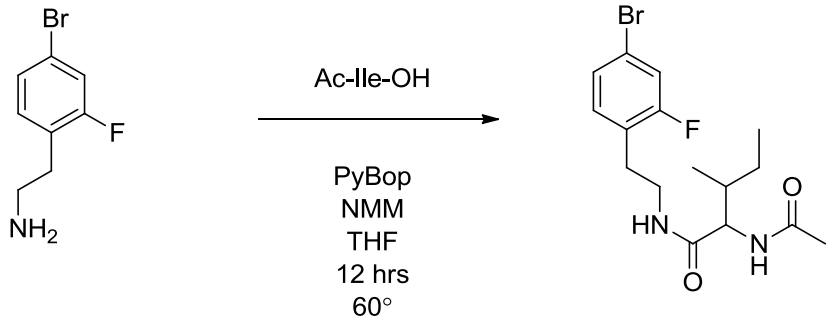

S10
15% yield

Synthesis of **S10**. In a dried, round-bottom flask equipped with a stir bar, 4-bromo, 2-fluorophenethyl amine (67.0 mg, 0.31 mmol) was added and dissolved in anhydrous THF (8 mL). Ac-Ile-OH (45 mg, 0.26 mol), PyBop (161.3 mg, 0.31 mmol) and n-methylmorpholine (0.860 mL, 0.78 mmol) were added and the solution was allowed to stir overnight at room temperature. The organics were removed under reduced pressure. The resulting oil was solubilized in DCM (20 mL) and washed with a brine solution (1 x 10 mL). The resulting organic layer was dried over anhydrous $MgSO_4$ and filtered. The solvent was removed under reduced pressure to provide the crude product, which was purified via reverse-phase chromatography (linear gradient of 5 → 95% CH_3CN (0.1% HOAc) in H_2O (0.1% HOAc)) to yield **S10** (17.7 mg, 0.05 mmol, 15% yield). **Spectral data**. ^{1}H NMR (500 MHz, DMSO-d_6) δ 8.05 (t, *J* = 5.9 Hz, 1H), 7.83 (d, *J* = 8.9 Hz, 1H), 7.46 (dd, *J* = 9.9, 2.0 Hz, 1H), 7.31 (dd, *J* = 8.4, 2.0 Hz, 1H), 7.23 (t, *J* = 8.1 Hz, 1H), 4.05 (t, *J* = 8.3 Hz, 1H), 3.34 – 3.19 (m, 2H), 2.70 (td, *J* = 7.1, 6.6, 2.2 Hz, 2H), 2.08 (s, 1H), 1.84 (d, *J* = 8.8 Hz, 3H), 1.61 (ddd, *J* = 16.7, 11.5, 7.7 Hz, 1H), 1.30 (dtd, *J* = 15.1, 7.5, 3.5 Hz, 1H), 1.06 – 0.93 (m, 1H), 0.82 – 0.68 (m, 6H). ^{13}C NMR (500 MHz, DMSO-d_6) δ 171.53, 169.46, 148.35, 133.36, 127.72, 118.94, 118.74, 109.99, 57.30, 36.77, 25.42, 24.70, 22.93, 15.75, 14.72, 11.44. HRMS-ESI (*m/z*): $[M+H]^+$ calcd for $C_{16}H_{22}BrFN_2O_2$ 373.0921; found 373.0924.

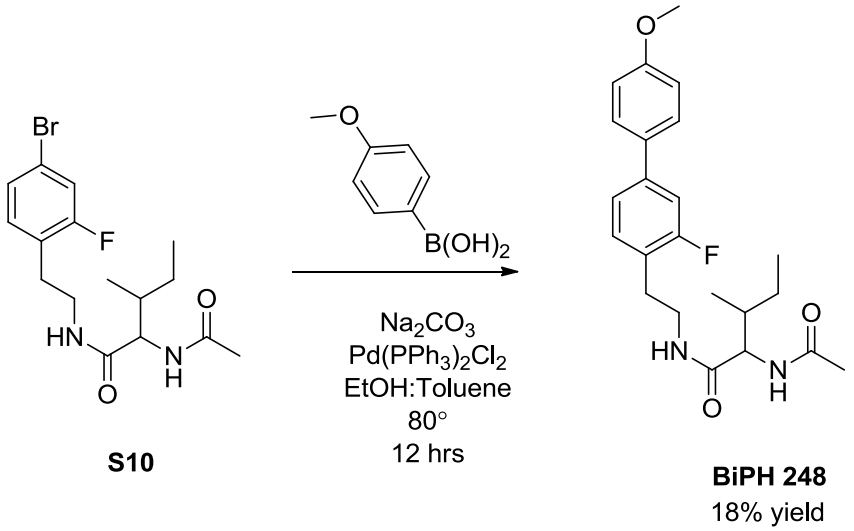

Synthesis of **BiPH 248**. In a dried, round-bottom flask equipped with a stir bar, **S10** (6.5 mg, 0.020 mmol), Palladium(II)bis(triphenylphosphine) dichloride (1.4 mg, 0.002 mmol), and sodium carbonate (1 mL,2 M solution), were dissolved in a 1:1 solution of ethanol:toluene (5 mL). 4-morpholinophenyl boronic acid (6.1 mg, 0.04 mmol) was added and the contents of the flask were heated to 80°C in an oil bath and allowed to stir overnight. The solvent was removed under reduced pressure to provide the crude product, which was purified via reverse-phase chromatography (linear gradient of 5 → 95% CH_3CN (0.1% HOAc) in H_2O (0.1% HOAc)) to yield **BiPH 248** (1.2 mg, 18% yield) as a white solid. **Spectral data**. ^{1}H NMR (500 MHz, DMSO-d_6) δ 8.07 (t, *J* = 5.8 Hz, 1H), 7.82 (d, *J* = 8.9 Hz, 1H), 7.62 (d, *J* = 8.2 Hz, 2H), 7.43 – 7.34 (m, 2H), 7.31 (t, *J* = 8.0 Hz, 1H), 7.01 (d, *J* = 8.3 Hz, 2H), 4.08 (t, *J* = 8.3 Hz, 1H), 3.79 (s, 3H), 3.37 (dd, *J* = 12.8, 6.9 Hz, 2H), 2.76 (t, *J* = 7.0 Hz, 2H), 1.85 (d, *J* = 9.3 Hz, 3H), 1.64 (d, *J* = 8.2 Hz, 1H), 1.41 – 1.30 (m, 1H), 1.02 (dt, *J* = 15.2, 7.7 Hz, 1H), 0.77 (dp, *J* = 16.8, 6.5, 5.6 Hz, 6H). ^{13}C NMR (500 MHz, DMSO-d_6) δ 171.50, 169.46, 160.58, 159.58, 133.85, 132.00, 128.13, 124.61, 124.48, 122.19, 114.82, 113.05, 112.87, 57.33, 55.64, 55.36, 38.96, 36.84, 28.60, 24.73, 22.94, 15.78, 11.46. HRMS-ESI (*m/z*): $[M+H]^+$ calcd for $C_{23}H_{29}FN_2O_3$ 401.2235; found 401.2234.

Synthesis of BiPH 250

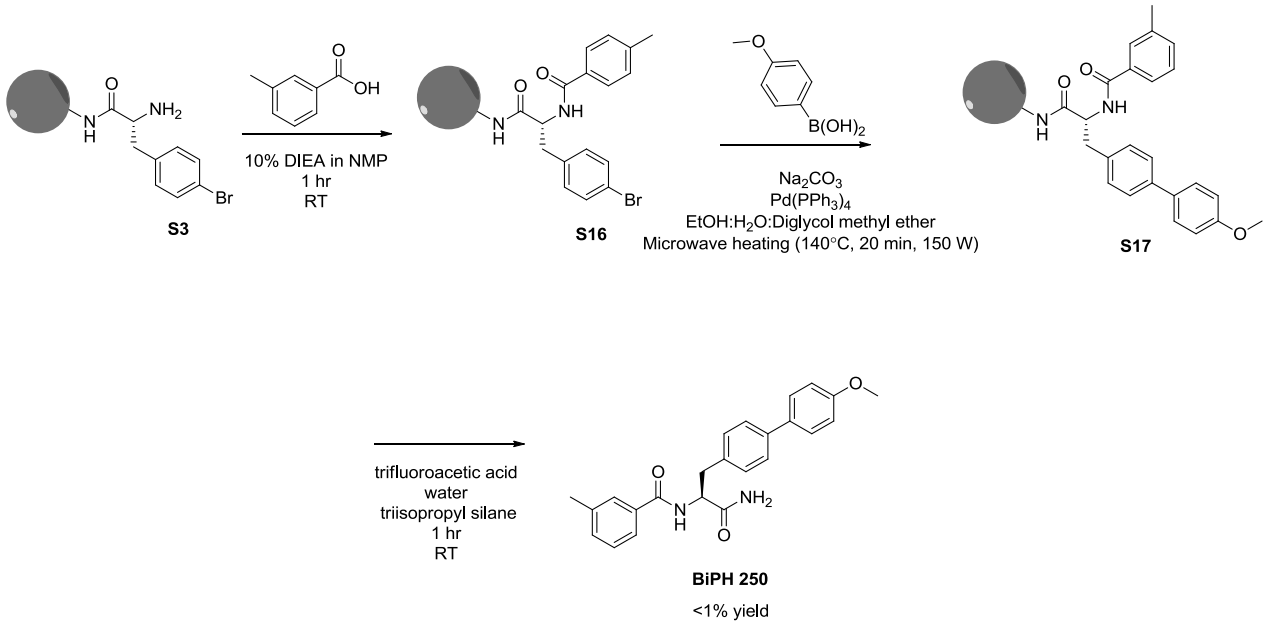

Synthesis of **S17**. To the resin beads of compound **S3** (400 mg), a solution of m-toluic acid (136 mg, 1.0 mmol, and HBTU (380 mg, 1.0 mmol) in 4 mL activator solution was added and allowed to shake at room temperature overnight. The vessel was then evacuated, washed with NMP (3 x 5 mL) and evaluated by Kaiser Test to ensure complete coupling. The beads were subsequently rinsed with DCM (3 x 5 mL) and dried arriving at compound **S17**.

Synthesis of compound **S18**. The resin beads containing compound **S17** were transferred to a dried, glass microwave vessel equipped with a stir bar. To this vessel, 4-methoxyphenyl boronic acid (304 mg, 2.0 mmol), sodium carbonate (212 mg, 2.0 mmol), tetrakis(triphenylphosphine)palladium (0) (24 mg, 0.021 mmol) were added. A solvent mixture of ethanol:water:diglycol methyl ether (2:1:10) was subsequently added and the reaction vessel was placed into a CEM microwave synthesizer. The reaction was heated to 140 °C for 20 minutes at 150 W of power. After cooling, the reaction mixture was washed with deionized water (~50 mL), NMP (3 x 10 mL), Methanol (3 x 10 mL), Diglycol methyl ether (3 x 10 mL), and DCM (3 x 10 mL), resulting in the preparation of compound **S18** on resin.

Synthesis of **BiPH 250**. Compound **S18** was separated from resin using cleavage conditions (trifluoroacetic acid 3.8 mL, water 0.1 mL, triisopropyl silane 0.1 mL) for 1 hour with intermittent stirring. The resulting solution was filtered, collected and the solvent was removed under reduced pressure. The resulting oil was purified via reverse-phase chromatography

(linear gradient of 5 → 95% CH_3CN (0.1% HOAc) in H_2O (0.1% HOAc)) to yield **BiPH 250** (2.0 mg, <1% yield). **Spectral data**. ^{1}H NMR (500 MHz, DMSO-d_6) δ 8.44 (d, *J* = 8.4 Hz, 1H), 7.66 – 7.42 (m, 6H), 7.41 – 7.24 (m, 4H), 7.11 (d, *J* = 2.5 Hz, 2H), 7.01 – 6.94 (m, 2H), 4.66 (ddd, *J* = 10.5, 8.4, 4.2 Hz, 1H), 3.77 (s, 3H), 3.20 – 3.08 (m, 1H), 3.08 – 2.97 (m, 1H), 2.34 (s, 3H). ^{13}C NMR (500 MHz, DMSO-d_6) δ 173.82, 166.76, 159.14, 138.10, 137.86, 137.53, 134.54, 132.73, 132.24, 128.51, 128.40, 127.98, 126.22, 124.99, 114.72, 55.58, 55.16, 37.27, 21.39. HRMS-ESI (*m/z*): $[M+H]^+$ calcd for $C_{24}H_{24}N_2O_3$ 389.1860; found 389.1862.

Synthesis of BiPH 259

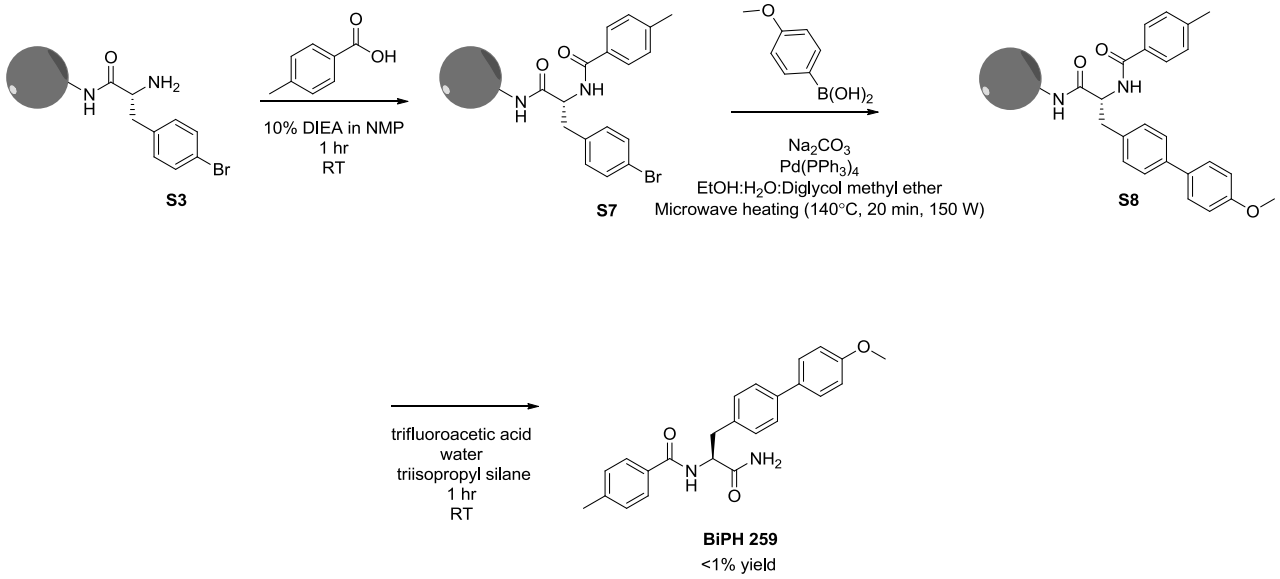

Synthesis of **S7**. To the resin beads of compound **S3** (400 mg), a solution of p-toluic acid (136 mg, 1.0 mmol, and HBTU (380 mg, 1.0 mmol) in 4 mL activator solution was added and allowed to shake at room temperature overnight. The vessel was then evacuated, washed with NMP (3 x 5 mL) and evaluated by Kaiser Test to ensure complete coupling. The beads were subsequently rinsed with DCM (3 x 5 mL) and dried arriving at compound **S7**.

Synthesis of compound **S8**. The resin beads containing compound **S7** were transferred to a dried, glass microwave vessel equipped with a stir bar. To this vessel, 4-methoxyphenyl boronic acid (304 mg, 2.0 mmol), sodium carbonate (212 mg, 2.0 mmol), tetrakis(triphenylphosphine)palladium (0) (24 mg, 0.021 mmol) were added. A solvent mixture of ethanol:water:diglycol methyl ether (2:1:10) was subsequently added and the reaction vessel was placed into a CEM microwave synthesizer. The reaction was heated to 140 °C for 20

minutes at 150 W of power. After cooling, the reaction mixture was washed with deionized water (~50 mL), NMP (3 x 10 mL), Methanol (3 x 10 mL), Diglycol methyl ether (3 x 10 mL), and DCM (3 x 10 mL), resulting in the preparation of compound **S8** on resin.

Synthesis of **BiPH 259**. Compound **S8** was separated from resin using cleavage conditions (trifluoroacetic acid 3.8 mL, water 0.1 mL, triisopropyl silane 0.1 mL) for 1 hour with intermittent stirring. The resulting solution was filtered, collected and the solvent was removed under reduced pressure. The resulting oil was purified via reverse-phase chromatography (linear gradient of 5 → 95% CH_3CN (0.1% HOAc) in H_2O (0.1% HOAc)) to yield **BiPH 259** as a white crystalline solid (2 mg, <1% yield). **Spectral data** ^{1}H NMR (500 MHz, DMSO-d_6) δ 8.43 (d, *J* = 8.4 Hz, 1H), 7.76 – 7.68 (m, 2H), 7.59 – 7.47 (m, 4H), 7.41 – 7.34 (m, 2H), 7.28 – 7.21 (m, 2H), 7.11 (s, 2H), 7.01 – 6.94 (m, 2H), 4.64 (ddd, *J* = 10.5, 8.3, 4.1 Hz, 1H), 3.77 (s, 3H), 3.11 (dd, *J* = 13.7, 4.2 Hz, 1H), 3.01 (dd, *J* = 13.7, 10.5 Hz, 1H), 2.33 (s, 3H).. ^{13}C NMR (500 MHz, DMSO-d_6) δ 173.86, 164.47, 158.07, 131.75, 130.17, 130.13, 129.18, 129.14, 128.01, 127.98, 127.89, 126.22, 114.72, 106.15, 62.52, 55.59, 25.47, 14.76. HRMS-ESI (*m/z*): $[M+H]^+$ calcd for $C_{24}H_{24}N_2O_3$ 389.1860; found 389.1857.

Synthesis of BiPH 264

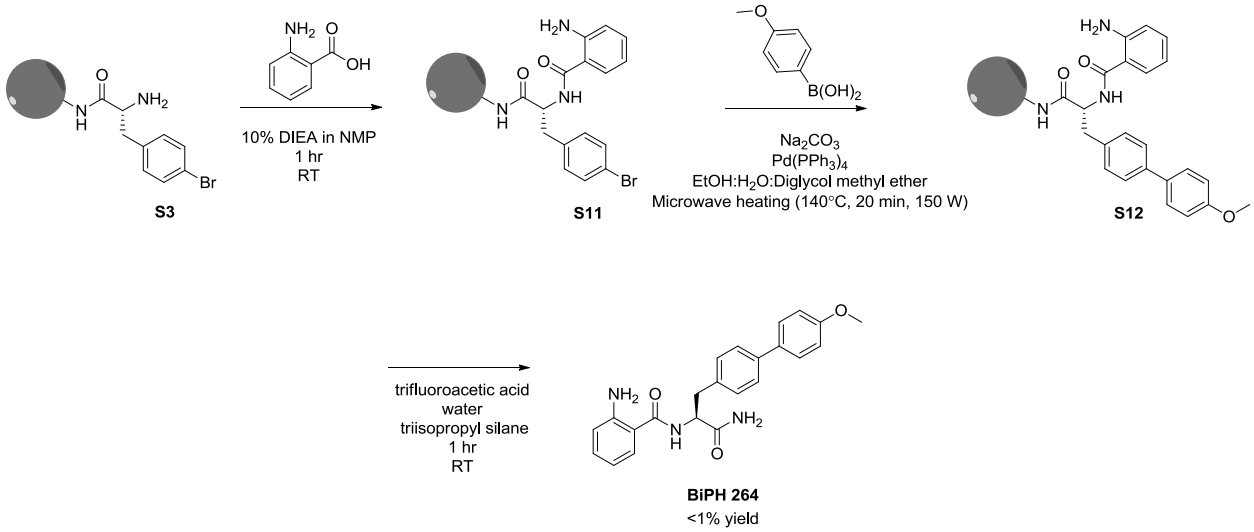

Synthesis of **S11**. To the resin beads of compound **S3** (200 mg), a solution of 2-aminobenzoic acid (200 mg, 1.46 mmol) and HBTU (380 mg, 1.0 mmol) in 4 mL activator solution was added and allowed to shake at room temperature overnight. The vessel was then evacuated, washed

with NMP (3 x 5 mL) and evaluated by Kaiser Test to ensure complete coupling. The beads were subsequently rinsed with DCM (3 x 5 mL) and dried arriving at compound **S11** on resin.

Synthesis of compound **S12**. The resin beads containing compound **S11** were transferred to a dried, glass microwave vessel equipped with a stir bar. To this vessel, 4-methoxyphenyl boronic acid (304 mg, 2.0 mmol), sodium carbonate (212 mg, 2.0 mmol), tetrakis(triphenylphosphine)palladium (0) (24 mg, 0.021 mmol) were added. A solvent mixture of ethanol:water:diglycol methyl ether (2:1:10) was subsequently added and the reaction vessel was placed into a CEM microwave synthesizer. The reaction was heated to 140 °C for 20 minutes at 150 W of power. After cooling, the reaction mixture was washed with deionized water (~50 mL), NMP (3 x 10 mL), Methanol (3 x 10 mL), Diglycol methyl ether (3 x 10 mL), and DCM (3 x 10 mL), resulting in the preparation of compound **S12** on resin.

Synthesis of **BiPH 264**. Compound **S12** was separated from resin using cleavage conditions (trifluoroacetic acid 3.8 mL, water 0.1 mL, triisopropyl silane 0.1 mL) for 1 hour with intermittent stirring. The resulting solution was filtered, collected and the solvent was removed under reduced pressure. The resulting oil was purified via reverse-phase chromatography (linear gradient of 5 → 95% CH_3CN (0.1% HOAc) in H_2O (0.1% HOAc)) to yield **BiPH 264** as a tan solid (3 mg, <1% yield). **Spectral data**. ^{1}H NMR (500 MHz, DMSO-d_6) δ 8.25 (d, *J* = 8.3 Hz, 1H), 7.60 – 7.47 (m, 6H), 7.42 – 7.34 (m, 2H), 7.24 – 7.07 (m, 2H), 7.03 – 6.95 (m, 2H), 6.69 (dd, *J* = 8.1, 1.3 Hz, 1H), 6.57 (t, *J* = 7.4 Hz, 1H), 4.60 (ddd, *J* = 10.5, 8.2, 4.2 Hz, 1H), 3.78 (s, 3H), 3.10 (dd, *J* = 13.8, 4.2 Hz, 1H), 3.01 (dd, *J* = 13.7, 10.5 Hz, 1H). ^{13}C NMR (500 MHz, DMSO-d_6) δ 174.01, 169.14, 159.14, 153.41, 137.62, 132.24, 130.11, 128.92, 128.88, 128.00, 126.25, 118.77, 116.82, 114.78, 114.75, 114.72, 62.45, 55.58, 14.71. HRMS-ESI (*m/z*): $[M+Na]^+$ calcd for $C_{23}H_{23}N_3O_3$ 412.1632; found 412.1635.

Synthesis of BiPH 280

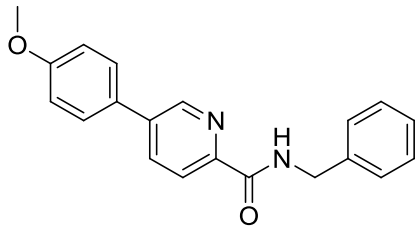

This compound was prepared by the methods set forth by Hangauer, David G.; et al.[2]

A.3: Spectral data for BiPH compounds

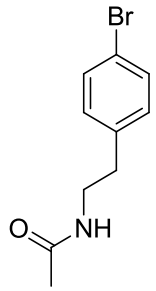

S1

^{1}H

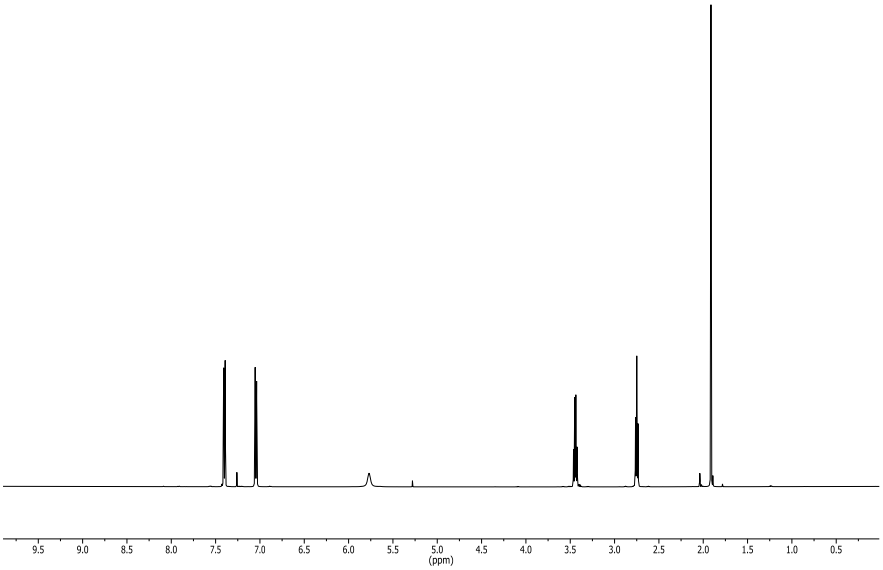

^{13}C

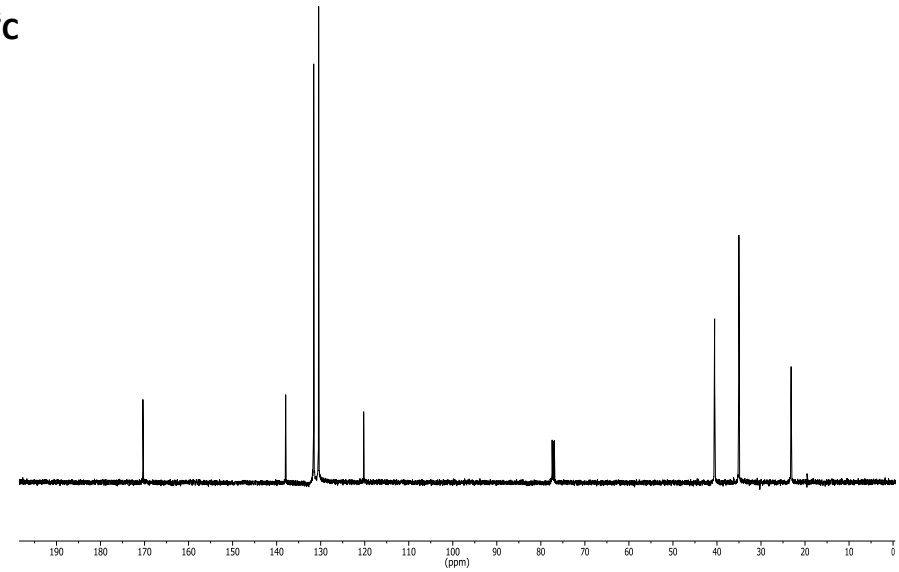

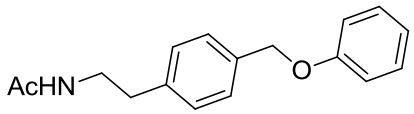

BiPH 47

^{1}H

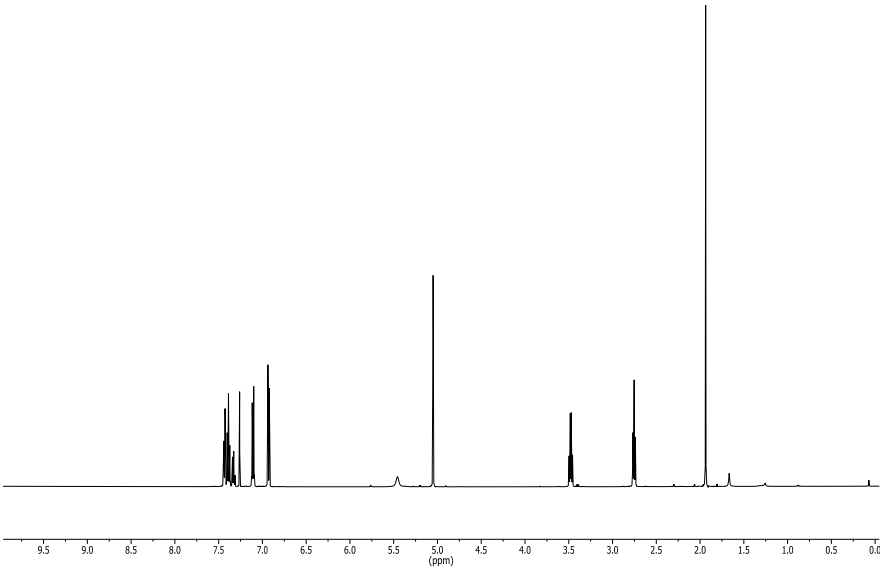

^{13}C

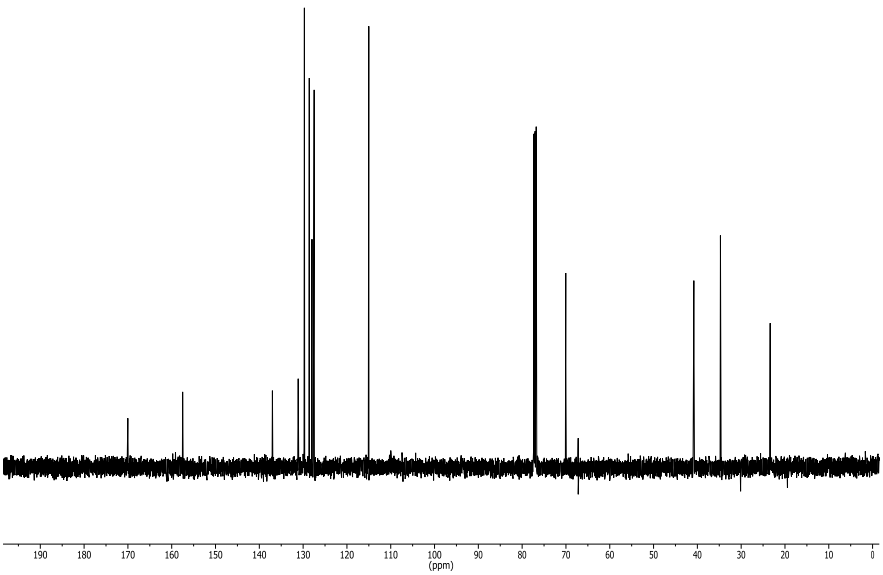

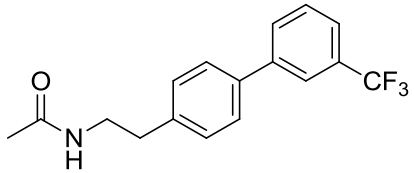

BiPH 50

^{1}H

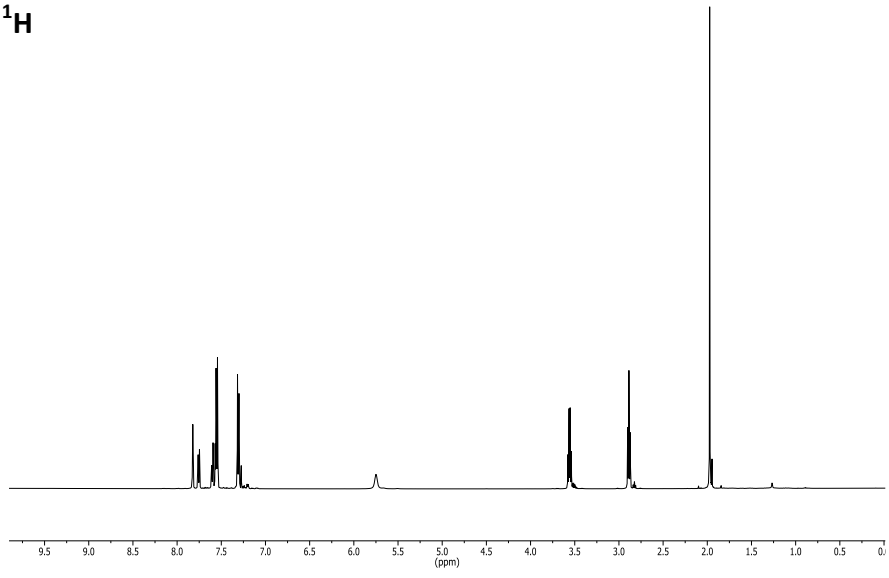

^{13}C

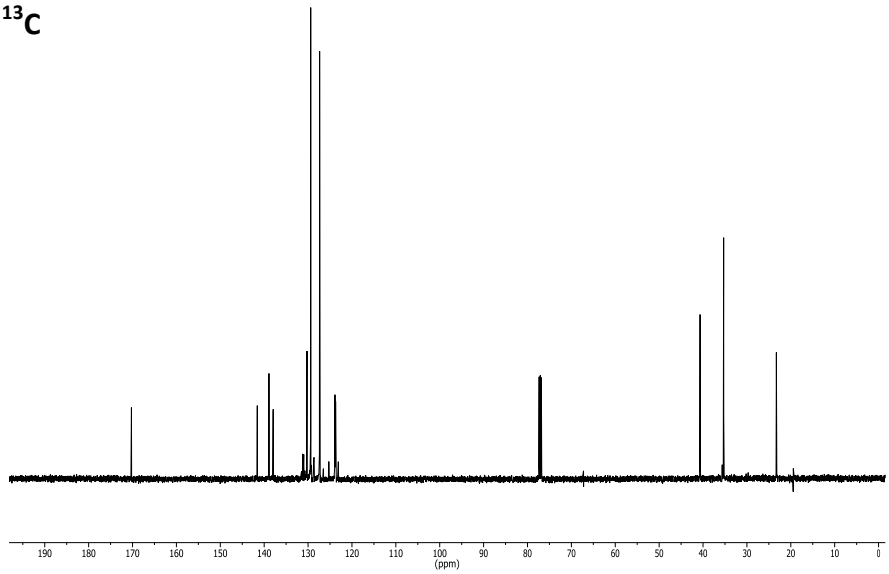

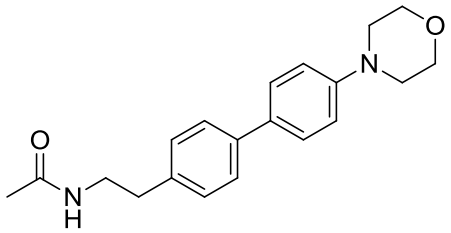

BiPH 65

^{1}H

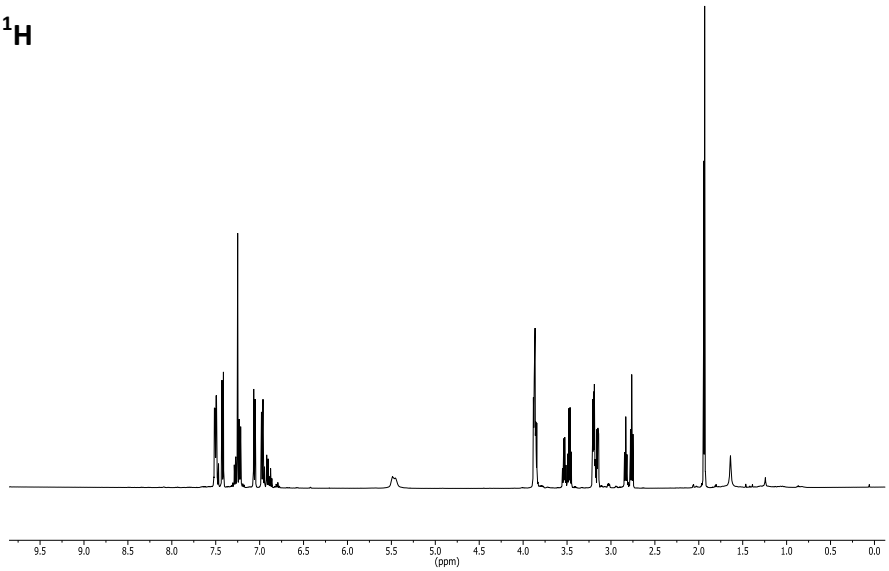

^{13}C

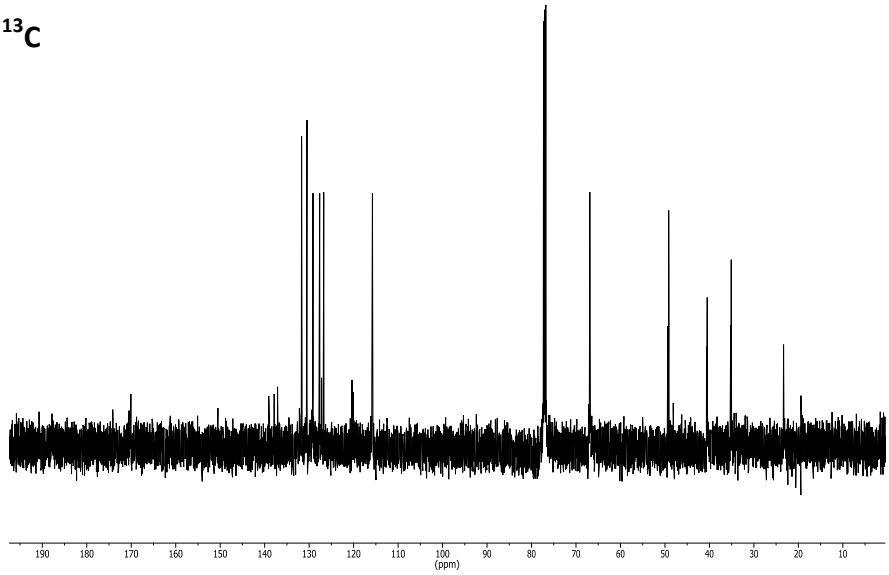

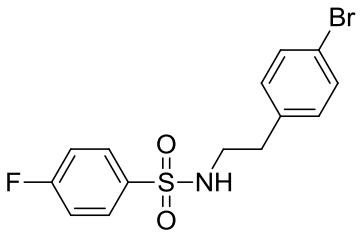
Br
O
F
S
NH
O

S9

^{1}H

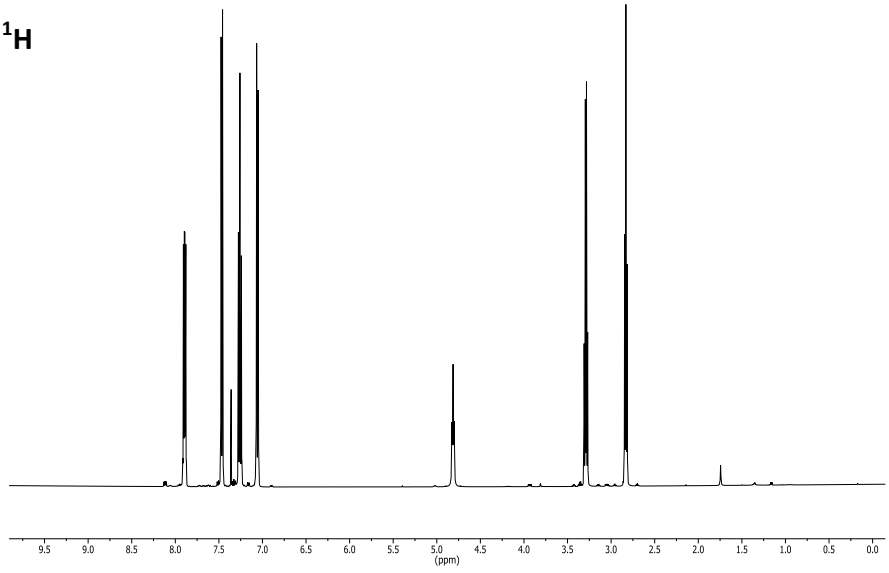
9.5 9.0 8.5 8.0 7.5 7.0 6.5 6.0 5.5 5.0 4.5 4.0 3.5 3.0 2.5 2.0 1.5 1.0 0.5 0.0
(ppm)

^{13}C

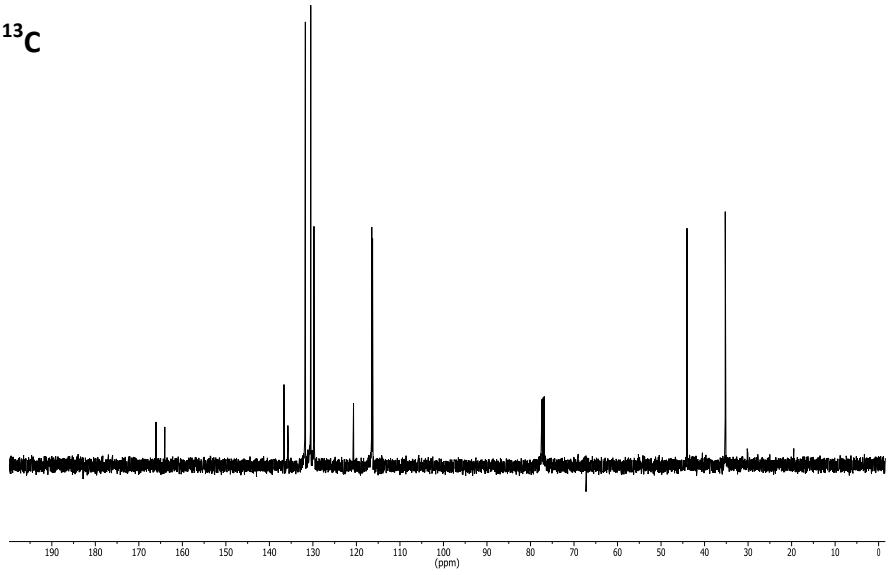
190 180 170 160 150 140 130 120 110 100 90 80 70 60 50 40 30 20 10 0
(ppm)

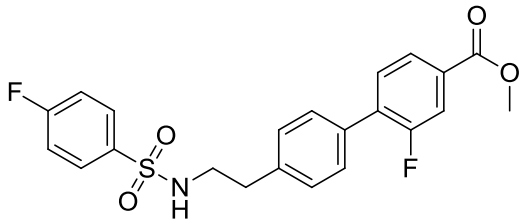

BiPH 85

^{1}H

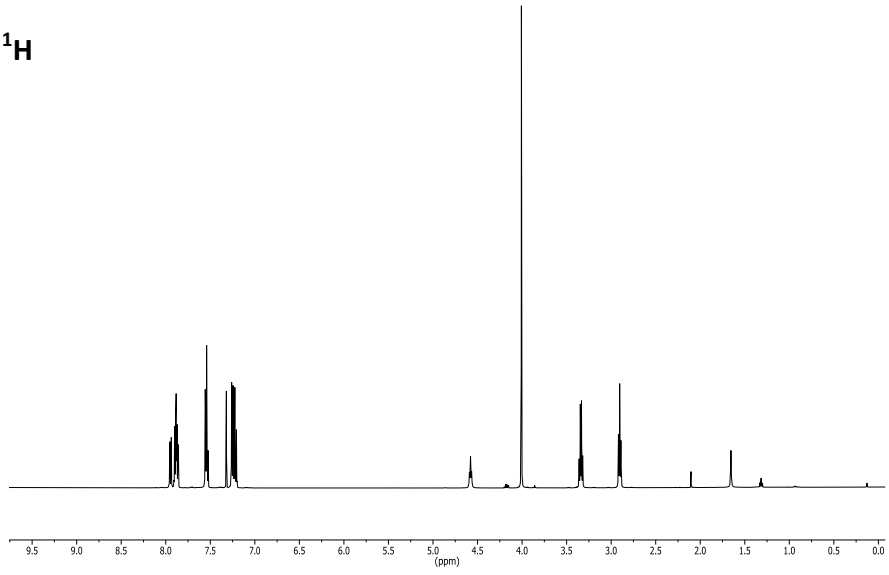

^{13}C

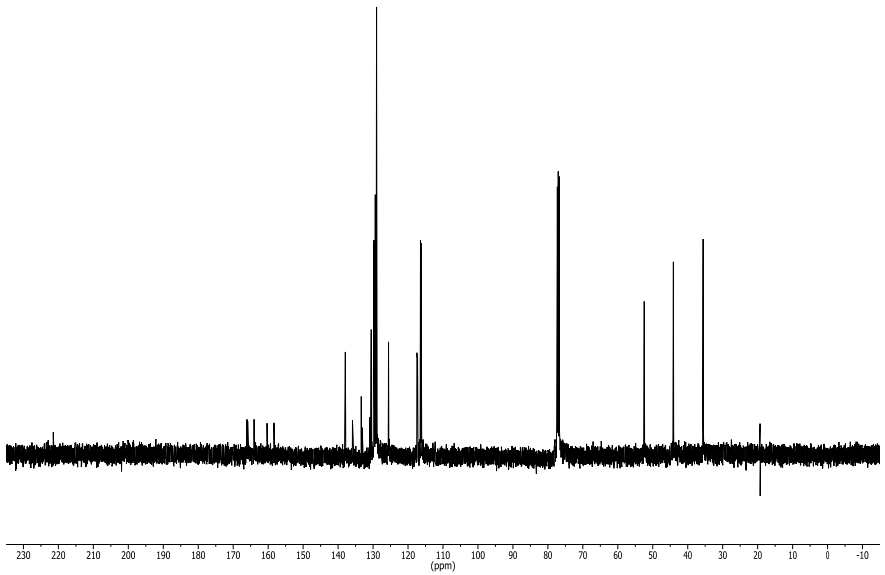

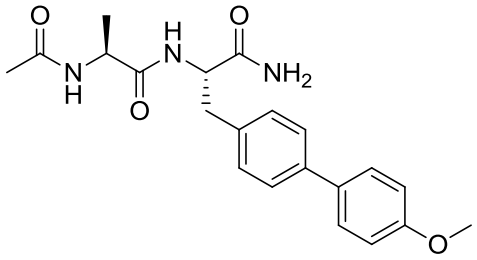

BiPH-101

^{1}H

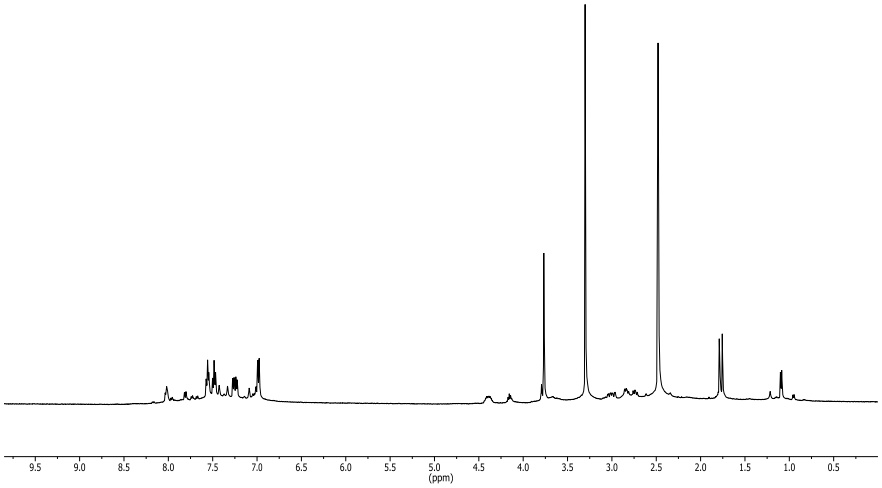

^{13}C

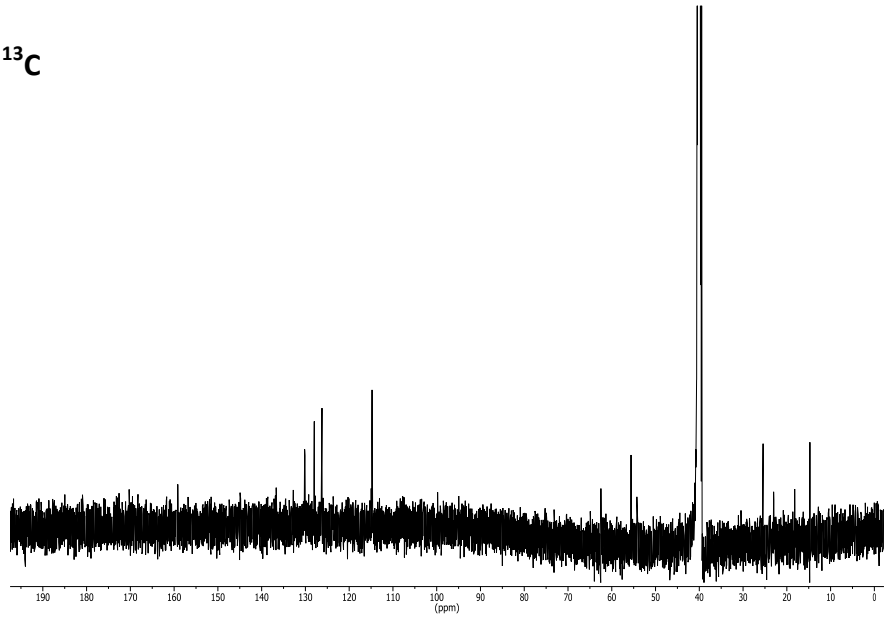

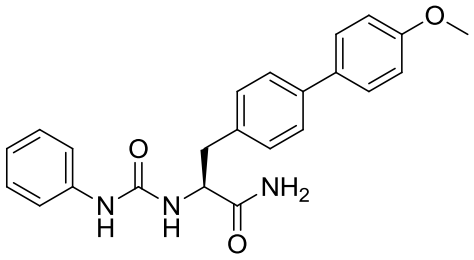

BiPH 108

^{1}H

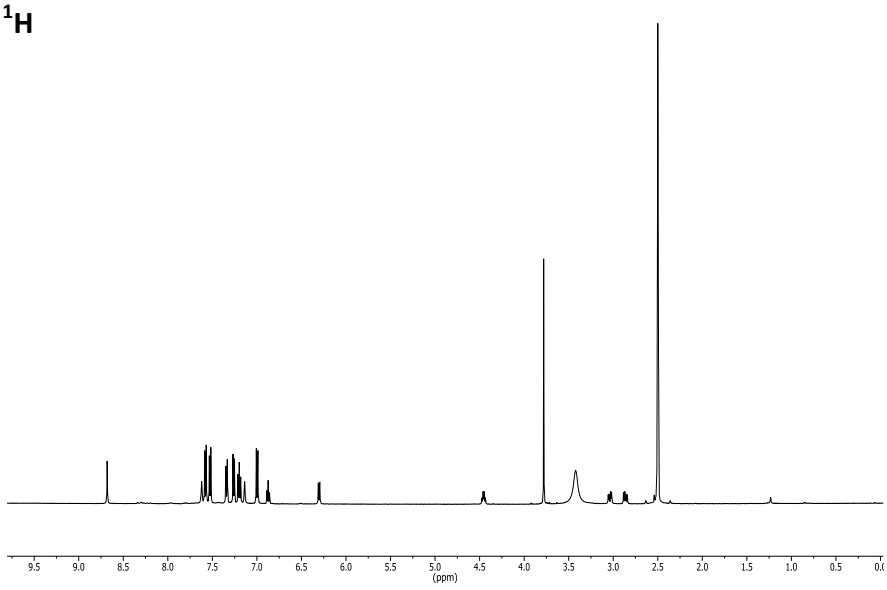

^{13}C

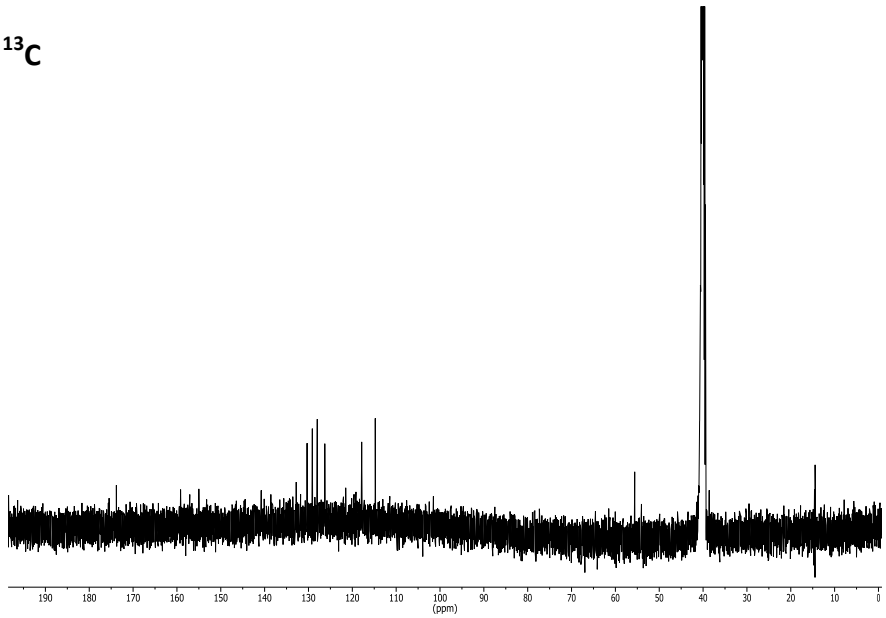

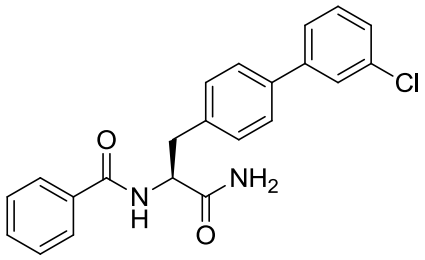

BiPH 142

^{1}H

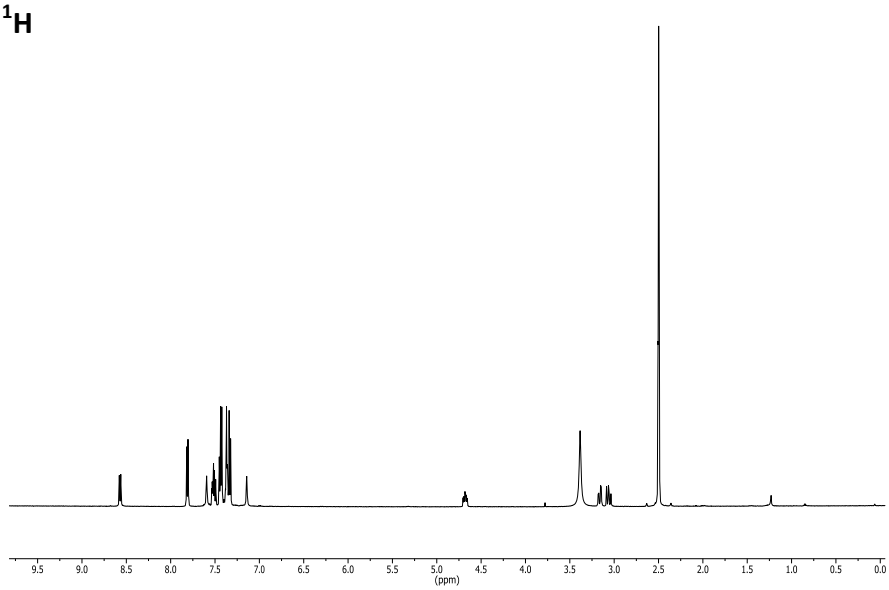

^{13}C

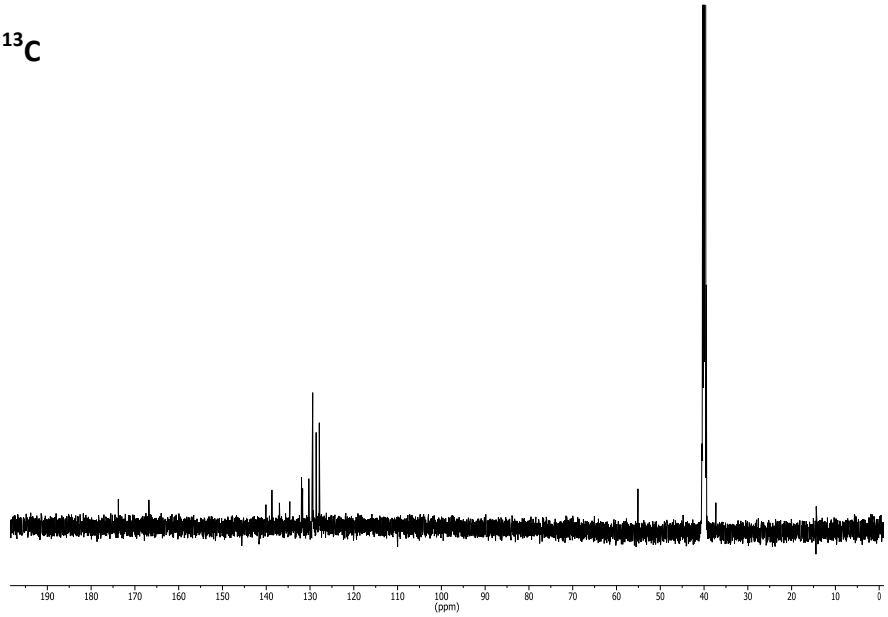

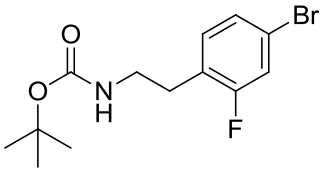
O
O
N
H
Br
F

S15

^{1}H

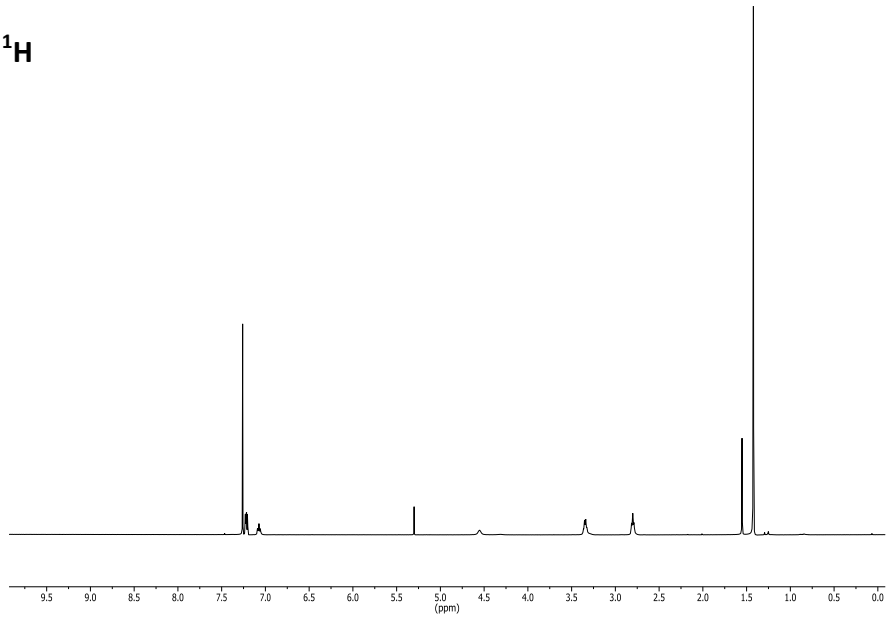
9.5 9.0 8.5 8.0 7.5 7.0 6.5 6.0 5.5 5.0 4.5 4.0 3.5 3.0 2.5 2.0 1.5 1.0 0.5 0.0
(ppm)

^{13}C

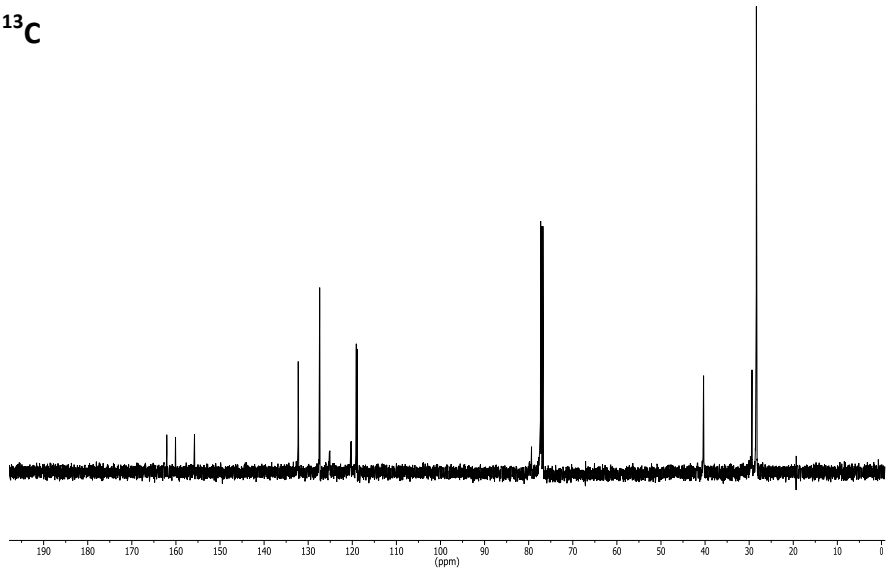
190 180 170 160 150 140 130 120 110 100 90 80 70 60 50 40 30 20 10 0
(ppm)

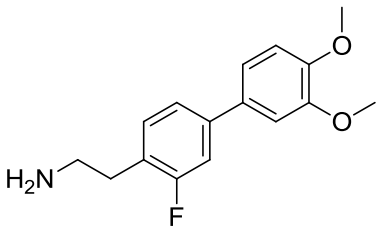

BiPH 230

^{1}H

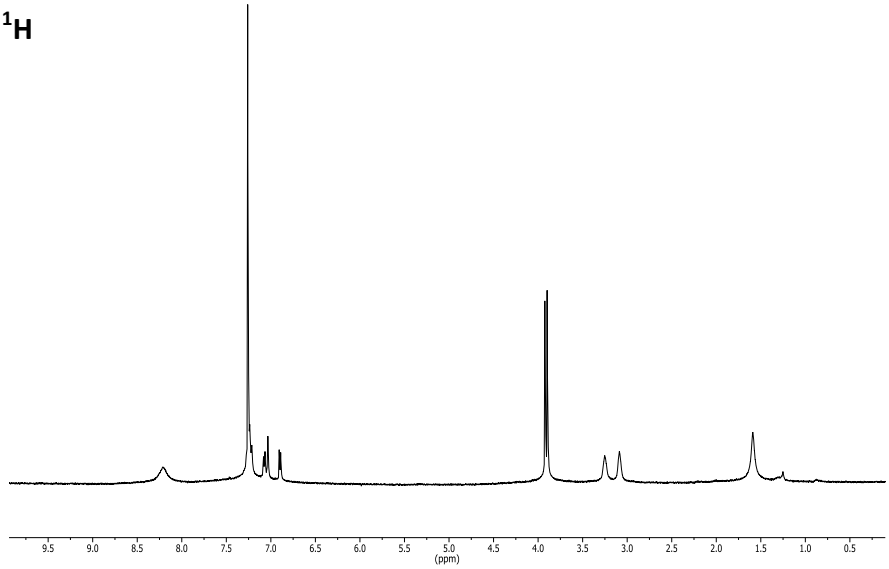

^{13}C

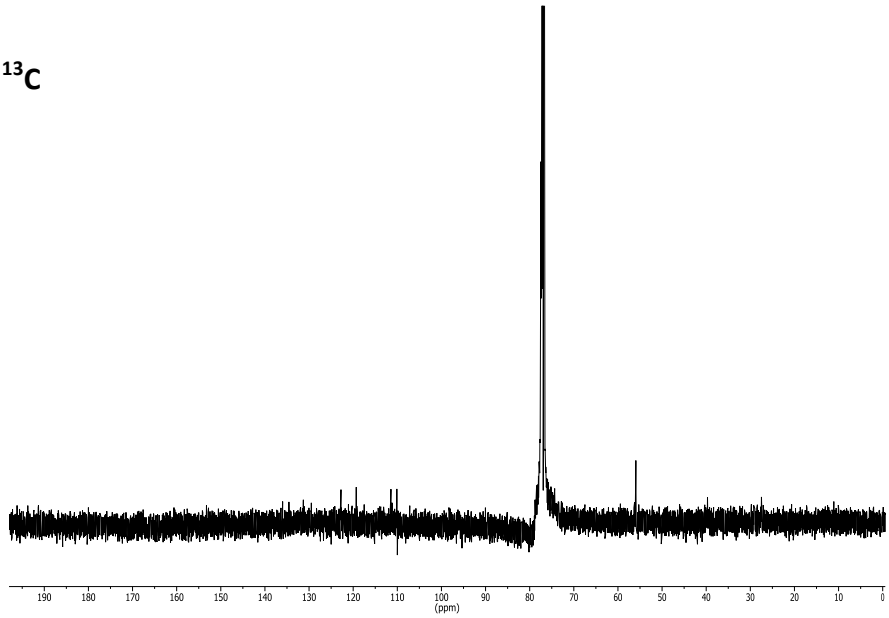

^{19}F

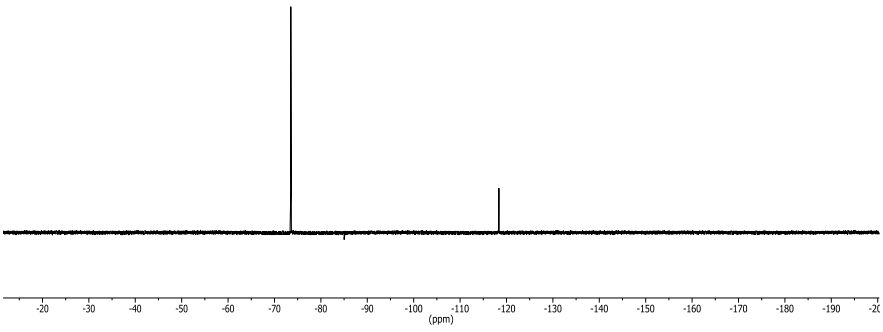

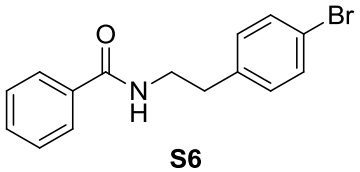
O
N
H
Br

S6

^{1}H

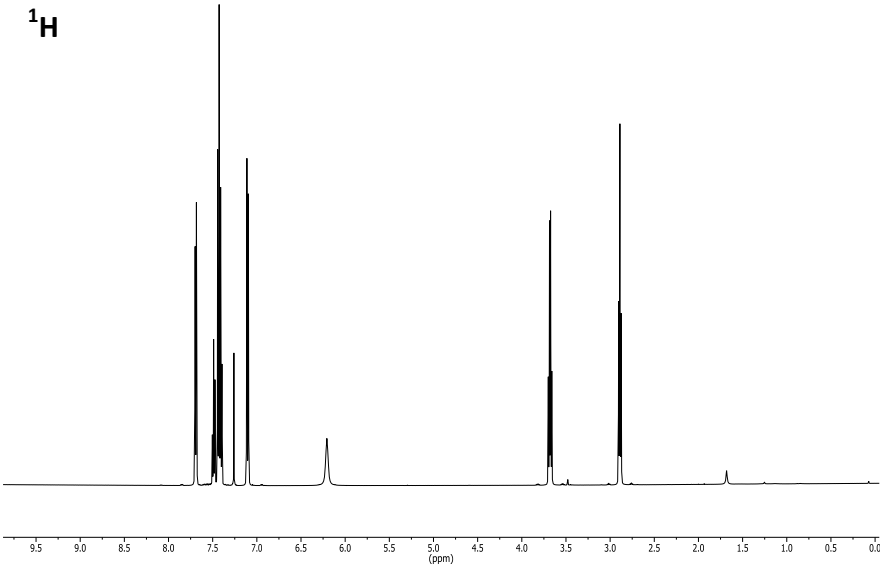
9.5 9.0 8.5 8.0 7.5 7.0 6.5 6.0 5.5 5.0 4.5 4.0 3.5 3.0 2.5 2.0 1.5 1.0 0.5
(ppm)

^{13}C

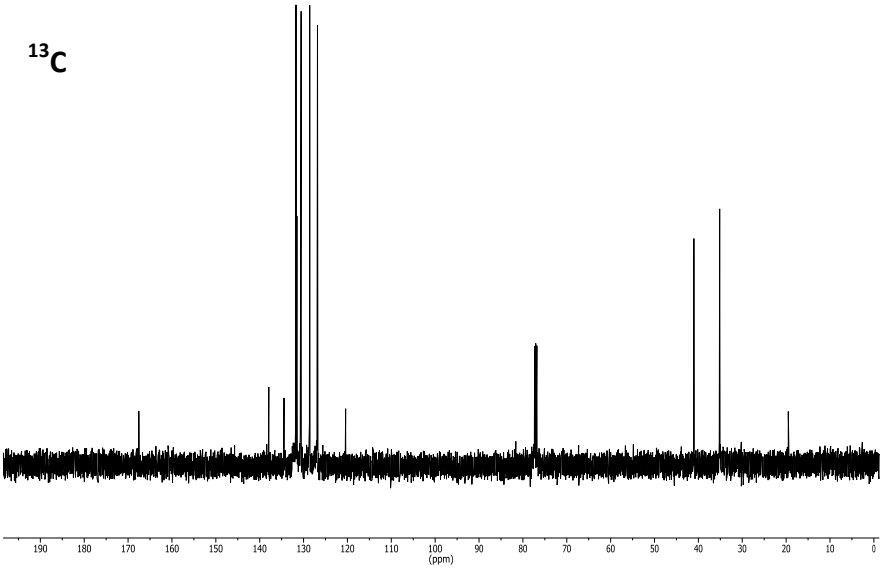
190 180 170 160 150 140 130 120 110 100 90 80 70 60 50 40 30 20 10 0
(ppm)

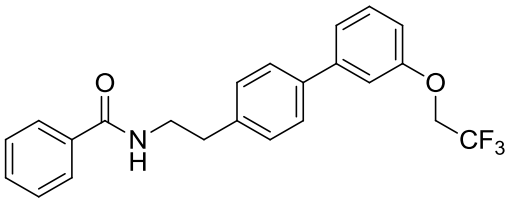

BiPH 240

^{1}H

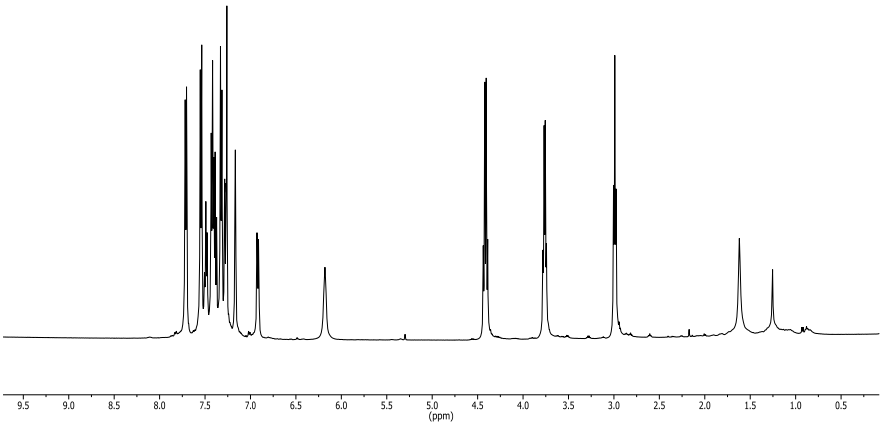

^{13}C

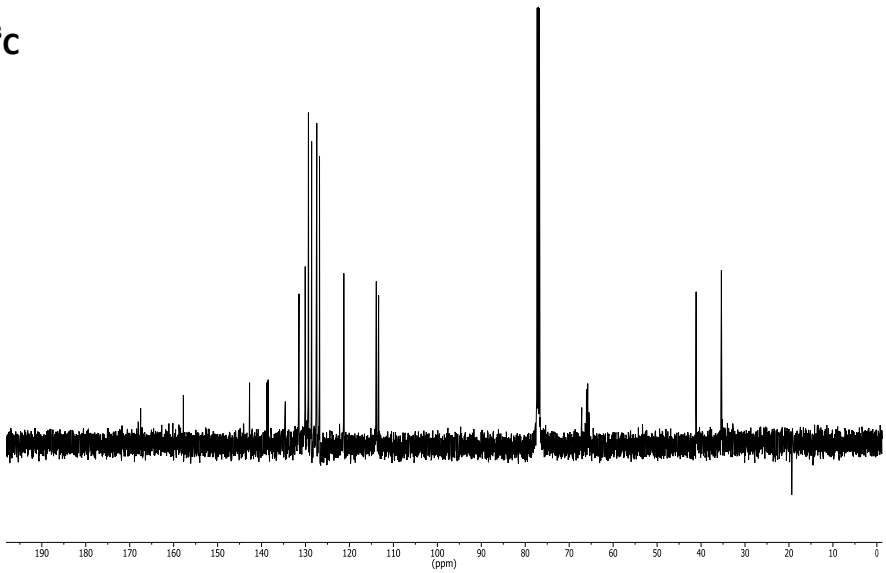

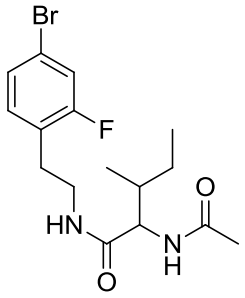
Br
F
HN
O
N
H
O

S10

^{1}H

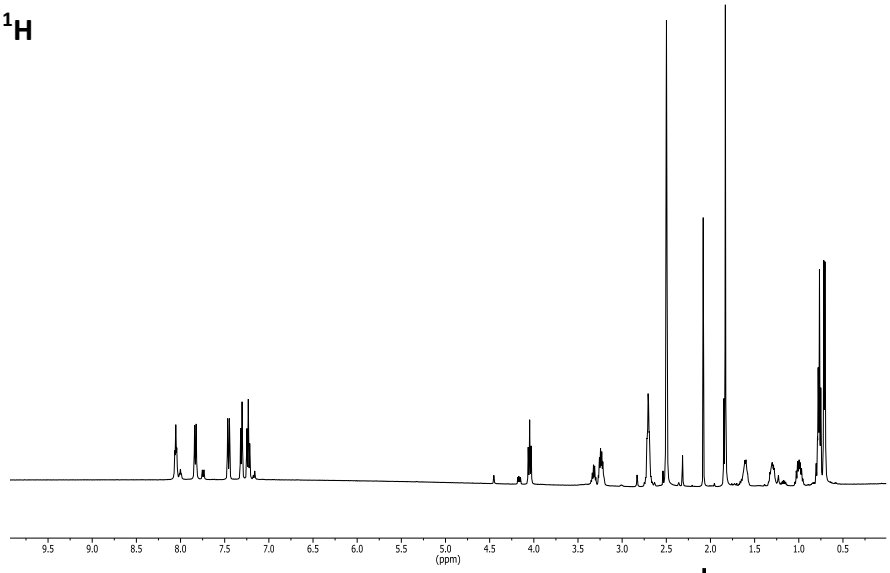
9.5 9.0 8.5 8.0 7.5 7.0 6.5 6.0 5.5 5.0 4.5 4.0 3.5 3.0 2.5 2.0 1.5 1.0 0.5
(ppm)

^{13}C

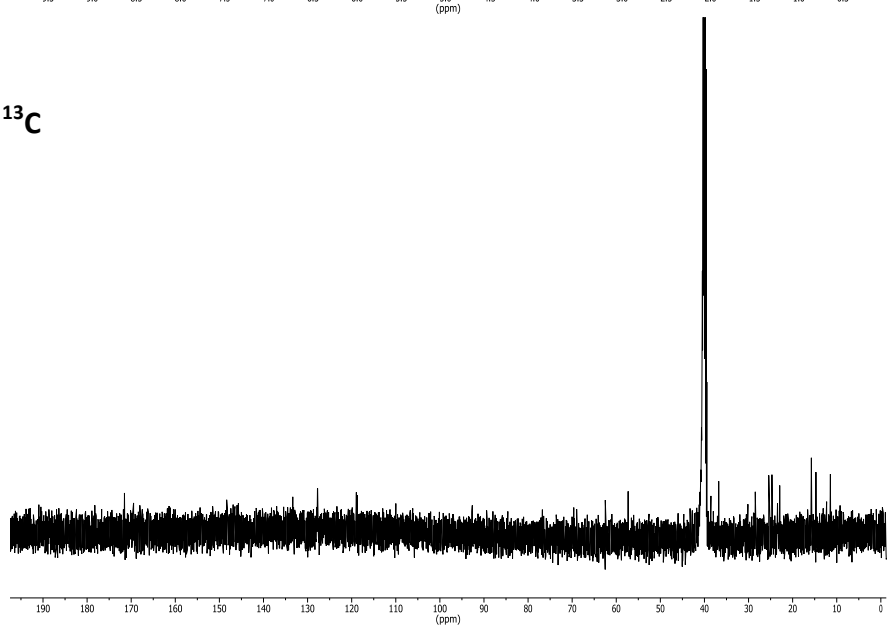
190 180 170 160 150 140 130 120 110 100 90 80 70 60 50 40 30 20 10 0
(ppm)

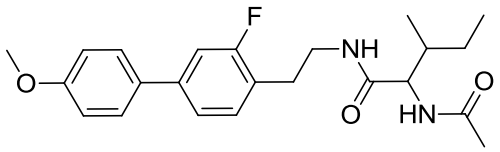

BiPH 248

^{1}H

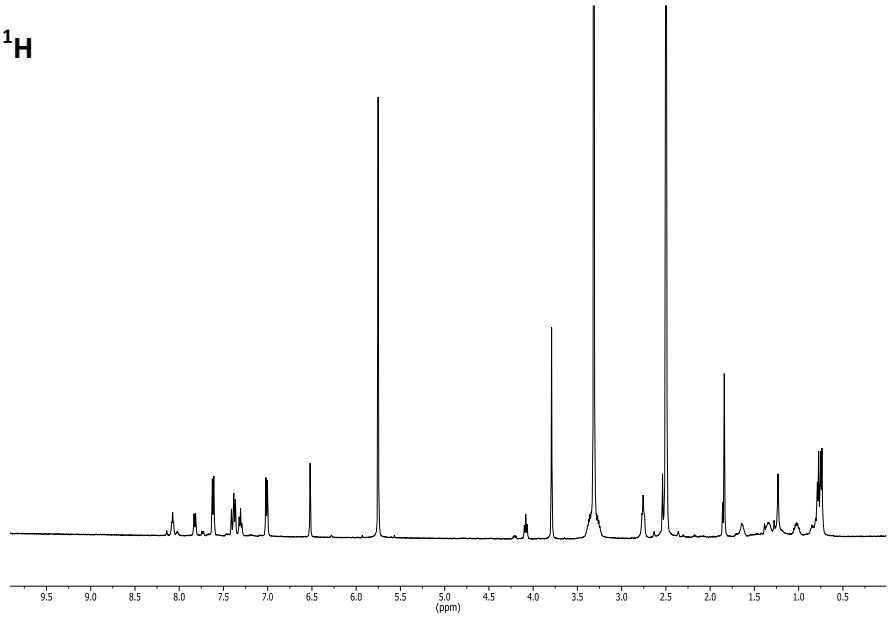

^{13}C

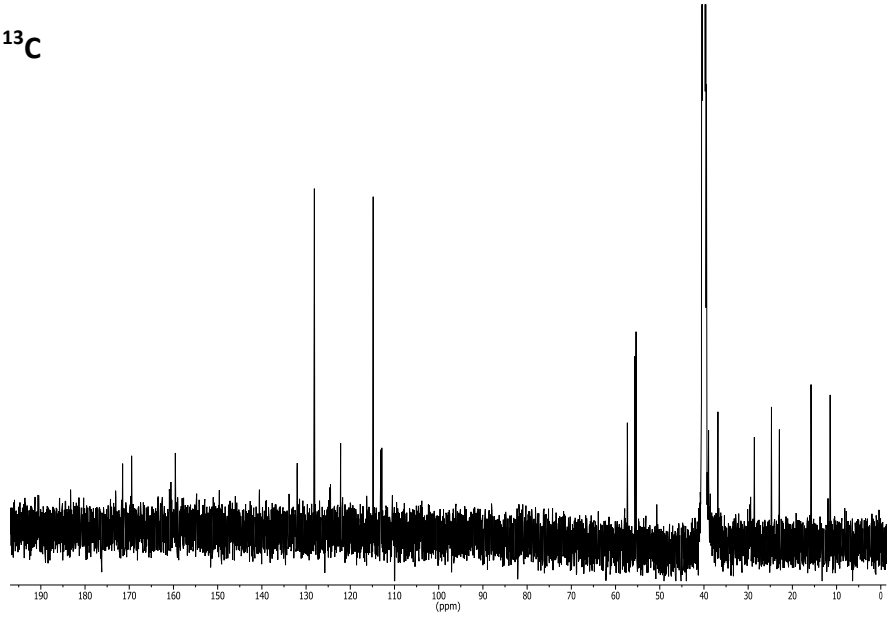

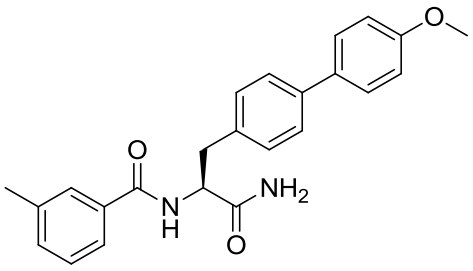

BiPH 250

^{1}H

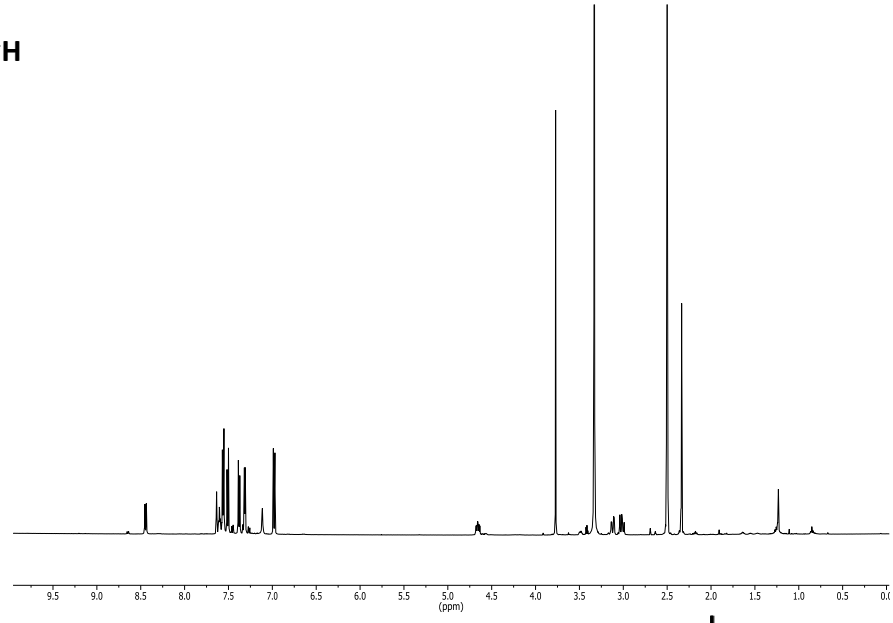

^{13}C

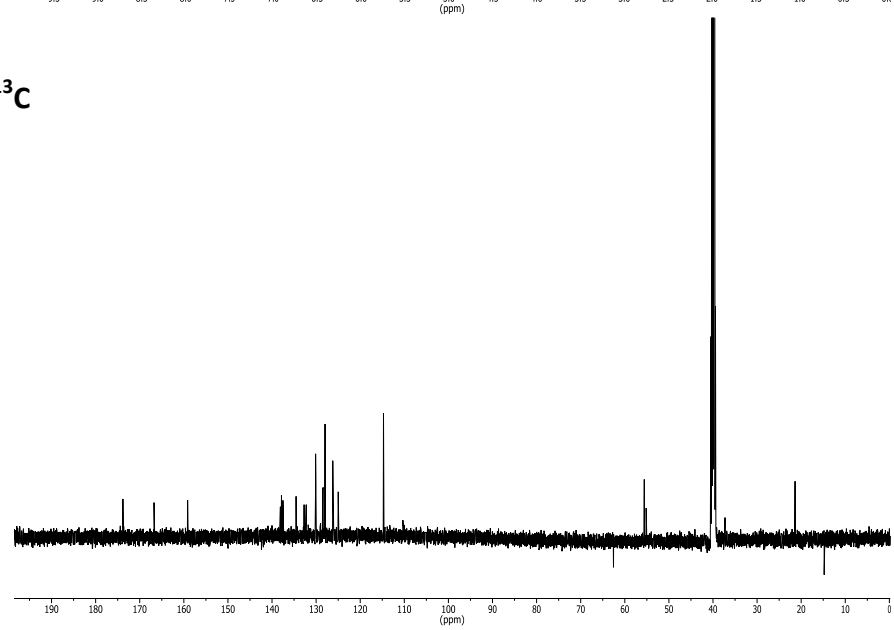

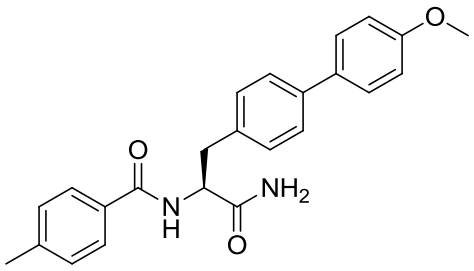

BiPH 259

^{1}H

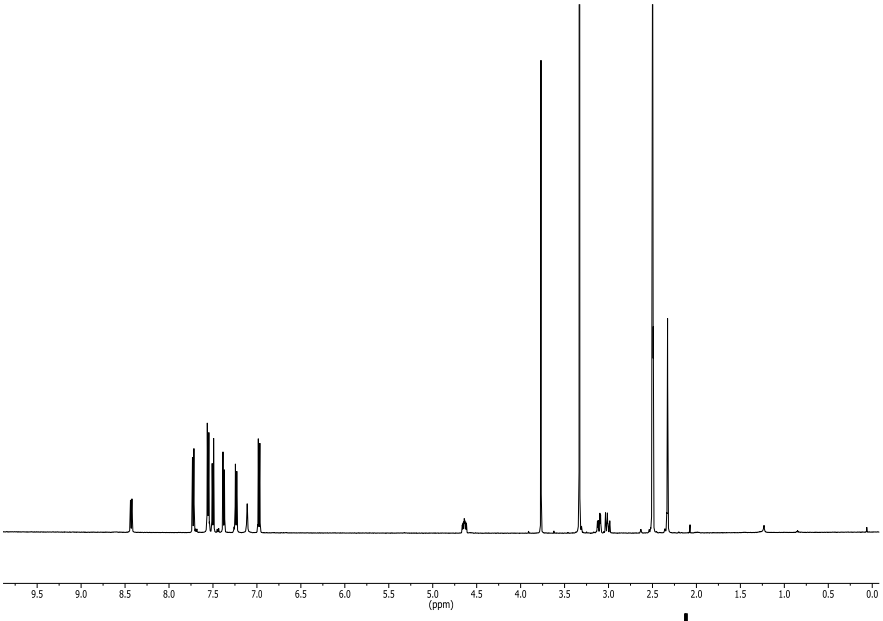

^{13}C

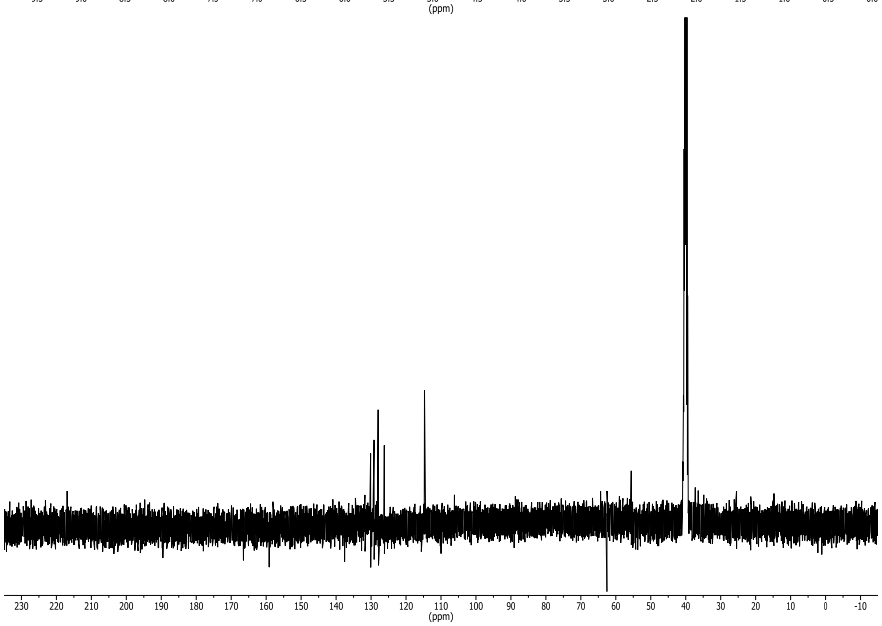

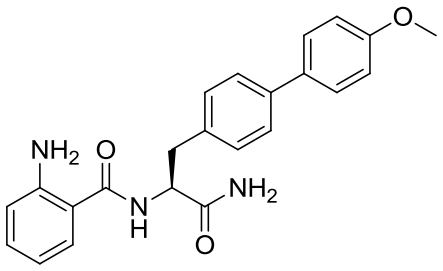

BiPH 264

^{1}H

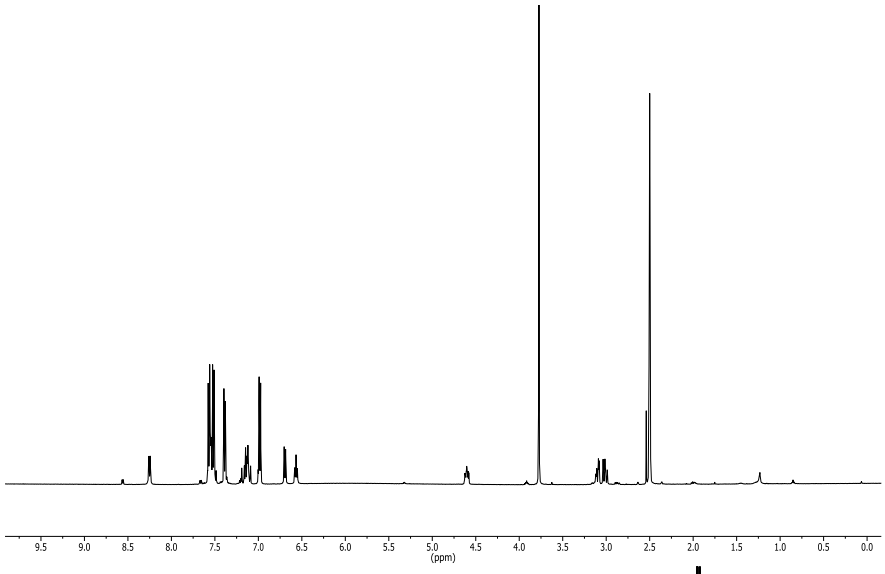

^{13}C

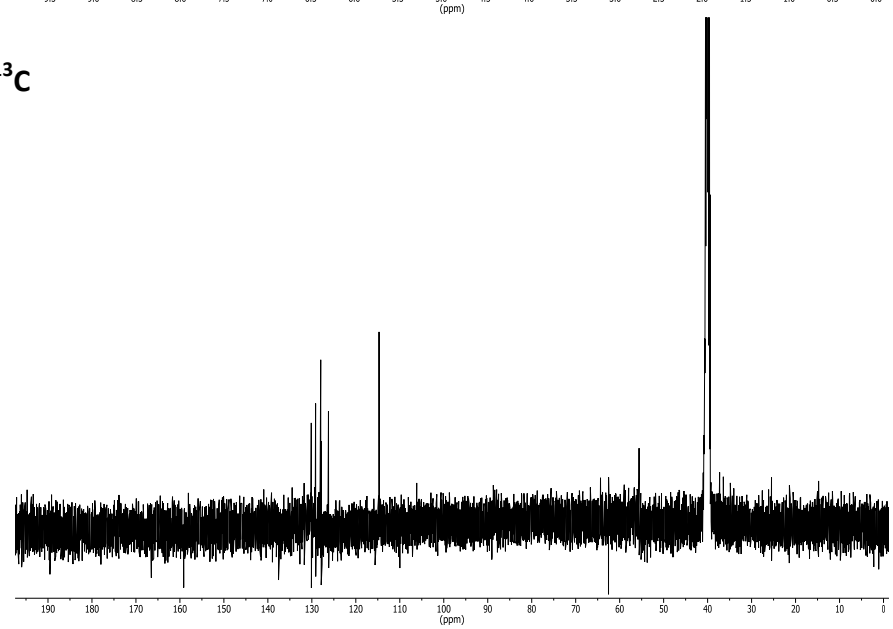

A.5: Biochemical characterization

General procedure for TR-FRET evaluation of inhibitor binding. The TR-FRET assay described here is adapted from a LanthaScreen© Eu Kinase Binding Assay protocol set forth by Invitrogen.[3,4] Reaction volumes of 50 µL were used in 384-well plates. 1 µL of inhibitor stock (5 mM) to wells, save 1 DMSO control well. 600 µL of Buffer F mix were prepared (3 µL of 1 µM enzyme with 6x His-Tag, 4 µL of 300 µM Eu^{3+} antibody, 1.5 µL of 40 µM probe in DMSO, 591.5 µL Buffer F) and 49 µL of the Buffer F mix were added to the wells. The plate was then spun down for 30 seconds at 4000 rpm to remove bubbles from wells. The plate was incubated for 30 minutes in the dark. Reactions had final concentrations of 5 nM enzyme with 6x His-Tag, 2 nM Eu^{3+} antibody, 100 nM ATP-binding probe or 1 nM bisubstrate-binding probe, 100 mM NaCl, 50 mM Tris buffer pH 8, and 0.1% BSA. Reaction progress was monitored at 620 nm and 665 nm (ex. 460 nm) at 30°C. Percent fluorescence data was evaluated for each compound against each probe. Compounds were selected for further evaluation based on their ability to outcompete the bisubstrate probe (fluorescence 50% or less) while not outcompeting the ATP probe (fluorescence above 50%). The probes utilized in this screen are shown below.

ATP-binding probe:

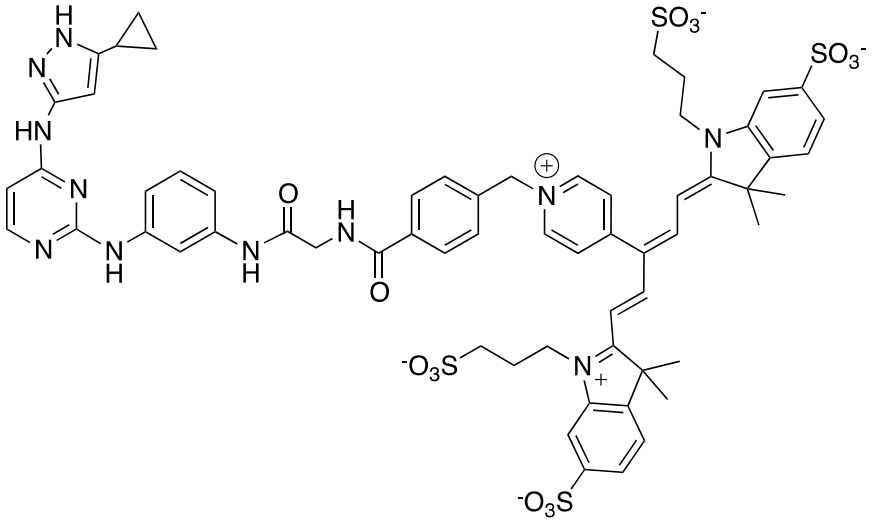

Bisubstrate-binding probe:

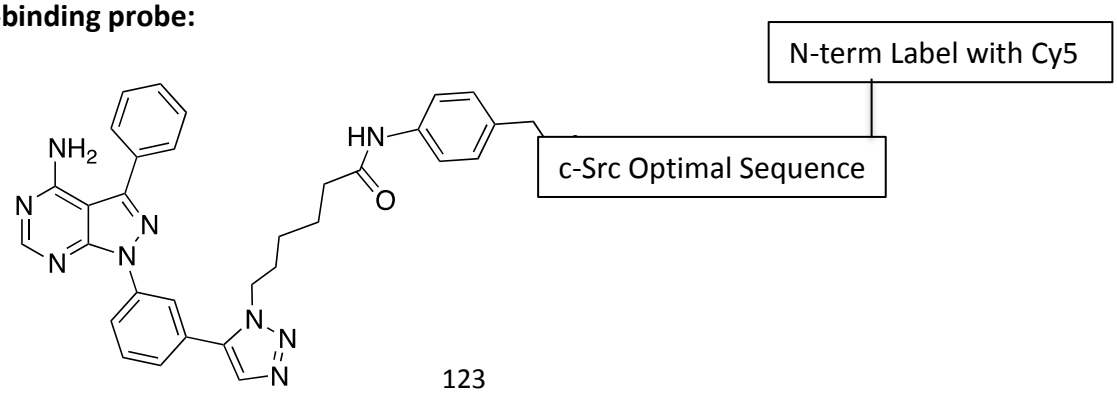

c-Src optimal binding sequence:

NH_2–A–E–E–E–I–Y–G–E–F–E–A–K–K–K–K–COOH

Cy5 structure:

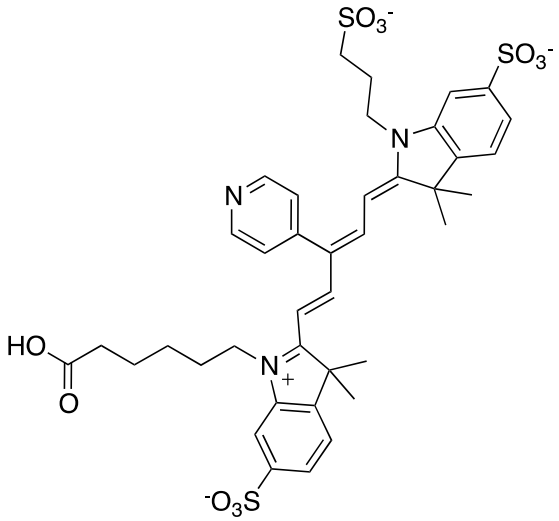

General procedure for determination of inhibitor K_i. A continuous fluorescence assay[5] was used to determine K_i. Reaction volumes of 100 µL were used in 96-well plates. 85 µL of enzyme in buffer was added to each well. 2.5 µL of the appropriate inhibitor dilution (final concentrations typically 1000, 500, 250, 125, 62.5, 31.25, 15.6, 7.8, 3.9 and 0 µM in DMSO) was then added. 2.5 µL of a substrate peptide ("compound 3" as described in Wang et al)[5] solution (1.8 mM in DMSO) was added. The reaction was initiated with 10 µL of ATP (10 mM in water), and reaction progress was immediately monitored at 405 nm (ex. 340 nm) for 10 minutes. Reactions had final concentrations of 30 nM enzyme, 45 µM peptide substrate, 1000 µM ATP, 100 µM Na_3VO_4, 100 mM Tris buffer (pH 8), 10 mM $MgCl_2$, 0.01% Triton X-100. The initial rate data collected was used for determination of K_i values. For K_i determination, the kinetic values were obtained directly from nonlinear regression of substrate-velocity curves in the presence of various concentrations of the inhibitor. The equation Y = Bottom + (Top – Bottom)/(1 + 10^X – LogEC50), X = log(concentration) and Y = binding; was used in the nonlinear regression.

Analytical data for c-Src Kinase Domain K_i determination. Each inhibitor K_i value was determined using two independent experiments, a representative inhibition curve is shown.

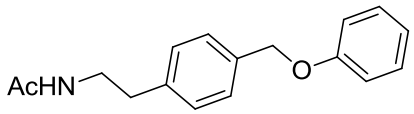

BiPH 47

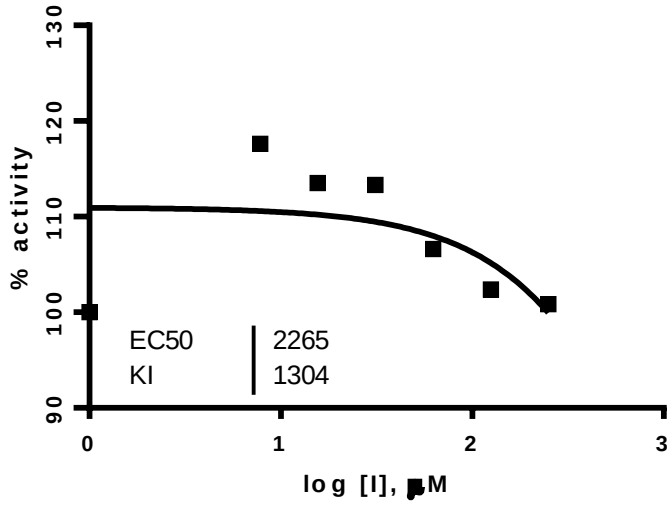

Average IC_{50}: > 1000 µM

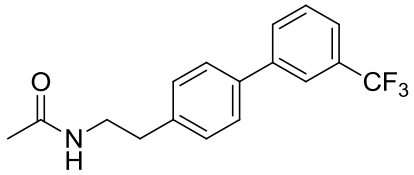

BiPH 50

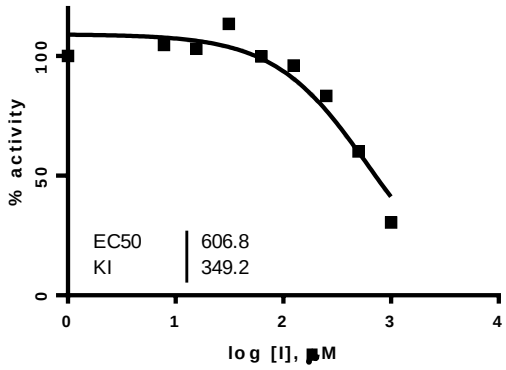

Average IC_{50}: 560.2 ± 65.9 µM

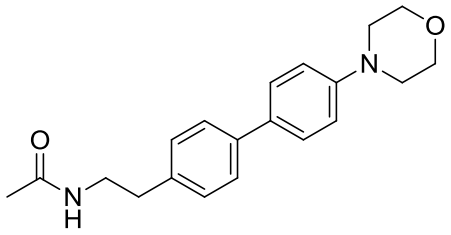

BiPH 65

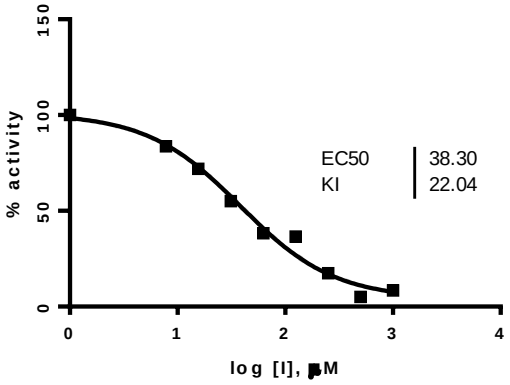

Average IC_{50}: 60.36 ± 31.2 µM

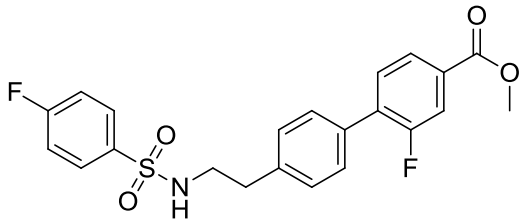

BiPH 85

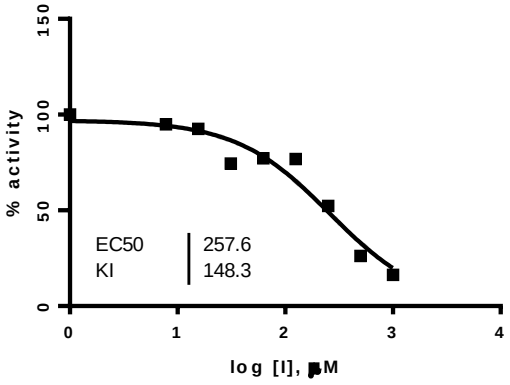

Average IC_{50}: 260.0 ± 3.3 µM

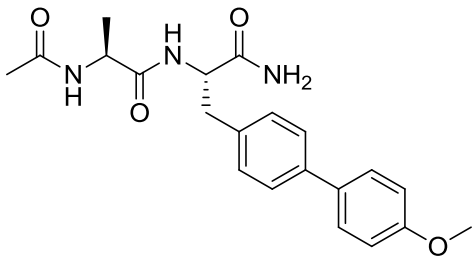

BiPH-101

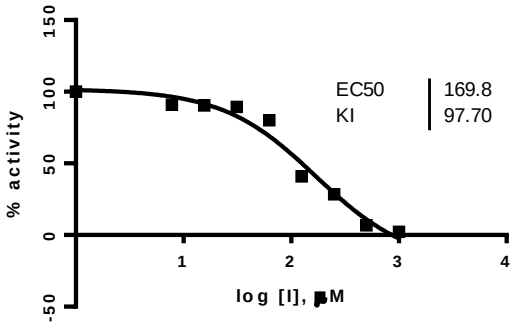

Average IC_{50}: 191.5 ± 30.6 µM

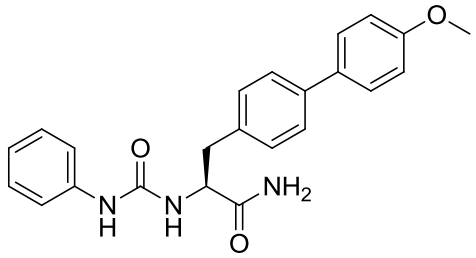

BiPH 108

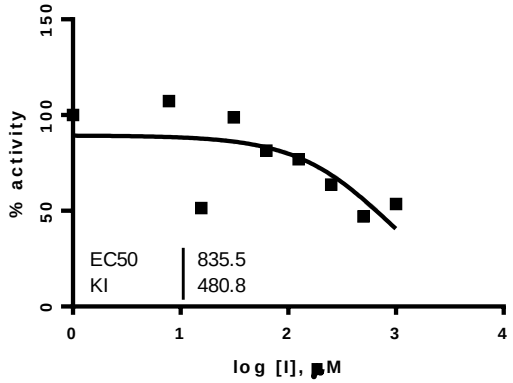

Average IC_{50}: 1147.3 ± 440.9 µM

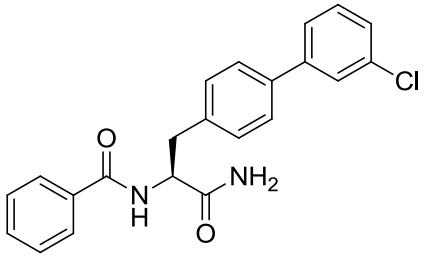

BiPH 142

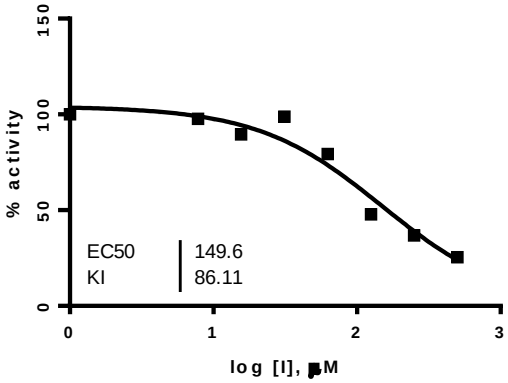

Average IC_{50}: 218.4 ± 97.2 µM

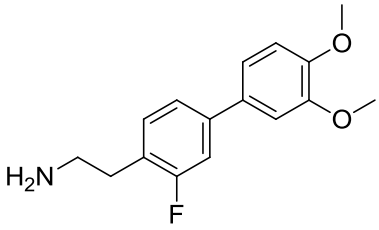

BiPH 230

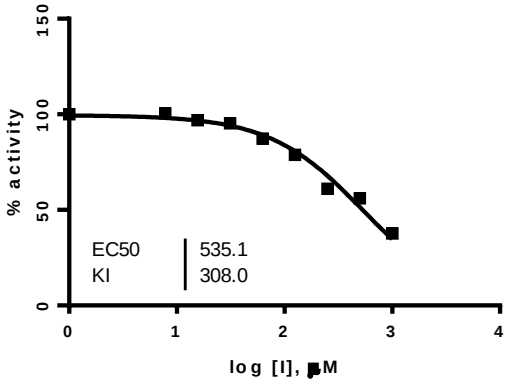

Average IC_{50}: 570.6 ± 50.1 µM

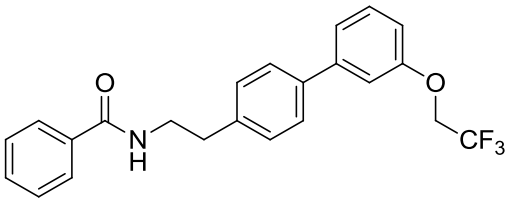

BiPH 240

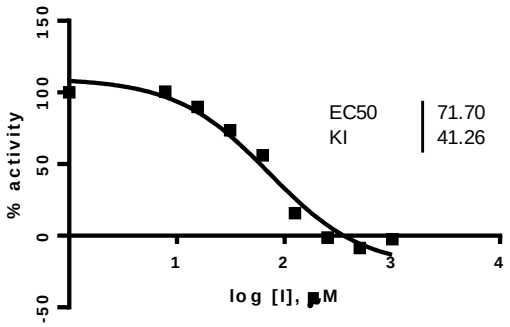

Average IC_{50}: 74.1 ± 3.3 µM

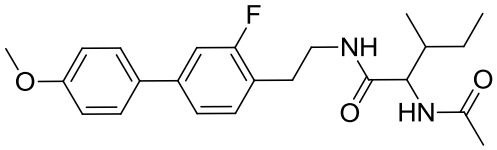

BiPH 248

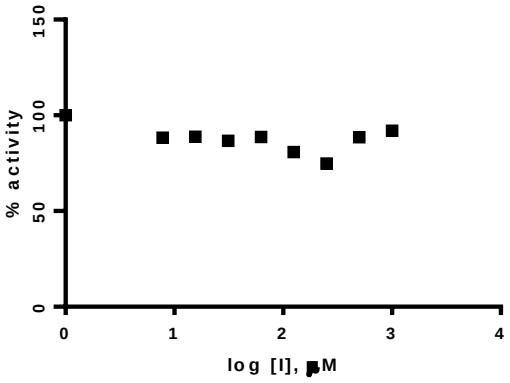

Average IC_{50}: > 1000 µM

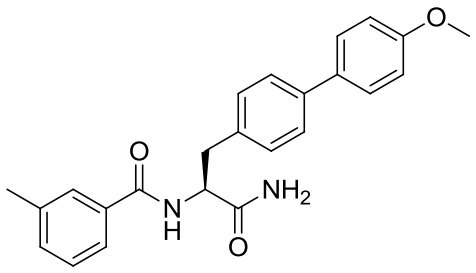

BiPH 250

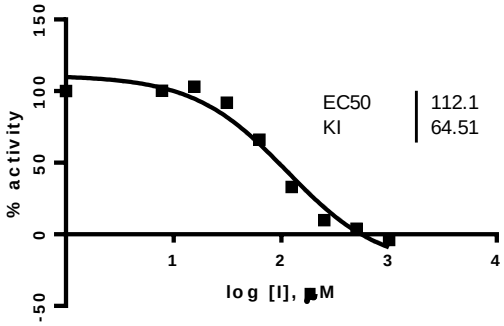

Average IC_{50}: 97.4 ± 20.9 µM

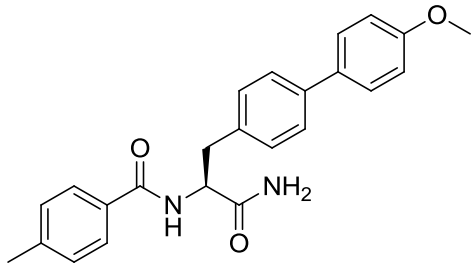

BiPH 259

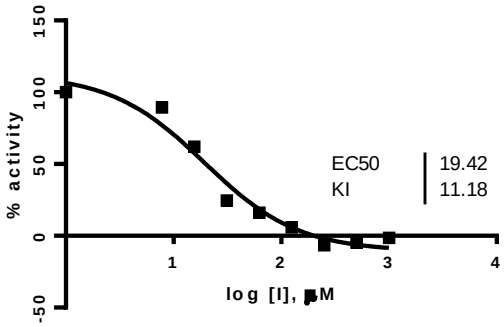

Average IC_{50}: 22.3 ± 4.0 µM

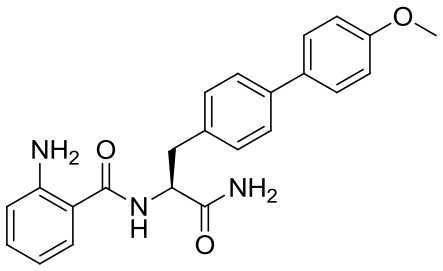

BiPH 264

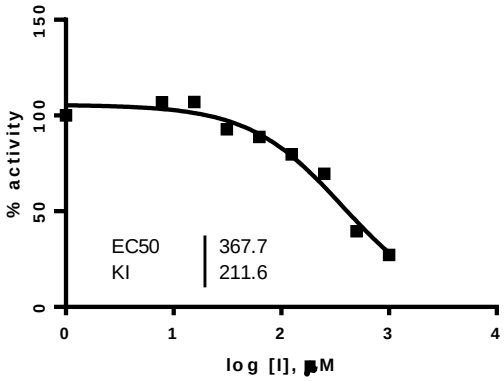

Average IC_{50}: 378.0 ± 14.5 µM

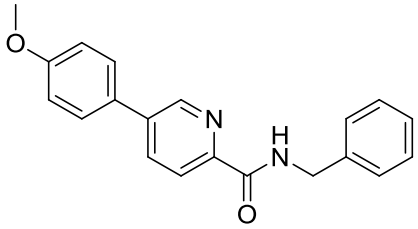

BiPH 280

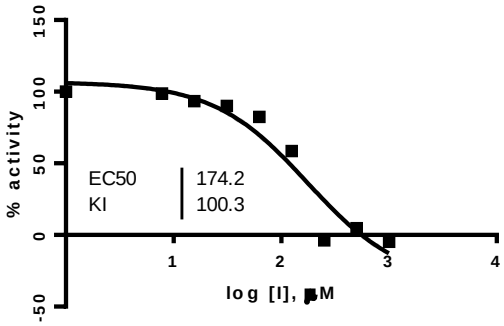

Average IC_{50}: 181.7 ± 10.5 µM

Analytical data for c-Src T341M K_i determination. Each inhibitor K_i value was determined using two independent experiments, a representative inhibition curve is shown.

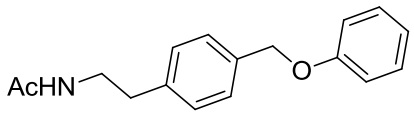

BiPH 47

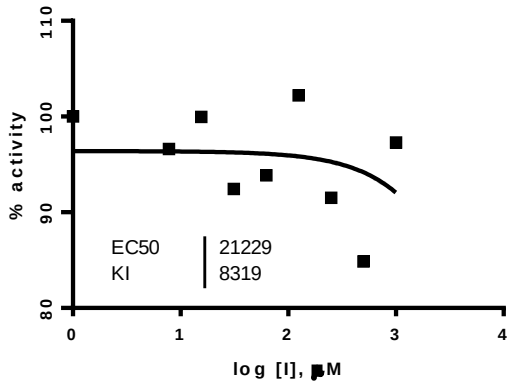

Average IC_{50}: > 1000 µM

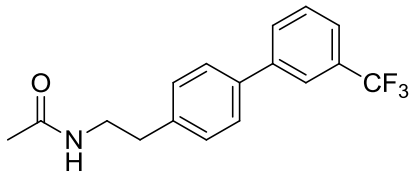

BiPH 50

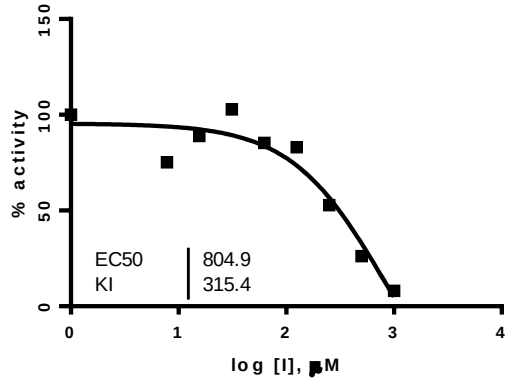

Average IC_{50}: 605.6 ± 281.9 µM

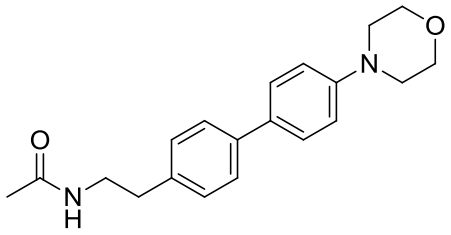

BiPH 65

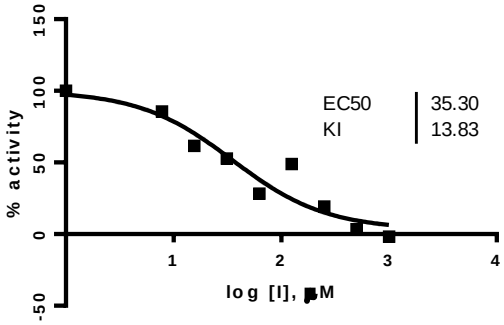

Average IC_{50}: 26.4 ± 12.6 µM

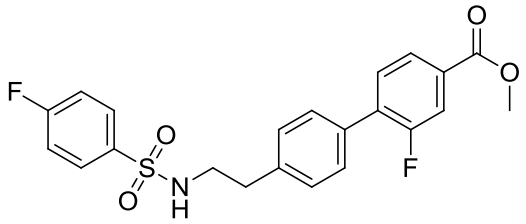

BiPH 85

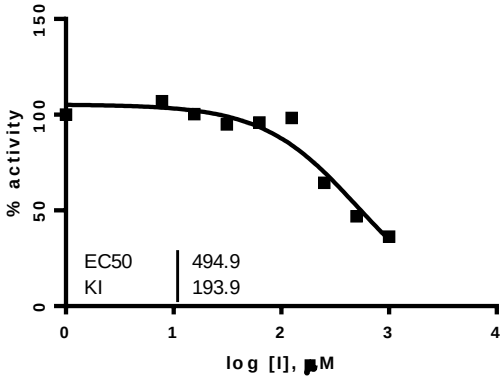

Average IC_{50}: 500.5 ± 7.9 µM

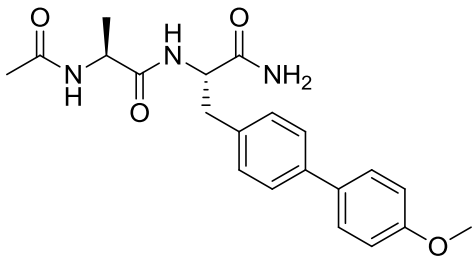

BiPH-101

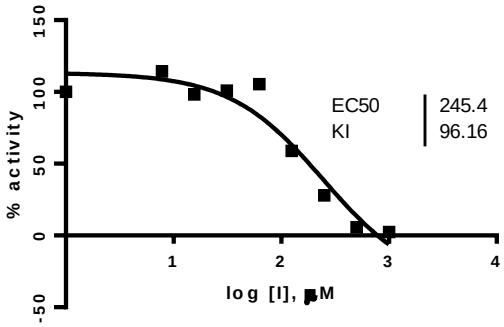

Average IC_{50}: 217.9 ± 39.0 µM

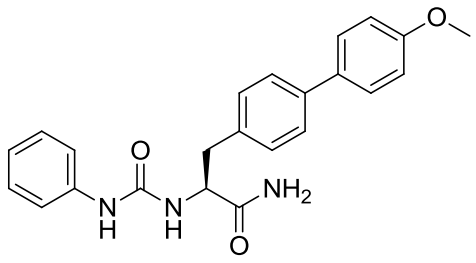

BiPH 108

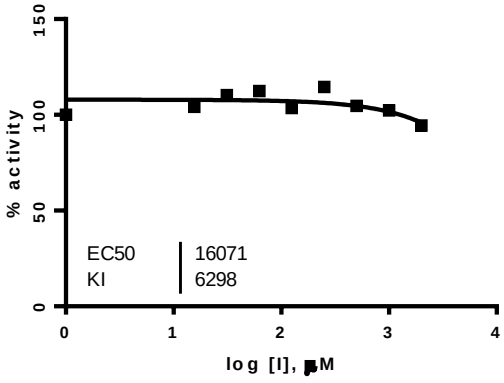

Average IC_{50}: > 1000 µM

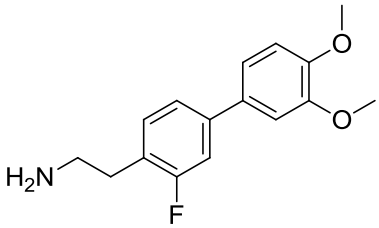

BiPH 230

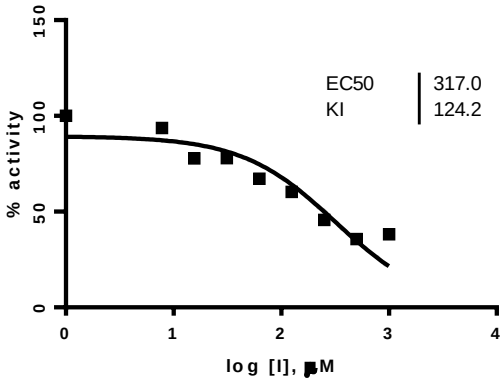

Average IC_{50}: 333.6 ± 23.5 µM

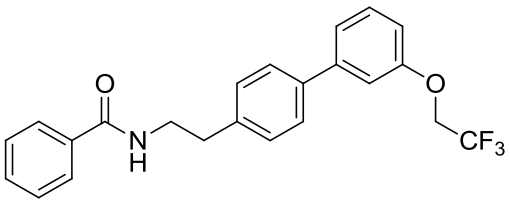

BiPH 240

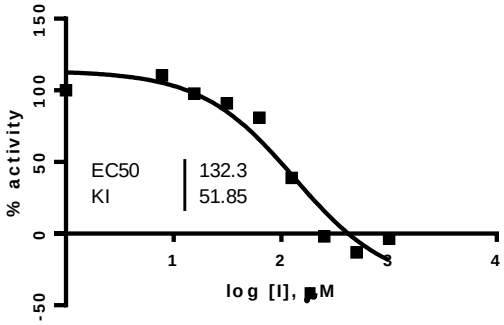

Average IC_{50}: 145.9 ± 19.2 µM

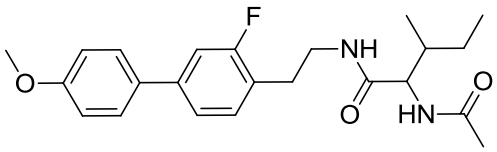

BiPH 248

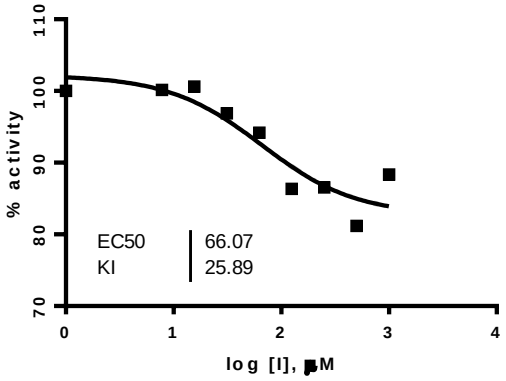

Average IC_{50}: 77.6 ± 16.3 µM

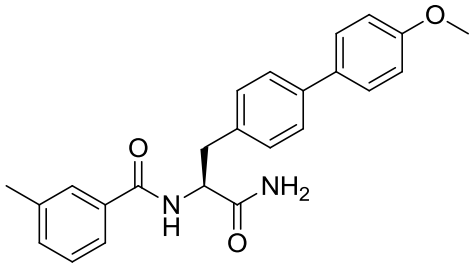

BiPH 250

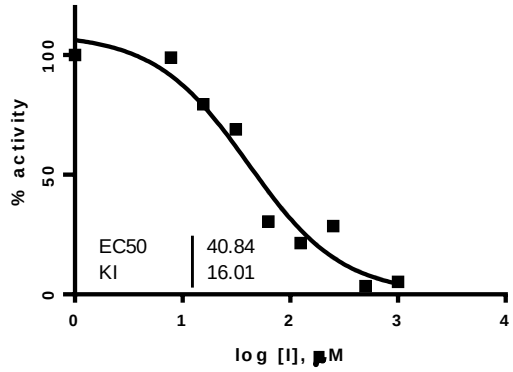

Average IC_{50}: 54.1 ± 18.8 µM

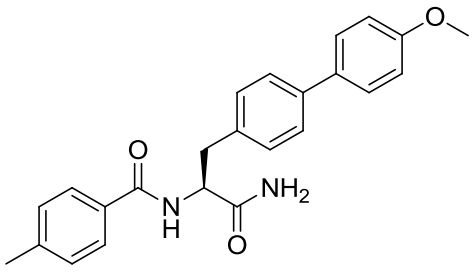

BiPH 259

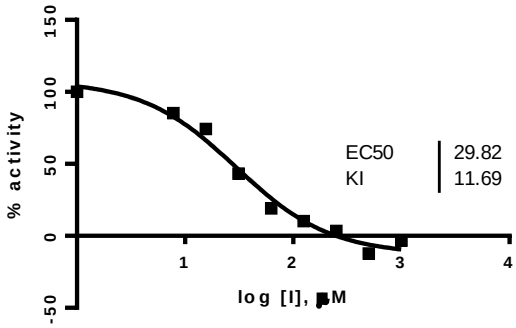

Average IC_{50}: 28.0 ± 2.7 µM

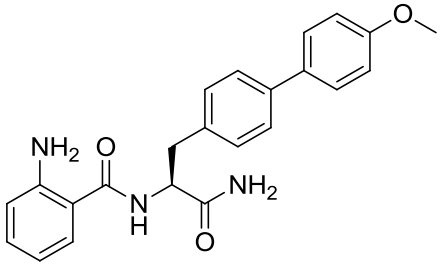

BiPH 264

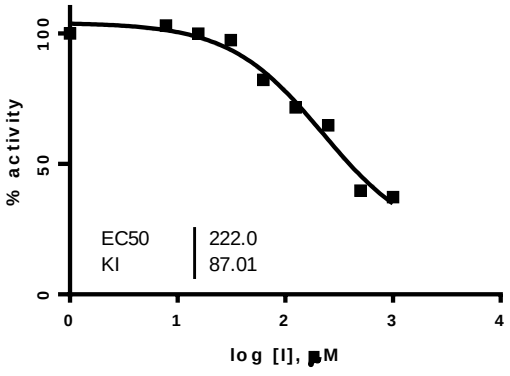

Average IC_{50}: 197.6 ± 34.6 µM

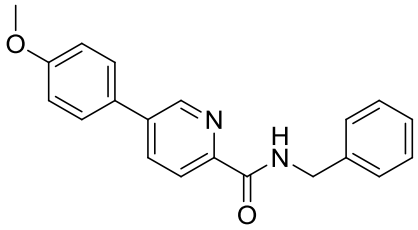

BiPH 280

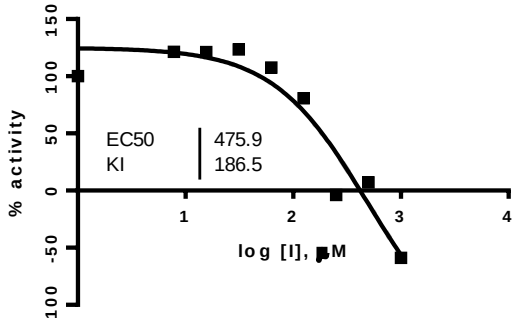

Average IC_{50}: 329.5 ± 207.0 µM

Analytical data for c-Src 3 Domain K_i determination. Each inhibitor K_i value was determined using two independent experiments, a representative inhibition curve is shown.

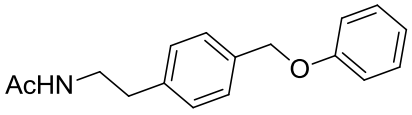

BiPH 47

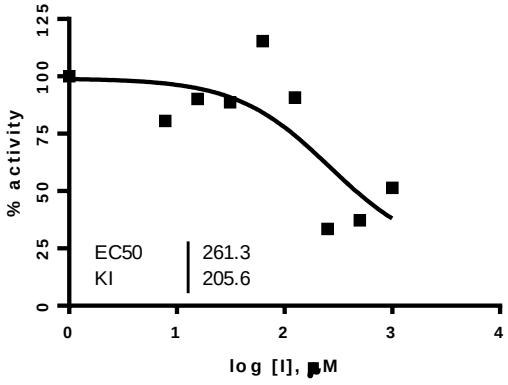

Average IC_{50}: 298.3 ± 52.3 µM

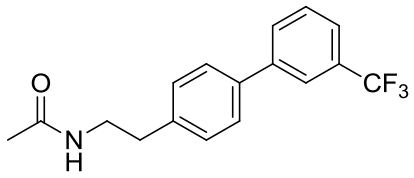

BiPH 50

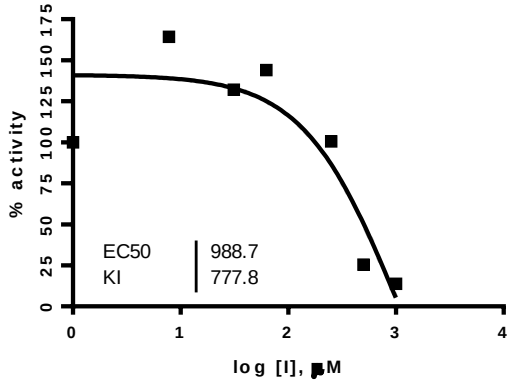

Average IC_{50}: 545.3 ± 627.0 µM

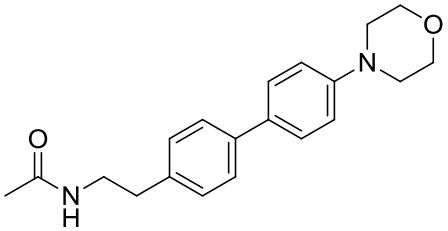

BiPH 65

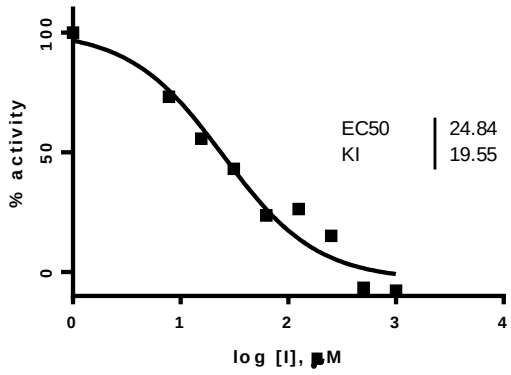

Average IC_{50}: 17.2 ± 10.9 µM

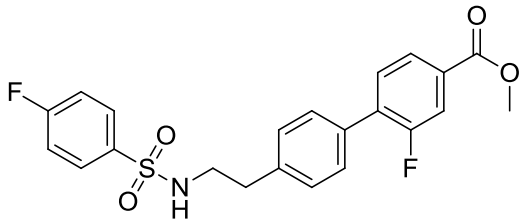

BiPH 85

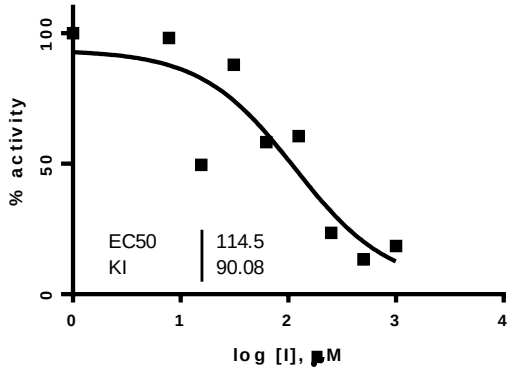

Average IC_{50}: 61.5 ± 75.0 µM

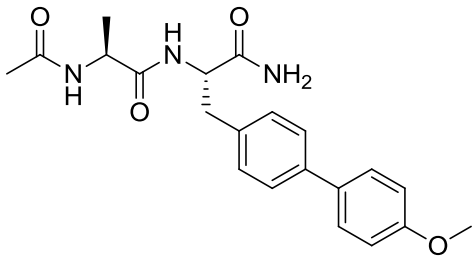

BiPH-101

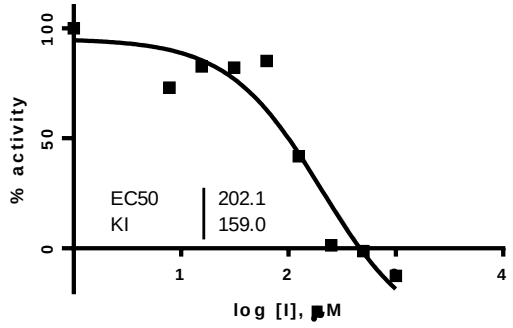

Average IC_{50}: 130.4 ± 101.4 µM

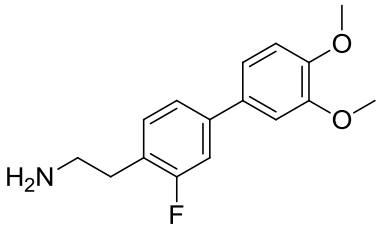

BiPH 230

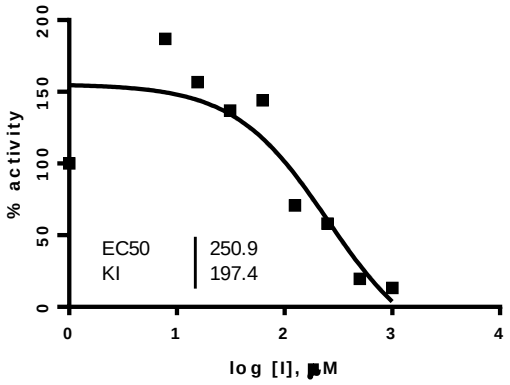

Average IC_{50}: 636.5 ± 545.3 µM

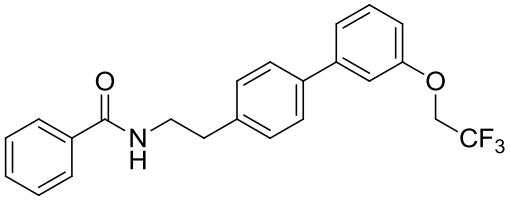

BiPH 240

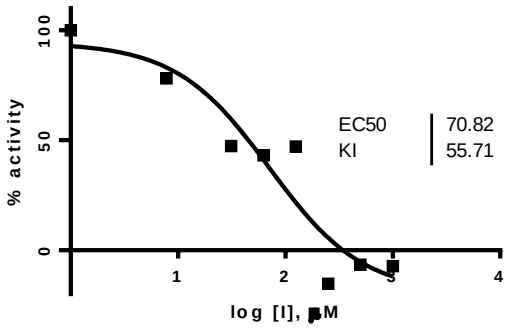

Average IC_{50}: 40.7 ± 42.6 µM

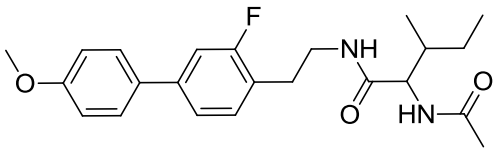

BiPH 248

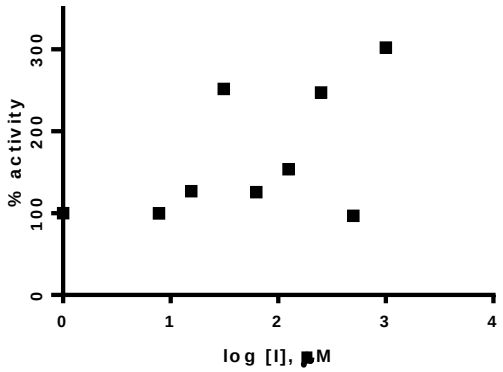

Average IC_{50}: > 1000 µM

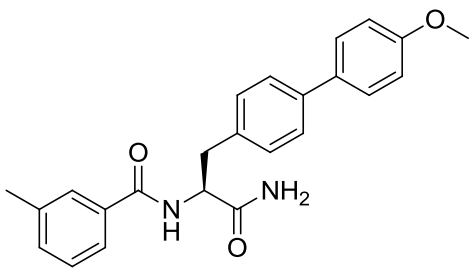

BiPH 250

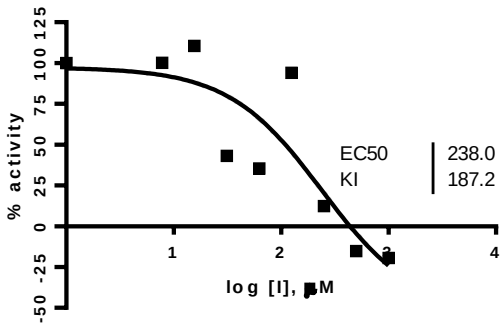

Average IC_{50}: 126.8 ± 157.2 µM

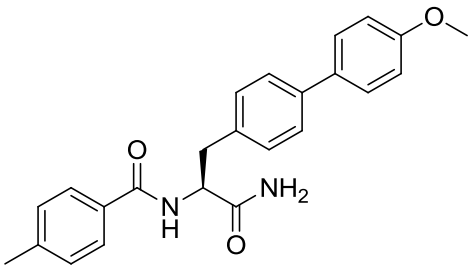

BiPH 259

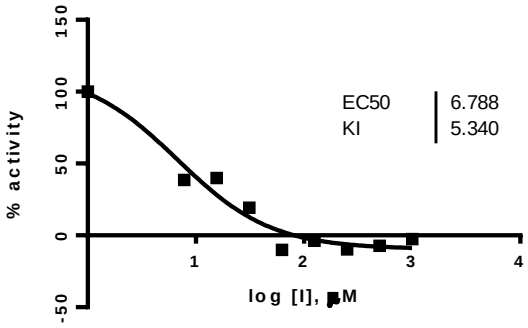

Average IC_{50}: 6.9 ± 0.2 µM

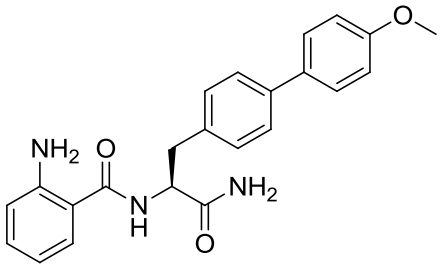

BiPH 264

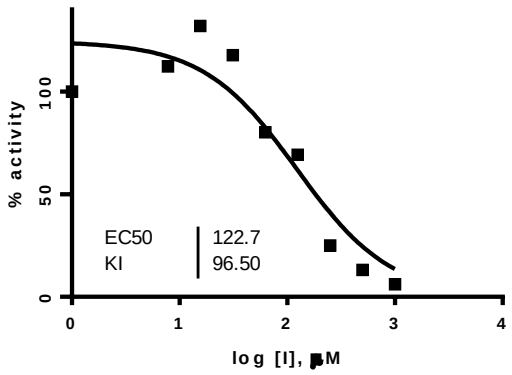

Average IC_{50}: 88.4 ± 48.6 µM

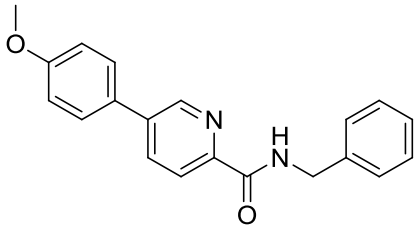

BiPH 280

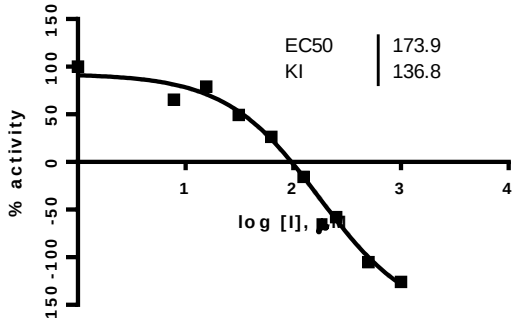

Average IC_{50}: 150.0 ± 33.9 µM

Analytical data for c-Src Kinase domain K_i determination at high [ATP] (5 mM final concentration, 45 µM substrate concentration). Each inhibitor K_i value was determined using at least four independent experiments; a representative inhibition curve is shown.

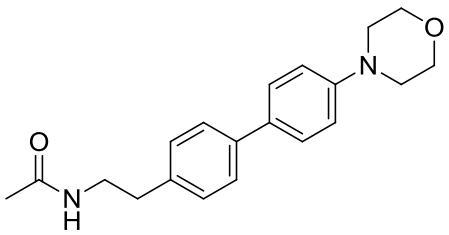

BiPH 65

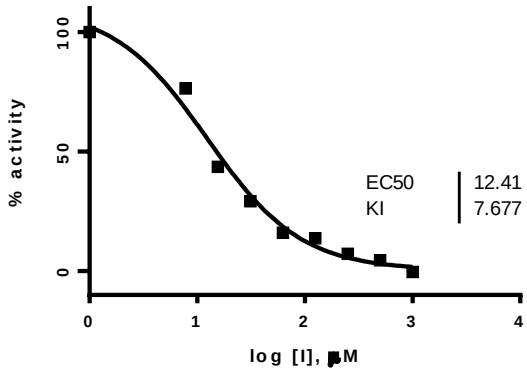

Average IC_{50}: 14.8 ± 2.1 µM

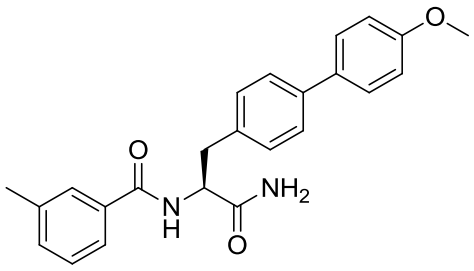

BiPH 250

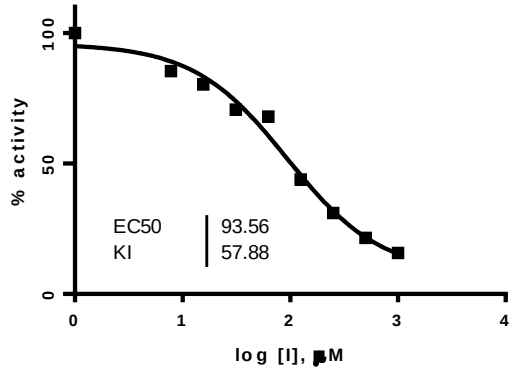

Average IC_{50}: 80.3 ± 43.3 µM

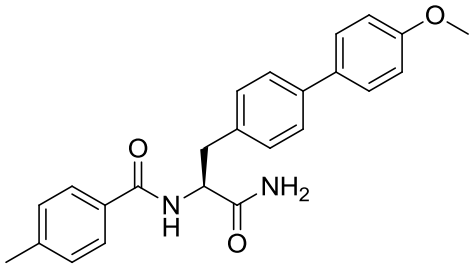

BiPH 259

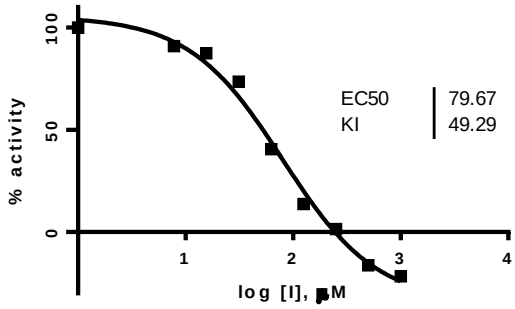

Average IC_{50}: 85.4 ± 8.0 µM

Analytical data for c-Src Kinase domain K_i determination at low [ATP] (100 µM final concentration, 45 µM substrate concentration). Each inhibitor K_i value was determined using at least four independent experiments; a representative inhibition curve is shown.

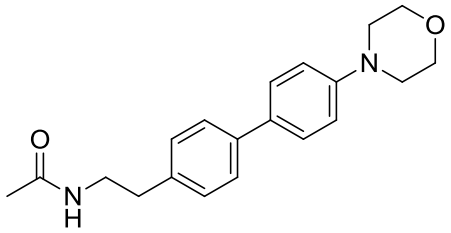

BiPH 65

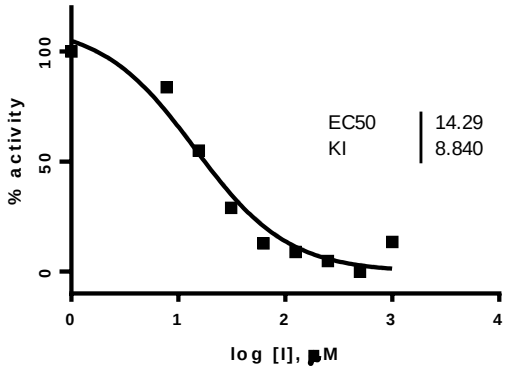

Average IC_{50}: 18.7 ± 6.1 µM

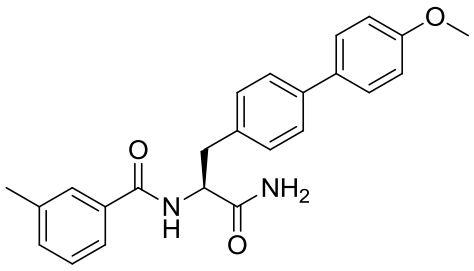

BiPH 250

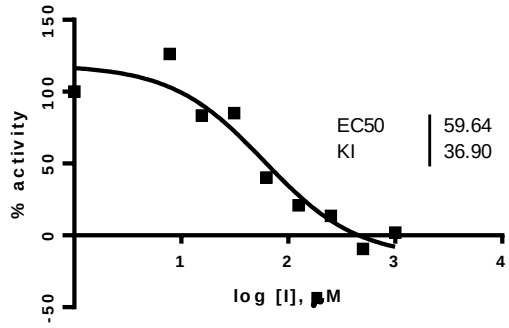

Average IC_{50}: 63.7 ± 5.8 µM

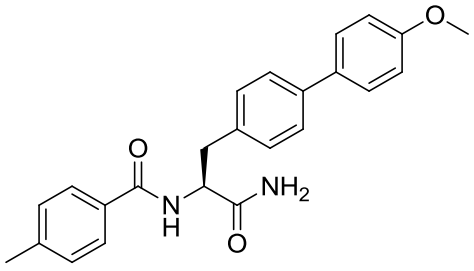

BiPH 259

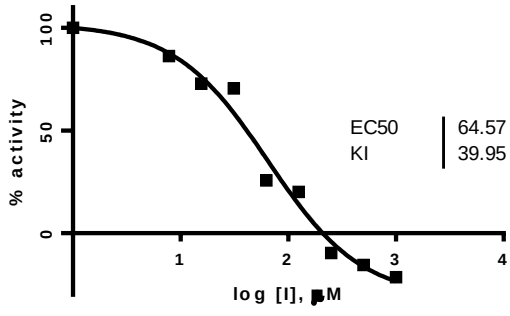

Average IC_{50}: 83.6 ± 27.0 µM

Analytical data for c-Src Kinase domain K_i determination at high [substrate] (500 µM final concentration, 1 mM ATP concentration). Each inhibitor K_i value was determined using at least four independent experiments; a representative inhibition curve is shown.

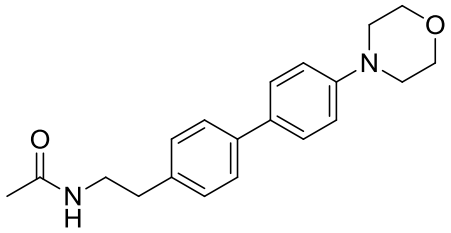

BiPH 65

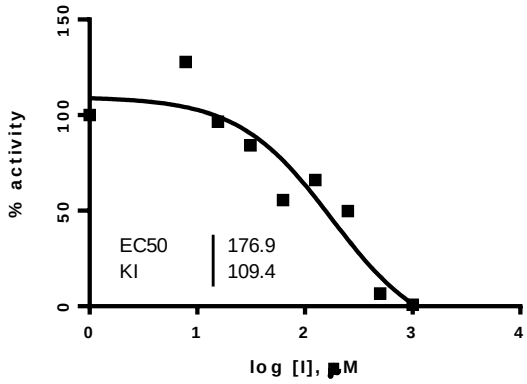

Average IC_{50}: 18.7 ± 6.1 µM

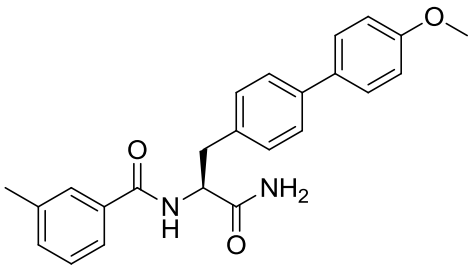

BiPH 250

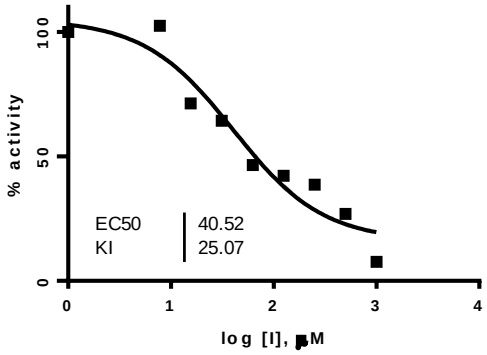

Average IC_{50}: 40.2 ± 0.5 µM

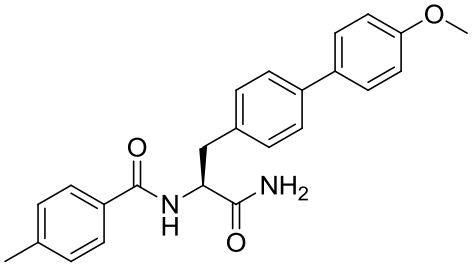

BiPH 259

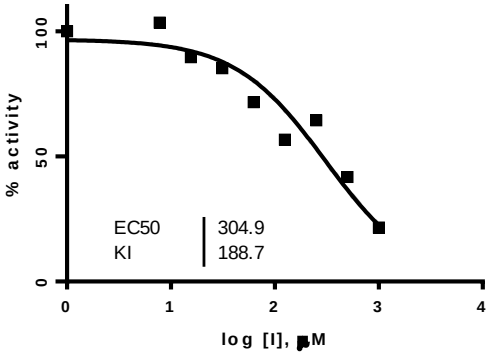

Average IC_{50}: 336.4 ± 44.5 µM

Analytical data for c-Abl K_i determination. Each inhibitor K_i value was determined using four independent experiments, a representative inhibition curve is shown.

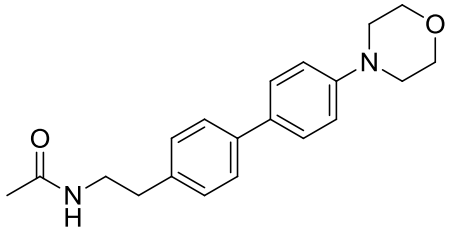

BiPH 65

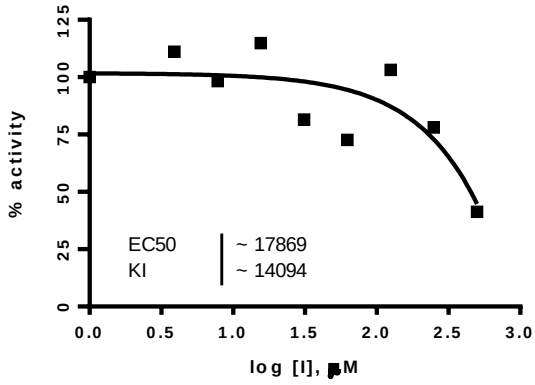

Average IC_{50} > 1000 µM

Analytical data for c-Hck K_i determination. Each inhibitor K_i value was determined using four independent experiments, a representative inhibition curve is shown.

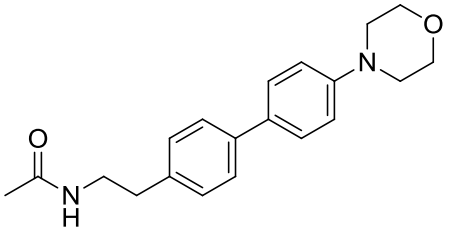

BiPH 65

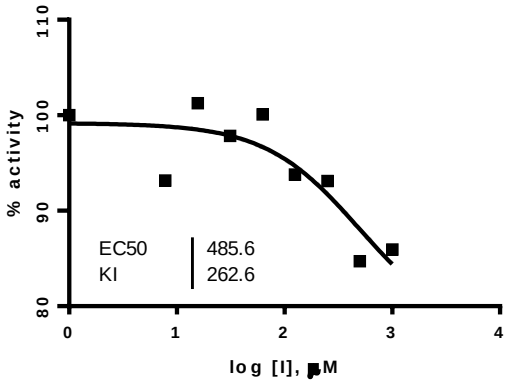

Average IC_{50} > 500 µM

General procedure for ATP Lineweaver-Burk analysis of inhibitor. A continuous fluorescence assay[5] was used to determine K_M. Reaction volumes of 100 µL were used in 96-well plates. 85 µL of enzyme in buffer was added to each well. 2.5 µL of the appropriate inhibitor dilution (fixed concentrations, typically 0, 35, 50, 70, 100, or 140 µM in DMSO) was then added. 2.5 µL of a substrate peptide ("compound 3" as described in Wang et al)[5] solution (1.8 mM in DMSO) was added. The reaction was initiated with 10 µL of ATP (Two-fold dilutions, final concentrations: 5mM → 0 in water), and reaction progress was immediately monitored at 405 nm (ex. 340 nm) for 10 minutes. Reactions had final concentrations of 30 nM enzyme, 45 µM peptide substrate, 100 µM Na_3VO_4, 100 mM Tris buffer (pH 8), 10 mM $MgCl_2$, 0.01% Triton X-100. The initial rate data collected was used for determination of K_M values. For K_M determination, the kinetic values were obtained directly from nonlinear regression of substrate-velocity curves in the presence of various concentrations of ATP. The equation Y = (Vmax * X)/(Km + X), X = substrate concentration (µM) and Y = enzyme velocity (RFU/s); was used in the nonlinear regression.

Analytical data for c-Src Kinase Domain ATP Lineweaver-Burk analysis of inhibitor. Each inhibitor K_M value was determined using at least 4 independent experiments; a representative K_M curve is shown.

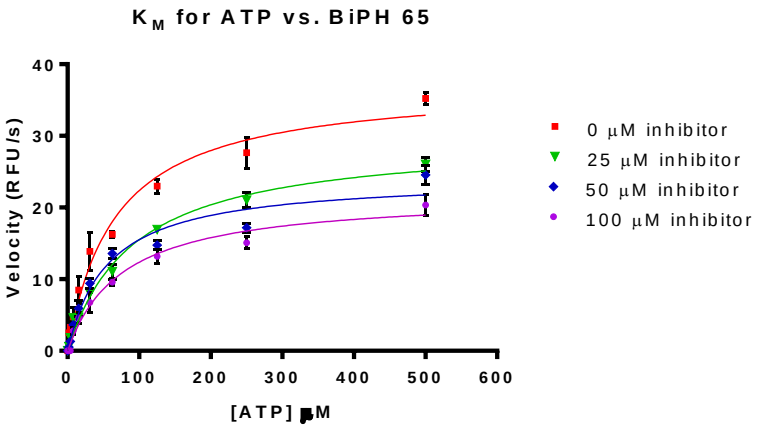

	0 µM inhibitor	25 µM inhibitor	50 µM inhibitor	100 µM inhibitor
Best-fit values				
Vmax	37.27	29.70	24.19	21.86
Km	66.73	91.59	56.05	76.88
Std. Error				
Vmax	1.898	1.112	1.134	1.254
Km	10.44	9.084	8.442	13.08
95% Confidence Intervals				
Vmax	33.41 to 41.13	27.45 to 31.96	21.88 to 26.49	19.27 to 24.45
Km	45.51 to 87.94	73.15 to 110.0	38.90 to 73.20	49.82 to 103.9

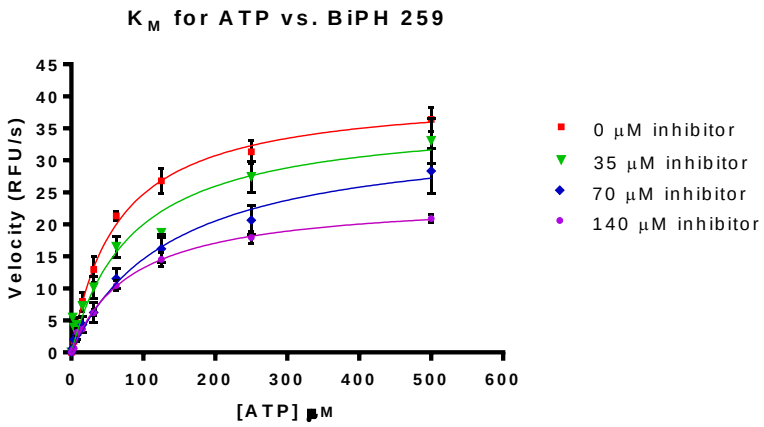

	0 µM inhibitor	35 µM inhibitor	70 µM inhibitor	140 µM inhibitor
Best-fit values				
Vmax	40.60	37.01	34.74	24.25
Km	64.35	85.25	138.7	84.23
Std. Error				
Vmax	1.649	2.527	3.386	0.8552
Km	8.113	16.75	33.78	8.635
95% Confidence Intervals				
Vmax	37.24 to 43.96	31.87 to 42.14	27.85 to 41.63	22.51 to 25.99
Km	47.84 to 80.87	51.18 to 119.3	69.93 to 207.5	66.69 to 101.8

General procedure for Substrate Lineweaver-Burk analysis of inhibitor. A continuous fluorescence assay[5] was used to determine K_M. Reaction volumes of 100 µL were used in 96-well plates. 85 µL of enzyme in buffer was added to each well. 2.5 µL of the appropriate inhibitor dilution (fixed concentrations, typically 0, 35, 50, 70, 100, or 140 µM in DMSO) was then added. 2.5 µL of a substrate peptide ("compound 3" as described in Wang et al)[5] solution (Final concentrations: 500 µM → 0 in DMSO) was added. The reaction was initiated with 10 µL of ATP (Final concentration 1 mM in water), and reaction progress was immediately monitored at 405 nm (ex. 340 nm) for 10 minutes. Reactions had final concentrations of 30 nM enzyme, 45 µM peptide substrate, 100 µM Na_3VO_4, 100 mM Tris buffer (pH 8), 10 mM $MgCl_2$, 0.01% Triton X-100. The initial rate data collected was used for determination of K_M values. For K_M determination, the kinetic values were obtained directly from nonlinear regression of substrate-velocity curves in the presence of various concentrations of substrate. The equation Y = (Vmax * X)/(Km + X), X = substrate concentration (µM) and Y = enzyme velocity (RFU/s); was used in the nonlinear regression.

Analytical data for c-Src Kinase Domain Substrate Lineweaver-Burk analysis of inhibitor. Each inhibitor K_M value was determined using at least 4 independent experiments; a representative K_M curve is shown.

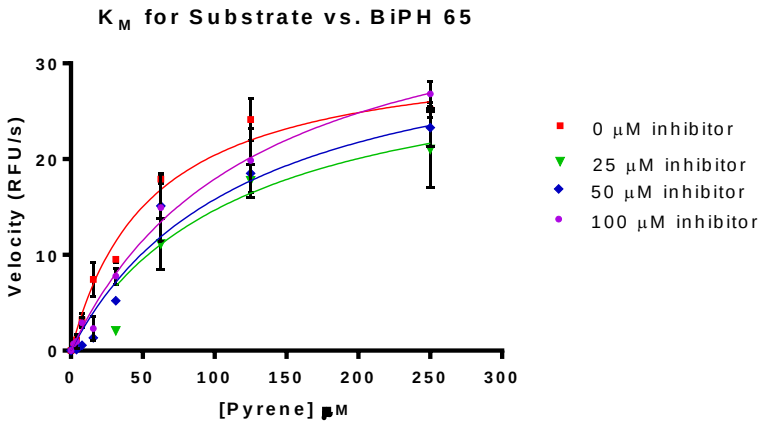

	0 µM inhibitor	25 µM inhibitor	50 µM inhibitor	100 µM inhibitor
Best-fit values				
Vmax	31.78	31.73	34.95	40.38
Km	55.74	116.4	121.4	125.4
Std. Error				
Vmax	1.651	10.58	6.538	4.494
Km	8.764	90.11	57.73	31.87
95% Confidence Intervals				
Vmax	28.30 to 35.26	8.168 to 55.30	20.16 to 49.74	30.90 to 49.86
Km	37.25 to 74.24	-84.37 to 317.1	-9.187 to 252.0	58.18 to 192.7

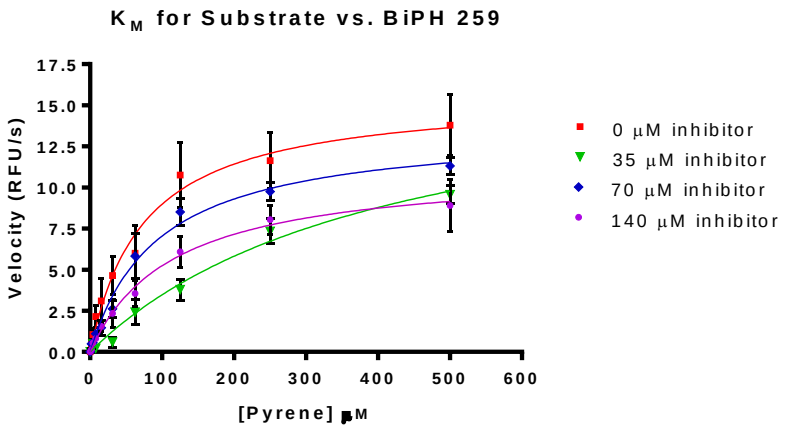

	0 µM inhibitor	35 µM inhibitor	70 µM inhibitor	140 µM inhibitor
Best-fit values				
Vmax	15.66	17.91	13.66	11.25
Km	74.33	415.8	93.96	114.8
Std. Error				
Vmax	1.567	3.252	0.9070	1.298
Km	22.18	133.5	17.51	35.94
95% Confidence Intervals				
Vmax	12.48 to 18.84	11.20 to 24.62	11.82 to 15.51	8.604 to 13.90
Km	29.35 to 119.3	140.3 to 691.4	58.40 to 129.5	41.42 to 188.2

A.5: Cancer cell growth inhibition assays

General procedure:

1. **Cell culture and seeding**: Cells are dispersed from flasks and collected by centrifugation (125xg for 5 minutes at room temperature). An aliquot of the resuspended cells is mixed with trypan blue solution and the cell number is quantified using a hemacytometer. In general, depending on the growth rate of the untreated cells, the cells will be plated at 5.0 – 7.5 x 10^3 cells per well. 100 µL of the cell mixture will be added to each well so the concentration should be 10X the cells per well in cells per mL. The cells are plated into sterile, clear bottom 96 well plates and cultured under normal growth conditions overnight prior to dosing with compound.
2. **Dosing**: The 100% DMSO compound stocks need to be prepared to 100X the final concentration that is desired in the assay. 3 µL of the DMSO stock solution is then added to 297 µL of the cell growth media to give a DMSO concentration of 1%. The cell media is removed by aspiration for adherent cells and replaced with 100 µL per well of the cell growth media containing the compound. In general each compound concentration is dosed in triplicate wells. The plates are returned to normal culture conditions for 24 – 72 hours.

3. **Assay**: After the required incubation period the plates are removed from the incubator and 10 µL per well of WST-1 reagent is added. The plates are returned to the incubator and the color change is visually monitored for 0.5 – 2 hours. When sufficient color change has occurred the plates are shaken on a plate shaker for 60 seconds and read in the appropriate plate reader.
4. **Data Analysis**: The reference absorbance reading is subtracted from the formazan absorbance and the data is plotted as a percentage of the vehicle (1% DMSO alone). Data analysis and curve fitting was performed using Graphpad Prism. For each cell line, there were n = 3 data points for each concentration. Each dose response curve was performed at least twice, providing n ≥ 6 for each data point.

BiPH 65 HT-29:

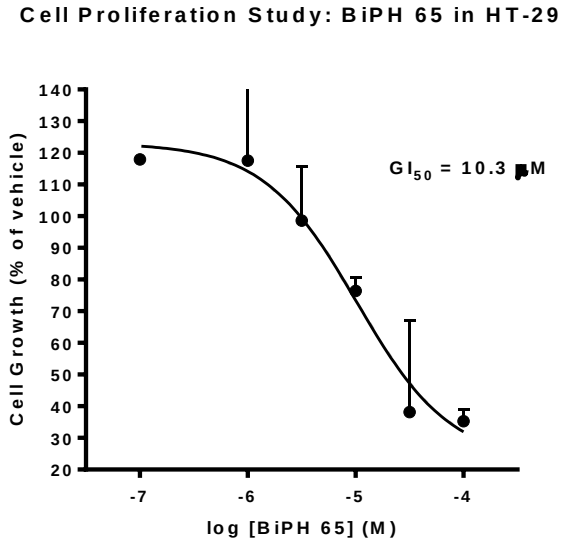

A.6: References

(1) Kaiser, E.; Colescott, R. L.; Bossinger, C. D.; Cook, P. I. *Anal Biochem* **1970**, *34*, 595.

(2) Hangauer, J. D. G.; Patra, D.; Cody, J. A.; Palmer, G. J.; Isbester, P. K.; Salsbury, J.; Kinex Pharmaceuticals, LLC Buffalo: United States, 2009; Vol. 20090318450.

(3) Invitrogen http://tools.invitrogen.com/content/sfs/manuals/SRC_LanthaScreen_Binding.pdf, LanthaScreen Eu Kinase Binding Assay for SRC.

(4) Lebakken, C. S.; Riddle, S. M.; Upinder, S.; Frazee, W. J.; Eliason, H. C.; Gao, Y.; Reichling, L. J.; Marks, B. D.; Vogel, K. W. *J. Biomol. Screen.* **2009**, *14*, 924.

(5) Wang, Q.; Cahill, S. M.; Blumenstein, M.; Lawrence, D. S. *J. Am. Chem. Soc.* **2006**, *128*, 1808.

Appendix B:

Supplemental Information for Chapter 3

B.1: General Synthetic Methods Unless otherwise noted, all reagents were obtained from commercially available sources and used without further purification. All ^{1}H and ^{19}F NMR spectra were measured with a Varian 400 MHz spectrometer. Samples were taken in $CDCl_3$ or DMSO-*d6***,** spectra were referenced to chloroform peak.

B.2: Synthesis of Compounds

Fmoc-(4F)Tyrosine-OH amino acid

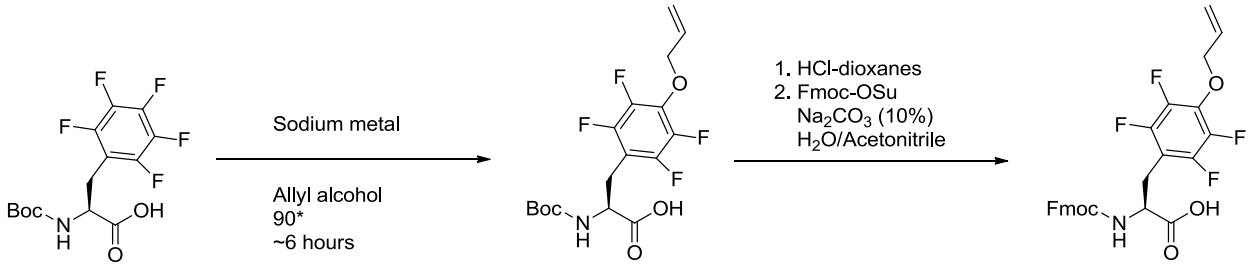

The Fmoc-(4F)Tyrosine amino acid was prepared and purified via methods set forth by Wang, et al.[1]

IV-sms-80

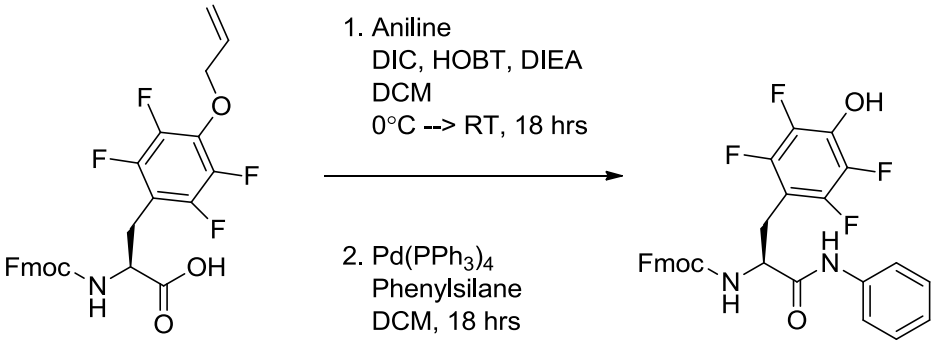

IV-sms-80

15.6% yield

In a dried, round-bottom flask equipped with a stir bar, and under nitrogen atmosphere, Fmoc-(4F)Tyrosine-OH (0.100 g, 0.194 mmol) was dissolved in 5 mL of dichloromethane. To this, N,N'-

dicyclohexylcarbodiimide (0.025 mL, 0.162 mmol), HOBT (0.021 g, 0.162 mmol), and DIEA (0.057 mL, 0.324 mmol) were added at 0°C and the reaction mixture was allowed to stir for 45 minutes before adding aniline (0.015 mL, 0.162 mmol). The reaction was allowed to stir overnight for 18 hours. The solvent was removed under reduced pressure and the resulting crude product was solubilized in ethyl acetate (50 mL) and washed with water (1 x 50 mL) followed by a wash with a brine solution (1 x 50 mL). The resulting organic layer was dried over anhydrous $MgSO_4$ and filtered. The solvent was removed under reduced pressure to afford the crude allyl protected product, which was purified via automated silica gel chromatography (Linear gradient of 7 → 60% ethyl acetate in hexanes) to yield the allyl protected intermediate product as a white crystalline solid (0.050 g, 52.3% yield). Removal of the allyl protecting groups subsequently followed, as the allyl protected intermediate (0.050 g, 0.085 mmol) was dissolved in 5 mL of dichloromethane. To this, tetrakis(triphenylphosphine)palladium(0) (0.005 g, 0.004 mmol) and phenylsilane (0.021 mL, 0.17 mmol) were added and the reaction was allowed to stir overnight for 18 hours at room temperature. The reaction mixture was washed with a solution of 10% aqueous citrate (2 x 20 mL) and the resulting organic layer was dried with anhydrous $MgSO_4$ and filtered. The solvent was removed under reduced pressure to afford the crude **IV-sms-80** product which was purified via automated silica gel chromatography (Linear gradient of 0 → 10% methanol in dichloromethane) as well as by reverse-phase chromatography (linear gradient of 5 → 95% CH_3CN (0.1% HOAc) in H_2O (0.1% HOAc)) to yield **IV-sms-80** as a crystalline solid (7.3 mg, 15.6% yield). **Spectral data**. ^{1}H NMR (500 MHz, DMSO-d_6) δ 11.24 (s, 1H), 9.94 (s, 1H), 7.88 (d, *J* = 7.7 Hz, 3H), 7.71 (d, *J* = 7.6 Hz, 2H), 7.49 (d, *J* = 7.9 Hz, 2H), 7.41 (t, *J* = 7.5 Hz, 2H), 7.30 (dd, *J* = 10.0, 4.0 Hz, 4H), 7.11 – 7.01 (m, 1H), 4.41 (q, *J* = 7.6 Hz, 1H), 4.29 (d, *J* = 8.2 Hz, 1H), 4.26 – 4.14 (m, 2H), 3.11 (s, 1H), 2.99 (d, *J* = 1.9 Hz, 1H), contains solvent peaks. ^{19}F NMR (400 MHz, DMSO-d_6) δ, -145.01, -145.07, -162.34, -162.40.

IV-sms-89

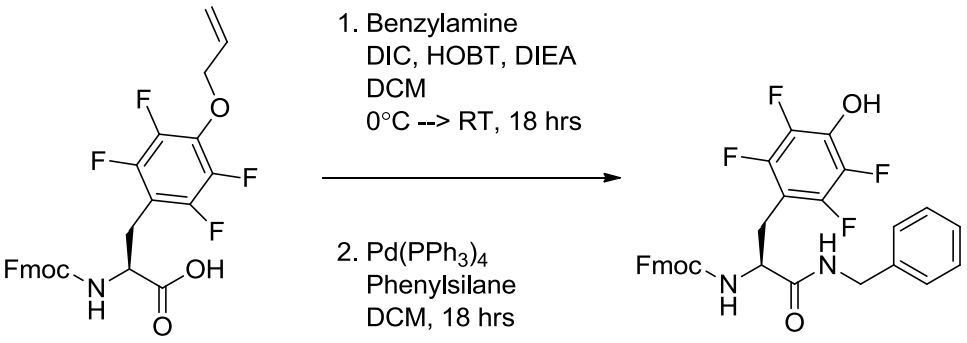

IV-sms-89
44% yield

In a dried, round-bottom flask equipped with a stir bar, and under nitrogen atmosphere, Fmoc-(4F)Tyrosine-OH (0.100 g, 0.194 mmol) was dissolved in 5 mL of dichloromethane. To this, N,N'-dicyclohexylcarbodiimide (0.025 mL, 0.162 mmol), HOBT (0.021 g, 0.162 mmol), and DIEA (0.057 mL, 0.324 mmol) were added at 0°C and the reaction mixture was allowed to stir for 45 minutes before adding benzylamine (0.017 mL, 0.162 mmol). The reaction was allowed to stir overnight for 18 hours. The solvent was removed under reduced pressure and the resulting crude product was solubilized in ethyl acetate (50 mL) and washed with water (1 x 50 mL) followed by a wash with a brine solution (1 x 50 mL). The resulting organic layer was dried over anhydrous $MgSO_4$ and filtered. The solvent was removed under reduced pressure to afford the crude allyl protected product, which was purified via automated silica gel chromatography (Linear gradient of 7 → 60% ethyl acetate in hexanes) to yield the allyl protected intermediate product as a white crystalline solid (0.060 g, 52.3% yield). Removal of the allyl protecting groups subsequently followed, as the allyl protected intermediate (0.050 g, 0.085 mmol) was dissolved in 5 mL of dichloromethane. To this, tetrakis(triphenylphosphine)palladium(0) (0.005 g, 0.004 mmol) and phenylsilane (0.021 mL, 0.17 mmol) were added and the reaction was allowed to stir overnight for 18 hours at room temperature. The reaction mixture was washed with a solution of 10% aqueous citrate (2 x 20 mL) and the resulting organic layer was dried with anhydrous $MgSO_4$ and filtered. The solvent was removed under reduced pressure to afford the crude **IV-sms-89** product which was purified via automated silica gel chromatography (Linear gradient of 0 → 10% methanol in dichloromethane) as well as by reverse-phase chromatography (linear gradient of 5 → 95% CH_3CN (0.1% HOAc) in H_2O (0.1% HOAc)) to yield **IV-sms-89** as a crystalline solid (21.1 mg, 44.0% yield). **Spectral data**. ^{1}H NMR (400 MHz, DMSO-d_6) δ 11.21 (s, 1H), 8.44 (t, *J* = 5.5 Hz, 1H), 7.89 – 7.81 (m, 2H), 7.77 – 7.70 (m, 1H), 7.68 – 7.61 (m, 2H), 7.38 (t, *J* = 7.7 Hz, 2H), 7.22 (ddd, *J* = 20.5, 14.3, 7.3 Hz, 3H), 7.11 – 7.04 (m, 2H), 4.32 – 4.07 (m, 6H), 3.06 (dd, *J* = 14.2, 7.5 Hz, 1H), 2.84 (dd, *J* = 13.8, 7.5 Hz, 1H), contains solvent peaks. ^{19}F NMR (400 MHz, DMSO-d_6) δ, -145.12, -145.18, -162.20, -162.26.

IV-sms-109

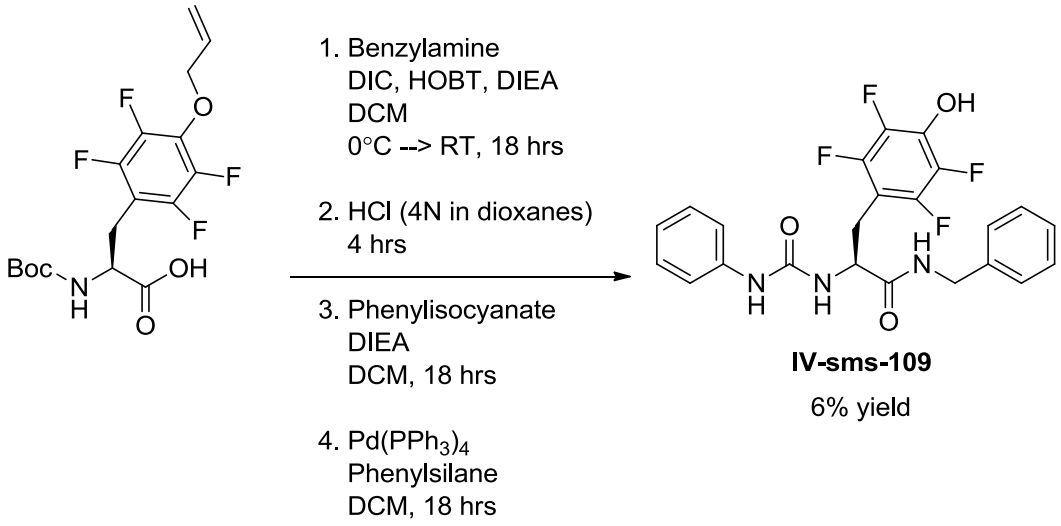

In a dried, round-bottomed flask equipped with a stir bar, and under nitrogen atmosphere, Boc-(4F)Tyrosine-OH (prepared via methods described in Wang, et al.[1] 0.500 g, 1.27 mmol) was solubilized in 10 mL of dichloromethane. To this, N,N'-dicyclohexylcarbodiimide (0.17 mL, 1.06 mmol), HOBT (0.143 g, 1.06 mmol), and DIEA (0.37 mL, 2.12 mmol) were added at 0°C and the reaction mixture was allowed to stir for 45 minutes before adding benzylamine (0.116 mL, 1.06 mmol). The reaction was allowed to stir overnight for 18 hours. The organics were removed under reduced pressure and the resulting crude product was solubilized in ethyl acetate (50 mL) and washed with water (1 x 50 mL) followed by a wash with a brine solution (1 x 50 mL). The resulting organic layer was dried over anhydrous $MgSO_4$ and filtered. The solvent was removed under reduced pressure to afford the crude allyl protected product, which was purified via automated silica gel chromatography (Linear gradient of 7 → 60% ethyl acetate in hexanes) to yield the allyl protected intermediate product as a white crystalline solid (0.440 g, 72% yield). The Boc- and allyl protected intermediate (0.410 g, 0.850 mmol) was immediately solubilized in 10 mL HCl (4N in dioxanes) and allowed to stir at room temperature for 4 hours to remove the Boc-protecting group. The reaction was concentrated under reduced pressure to dryness to yield the free amine and allyl protected intermediate as the HCl salt, a tan crystalline solid (0.360 g, 100% yield). This intermediate (0.047 mg, 0.123 mmol) was solubilized in 4 mL of dichloromethane. To this, diisopropylamine (0.090 mL, 0.492 mmol) and phenylisocyanate (0.017 mL, 0.148 mmol) were added and the reaction was allowed to stir overnight at room temperature. The organics were removed under reduced pressure and the resulting crude product was dissolved in ethyl acetate (50 mL) and washed with water (1 x 50 mL) followed by a wash with a brine solution (1 x 50 mL). The resulting organic layer was dried over anhydrous $MgSO_4$ and filtered. The solvent was removed under reduced pressure to yield the crude allyl protected intermediate which was purified via automated silica gel chromatography (Linear

gradient of 0 → 10% methanol in dichloromethane) to afford the allyl protected intermediate (0.055 g, 88.6%). Removal of the allyl protecting groups subsequently followed, as the allyl protected intermediate (0.055 g, 0.109 mmol) was dissolved in 5 mL of dichloromethane. To this, tetrakis(triphenylphosphine)palladium(0) (0.006 g, 0.005 mmol) and phenylsilane (0.027 mL, 0.22 mmol) were added and the reaction was allowed to stir overnight for 18 hours at room temperature. The reaction mixture was washed with a solution of 10% aqueous citrate (2 x 20 mL) and the resulting organic layer was dried with anhydrous $MgSO_4$ and filtered. The solvent was removed under reduced pressure to afford the crude **IV-sms-89** product which was purified via automated silica gel chromatography (Linear gradient of 0 → 10% methanol in dichloromethane) as well as by reverse-phase chromatography (linear gradient of 5 → 95% CH_3CN (0.1% HOAc) in H_2O (0.1% HOAc)) to yield **IV-sms-109** as a crystalline solid (2.9 mg, 6.0% yield). **Spectral data**. ^{1}H NMR (400 MHz, DMSO-d_6) δ 11.23 (s, 1H), 8.68 (d, *J* = 10.1 Hz, 2H), 7.07 – 7.02 (m, 6H), 6.84 (d, *J* = 7.6 Hz, 2H), 6.44 (d, *J* = 9.5 Hz, 2H), 4.51 (d, *J* = 7.6 Hz, 1H), 4.21 (s, 1H), 3.10 – 2.83 (m, 2H), contains solvent peaks.^{19}F NMR (400 MHz, DMSO-d_6) δ, -144.91, -144.97, -162.38, -162.44.

IV-sms-93

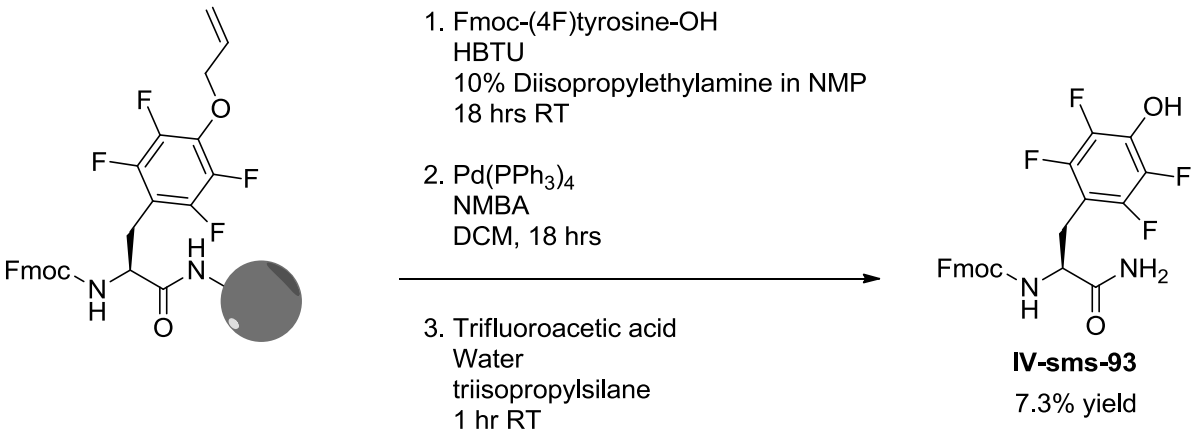

Into a plastic, microwave peptide vessel, Rink Amide resin (340 mg, 0.160 mmol) was added and swollen with n-methyl-2-pyrrolidone (7 mL). The vessel was placed on a shake plate for 1 hour at room temperature. Following this period, the solvent in the vessel was evacuated and to it, deprotection solution (7 mL, 20% piperidine, 0.15 M HOBT in NMP) was added. Again, the vessel was placed on a shake plate for 1 hour at room temperature and subsequently the solvent was evacuated and the beads were washed with NMP (3 x 10 mL). The resin beads were evaluated for complete Fmoc deprotection through the use of the Kaiser test.[2] The resin beads were washed with DCM (3 x 5 mL) and dried. A solution of Fmoc-(4F)tyrosine-OH (400 mg, 0.780 mmol) and HBTU (296 mg, 0.780 mmol) and activator solution (10% Diisopropyl ethyl

amine in NMP, 4 mL) was prepared and added to the vessel containing the deprotected rink amide resin beads. The vessel was allowed to shake at room temperature overnight. Upon solvent evacuation and the washing of the beads (NMP, 3 x 10 mL), the resin beads were evacuated with the Kaiser test to insure complete coupling of the amino acid to the resin beads. Removal of the allyl protecting groups subsequently followed. To the vessel containing the resin beads, tetrakis(triphenylphosphine)palladium(0) (0.037 g, 0.032 mmol) and 1.3-dimethylbarbituric acid (0.100 g, 0.640 mmol) were added and the reaction was allowed to stir overnight for 18 hours at room temperature. The resin beads were washed with dichloromethane (3 x 10 mL) and dried. Compound **IV-sms-93** was separated from resin using cleavage conditions (trifluoroacetic acid 3.8 mL, water 0.1 mL, triisopropylsilane 0.1 mL) for 1 hour with intermittent stirring. The resulting solution was filtered, collected and the solvent was removed under reduced pressure. The resulting oil was purified via reverse-phase chromatography (linear gradient of 5 → 95% CH_3CN (0.1% HOAc) in H_2O (0.1% HOAc)) to yield **IV-sms-93** as a white crystalline solid (5.3 mg, 7.3% yield). **Spectral data**. ^{1}H NMR (400 MHz, DMSO-d_6) δ 11.39 – 11.13 (m, 1H), 8.23 (s, 1H), 7.84 (d, *J* = 7.8 Hz, 2H), 7.68 – 7.46 (m, 2H), 7.31 (dt, *J* = 31.9, 7.6 Hz, 3H), 7.12 (s, 1H), 5.28 (s, 1H), 4.29 – 4.05 (m, 3H), 3.69 (s, 1H), 3.29 (s, 4H), 3.07 – 2.73 (m, 2H), contains solvent peaks.^{19}F NMR (400 MHz, DMSO-d_6) δ, -145.28, -162.44.

V-sms-57

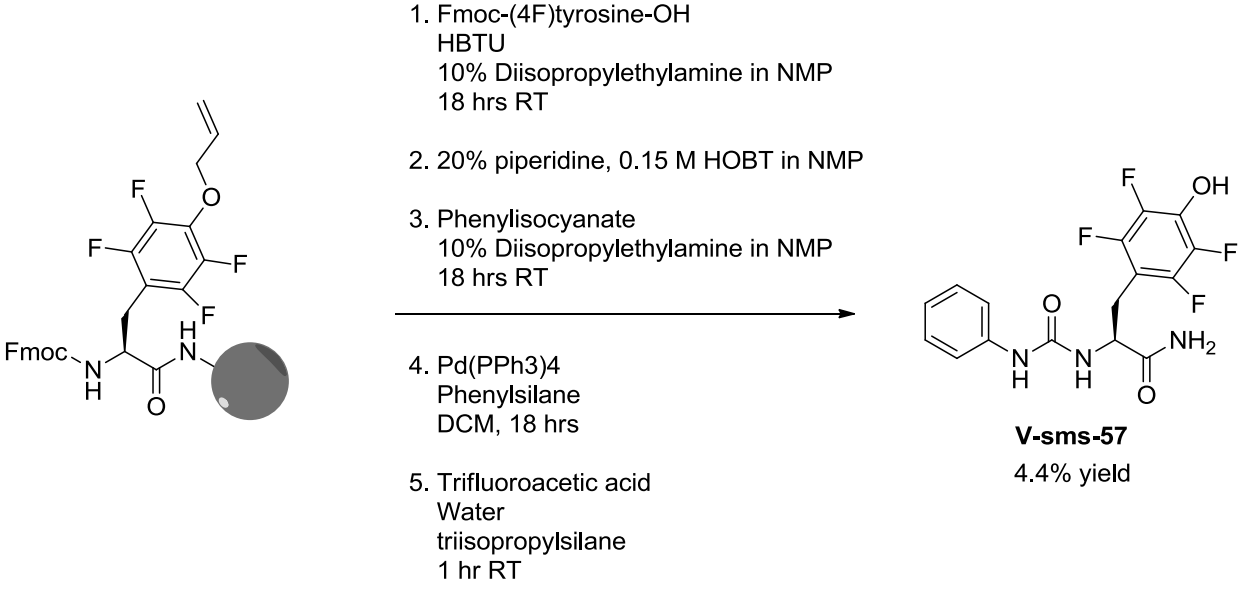

Prepared as previously described for compound **IV-sms-93**, the Fmoc-(4F)Tyrosine-OH was appended to Rink amide resin. The Fmoc protecting group was removed by adding 7 mL of deprotection solution (20% piperidine, 0.15 M HOBt in NMP) to the beads and allowing the

vessel to shake for 1 hour at room temperature. Subsequently, the solvent was evacuated, the beads were washed with NMP (3 x 10 mL), and the beads were evaluated for complete Fmoc removal through the use of the Kaiser test. To the vessel containing the Fmoc deprotected (4F)tyrosine resin beads, a solution of phenylisocyanate (5% in 4 mL of 10% diisopropylethylamine in NMP) was added and allowed to shake at room temperature overnight. The vessel was then evacuated, washed with NMP (3 x 5 mL) and evaluated by Kaiser test to ensure complete coupling of the phenylisocyanate. Removal of the allyl protecting groups subsequently followed. To the vessel containing the resin beads, tetrakis(triphenylphosphine)palladium(0) (0.037 g, 0.032 mmol) and 1.3-dimethylbarbituric acid (0.100 g, 0.640 mmol) were added and the reaction was allowed to stir overnight for 18 hours at room temperature. The resin beads were washed with dichloromethane (3 x 10 mL) and dried. Compound **V-sms-57** was separated from resin using cleavage conditions (trifluoroacetic acid 3.8 mL, water 0.1 mL, triisopropylsilane 0.1 mL) for 1 hour with intermittent stirring. The resulting solution was filtered, collected and the solvent was removed under reduced pressure. The resulting oil was purified via reverse-phase chromatography (linear gradient of 5 → 95% CH_3CN (0.1% HOAc) in H_2O (0.1% HOAc)) to yield **V-sms-57** as a crystalline solid (2.6 mg, 4.4% yield). **Spectral data**. ^{1}H NMR (400 MHz, DMSO-d_6) ^{1}H NMR (400 MHz, DMSO-d_6) δ 11.17 (s, 1H), 8.66 (s, 1H), 7.62 (s, 1H), 7.26 (d, *J* = 8.0 Hz, 2H), 7.23 – 7.11 (m, 3H), 6.84 (t, *J* = 7.3 Hz, 1H), 6.32 (d, *J* = 8.2 Hz, 1H), 4.41 (t, *J* = 6.8 Hz, 1H), 3.42 (s, 1H), 3.05 – 2.82 (m, 2H), contains solvent peaks.^{19}F NMR (400 MHz, DMSO-d_6) δ -144.58, -144.64, -162.56, -162.60.

V-sms-174

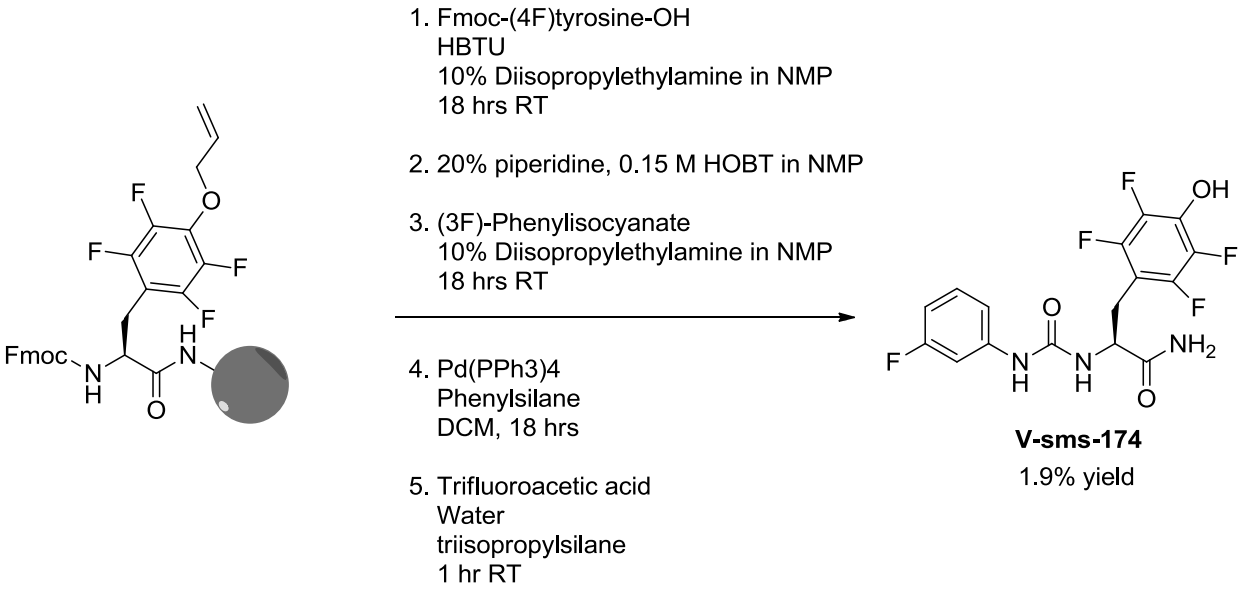

Prepared as previously described for compounds **IV-sms-93** and **V-sms-57**, the Fmoc-(4F)Tyrosine-OH was appended to Rink amide resin. The Fmoc protecting group was removed by adding 7 mL of deprotection solution (20% piperidine, 0.15 M HOBt in NMP) to the beads and allowing the vessel to shake for 1 hour at room temperature. Subsequently, the solvent was evacuated, the beads were washed with NMP (3 x 10 mL), and the beads were evaluated for complete Fmoc removal through the use of the Kaiser test. To the vessel containing the Fmoc deprotected (4F)tyrosine resin beads, a solution of (3F)-phenylisocyanate (5% in 4 mL of 10% diisopropylethylamine in NMP) was added and allowed to shake at room temperature overnight. The vessel was then evacuated, washed with NMP (3 x 5 mL) and evaluated by Kaiser test to ensure complete coupling of the phenylisocyanate. Removal of the allyl protecting groups subsequently followed. To the vessel containing the resin beads, tetrakis(triphenylphosphine)palladium(0) (0.037 g, 0.032 mmol) and 1.3-dimethylbarbituric acid (0.100 g, 0.640 mmol) were added and the reaction was allowed to stir overnight for 18 hours at room temperature. The resin beads were washed with dichloromethane (3 x 10 mL) and dried. Compound **V-sms-174** was separated from resin using cleavage conditions (trifluoroacetic acid 3.8 mL, water 0.1 mL, triisopropylsilane 0.1 mL) for 1 hour with intermittent stirring. The resulting solution was filtered, collected and the solvent was removed under reduced pressure. The resulting oil was purified via reverse-phase chromatography (linear gradient of 5 → 95% CH_3CN (0.1% HOAc) in H_2O (0.1% HOAc)) to yield **V-sms-174** as a crystalline solid (1.2 mg, 1.9% yield). **Spectral data**. ^{1}H NMR (400 MHz, DMSO-d_6) ^{1}H NMR (400 MHz, DMSO-d_6) δ δ 11.19 (s, 1H), 8.91 (s, 1H), 7.64 (s, 1H), 7.43 – 7.26 (m, 1H), 7.24 – 7.11 (m, 1H), 6.89 (d, *J* = 8.3 Hz, 1H), 6.66 (t, *J* = 8.6 Hz, 1H), 6.39 (d, *J* = 8.1 Hz, 1H), 5.28 (s, 1H), 4.41 (q, *J* = 7.0 Hz, 1H), 3.07 – 2.80 (m, 1H), contains solvent peaks.^{19}F NMR (400 MHz, DMSO-d_6) δ -112.41, -144.57, -144.63, -162.52, -162.58.

B.3: Spectral Data

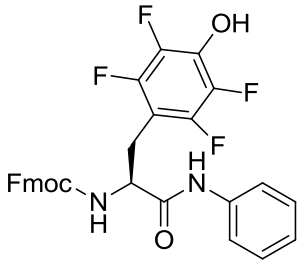

IV-sms-80

^{1}H

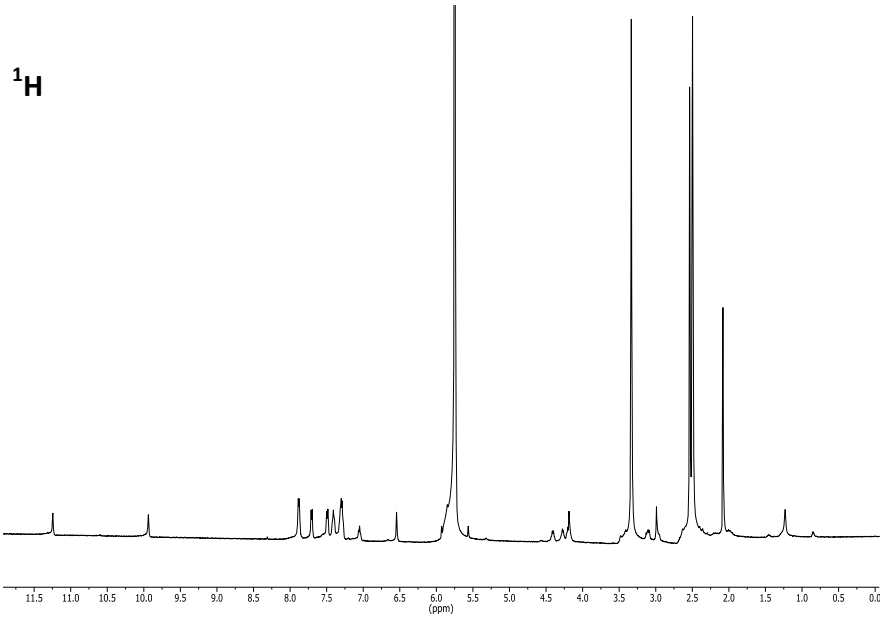

^{19}F

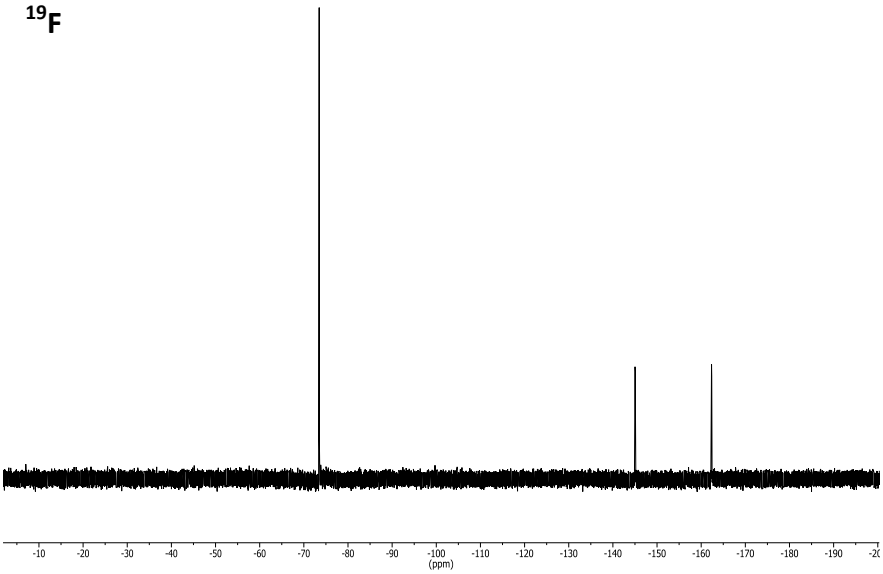

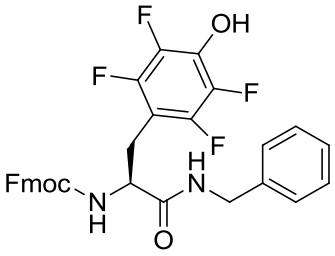

IV-sms-89

^{1}H

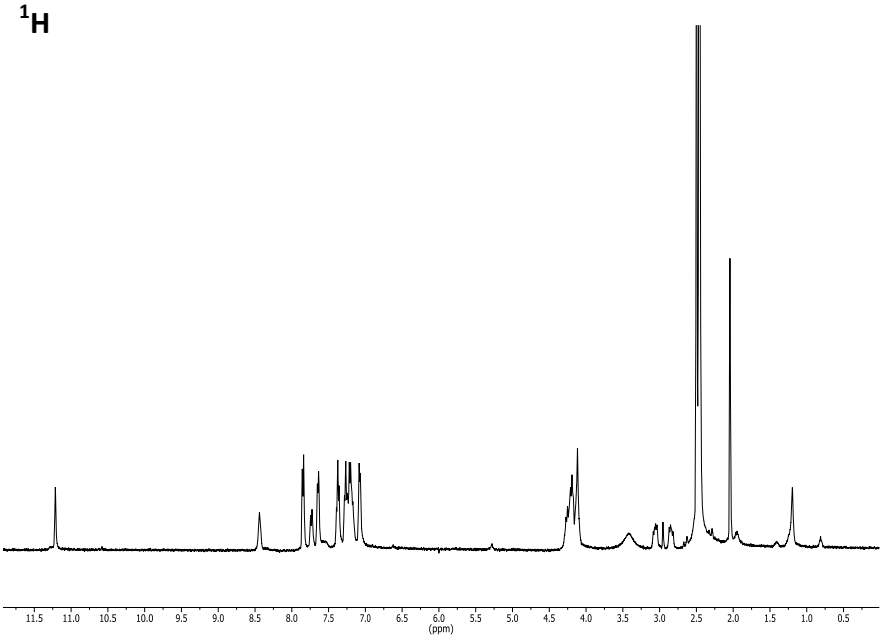

^{19}F

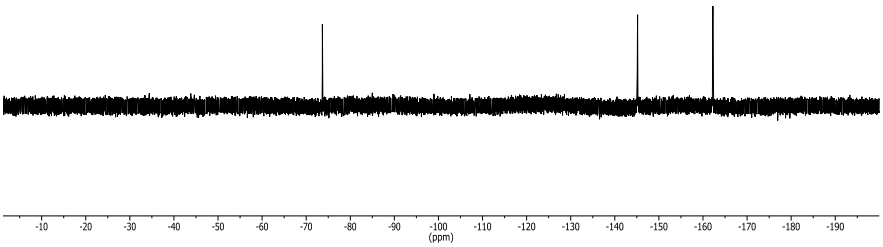

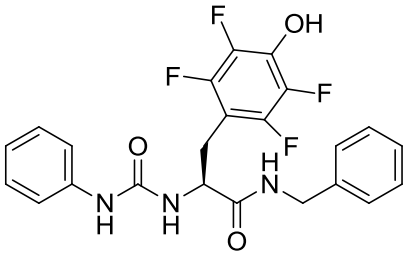

IV-sms-109

^{1}H

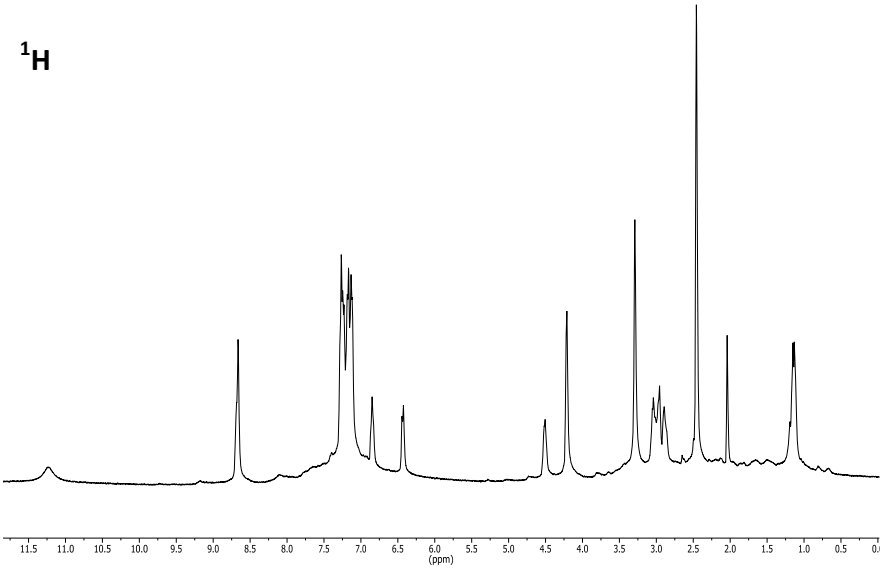

^{19}F

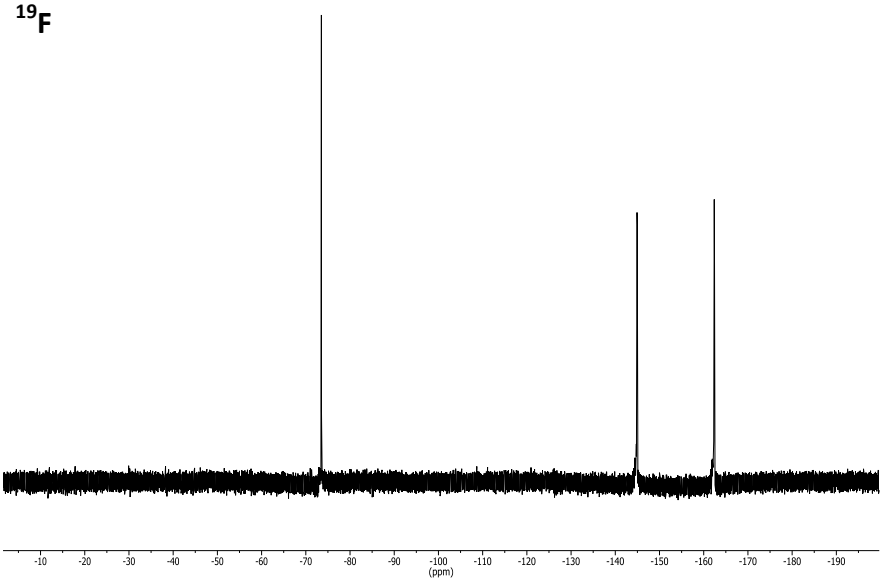

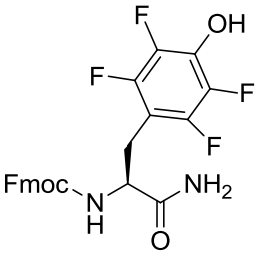

IV-sms-93

^{1}H

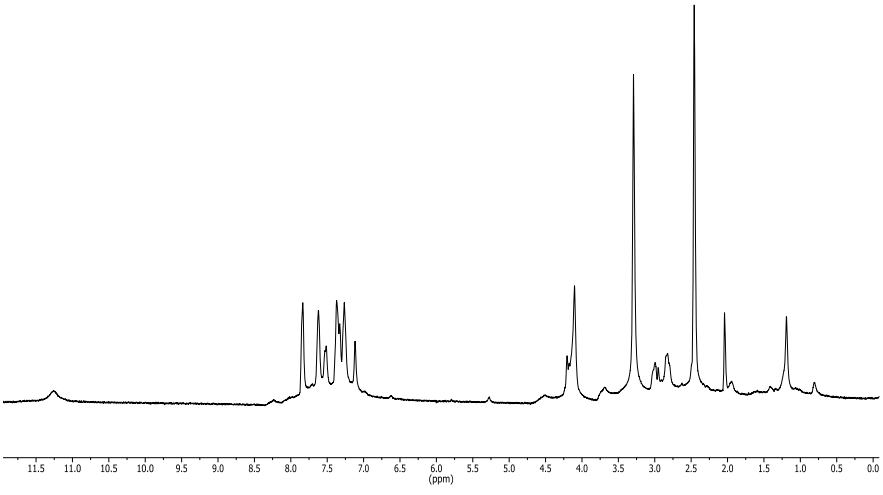

^{19}F

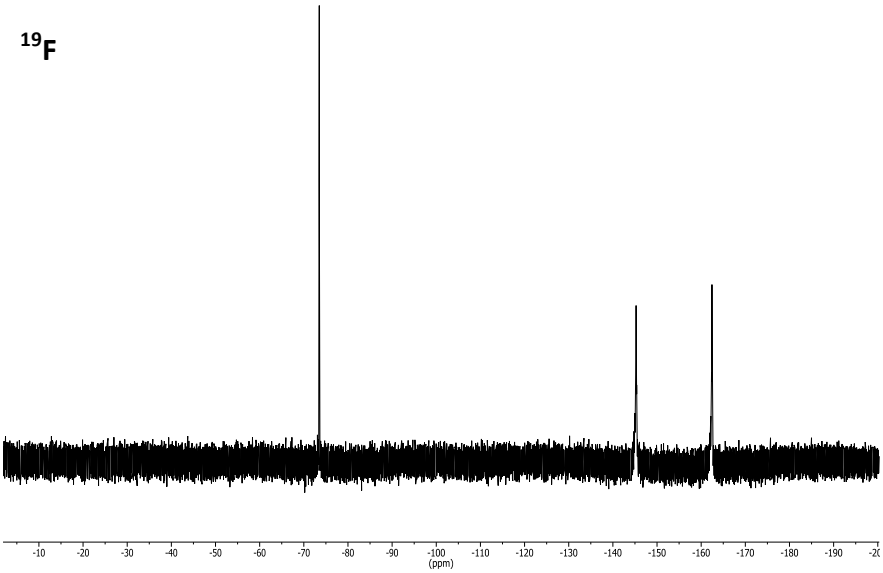

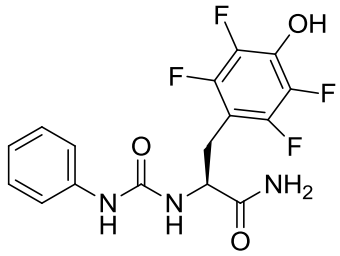

V-sms-57

^{1}H

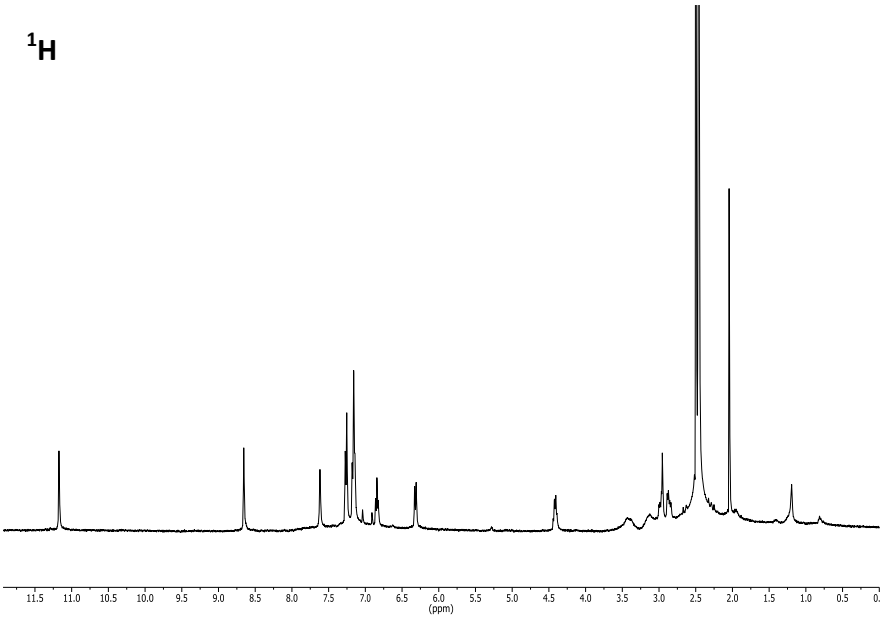

^{19}F

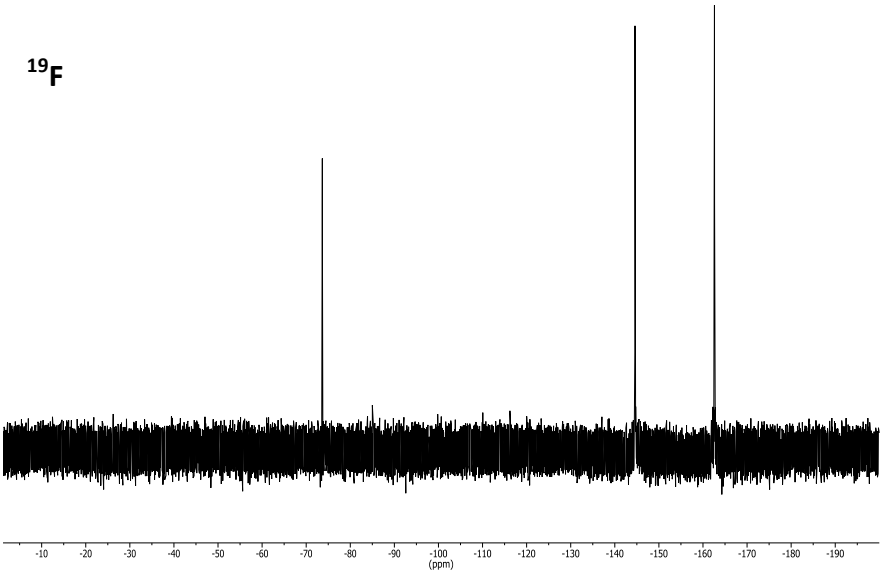

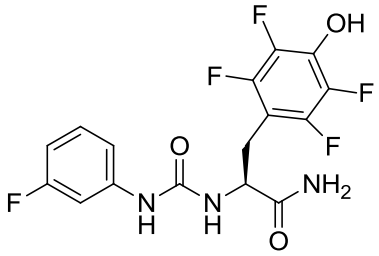

V-sms-174

^{1}H

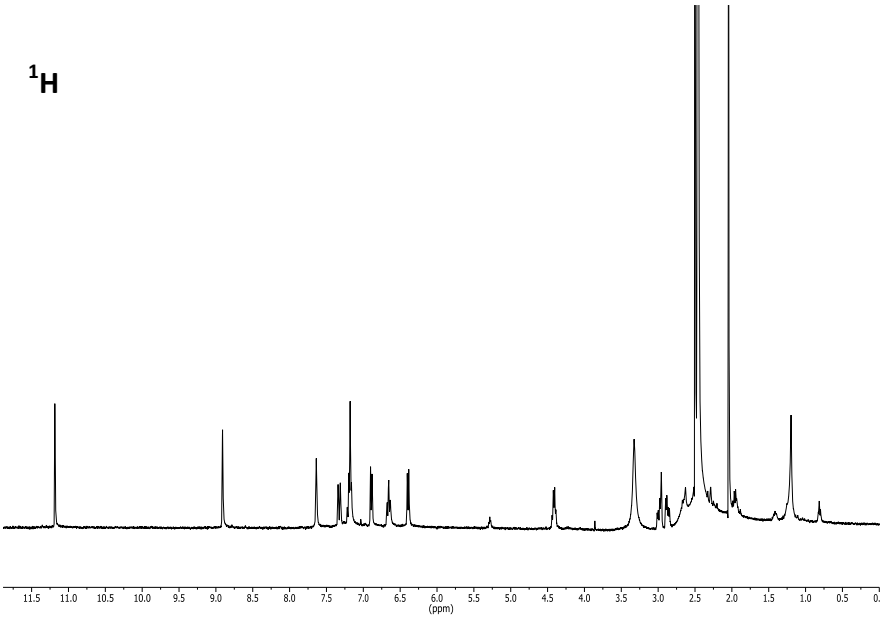

^{19}F

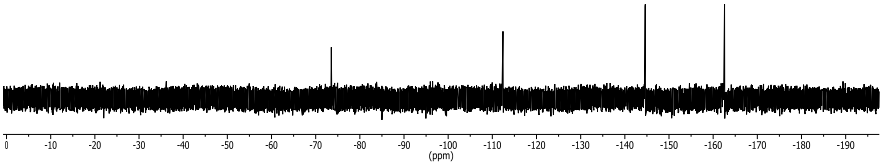

B.4: Biochemical Characterization

General procedure for determination of inhibitor K_i. A continuous fluorescence assay[3] was used to determine K_i. Reaction volumes of 100 µL were used in 96-well plates. 85 µL of enzyme in buffer was added to each well. 2.5 µL of the appropriate inhibitor dilution (final concentrations typically 1000, 500, 250, 125, 62.5, 31.25, 15.6, 7.8, 3.9 and 0 µM in DMSO) was then added. 2.5 µL of a substrate peptide ("compound 3" as described in Wang et al)[3] solution (1.8 mM in DMSO) was added. The reaction was initiated with 10 µL of ATP (10 mM in water), and reaction progress was immediately monitored at 405 nm (ex. 340 nm) for 10 minutes. Reactions had final concentrations of 30 nM enzyme, 45 µM peptide substrate, 1000 µM ATP, 100 µM Na_3VO_4, 100 mM Tris buffer (pH 8), 10 mM $MgCl_2$, 0.01% Triton X-100. The initial rate data collected was used for determination of K_i values. For K_i determination, the kinetic values were obtained directly from nonlinear regression of substrate-velocity curves in the presence of various concentrations of the inhibitor. The equation Y = Bottom + (Top – Bottom)/(1 + 10^X – LogEC50), X = log(concentration) and Y = binding; was used in the nonlinear regression.

Analytical data for c-Src Kinase Domain K_i determination. Each inhibitor K_i value was determined using at least four independent experiments, a representative inhibition curve is shown.

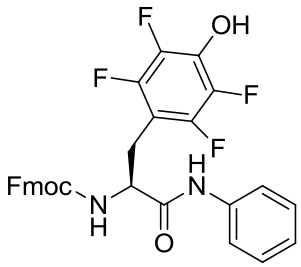

IV-sms-80

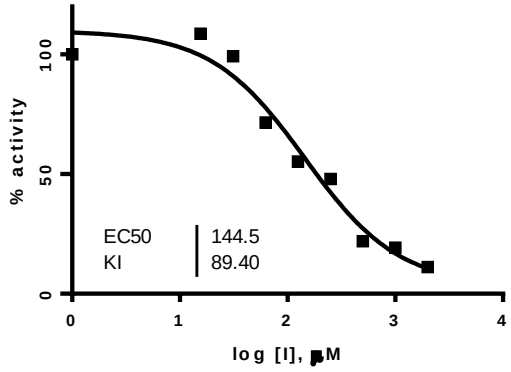

Average IC_{50}: 144.6 ± 21.2 µM

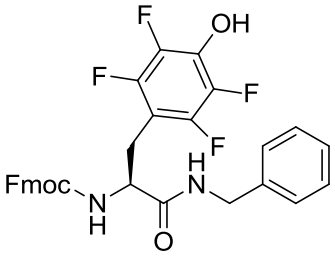

IV-sms-89

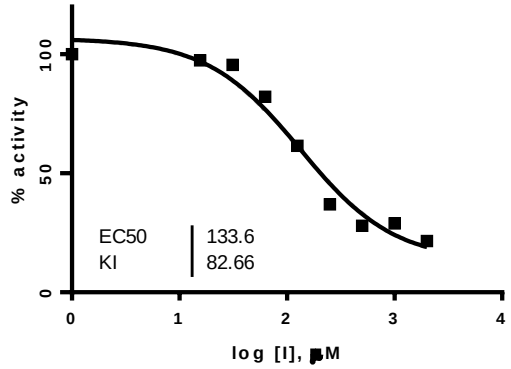

Average IC_{50}: 131.2 ± 22.3 µM

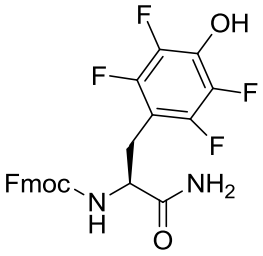

IV-sms-93

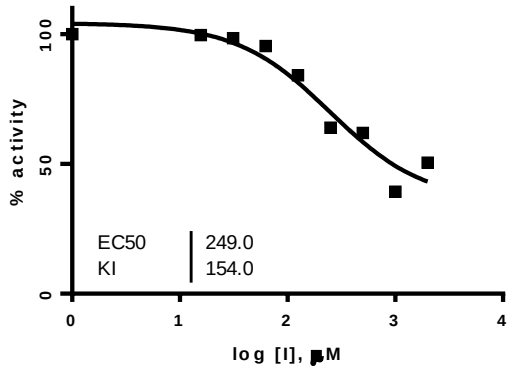

Average IC_{50}: 302.1 ± 141.8 µM

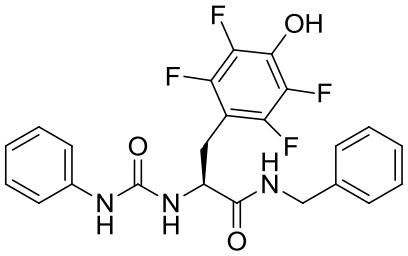

IV-sms-109

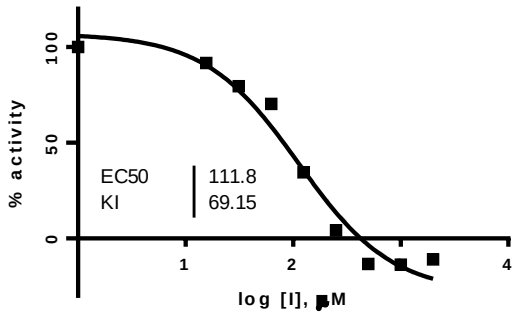

Average IC_{50}: 129.2 ± 24.6 µM

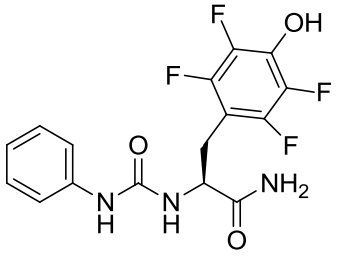

V-sms-57

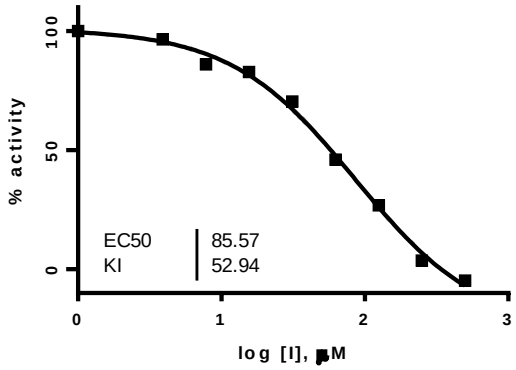

Average IC_{50}: 86.4 ± 15.0 µM

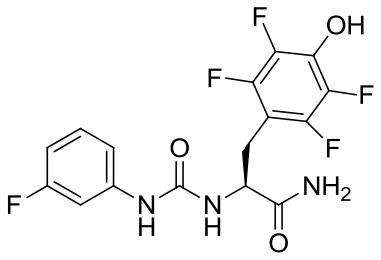

V-sms-174

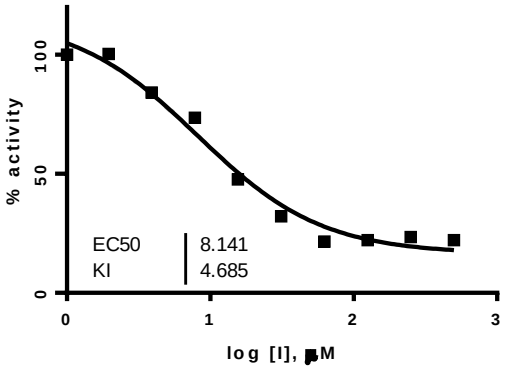

Average IC_{50}: 12.3 ± 4.4 µM

Analytical data for c-Src T338M K_i determination. Each inhibitor K_i value was determined using at least four independent experiments, a representative inhibition curve is shown.

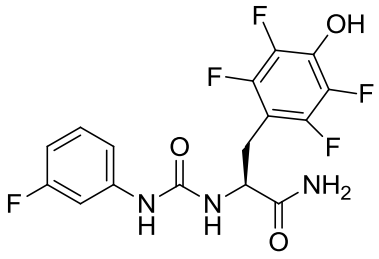

V-sms-174

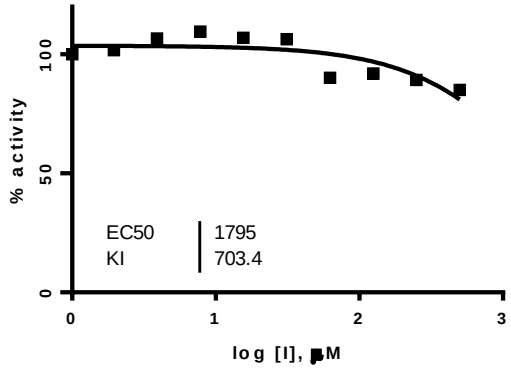

Average IC_{50}: > 500 µM

Analytical data for c-Src 3D K_i determination. Each inhibitor K_i value was determined using at least four independent experiments, a representative inhibition curve is shown

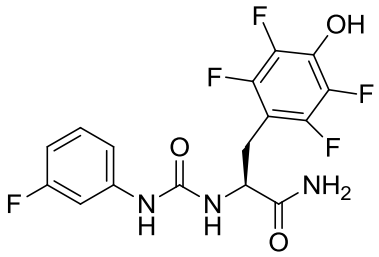

V-sms-174

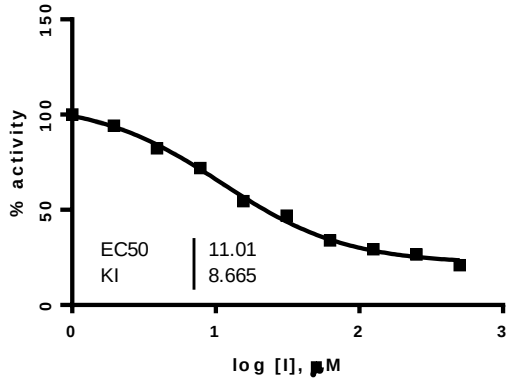

Average IC_{50}: 11.5 ± 0.4 µM

Analytical data for c-Abl K_i determination. Each inhibitor K_i value was determined using at least four independent experiments, a representative inhibition curve is shown

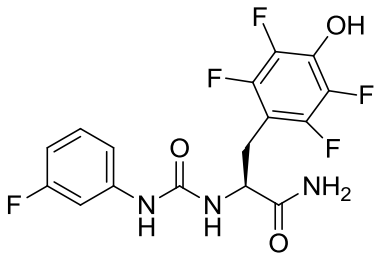

V-sms-174

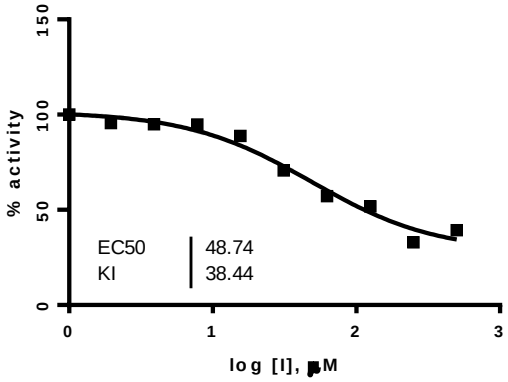

Average IC_{50}: 46.4 ± 17.6 µM

Analytical data for c-Hck K_i determination. Each inhibitor K_i value was determined using at least four independent experiments, a representative inhibition curve is shown.

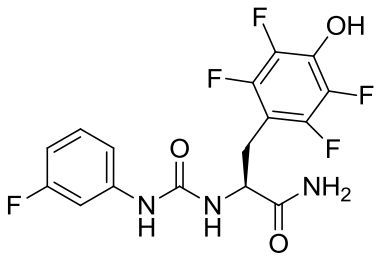

V-sms-174

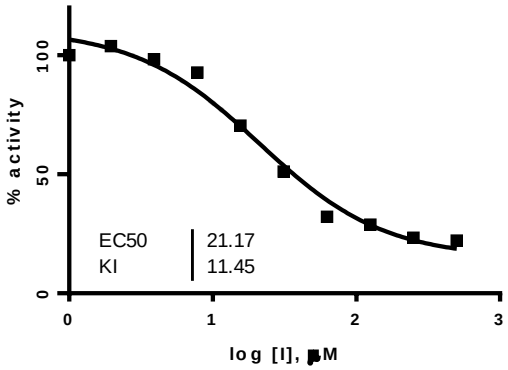

Average IC_{50}: 23.1 ± 2.2 µM

Analytical data for c-Src Kinase domain K_i determination at high [ATP] (5 mM final concentration, 45 µM substrate concentration). Each inhibitor K_i value was determined using at least four independent experiments; a representative inhibition curve is shown.

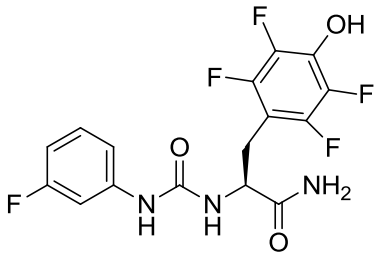

V-sms-174

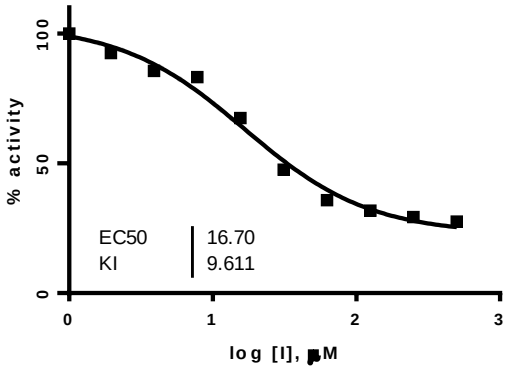

Average IC_{50}: 16.4 ± 2.1 µM

Analytical data for c-Src Kinase domain K_i determination at low [ATP] (100 µM final concentration, 45 µM substrate concentration). Each inhibitor K_i value was determined using at least four independent experiments; a representative inhibition curve is shown.

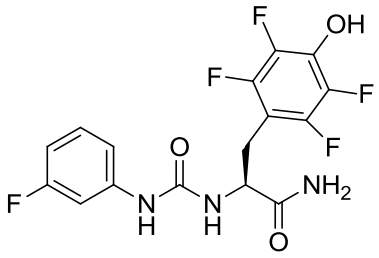

V-sms-174

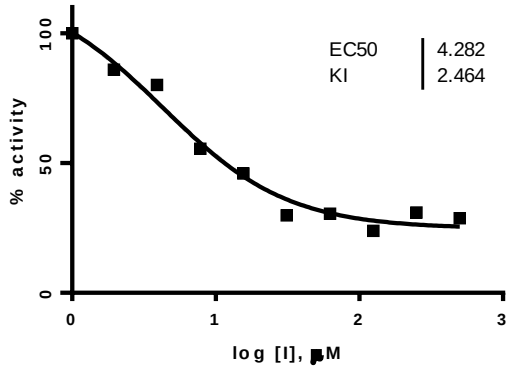

Average IC_{50}: 5.3 ± 2.2 µM

Analytical data for c-Src Kinase domain K_i determination at high [substrate] (500 µM final concentration, 1 mM ATP concentration). Each inhibitor K_i value was determined using at least four independent experiments; a representative inhibition curve is shown.

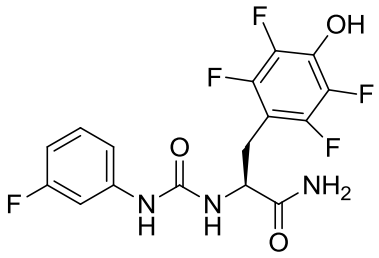

V-sms-174

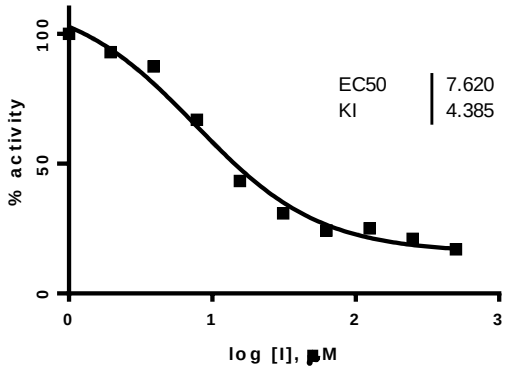

Average IC_{50}: 4.6 ± 2.9 µM

General procedure for ATP Lineweaver-Burk analysis of inhibitor. A continuous fluorescence assay[3] was used to determine K_M. Reaction volumes of 100 µL were used in 96-well plates. 85 µL of enzyme in buffer was added to each well. 2.5 µL of the appropriate inhibitor dilution (fixed concentrations, typically 0, 35, 50, 70, 100, or 140 µM in DMSO) was then added. 2.5 µL of a substrate peptide ("compound 3" as described in Wang et al)[3] solution (1.8 mM in DMSO) was added. The reaction was initiated with 10 µL of ATP (Two-fold dilutions, final concentrations: 5mM → 0 in water), and reaction progress was immediately monitored at 405 nm (ex. 340 nm) for 10 minutes. Reactions had final concentrations of 30 nM enzyme, 45 µM peptide substrate, 100 µM Na_3VO_4, 100 mM Tris buffer (pH 8), 10 mM $MgCl_2$, 0.01% Triton X-100. The initial rate data collected was used for determination of K_M values. For K_M determination, the kinetic values were obtained directly from nonlinear regression of substrate-velocity curves in the presence of various concentrations of ATP. The equation Y = (Vmax * X)/(Km + X), X = substrate concentration (µM) and Y = enzyme velocity (RFU/s); was used in the nonlinear regression.

Analytical data for c-Src Kinase Domain ATP Lineweaver-Burk analysis of inhibitor. Each inhibitor K_M value was determined using at least 4 independent experiments; a representative K_M curve is shown.

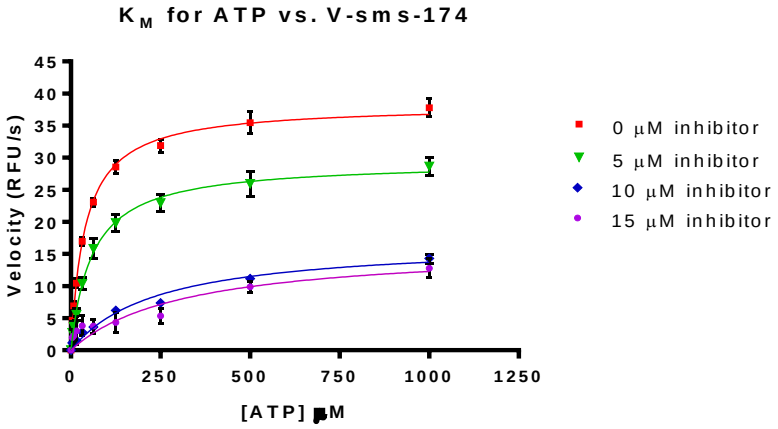

	0 µM inhibitor	5 µM inhibitor	10 µM inhibitor	15 µM inhibitor
Best-fit values				
Vmax	38.22	29.38	17.04	16.18
Km	40.13	58.70	242.0	317.3
Std. Error				
Vmax	0.6888	0.9834	0.9505	2.618
Km	2.884	7.533	35.38	128.1
95% Confidence Intervals				
Vmax	36.85 to 39.59	27.42 to 31.35	15.15 to 18.94	10.91 to 21.45
Km	34.38 to 45.88	43.67 to 73.73	171.4 to 312.6	59.60 to 575.1

General procedure for Substrate Lineweaver-Burk analysis of inhibitor. A continuous fluorescence assay[3] was used to determine K_M. Reaction volumes of 100 µL were used in 96-well plates. 85 µL of enzyme in buffer was added to each well. 2.5 µL of the appropriate inhibitor dilution (fixed concentrations, typically 0, 35, 50, 70, 100, or 140 µM in DMSO) was then added. 2.5 µL of a substrate peptide ("compound 3" as described in Wang et al)[3] solution (Final concentrations: 500 µM → 0 in DMSO) was added. The reaction was initiated with 10 µL of ATP (Final concentration 1 mM in water), and reaction progress was immediately monitored at 405 nm (ex. 340 nm) for 10 minutes. Reactions had final concentrations of 30 nM enzyme, 45 µM peptide substrate, 100 µM Na_3VO_4, 100 mM Tris buffer (pH 8), 10 mM $MgCl_2$, 0.01% Triton X-100. The initial rate data collected was used for determination of K_M values. For K_M determination, the kinetic values were obtained directly from nonlinear regression of substrate-velocity curves in the presence of various concentrations of substrate. The equation Y = (Vmax * X)/(Km + X), X = substrate concentration (µM) and Y = enzyme velocity (RFU/s); was used in the nonlinear regression.

Analytical data for c-Src Kinase Domain Substrate Lineweaver-Burk analysis of inhibitor. Each inhibitor K_M value was determined using at least 4 independent experiments; a representative K_M curve is shown.

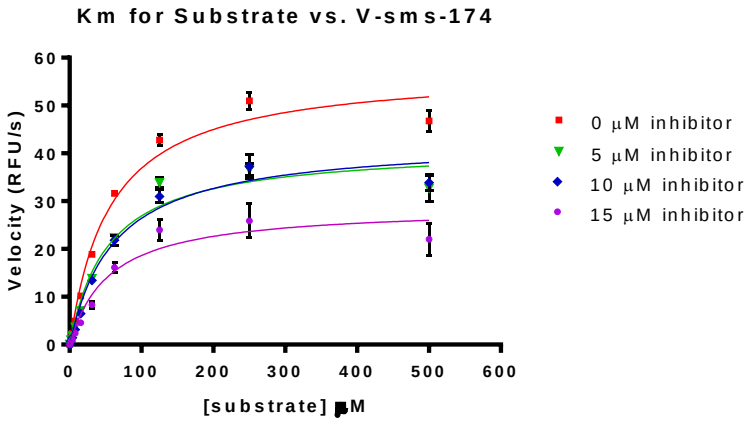

	0 µM inhibitor	5 µM inhibitor	10 µM inhibitor	15 µM inhibitor
Best-fit values				
Vmax	57.64	41.34	42.79	28.85
Km	56.34	53.69	62.18	54.89
Std. Error				
Vmax	1.468	1.476	1.566	2.025
Km	4.588	6.204	7.040	12.40
95% Confidence Intervals				
Vmax	54.71 to 60.57	38.40 to 44.29	39.67 to 45.92	24.81 to 32.88
Km	47.19 to 65.49	41.32 to 66.06	48.14 to 76.23	30.16 to 79.62

B.5: References

(1) Wang, F.; Luoheng, Q.; Wong, P.; Gao, J. *Org. Lett.* **2011**, *13*, 236.

(2) Kaiser, E.; Colescott, R. L.; Bossinger, C. D.; Cook, P. I. *Anal Biochem* **1970**, *34*, 595.

(3) Wang, Q.; Cahill, S. M.; Blumenstein, M.; Lawrence, D. S. *J. Am. Chem. Soc.* **2006**, *128*, 1808.

Appendix C:

Supplemental Information for Chapter 4

C.1: General Synthetic Methods Unless otherwise noted, all reagents were obtained from commercially available sources and used without further purification. All ^{1}H and ^{13}C NMR spectra were measured with a Varian 400 MHz spectrometer. Samples were taken in $CDCl_3$ or DMSO-*d6***,** spectra were referenced to chloroform peak. High resolution mass spectrometry (HRMS) was carried out by the University of Michigan Mass Spectrometry Facility (J. Windak, Director).

C.2: Synthesis of Compounds

Compounds [1], [1d], [1e], [1f], [1g]:

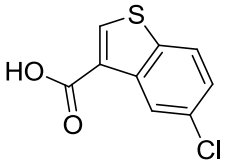

[1]

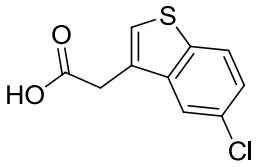

[1d]

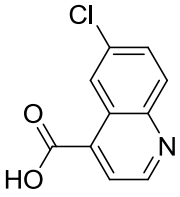

[1e]

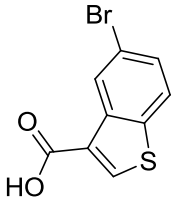

[1f]

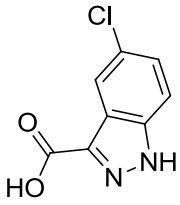

[1g]

These commercially available compounds were purchased from Maybridge Chemical, a part of Thermo Fisher Scientific Company and were used without further purification.[1]

Synthesis of compound [1a]

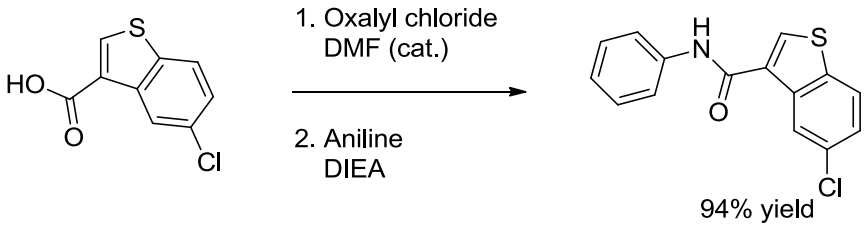

In a dried, round-bottom flask equipped with a stir bar, and under nitrogen atmosphere, 5-chlorobenzo[b]thiophene-3-carboxylic acid **[1]** (0.100 g, 0.472 mmol) was dissolved in 3 mL of dichloromethane. To this, oxalyl chloride (0.060 mL, 0.66 mmol) was added slowly, drop-wise.

Following this, one drop of dimethylformamide was added. The reaction was allowed to stir at room temperature for thirty minutes at which point, the solvent was concentrated to yield the crude oil intermediate which was immediately used without further purification and dissolved in 2 mL of dichloromethane. To this, diisopropylethylamine (0.12 mL, 0.742 mmol) and aniline (0.033 mL, 0.362 mmol) were added at 0°C. The reaction was allowed to warm to room temperature overnight. The solvent was removed under reduced pressure and the resulting crude product was solubilized in ethyl acetate (50 mL) and washed with water (1 x 50 mL) followed by a wash with a brine solution (1 x 50 mL). The resulting organic layer was dried over anhydrous $MgSO_4$ and filtered. The solvent was removed under reduced pressure to afford the crude product, which was purified via automated silica gel chromatography (Linear gradient of 7 → 100% ethyl acetate in hexanes) to yield compound **[1a]** as a yellow crystalline solid (117 mg, 94% yield). **Spectral data**. ^{1}H NMR (400 MHz, DMSO-d_6) δ 10.35 (s, 1H), 8.68 (s, 1H), 8.42 (s, 1H), 8.10 (d, *J* = 8.4 Hz, 1H), 7.74 (d, *J* = 8.1 Hz, 2H), 7.46 (dd, *J* = 8.6, 2.4 Hz, 2H), 7.34 (t, *J* = 8.0 Hz, 1H), 7.08 (t, *J* = 7.5 Hz, 1H). ^{13}C NMR (400 MHz, DMSO-d_6) δ 161.82, 139.30, 138.91, 138.43, 134.77, 130.70, 130.47, 129.41, 129.10, 125.53, 125.03, 124.15, 124.01, 120.70. HRMS-ESI (*m/z*): $[M+H]^+$ calcd for $C_{15}H_{10}ClNOS$ 288.0244; found 288.0239.

Synthesis of compound [1b]:

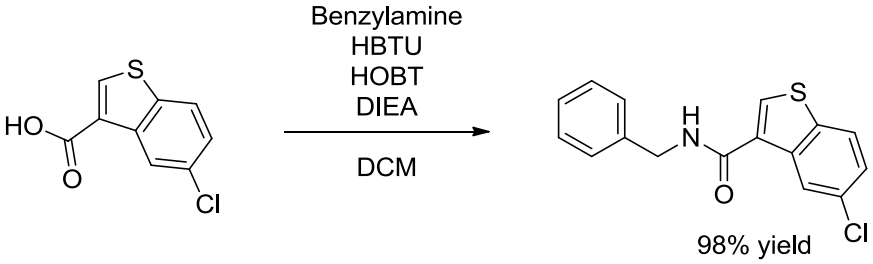

In a dried, round-bottom flask equipped with a stir bar, and under nitrogen atmosphere, 5-chlorobenzo[b]thiophene-3-carboxylic acid **[1]** (0.100 g, 0.472 mmol) was dissolved in 5 mL of

dichloromethane. To this, HBTU (0.197 g, 0.519 mmol), HOBT (0.070 g, 0.519 mmol), diisopropylethylamine (0.090 mL, 0.519 mmol), and benzylamine (0.052 mL, 0.472 mmol) were added at 0°C. The reaction was allowed to warm to room temperature overnight. The organics were removed under reduced pressure and the resulting crude product was solubilized in ethyl acetate (50 mL) and washed with water (1 x 50 mL) followed by a wash with a brine solution (1 x 50 mL). The resulting organic layer was dried over anhydrous $MgSO_4$ and filtered. The solvent was removed under reduced pressure to afford the crude product, which was purified via automated silica gel chromatography (Linear gradient of 7 → 100% ethyl acetate in hexanes) to yield compound **[1a]** as a crystalline solid (140 mg, 98% yield). **Spectral data**. ^{1}H NMR (400 MHz, DMSO-d_6) δ 9.07 (t, *J* = 5.9 Hz, 1H), 8.51 (d, *J* = 10.0 Hz, 2H), 8.05 (d, *J* = 8.6 Hz, 1H), 7.42 (dd, *J* = 8.7, 2.3 Hz, 1H), 7.31 (d, *J* = 6.9 Hz, 4H), 7.22 (d, *J* = 6.8 Hz, 1H), 4.47 (d, *J* = 5.9 Hz, 2H). ^{13}C NMR (400 MHz, DMSO-d_6) δ 163.08, 139.90, 139.04, 138.45, 133.70, 130.55, 130.16, 128.75, 127.71, 127.24, 125.35, 124.90, 124.23, 42.70. HRMS-ESI (*m/z*): $[M+H]^+$ calcd for $C_{16}H_{12}ClNOS$ 302.0401; found 302.0398.

Synthesis of compound [1c]

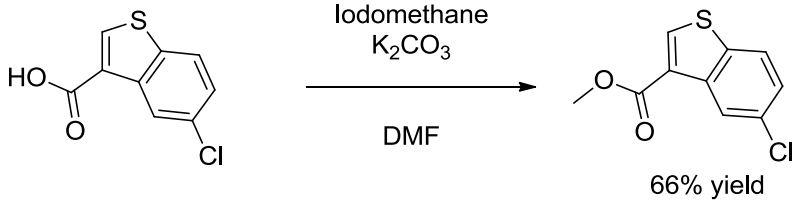

In a dried, round-bottom flask equipped with a stir bar, and under nitrogen atmosphere, 5-chlorobenzo[b]thiophene-3-carboxylic acid **[1]** (0.100 g, 0.472 mmol) was dissolved in 3 mL of dimethylformamide. To this, iodomethane (0.040 mL, 0.705 mmol), potassium carbonate (0.098 mL, 0.709 mmol) were added and was allowed to stir overnight at room temperature. The reaction was quenched with water (50 mL) and extracted with ethyl acetate (3 x 50 mL). The resulting organic layer was washed with a saturated sodium bicarbonate solution (1 x 50 mL) followed by a wash with a brine solution (1 x 50 mL). The resulting organic layer was dried over anhydrous $MgSO_4$ and filtered. The solvent was removed under reduced pressure to afford the crude product, which was purified via automated silica gel chromatography (Linear gradient of 7 → 100% ethyl acetate in hexanes) to yield compound **[1a]** as a white crystalline solid (70 mg, 66% yield). **Spectral data**. ^{1}H NMR (400 MHz, DMSO-d_6) δ 8.70 (s, 1H), 8.33 (d, *J* = 2.3 Hz, 1H), 8.05 (d, *J* = 8.7 Hz, 1H), 7.50 – 7.33 (m, 1H), 3.84 (s, 3H). ^{13}C NMR (100 MHz, dmso) δ 162.59, 140.92, 138.55, 137.88, 131.22, 129.69, 125.56, 125.17, 123.44, 52.28. HRMS-ESI (*m/z*): $[M+H]^+$ calcd for $C_{10}H_7ClNO_2S$ 226.9855; found 226.1791.

C.3: Spectral Data for compounds [1a-c]

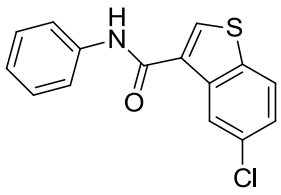

[1a]

^{1}H

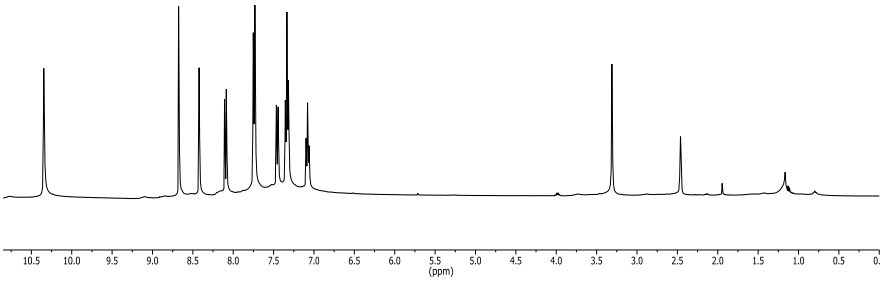

^{13}C

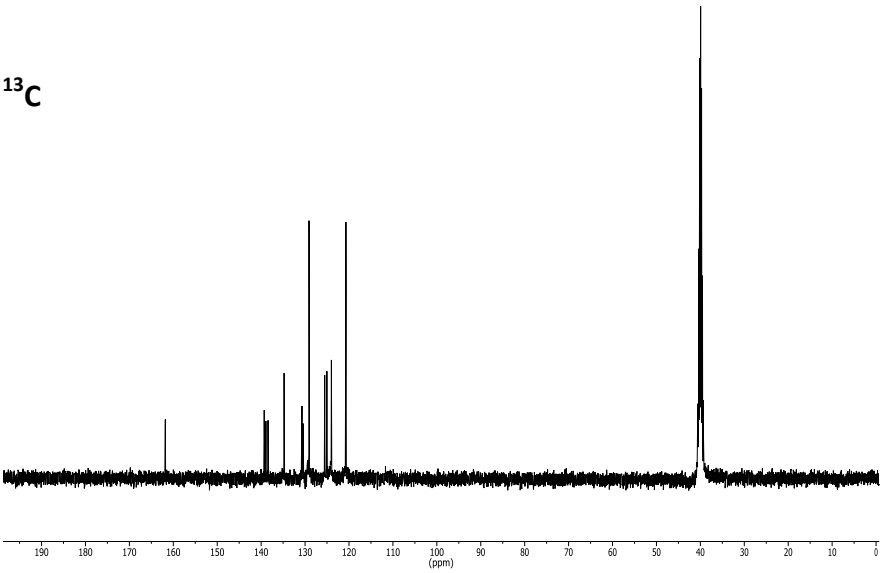

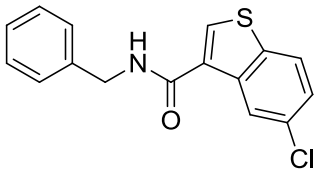
S
H
N
O
Cl

[1b]

^{1}H

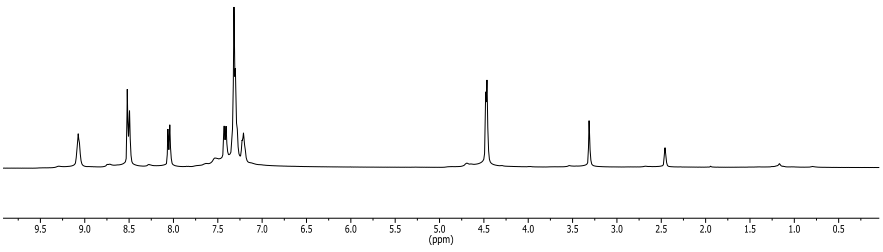
9.5 9.0 8.5 8.0 7.5 7.0 6.5 6.0 5.5 5.0 4.5 4.0 3.5 3.0 2.5 2.0 1.5 1.0 0.5
(ppm)

^{13}C

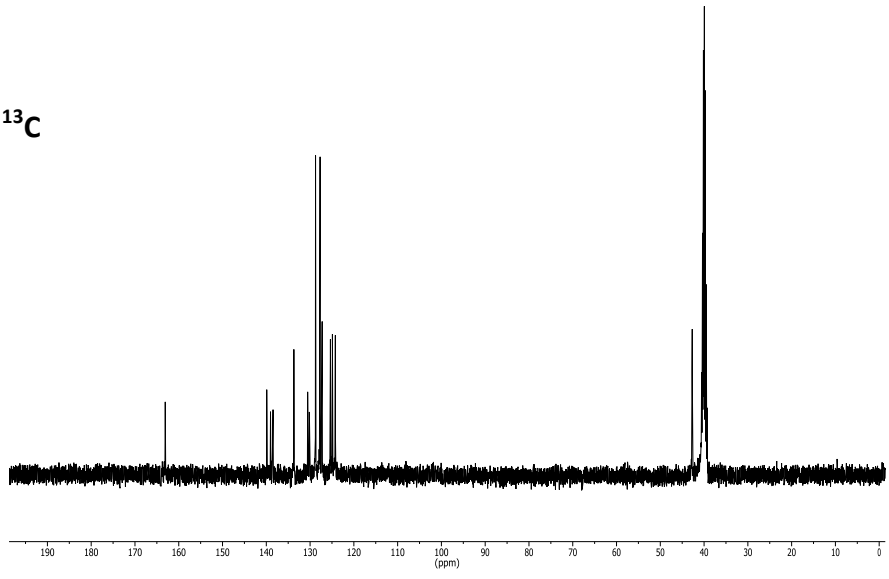
190 180 170 160 150 140 130 120 110 100 90 80 70 60 50 40 30 20 10 0
(ppm)

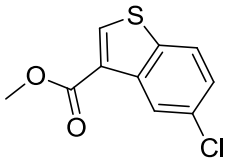
S
O
O
Cl

[1c]

^{1}H

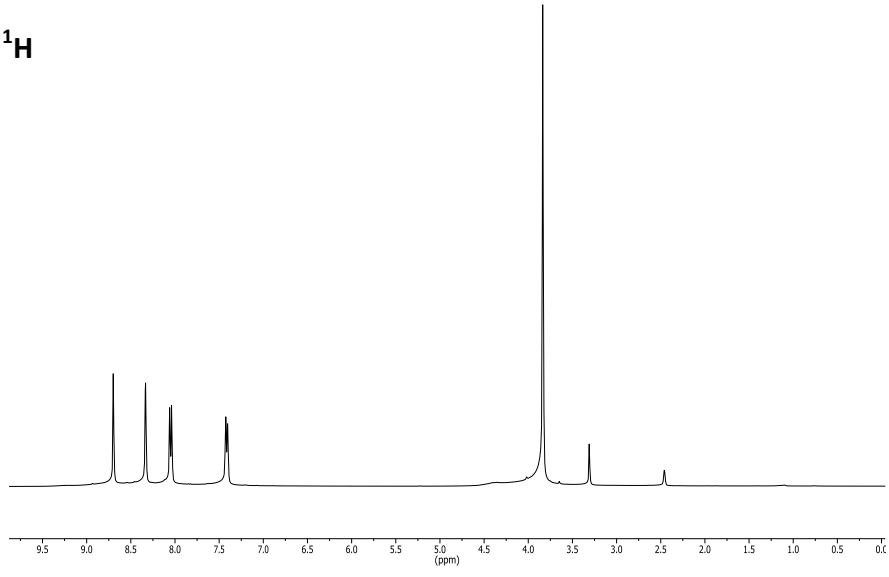
9.5
9.0
8.5
8.0
7.5
7.0
6.5
6.0
5.5
5.0
4.5
4.0
3.5
3.0
2.5
2.0
1.5
1.0
0.5
(ppm)

^{13}C

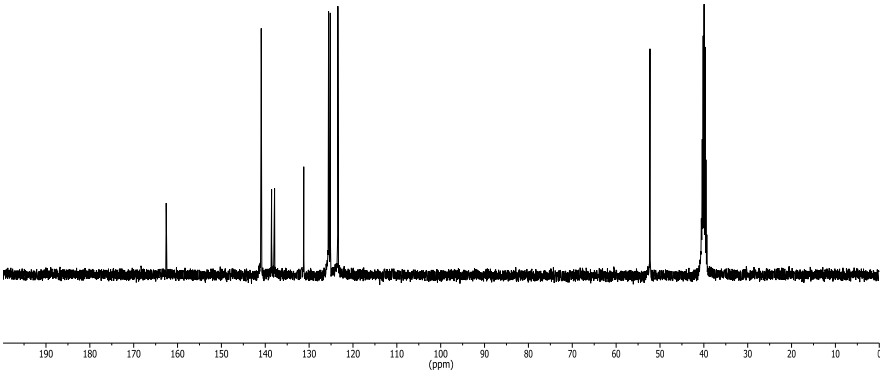
190
180
170
160
150
140
130
120
110
100
90
80
70
60
50
40
30
20
10
(ppm)

C.4: Biochemical Characterization

General procedure for determination of inhibitor K_i. A continuous fluorescence assay[2] was used to determine K_i. Reaction volumes of 100 µL were used in 96-well plates. 85 µL of enzyme in buffer was added to each well. 2.5 µL of the appropriate inhibitor dilution (final concentrations typically 1000, 500, 250, 125, 62.5, 31.25, 15.6, 7.8, 3.9 and 0 µM in DMSO) was then added. 2.5 µL of a substrate peptide ("compound 3" as described in Wang et al)[2] solution (1.8 mM in DMSO) was added. The reaction was initiated with 10 µL of ATP (10 mM in water), and reaction progress was immediately monitored at 405 nm (ex. 340 nm) for 10 minutes. Reactions had final concentrations of 30 nM enzyme, 45 µM peptide substrate, 1000 µM ATP, 100 µM Na_3VO_4, 100 mM Tris buffer (pH 8), 10 mM $MgCl_2$, 0.01% Triton X-100. The initial rate data collected was used for determination of K_i values. For K_i determination, the kinetic values were obtained directly from nonlinear regression of substrate-velocity curves in the presence of various concentrations of the inhibitor. The equation Y = Bottom + (Top – Bottom)/(1 + 10^X – LogEC50), X = log(concentration) and Y = binding; was used in the nonlinear regression.

Analytical data for c-Src Kinase Domain K_i determination. Each inhibitor K_i value was determined using at least four independent experiments, a representative inhibition curve is shown.

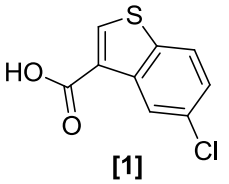

[1]

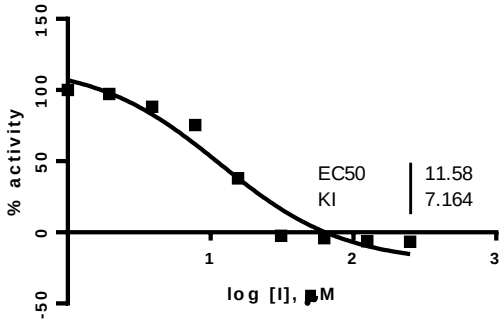

Average IC_{50}: 9.4 ± 2.8 µM

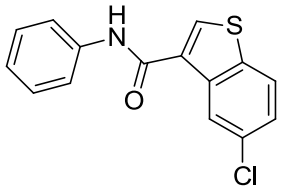

[1a]

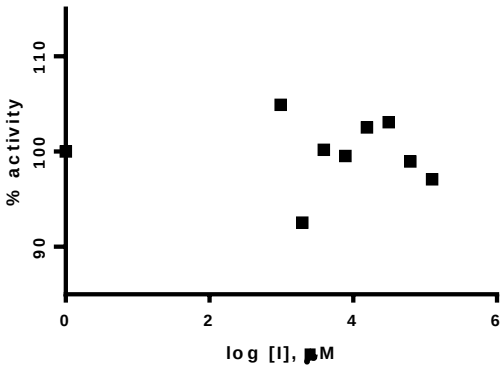

Average IC_{50}: > 125 µM

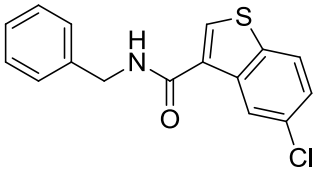

[1b]

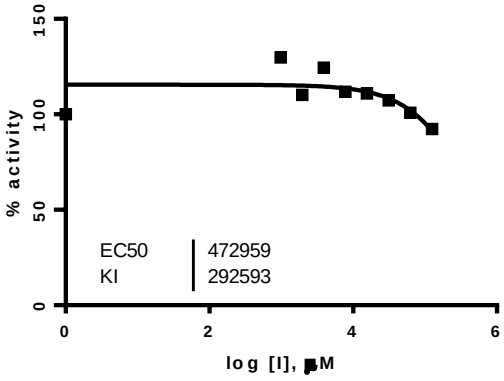

Average IC_{50}: > 125 µM

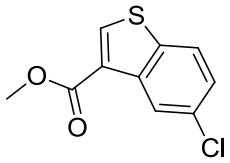

[1c]

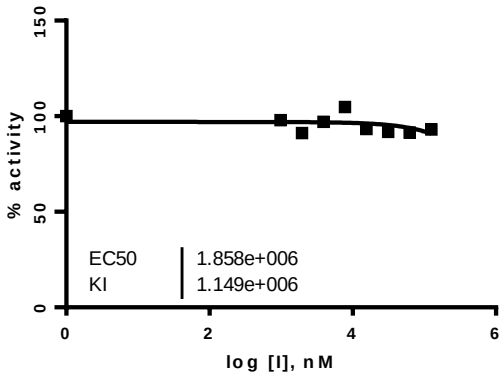

Average IC_{50}: > 125 µM

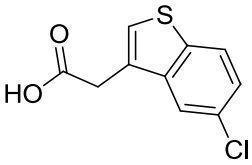

[1d]

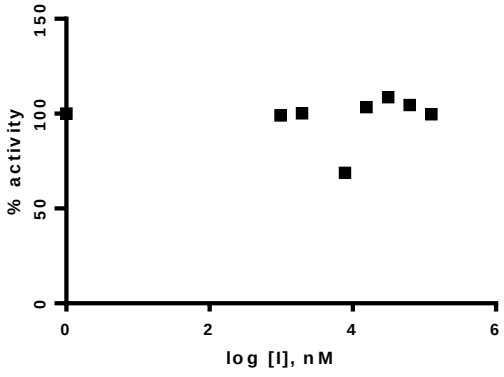

Average IC_{50}: > 125 µM

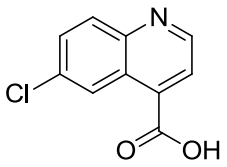

[1e]

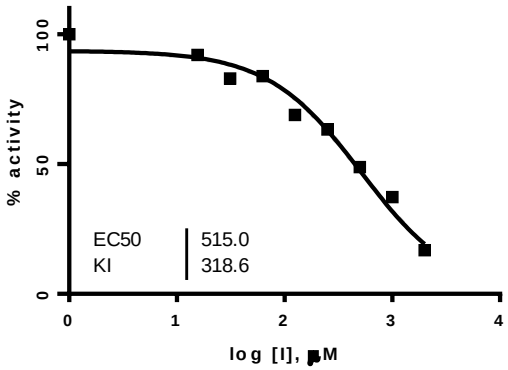

Average IC_{50}: > 125 µM

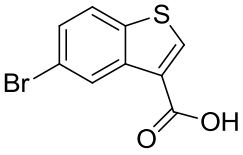

[1f]

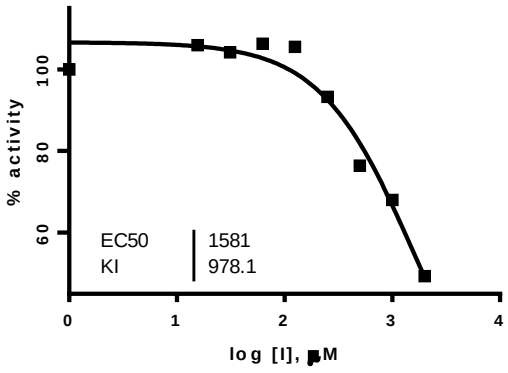

Average IC_{50}: > 125 µM

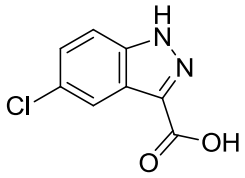

[1g]

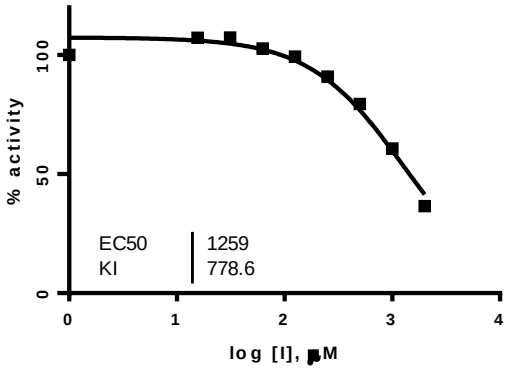

Average IC_{50}: > 125 µM

Analytical data for c-Abl Kinase Domain K_i determination. Each inhibitor K_i value was determined using nine independent experiments, a representative inhibition curve is shown.

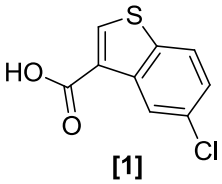

[1]

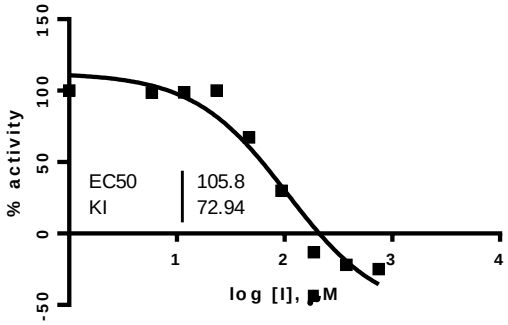

Average IC_{50}: 195.0 ± 84.9 µM

Analytical data for c-Hck Kinase Domain K_i determination. Each inhibitor K_i value was determined using six independent experiments, a representative inhibition curve is shown.

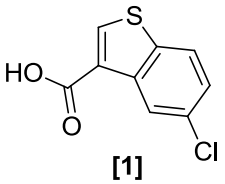

[1]

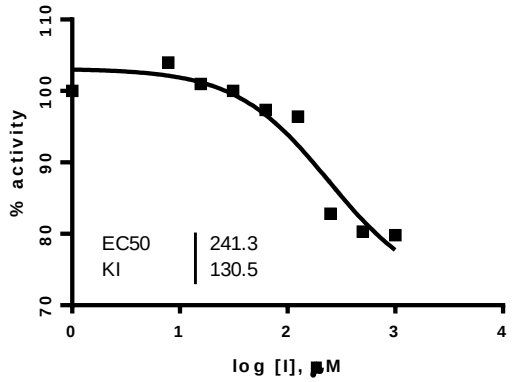

Average IC_{50}: > 125 µM

Analytical data for c-Src T338M Kinase Domain K_i determination. Each inhibitor K_i value was determined using four independent experiments, a representative inhibition curve is shown.

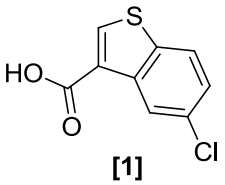

[1]

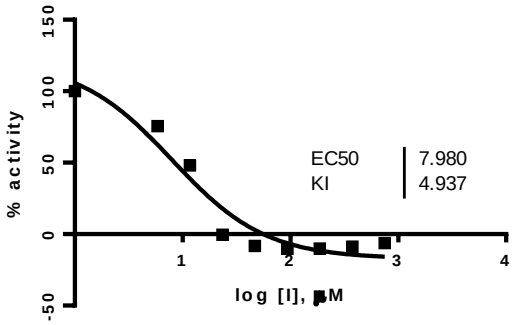

Average IC_{50}: 7.93 ± 2.23 µM

Analytical data for c-Src Kinase domain K_i determination at high [ATP] (5 mM final concentration, 45 µM substrate concentration). Each inhibitor K_i value was determined using at least four independent experiments; a representative inhibition curve is shown.

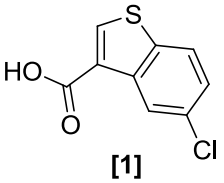

[1]

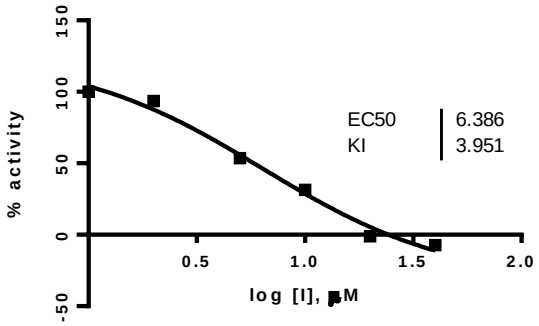

Average IC_{50}: 7.72 ± 1.47 µM

Analytical data for c-Src Kinase domain K_i determination at low [ATP] (100 µM final concentration, 45 µM substrate concentration). Each inhibitor K_i value was determined using at least four independent experiments; a representative inhibition curve is shown.

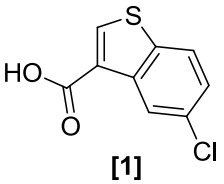

[1]

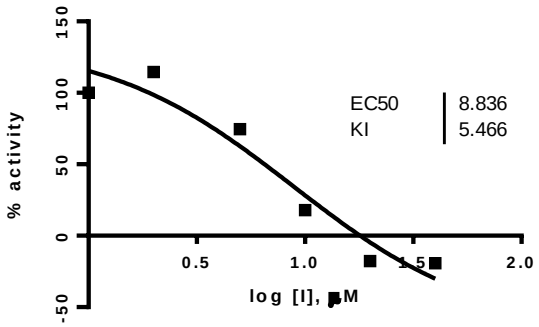

Average IC_{50}: 9.01 ± 3.38 µM

General procedure for ATP Lineweaver-Burk analysis of inhibitor. A continuous fluorescence assay[2] was used to determine K_M. Reaction volumes of 100 µL were used in 96-well plates. 85 µL of enzyme in buffer was added to each well. 2.5 µL of the appropriate inhibitor dilution (fixed concentrations, typically 0, 35, 50, 70, 100, or 140 µM in DMSO) was then added. 2.5 µL of a substrate peptide ("compound 3" as described in Wang et al)[2] solution (1.8 mM in DMSO) was added. The reaction was initiated with 10 µL of ATP (Two-fold dilutions, final concentrations: 5mM → 0 in water), and reaction progress was immediately monitored at 405 nm (ex. 340 nm) for 10 minutes. Reactions had final concentrations of 30 nM enzyme, 45 µM peptide substrate, 100 µM Na_3VO_4, 100 mM Tris buffer (pH 8), 10 mM $MgCl_2$, 0.01% Triton X-100. The initial rate data collected was used for determination of K_M values. For K_M determination, the kinetic values were obtained directly from nonlinear regression of substrate-velocity curves in the presence of various concentrations of ATP. The equation Y = (Vmax * X)/(Km + X), X = substrate concentration (µM) and Y = enzyme velocity (RFU/s); was used in the nonlinear regression.

Analytical data for c-Src Kinase Domain ATP Lineweaver-Burk analysis of inhibitor. Each inhibitor K_M value was determined using at least 4 independent experiments; a representative K_M curve is shown.

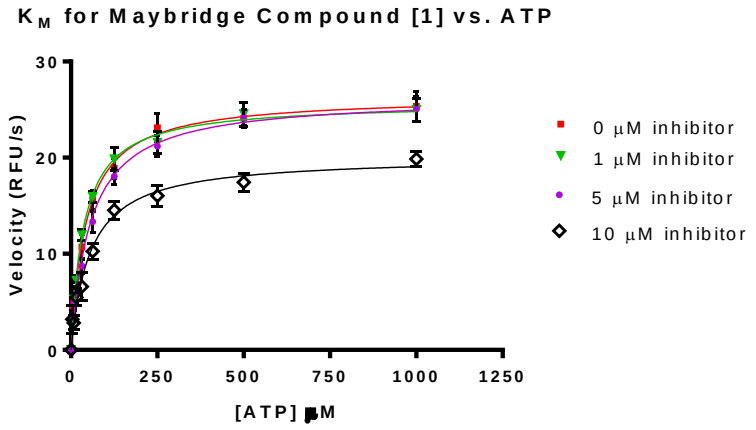

	0 µM inhibitor	1 µM inhibitor	5 µM inhibitor	10 µM inhibitor
Best-fit values				
Vmax	26.40	25.71	26.32	20.10
Km	43.82	37.09	55.81	54.98
Std. Error				
Vmax	0.8003	0.6059	0.7232	0.7665
Km	5.237	3.537	5.755	8.042
95% Confidence Intervals				
Vmax	24.80 to 27.99	24.51 to 26.92	24.88 to 27.76	18.57 to 21.63
Km	33.37 to 54.26	30.04 to 44.14	44.33 to 67.29	38.92 to 71.03

General procedure for Substrate Lineweaver-Burk analysis of inhibitor. A continuous fluorescence assay[2] was used to determine K_M. Reaction volumes of 100 µL were used in 96-well plates. 85 µL of enzyme in buffer was added to each well. 2.5 µL of the appropriate inhibitor dilution (fixed concentrations, typically 0, 35, 50, 70, 100, or 140 µM in DMSO) was then added. 2.5 µL of a substrate peptide ("compound 3" as described in Wang et al)[2] solution (Final concentrations: 500 µM → 0 in DMSO) was added. The reaction was initiated with 10 µL of ATP (Final concentration 1 mM in water), and reaction progress was immediately monitored at 405 nm (ex. 340 nm) for 10 minutes. Reactions had final concentrations of 30 nM enzyme, 45 µM peptide substrate, 100 µM Na_3VO_4, 100 mM Tris buffer (pH 8), 10 mM $MgCl_2$, 0.01% Triton X-100. The initial rate data collected was used for determination of K_M values. For K_M determination, the kinetic values were obtained directly from nonlinear regression of substrate-velocity curves in the presence of various concentrations of substrate. The equation Y = (Vmax * X)/(Km + X), X = substrate concentration (µM) and Y = enzyme velocity (RFU/s); was used in the nonlinear regression.

Analytical data for c-Src Kinase Domain Substrate Lineweaver-Burk analysis of inhibitor. Each inhibitor K_M value was determined using at least 4 independent experiments; a representative K_M curve is shown.

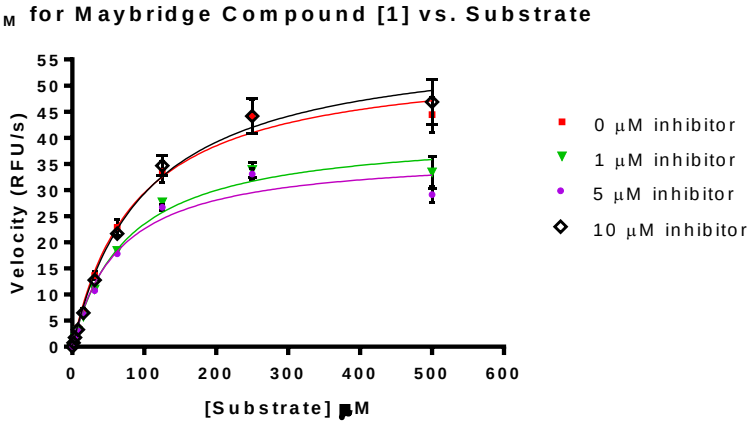

	0 µM inhibitor	1 µM inhibitor	5 µM inhibitor	10 µM inhibitor
Best-fit values				
Vmax	55.41	41.30	37.10	59.02
Km	88.16	75.91	64.45	101.3
Std. Error				
Vmax	2.468	1.541	1.096	2.896
Km	11.18	8.399	5.892	13.62
95% Confidence Intervals				
Vmax	50.49 to 60.34	38.22 to 44.37	34.91 to 39.28	53.24 to 64.79
Km	65.87 to 110.5	59.16 to 92.66	52.71 to 76.20	74.16 to 128.5

C.5: Cancer cell growth inhibition assays

General procedure:

1. **Cell culture and seeding**: Cells are dispersed from flasks and collected by centrifugation (125xg for 5 minutes at room temperature). An aliquot of the resuspended cells is mixed with trypan blue solution and the cell number is quantified using a hemacytometer. In general, depending on the growth rate of the untreated cells, the cells will be plated at 5.0 – 7.5 x 10^3 cells per well. 100 µL of the cell mixture will be added to each well so the concentration should be 10X the cells per well in cells per mL. The cells are plated into sterile, clear bottom 96 well plates and cultured under normal growth conditions overnight prior to dosing with compound.
2. **Dosing**: The 100% DMSO compound stocks need to be prepared to 100X the final concentration that is desired in the assay. 3 µL of the DMSO stock solution is then added to 297 µL of the cell growth media to give a DMSO concentration of 1%. The cell media is removed by aspiration for adherent cells and replaced with 100 µL per well of the cell growth media containing the compound. In general each compound concentration is dosed in triplicate wells. The plates are returned to normal culture conditions for 24 – 72 hours.
3. **Assay**: After the required incubation period the plates are removed from the incubator and 10 µL per well of WST-1 reagent is added. The plates are returned to the incubator and the color change is visually monitored for 0.5 – 2 hours. When sufficient color change has occurred the plates are shaken on a plate shaker for 60 seconds and read in the appropriate plate reader.
4. **Data Analysis**: The reference absorbance reading is subtracted from the formazan absorbance and the data is plotted as a percentage of the vehicle (1% DMSO alone). Data analysis and curve fitting was performed using Graphpad Prism. For each cell line, there were n = 3 data points for each concentration. Each dose response curve was performed at least twice, providing $n \geq 6$ for each data point.

Maybridge Compound [1] and SK-BR-3 cell line:

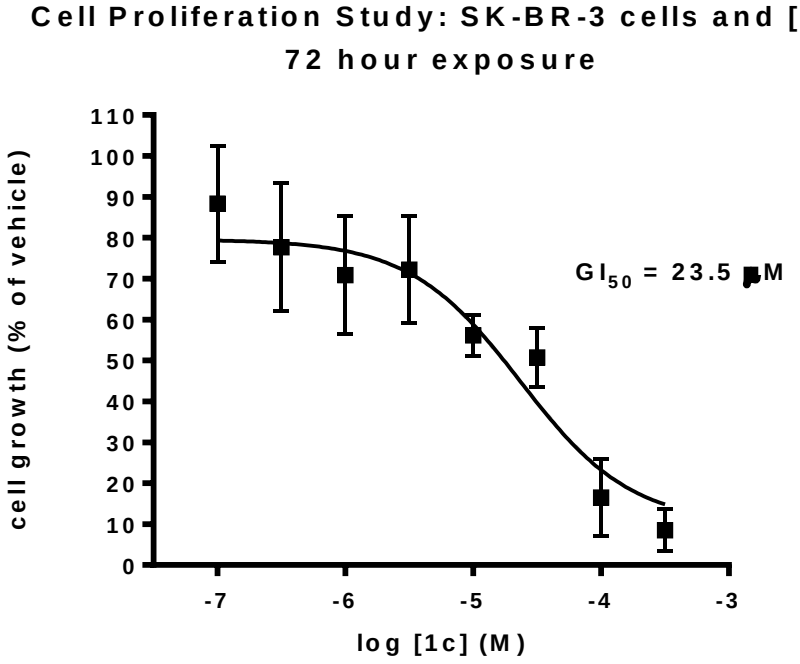

C.6: References

(1) Maybridge; 2013, http://www.maybridge.com/images/pdfs/ro3frag.pdf.

(2) Wang, Q.; Cahill, S. M.; Blumenstein, M.; Lawrence, D. S. *J. Am. Chem. Soc.* **2006**, *128*, 1808.

Appendix D:

Supplemental Plots for Compounds of Interest

D.1: Chapter 2

Hanes Plots

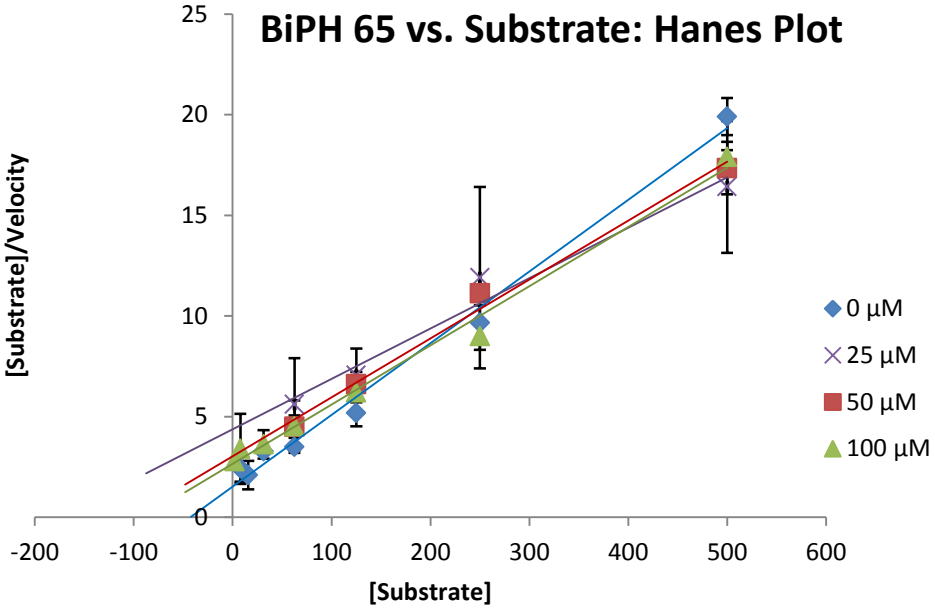

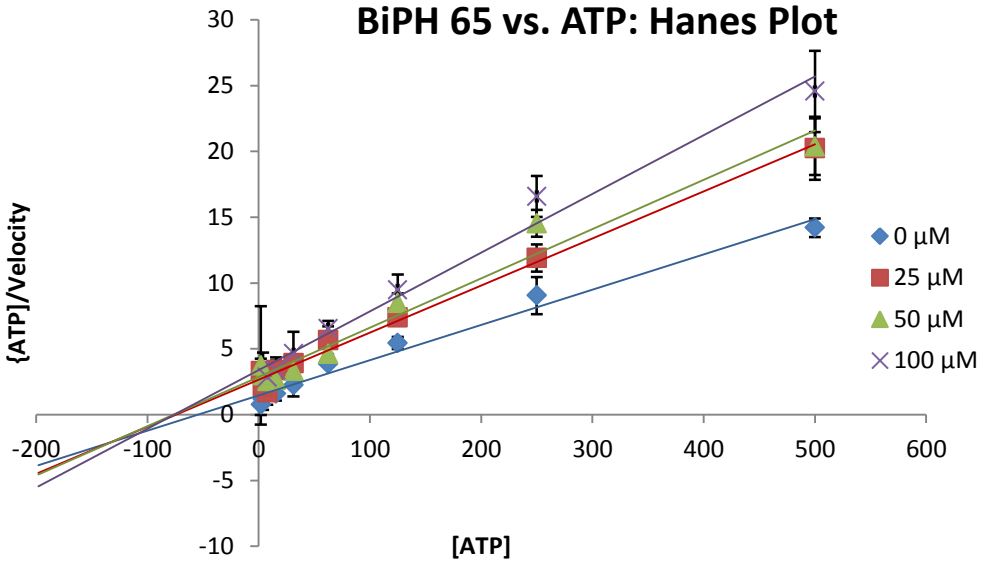

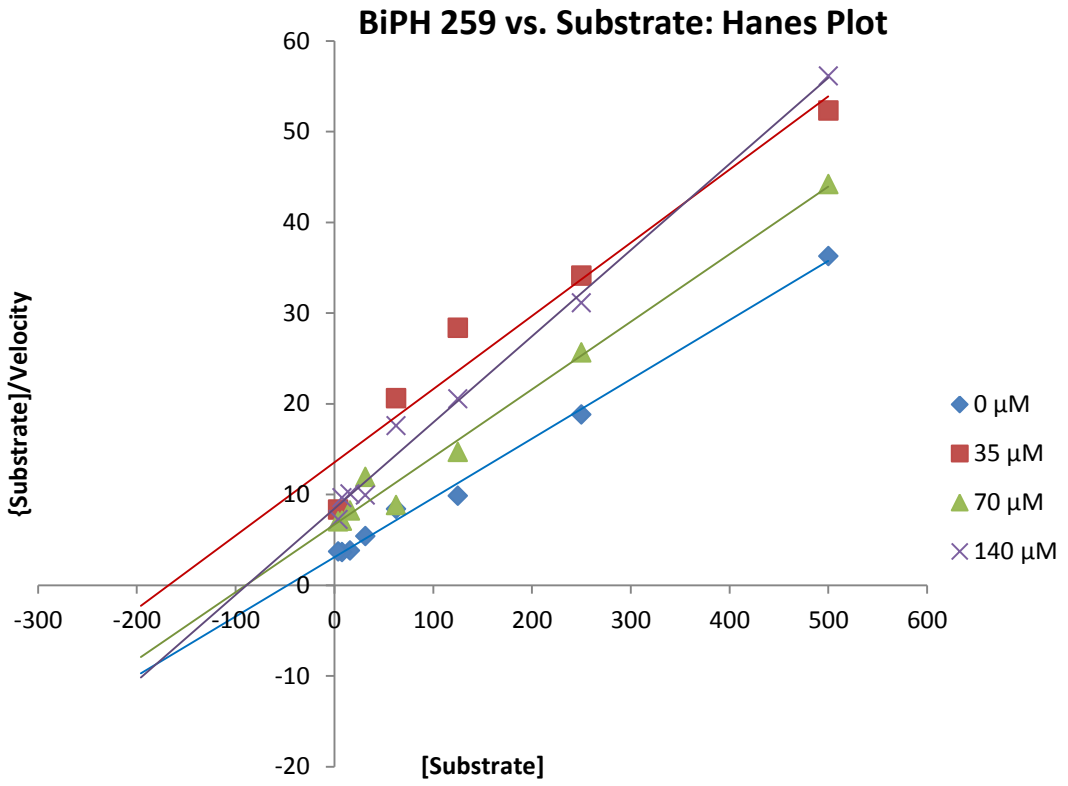
BiPH 259 vs. Substrate: Hanes Plot
{Substrate]/Velocity
[Substrate]
60
50
40
30
20
10
0
-10
-20
-300
-200
-100
0
100
200
300
400
500
600
0 µM
35 µM
70 µM
140 µM

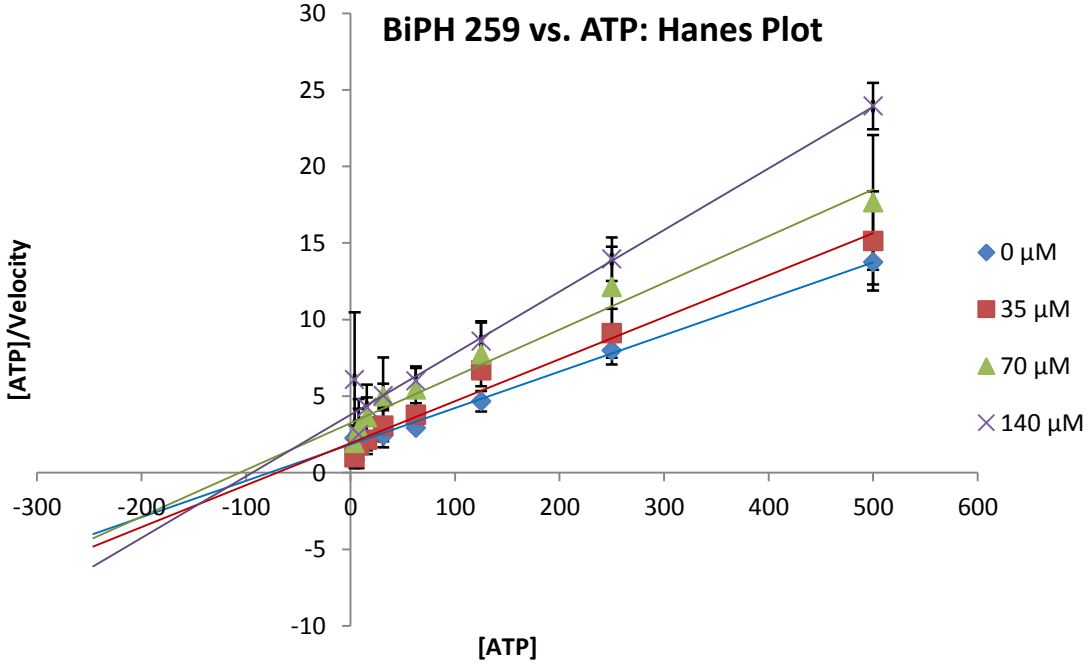
BiPH 259 vs. ATP: Hanes Plot
[ATP]/Velocity
[ATP]
30
25
20
15
10
5
0
-5
-10
-300
-200
-100
0
100
200
300
400
500
600
0 µM
35 µM
70 µM
140 µM

Additional Lineweaver-Burk Analysis

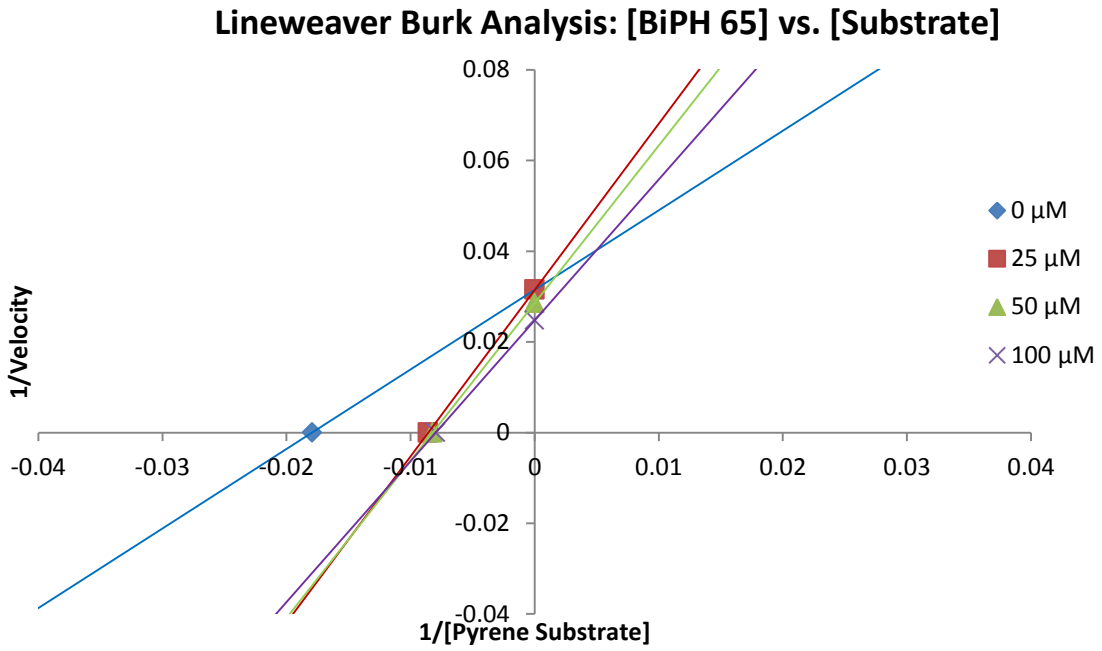

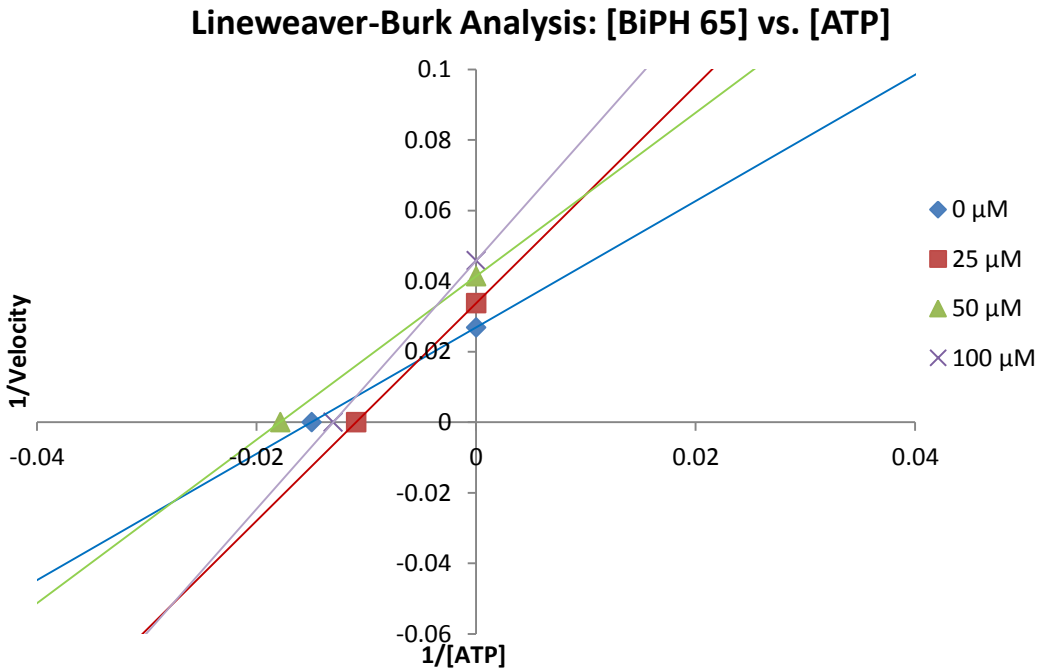

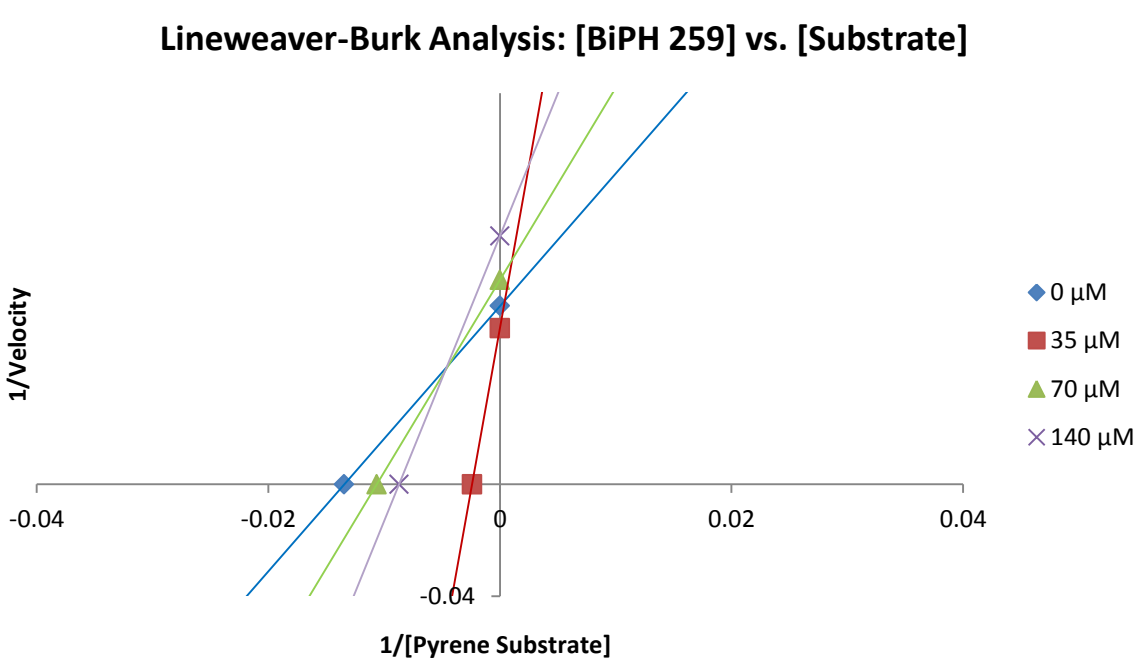
Lineweaver-Burk Analysis: [BiPH 259] vs. [Substrate]
1/Velocity
-0.04
-0.02
0
0.02
0.04
-0.04
1/[Pyrene Substrate]
0 µM
35 µM
70 µM
140 µM

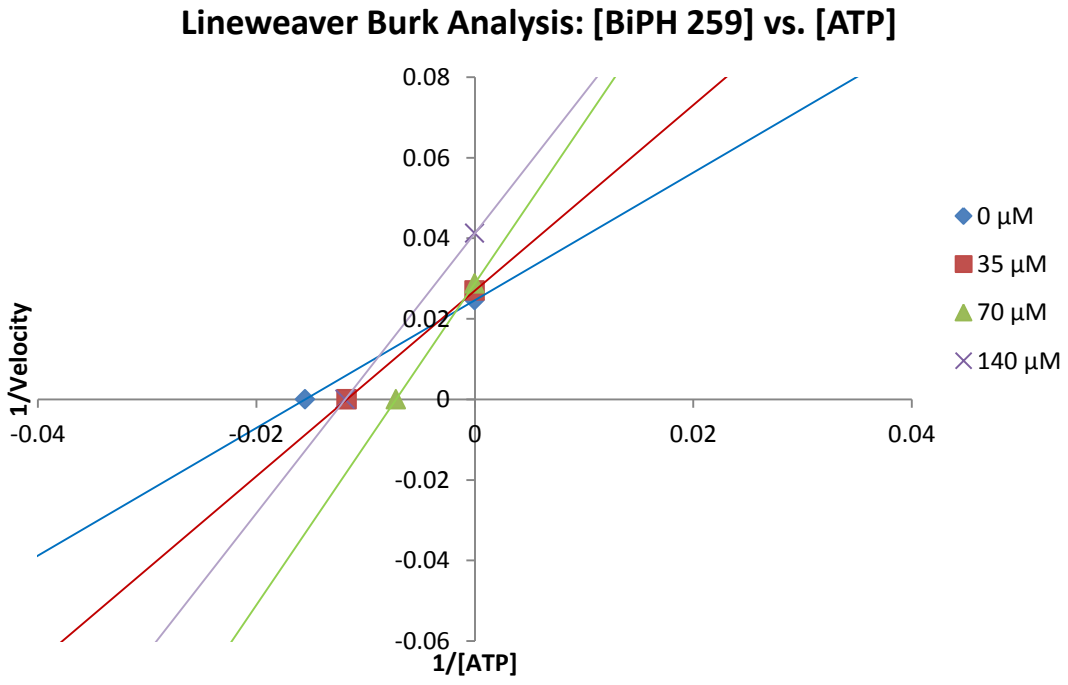
Lineweaver Burk Analysis: [BiPH 259] vs. [ATP]
1/Velocity
0.08
0.06
0.04
0.02
0
-0.02
-0.04
-0.06
-0.04
-0.02
0
0.02
0.04
1/[ATP]
0 µM
35 µM
70 µM
140 µM

D.2: Chapter 3

Hanes Plots

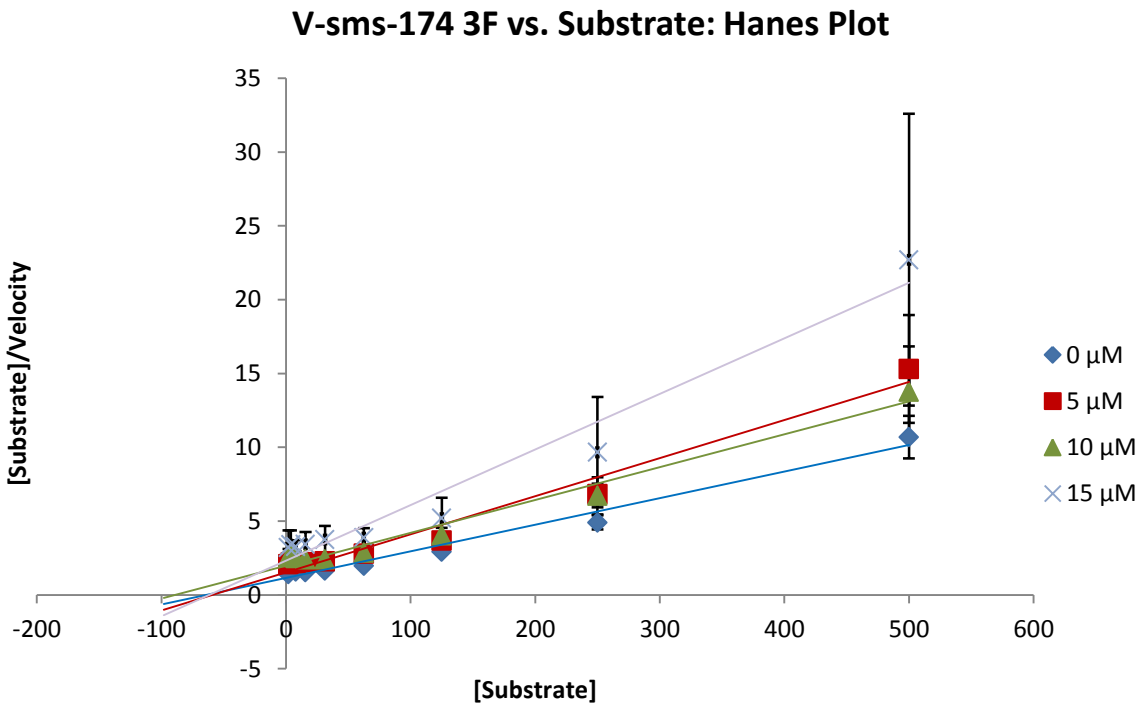

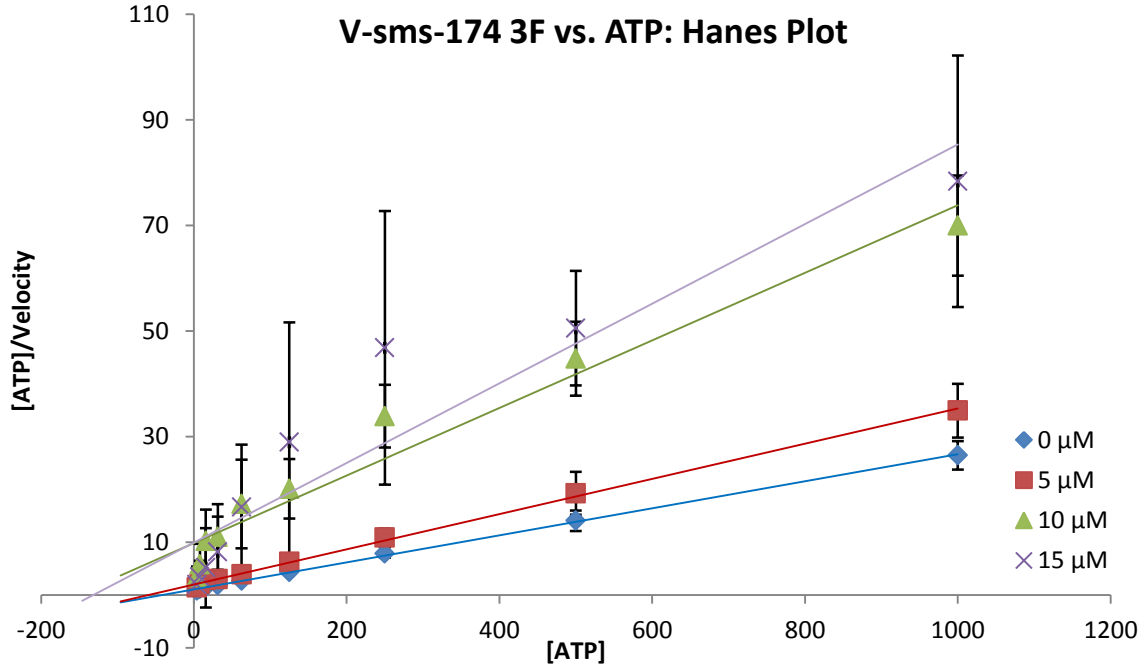

Additional Lineweaver-Burk Analysis

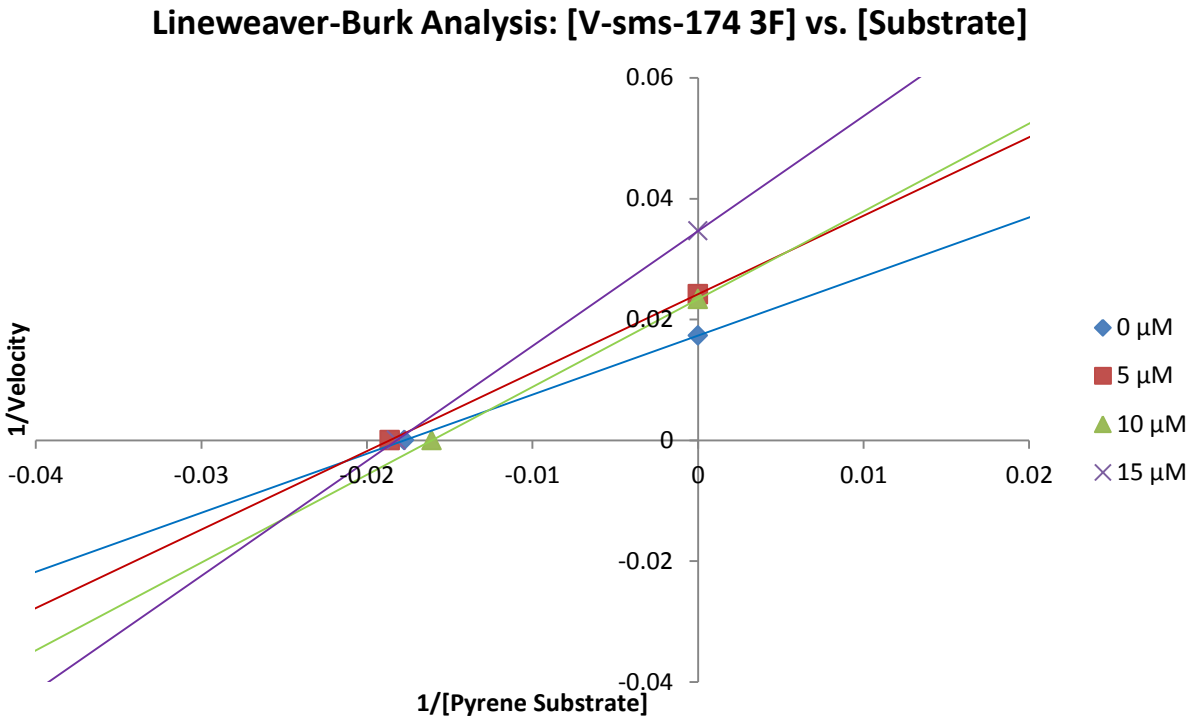

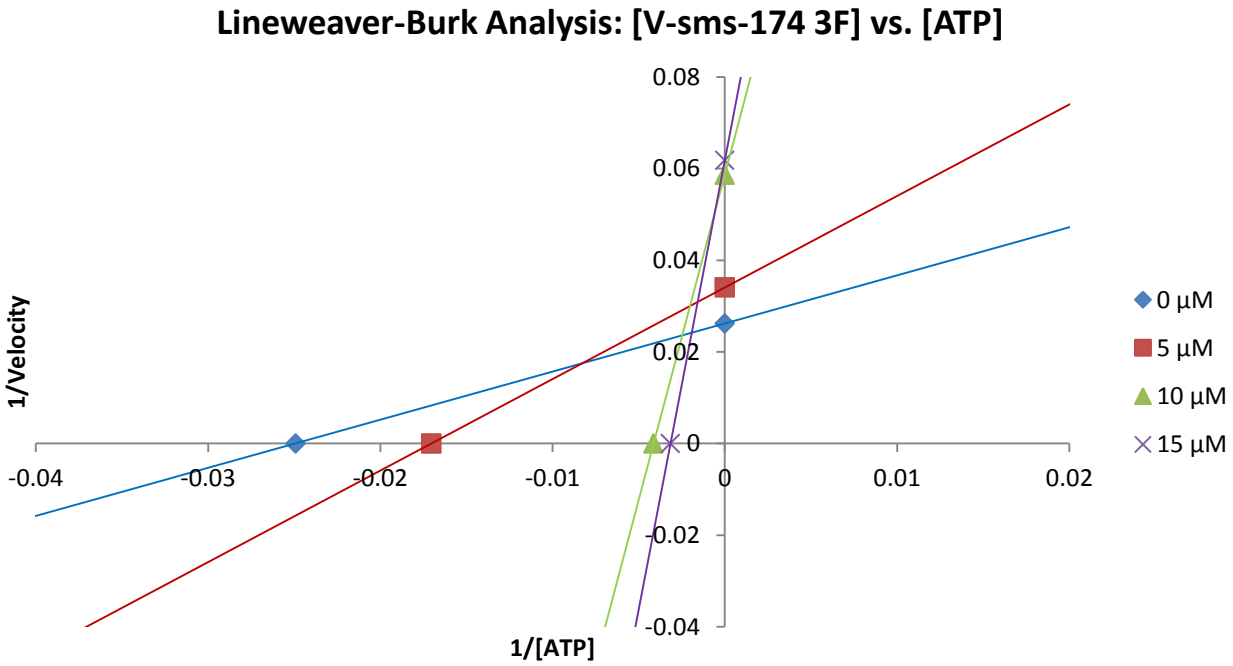

D.3: Chapter 4

Hanes Plots:

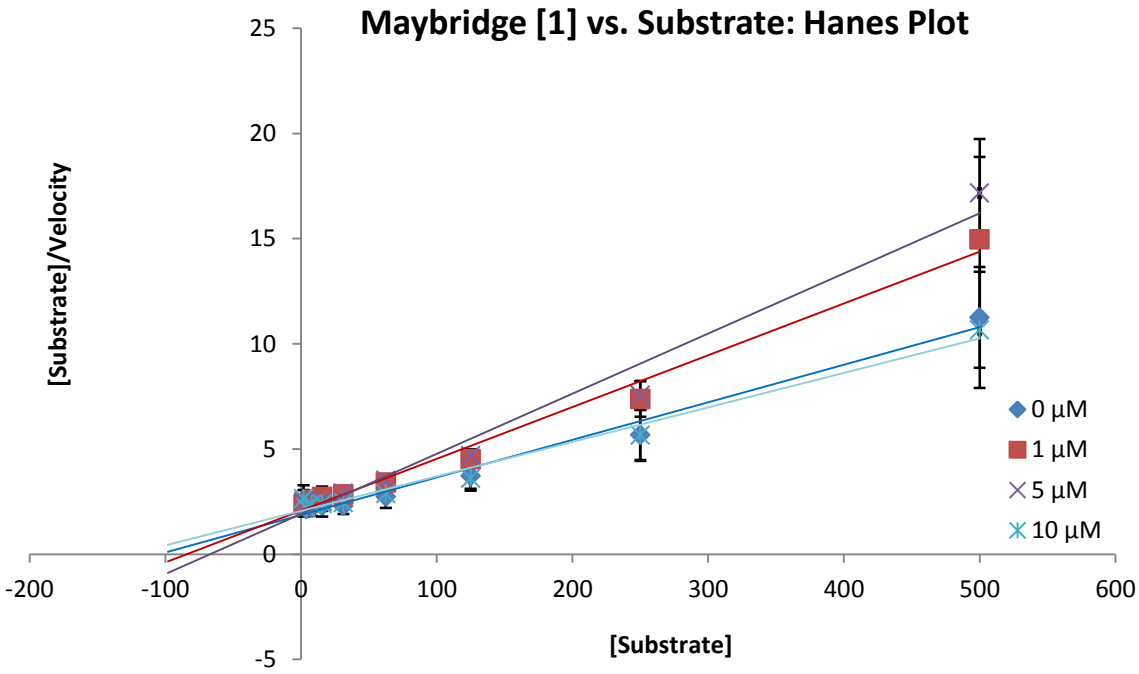

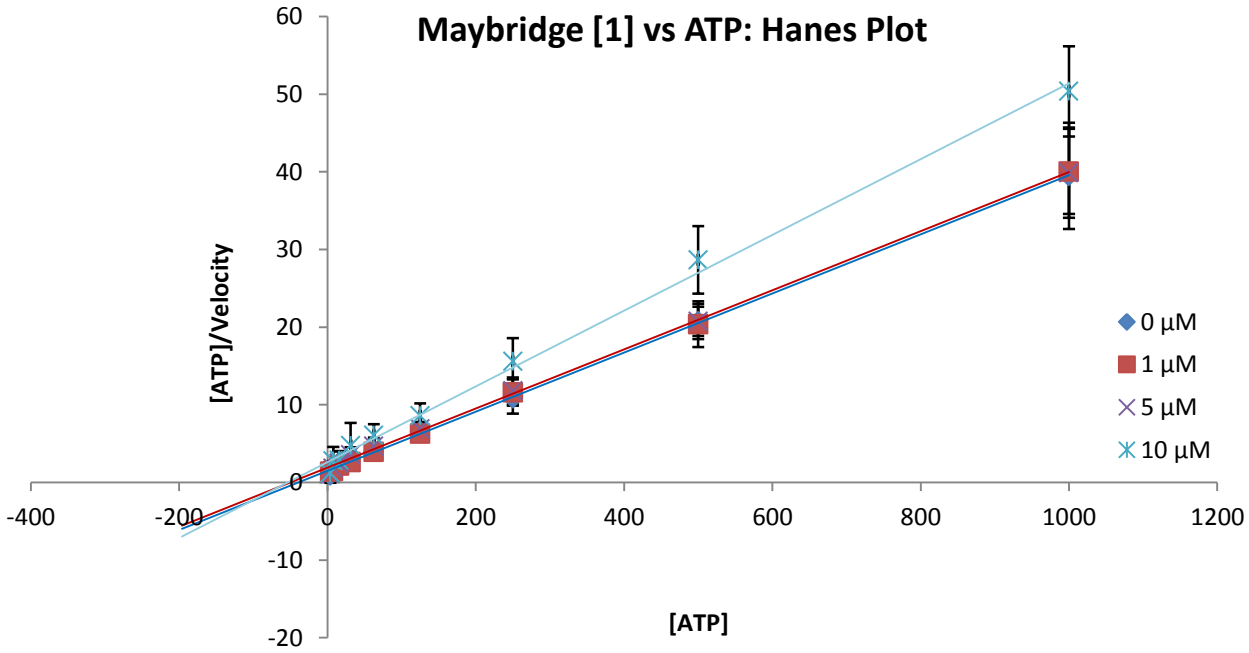

Additional Lineweaver-Burk Analysis: